Originally Processed With FOIA(s):
2005-0336-F

FOIA Number:
2005-0336-F

FOIA MARKER

This is not a textual record. This is used as an administrative marker by the George Bush Presidential Library Staff.

Record Group/Collection:	George H.W. Bush Presidential Records
Collection/Office of Origin:	Science and Technology Policy, Office of (OSTP)
Series:	Publications
Subseries:	Reports and Publications Files

OA/ID Number:	62111
Folder ID Number:	62111-006

Folder Title:
Non-Government [3 of 3]

Stack:	Row:	Section:	Shelf:	Position:
	0	0	0	0

Wavelets

JASON

MITRE

Wavelets

H. Abarbanel
K. Case
F. Dyson
D. Eardley
M. Freedman
J. Harvey
S. Koonin
G. MacDonald
W. Press
O. Rothaus

September 1992

JSR-90-150

Approved for public release; distribution unlimited.

JASON
The MITRE Corporation
7525 Colshire Drive
McLean, Virginia 22102-3481
(703) 883-6997

REPORT DOCUMENTATION PAGE

Form Approved
OMB No. 0704-0188

Public reporting burden for this collection of information is estimated to average 1 hour per response, including the time for reviewing instructions, searching existing data sources, gathering and maintaining the data needed, and completing and reviewing the collection of information. Send comments regarding this burden estimate or any other aspect of this collection of information, including suggestions for reducing this burden, to Washington Headquarters Services, Directorate for information Operations and Reports, 1215 Jefferson Davis Highway, Suite 1204, Arlington, VA 22202-4302, and to the Office of Management and Budget, Paperwork Reduction Project (0704-0188), Washington, DC 20503.

1. AGENCY USE ONLY (Leave blank)	2. REPORT DATE	3. REPORT TYPE AND DATES COVERED
	September 22, 1992	

4. TITLE AND SUBTITLE

WAVELETS

5. FUNDING NUMBERS

PR-8503A

6. AUTHOR(S)

H. Abarbanel, K. Case, F. Dyson, D. Eardley,
S. Koonin, G. MacDonald, W. Press, O. Rothaus

7. PERFORMING ORGANIZATION NAME(S) AND ADDRESS(ES)

The MITRE Corporation
JASON Program Office, A10
7525 Colshire Drive
McLean, VA 22102

8. PERFORMING ORGANIZATION REPORT NUMBER

JSR-90-150

9. SPONSORING/MONITORING AGENCY NAME(S) AND ADDRESS(ES)

DARPA/TIO
3701 North Fairfax Drive
Arlington, VA 22203-1714

10. SPONSORING/MONITORING AGENCY REPORT NUMBER

JSR-90-150

11. SUPPLEMENTARY NOTES

12a. DISTRIBUTION/AVAILABILITY STATEMENT

Distribution limited to U.S. Government agencies
and their contractors.

12b. DISTRIBUTION CODE

13. ABSTRACT *(Maximum 200 words)*

This report provides a relatively detailed description of wavelet research, including some JASON research, through roughly mid 1991, with a discussion of potential applications to DOD and other problems.

Some software for experimentation is included.

14. SUBJECT TERMS

discrete wavelet transform, image processing,
Daubechies wavelet filter coefficients

15. NUMBER OF PAGES

16. PRICE CODE

17. SECURITY CLASSIFICATION OF REPORT	18. SECURITY CLASSIFICATION OF THIS PAGE	19. SECURITY CLASSIFICATION OF ABSTRACT	20. LIMITATION OF ABSTRACT
UNCLASSIFIED	UNCLASSIFIED	UNCLASSIFIED	SAR

Contents

Abstract

This report provides a relatively detailed description of the state of wavelet research, including some JASON research, through roughly mid 1991, with a discussion of potential applications to problems of interest to DoD.

Some software for experimentation is included.

The sections of the report were written by many authors, in some cases totally independent of the others and without substantial editorial revision. While this has the advantage that many of the sections are self-contained and can stand alone on their own merits, it has the obvious defect of introducing repetitiveness, notational inconsistencies, and jarring stylistic breaks.

At the last moment, Ms. Margaret Jennings made an heroic effort to create some overall unity in the presentation, and we owe an enormous debt to her insight and perseverance. The obvious flaws still remaining are the responsibility solely of the authors.

1 EXECUTIVE SUMMARY

A large number of JASONs were involved to a greater or lesser degree in the Wavelet Study: H. Abarbanel, K. Case, F. Dyson, D. Eardley, M. Freedman, J. Harvey, S. Koonin, G. MacDonald, W. Press, and O. Rothaus. We listened to several briefings throughout the summer:

S. Mallat — Courant Institute

H. Resnikoff — Aware Corporation

R. Coifman, V. Rokhlin — Yale University

L. Auslander — DARPA

G. Wornell (for A. Oppenheim) — M.I.T.

G. Jacyna, M. Dellomo — The MITRE Corporation.

Additionally, a subgroup had heard short briefings in Washington before the summer study began, which included, beyond briefings mentioned above:

Richard Orr — Atlantic Aerospace

Leonid Rudin — Cognitech.

We viewed as our main responsibilities in this study the formulation of a judgment as to the general purview of wavelet theory, and the identification of areas of interest to DARPA to which wavelet theory might be applied.

We did not regard it as our task to critique the DARPA Wavelet Program, and indeed we were not briefed on all aspects, by any means, of that program. It is quite possible, of course, that the DARPA program is already supporting research in areas that we would regard as appropriate for wavelet

application, and of which we are not aware.

Since wavelet theory is fundamentally another form of harmonic or Fourier analysis, it is immediately reasonable to suppose that the theory will be applicable in any area in which Fourier analysis is used. In the interest of seeing that all prospective users hear the good news, this report includes a Wavelet primer, primarily addressed to physicists, which we hope to circulate widely.

It is also apparent that wavelet theory is an attractive mathematical study, with a reasonably large and probably growing number of mathematical practitioners. As a consequence, new theoretical developments will almost certainly continue to emerge for the next several years, especially so since the subject is in its relative infancy. (From a certain point of view, wavelets have been around 30 years or so, but it is the significant advances of Mallat in 1987 and Daubechies in 1988 that have given the theory its current vitality). The purely mathematical and other theoretical research will be carried forward by its own momentum, with the help of the usual funding agencies, although it is appropriate for DARPA to support some leading researchers in order to maintain a presence in the field and to keep abreast of developments.

There are a number of areas where wavelet theory will find adequate commercial backing — particularly speech and image processing, more particularly compression of such signals. A large volume of excellent work has already been done in this area, and further work probably does not need DARPA support. The commercial possibilities alone will carry it forward, though it is not yet clear how much better than "state of the art" techniques

wavelet theory will turn out to be. Because of its potential, however, the military and classified applications deserve support from DARPA.

A related area of wavelet application could use help from DARPA: the problem of data compression, data not structured in any particular way, in contrast to speech and visual images. In connection with the climate problem, vast quantities of numerical and other data may be produced, such as Earth Observation System (EOS) observations, and atmospheric measurements in the Atmospheric Radiation Measurement (ARM) program. Additionally, many military programs produce vast quantities of data to be stored for possible later use. Judging by the success of wavelet theory in analyzing and compressing images and speech, and in finding and classifying sharp contrasts, there could very well be general and specific data compression techniques of enough interest to DARPA to deserve encouragement and support.

There is still another area, related to the above, but with a distinct flavor of its own, that could use DARPA help. It is originally an application of wavelet theory, but it may go off in its own direction. This is the topic we will call fast linear algebra. Everyone knows the success of the fast Fourier transform (FFT) in certain linear problems. Because of the ability of wavelets to compress images, the numerical burden of multiplying two large matrices can be reduced in many cases by finding (using wavelets) a basis in which both matrices are sparse. This ability can have revolutionary consequences for all numerical computer problems. Some of the work in this area is being carried out by the Yale group; they even have discussed procedures using

change of bases much more general than those wavelet theory permits. This area of work should be strongly encouraged. It may turn out to be much more important for application than the Wavelet Theory that gave it birth.

Next we should mention wavelets and partial differential equations (PDEs). It seems reasonable to suppose that wavelets can be used as a "pseudo-spectral" method for numerical solution of all sorts of linear and non-linear PDEs. In addition, given their remarkable ability to resolve contrasts, they should be useful in following shock fronts in various PDEs. A reasonable amount of exploratory work using wavelet expansion has already been carried out; the very great flexibility and variety of wavelet expansion suggests their utility, but also makes it more difficult to know how and which to choose. The question of how far to carry a given wavelet expansion, or of how to increase or decrease the number of terms adaptively, is hardly addressed. Indeed the bulk of the work we have examined hardly uses wavelet theory at all — a preliminary choice of resolution is made and then the linear space of translates of the scaling function is used, rather than the full wavelet basis adaptively.

In a nutshell, wavelet PDE theory is hardly off the ground. But more significantly, it has a hard row to hoe. There is by this time an enormous investment in software algorithms for solving PDEs, and an enormous store of experience about the relative efficacy of competing methods. If this investment is to be set aside in favor of wavelets, there would have to be a very significant improvement in computational efficiency, or a remarkably heightened ability to solve at all. Even if it is possible for wavelet theory to

gain this ground, it will take a fair amount of time. While it comes of age, it should be encouraged and supported.

The facility, noted above, of wavelets to achieve fast linear algebra manipulation, will, of its own, have direct consequences for fast numerical PDEs.

There is another prospectively useful area of wavelet theory which is hardly off the ground, and that is an adaptive theory. The very wide choice of wavelet expansions raises naturally the question of "optimal" choice of wavelet basis. Very clever adaptive procedures, called wavelet packets, have been used by Coifman in speech compression; a little general work has been carried out by the MITRE group. The subject as a whole, though, is untouched — progress here will probably have important consequences for numerical PDEs. In connection with the problem of adaption, one should mention the more general question of wavelet frames. In all the enthusiasm over orthonormal wavelet bases, these seem to have been set aside, but they may offer better hope for adaptive procedures, and they do seem to show more numerical robustness.

Finally, there are a number of purely military applications, where DARPA support would be quite natural. We allude principally to wavelets and radar theory, wavelets and feature extraction for target identification, wavelets and acoustic transients for ASW.

2 INTRODUCTION

2.1 JASON Involvement

The question always asked is "What are wavelets and what are they good for?" Well, a part of DARPA, under the guidance of Dr. Louis Auslander, was funding a wavelet research program, and while the researchers knew what wavelets are, they hoped JASON would tell them a few things that wavelets might be good for of which they were not aware.

We had first to find out ourselves what wavelets are. After some very preliminary briefings at MITRE, work began in earnest in Summer '90 with an extensive exploration of the literature and a number of detailed briefings by outside experts. In the sequence in which they occurred these were:

1. S. Mallat — Courant Institute
2. H. Resnikoff — Aware Corporation
3. R. Coifman and V. Rokhlin — Yale University
4. L. Auslander — DARPA
5. G. Wornell — (reporting work of self and A. Oppenheim) MIT
6. G. Jacyna, M. Dellomo — The MITRE Corporation.

These acknowledgments made, we may now give a brief answer to the initial question.

Wavelets and wavelet theory constitute a systematic collection, and study of, alternative ways of doing Fourier analysis. The theory is very well adapted to the computer, and enjoys the computational efficiency of the FFT. Moreover, wavelets give a very good localization of signal in phase space — i.e., time and frequency. (The Fourier transform is of course very poorly localized in time and very sharply localized in frequency.)

Wavelets are currently "BIG NEWS," with a very large number of active researchers and conferences, very many claims and some of the usual hyperbole. It is clear that there are many promising aspects and possible applications of wavelet theory — some parts of it are already proved, but by and large there is still, we believe, a great deal of work to be done before wavelet analysis overtakes or replaces more traditional Fourier methods as a general tool.

The areas in which we were briefed, or the areas in which we see possible applications, include a number that are quite familiar:

1. signal processing and compression, especially speech signals
2. image processing and compression
3. linear and non-linear
4. seismology

5. radar

6. theoretical mathematics,

plus a number of others which struck us as peculiar to wavelet theory:

7. fast linear algebra

8. data compression

9. feature extraction

10. modeling $1/f$ processes.

2.2 Some History

The word wavelet itself probably comes from the French *ondelettes*, the French probably got *ondelettes* from American seismologists who used the word wavelet. This round trip and the birth and use of wavelets in seismology are explored in Section 6 of this report.

Still earlier roots of modern wavelet theory are to be found in the so-called Gabor Transform (1943) and its generalization to the Weyl-Heisenberg Transform. Using modern language, we will start with a function g called the analyzing wavelet (picked by the user in a special way), and a function f, the signal to be analyzed. One forms

$$F(\gamma, \tau) = \int_{-\infty}^{\infty} f(x) g(x - \gamma) e^{2\pi i \tau x} dx \, .$$

The reader will recognize F as a windowed Fourier transform; F is called a Weyl-Heisenberg transform. Gabor concentrated on $g(x) = e^{-x^2/2}$, which is

local in time and frequency. In general F overdetermines f and given F we can recover f in a continuous linear fashion. This being so, it is natural to inquire if from the discretization:

$$F(m,n) = \int_{-\infty}^{\infty} f(x)g(x - m\gamma)e^{2\pi i n\tau x}dx,$$

one can continuously recover f. If this is so, the collection of functions $\{g(x - m\gamma)e^{2\pi i n\tau x}\}$ is called a Weyl-Heisenberg frame. Weyl-Heisenberg frames are useful in quantum mechanics — the Weyl-Heisenberg transform is important in radar theory, related as it is to the radar cross ambiguity function and the Wigner-Ville distribution.

One natural question to ask is, given a frame, how efficient is it? Put another way, can one select g, γ, and τ so that the frame $\{g(x - m\gamma)e^{2\pi i n\tau x}\}$ is an orthonormal basis for L^2 ?

The somewhat discouraging answer is given by the Balian-Low Theorem:

1. If $\gamma\tau > 1$, no frames exist.

2. If $\gamma\tau = 1$, orthonormal bases are possible, but either g' or $(\hat{g})'$ decays "slowly."

3. If $\gamma\tau < 1$, there are frames, but none of them are orthonormal bases.

What this means, of course, is that the information given by $F(m,n)$ is redundant, or if not redundant is not well localized in phase space.

Another general difficulty with this kind of analysis is the difficulty of

representing a pulse — the $F(m,n)$ will be large for a large range of values of m and n.

Interest in this kind of Fourier analysis flagged, despite the importance in radar theory. (We tend to believe however, that Weyl-Heisenberg frames, in the regime $\gamma\tau < 1$, are still of great potential utility, even though they are redundant.)

More recently, a group other than the Heisenberg group has been emphasized, and an alternative analysis has surfaced. Now we concentrate on the affine group of the line, and following Grossman and Morlet select an analyzing function $g(x)$, (subject to $\int_{-\infty}^{\infty} g(x)dx = 0$ for technical reasons), and form, for a function f to be analyzed:

$$F(\gamma,\tau) = \sqrt{\gamma}\int_{-\infty}^{\infty} f(x)g(\gamma x - z)dx.$$

Again we can continuously recover f from F. The discretization selected in this case is:

$$F(m,n) = 2^{m/2}\int_{-\infty}^{\infty} f(x)g(2^m x - n)dx.$$

Here the various versions of the analyzing function in the integrand, i.e., $2^{m/2}g(2^m x - n)$, are all translates of the same shape curve, dilated or expanded by a power of 2. Consequently, if g is compactly supported, this analysis of f gives great temporal resolution, and great phase space resolution at high frequencies.

2.3 The Recent Developments

We may ask now the same question for affine wavelets as we did in the Weyl-Heisenberg case. The answers are what modern wavelet theory is all about.

First, it is known that frames often exist — they are called wavelet frames. In our view they have been sadly neglected in favor of the more glamorous orthonormal frames we are about to describe, but it should be noted that general frames may be more robust numerically than orthonormal frames.

So there are choices of g for which the family $\{2^{m/2}g(2^m x - n)\}$ form an orthonormal basis for L^2. One such obvious choice is the Haar wavelet.

$$g(x) = \begin{cases} 1 & 0 \leq x < 1/2 \\ -1 & 1/2 \leq x < 1 \\ 0 & \text{otherwise.} \end{cases}$$

For analysis of smooth functions f, the Haar wavelet family is not too good — it leads to too many large $F(m,n)$. So it would be desirable to have a differentiable wavelet, in fact highly differentiable, and compactly supported, if possible, to get good temporal resolution. (The merit of high differentiability is roughly the same as the case in Fourier series where integration by parts shows rapid decay of the Fourier coefficients.)

In 1985, Y. Meyer produced the first really interesting wavelet — it was infinitely differentiable, decayed rapidly and had, as a matter of fact, a compactly supported Fourier transform. Shortly afterward, Lemarié and, in-

dependently, Battle produced a highly differentiable wavelet with even more rapid decay than that of Meyer.

At this time, there was no general theory for the construction of these remarkable wavelets, but it was soon to emerge in the multi-resolution analysis of S. Mallat, itself an outgrowth of the Laplacian pyramid schemes of Burt and Adelson. Mallat was interested in image compression, but his analysis is perfectly general and works in all dimensions.

We are given a bilaterally infinite scale of (closed) subspaces of $L^2(R)$:

$$\ldots \subset V_{-2} \subset V_{-1} \subset V_0 \subset V_1 \subset V_2 \subset \ldots$$

whose union is dense in $L^2(R)$, and whose intersection is empty. Moreover, $f(x)$ is in V_i if and only if $f(2x) \in V_{i+1}$, so all the V_is are determined by any one of them. And finally, $\exists \phi$ such that the collection $\{\phi(x-n)\}$ is an orthonormal basis for V_0.

A simple example of a multi-resolution analysis consists in taking $V_0 =$ collection of functions, each of which is constant on $[i, i+1]$ for all i, and

$$\phi(x) = \begin{cases} 1 & 0 \leq x \leq 1 \\ 0 & \text{otherwise} \end{cases} .$$

Mallat proved that for every multi-resolution analysis, there exists a function ψ, called the mother function, such that the collection (m, n running through integers)

$$\{2^{m/2}\psi(2^m x - n)\}$$

is an orthonormal base for $L^2(R)$. The translates of ψ span the orthocomplement of V_0 in V_1. For a function in V_0, its part in V_{-1} is its smooth part or

part at a coarser resolution, while its part in the orthocomplement of V_{-1} in V_0 is its fine detail. For the example we gave above, the mother, or analyzing, wavelet is the Haar wavelet.

Inspired by the work of Mallatt, I. Daubechies (1988) was able to produce compactly supported wavelets of arbitrarily high differentiability. We will now indicate briefly how the analysis of Mallatt and Daubechies works. Since V_0 is contained in V_1, we must have

$$\phi(x) = \sum_{-\infty}^{\infty} c_n \phi(2x - n). \qquad (2-1)$$

(Daubechies noticed that if only finitely many c_is were different from zero, she could construct a compactly supported ϕ.) ϕ perpendicular to its translates requires

$$\sum_{-\infty}^{\infty} c_v c_{v-2n} = 2\delta_{0n}, \qquad (2-2)$$

and a technical requirement $\int_{-\infty}^{\infty} \phi(x)dx \neq 0$, demands

$$\sum_{-\infty}^{\infty} c_v = 2. \qquad (2-3)$$

In terms of the c_is, the mother wavelet is given by:

$$\psi(x) = \sum_{k=-\infty}^{\infty} (-1)^k c_{1-k} \phi(2x - k).$$

(If, for example, $c_o = c_1 = 1$, all c_is remaining are zero, then ϕ = box function, and ψ is the Haar wavelet.)

Notice the easy iterative computation of ϕ suggested by Equation (2–1). Knowing ϕ at the integers gives ϕ at all half integers, gives ϕ at all quarter integers, etc. This is quite the typical situation in wavelet theory: the computations are all recursive and made on the fly as needed. (By careful

choice of ϕ on the integers, Daubechies was able to construct compactly supported ϕ.)

If one puts $P(\epsilon) = \frac{1}{2}\sum_n c_n e^{in\epsilon}$, the identity (2–2) may be rewritten

$$|P(\epsilon)|^2 + |P(\epsilon + \pi)|^2 = 1,$$

while Equation (2–3) says $P(0) = 1$. If one takes Fourier transform of Equation (2–1), one obtains the identity $\hat{\phi}(\epsilon) = P(\epsilon/2)\hat{\phi}(\epsilon/2)$. If ϕ is normalized so that $\int \phi(x)dx = 1$, i.e., $\hat{\phi}(0) = 1$, the last equation yields formally

$$\hat{\phi}(\epsilon) = P(\epsilon/2)P(\epsilon/4)P(\epsilon/8)\dots .$$

This determination of ϕ is used extensively by Daubechies (and others) in an analysis of its properties.

As a non-trivial illustration of all the above we give:

Ex D_4 (Daubechies 4)

$$\begin{aligned} c_0 &= \tfrac{1}{4}(1+\sqrt{3}), c_1 = \tfrac{1}{4}(3+\sqrt{3}) \\ c_2 &= \tfrac{1}{4}(3-\sqrt{3}), c_3 = \tfrac{1}{4}(1-\sqrt{3}), \text{all other } c_i\text{s zero} \\ & \phi(1) = \tfrac{1}{2}(1+\sqrt{3}), \phi(2) = \tfrac{1}{2}(1-\sqrt{3}), \phi(k) = 0 \end{aligned}$$

for all other integers. D_4, the associated wavelet, is continuous, supported on [0,3], and .55 differentiable (in Lipschitz sense).

Daubechies has a whole infinite family of wavelets — the support increases with the number of non-vanishing cs, and so does the degree of differentiability. None of the Daubechies wavelets are symmetric about zero.

The Meyer and Lemarié-Battle (L-B) wavelets are associated with multi-resolution analyses also, but are not compactly supported. The L-B wavelet is left-right symmetric. It is known that there are affine wavelets not associated with a multi-resolution analysis, so their origins are somewhat obscure.

We have only discussed one-dimensional wavelets. The higher dimensional ones in use are formed by a straightforward algebraic direct sum construction from the one-dimensional version. No one seems to have worked on genuinely irreducible two-dimensional wavelets — they might be useful in image processing or pattern recognition, since they will not have a preferred pair of directions.*

As we have noted earlier, use of the fundamental relation, given in Equation (2–1) makes it simple to compute the values of ϕ, and hence ψ, recursively, but it also makes it simple to compute the wavelet expansive of a function f. For once the inner products of f with translates of ϕ are known, the inner products of f with $\{\phi(\frac{1}{2}x-k)\}$ are known, $\{\phi(\frac{1}{4}x-k)\}$ are known, etc. What this means, put another way, is that if the function f is to be specified at the resolution afforded by V_0, all of its expansion coefficients are computed readily in terms of a few of them. Since this observation will become more significant when we discuss the "discrete wavelet transform," we will spell out some of the details now.

Given a waveform f, one must first decide what resolution is required to represent it adequately. Though in some cases this will be determined on the basis of purely physical requirements or on the nature of the waveform

*The situation has changed since this report was first written.

source, as a purely sampling problem, it does not appear to have been dealt with much in the literature. It is, as a matter of fact, not at all difficult to handle, though it is a little subtler than first glance suggests, for our intuitive notion of adequate resolution is Euclidean invariant, but this is not the case for wavelet resolutions. Thus if $\psi(x)$ is the Daubechies 4 wavelet, it is perfectly resolved in V_0, but its translate, $\varphi(x + 1/2)$, is in V_1 and not in V_0, and only about 70 percent of its energy is in V_0. As a further example, $\varphi(x + 1/3)$ does not belong to any V_n.

Here is a fairly simple way of deciding adequate resolution. Without losing generality, we may suppose we have tried to resolve f in V_0 — any other V_i will lead to similar arguments. So we suppose $f(x) \approx \sum a_v \phi(x - v)$, with $a_v = \int_{-\infty}^{\infty} f(x)\phi(x - v)dx$. If f were perfectly resolved in V_0, then $\int_{-\infty}^{\infty} f^2(x)dx = \sum a_v^2$; in any case $\int f^2 dx \geq \sum a_v^2$ and the size of $\int f^2 - \sum a_v^2$, relative to $\int f^2$ is a reasonable measure of resolution.

One can be a little more sophisticated. Try instead to resolve f in V_1; $f \approx \sum \ell_v \phi(2x - v)$, with $\ell_v = \frac{1}{2}\int_{-\infty}^{\infty} f(x)\phi(2x - v)dx$. $\sqrt{\frac{1}{2}\sum \ell_v^2 - \sum a_v^2}$ is the length of the "detail", or "fine", part of f in V_1 relative to V_0, and so $\frac{1}{2}\sum \ell_v^2 - \sum a_v^2$ relative to $\sum a_v^2$ is a measure of the improvement available in resolving f in V_1 rather than V_0.

For the moment now, we suppose the question of level of resolution has been settled, and without losing generality we take f to have been resolved in V_0. This is to say we know all the coefficients $a_v = \int_{-\infty}^{\infty} f(x)\phi(x - v)dx$. From the basic relations in a multi-resolution analysis, we have $\phi(\frac{1}{2}x - \ell) = \sum_k c_k \phi(x - 2\ell - k)$ and $\psi(\frac{1}{2}x - \ell) = \sum_k (-1)^k c_{1-k}\psi(x - 2\ell - k)$. Thus the

detail part of f in V_0 relative to V_{-1} is known, since we may compute without integration $\int f(x)\psi(\frac{1}{2}x - \ell)dx$, and the wavelet expansion of f in V_{-1} is also completely known. With the resolution of f in V_{-1} at hand, the whole process described above may be repeated to get the detail part of f in V_{-1} relative to V_{-2}, and the resolution of f in V_{-2}, etc. The continuing procedure is very simply encoded algorithmically in what is called the (fast) wavelet expansion algorithm. What is left at the end is the detail part of f; i.e., the expansion of f in terms of the mother wavelet.

2.4 Connection with Signal Processing and Quadrature Mirror Filters

The signal processing community has, for a number of years, been investigating subband coding procedures, in which a signal is divided into frequency bins, each bin is down sampled depending upon its average energy, and the bin samples are multiplexed and transmitted. Under some circumstances, the original signal can be recovered perfectly from the multiplexed one. For high- and low-pass binning, analysis of the reconstruction led in the early 1980s to the notion of quadrature mirror filters. Interestingly enough, the condition derived from Equation (2–2), i.e., $|P(\epsilon)|^2 + |P(\epsilon + \pi)|^2 = 1$, appears in the signal processing literature as one leading to a perfect reconstruction quadrature mirror filter. Therefore, one may fairly say that some of the developments in wavelet theory application to speech and image compression were already anticipated and worked out by the signal processing community. What they did not do was pass to the continuum limit, and see

the orthogonality of the wavelet family, nor did they have systematic procedures for constructing compactly supported wavelets. Not all quadrature mirror filters come from wavelets, but the wavelet theory quadrature mirror filters appear to have exceptionally good signal processing features, and have consequently been picked up and stimulated further signal processing research.

2.5 The Discrete Wavelet Transform

The discrete wavelet transform is a formal extension of the pyramidal algorithm described earlier for fast computation of wavelet coefficients, but one does not need an analog signal to begin. A discrete signal $\{a_v\}$ is given, and it is imagined that these are the wavelet coefficients of a waveform in V_0; $f(x) = \sum a_v \phi(x - v)$. (The processing really only uses the quadrature mirror filter features of the wavelet construction.)

The smooth and detail parts of f are determined as before, and the process is repeated for the smooth part, lying in V_{-1}, etc., till only detail coefficients are left.

One should not tend to think that the $\{a_v\}$ have a direct relationship to the shape of $f(x)$, though this is clearly close to true for Haar wavelets, and still approximately true for very compactly supported wavelet bases.

One might have equally well imagined that the $\{a_v\}$ were the wavelet

coefficients in some other scale, i.e., $f(x) = \sum_v a_v 2^{k/2} \phi(2^k x - v)$, but only the scales have changed, not the "shape."

Given a waveform $f(x)$, and a wavelet ϕ, there is a fairly delicate balance between support properties of ϕ and choice of sampling interval in order that $f(x) \approx \sum_v a_v \phi(x - v)$ to a good approximation, where the $\{a_v\}$ are regularly spaced samples of $f(x)$. If ϕ is unimodal, or compactly supported, then for sufficiently large k one may write $f(x) \approx \sum_v a_v 2^{k/2} \phi(2^k x - v)$, with the $\{a_v\}$ now really being approximate values of $f(x)$ at regular spacing.

Suppose one begins, as is often the case, with an analog signal $f(x)$, samples it regularly and processes the sample stream by the discrete wavelet transform. One need not think of this as a wavelet analysis of the analog signal: it is a surrogate analysis that is just as effective in practice as the continuous waveform analysis earlier described.

The continuous wavelet transform and the discrete wavelet transform simply do not bear the same relation to each other as the Fourier transform does to the discrete Fourier transform.

In order to make the discrete wavelet analysis more uniform in structure, the following modification of the usual procedure is adopted. It is supposed that there is precisely a power of 2, 2^N, points in the original data stream a_v, $v = 0, 1, 2, \ldots 2^N - 1$, which is then repeated periodically. With this supposition, we get 2^{N-1} points, repeated periodically, for the smooth part in V_{-1}, and 2^{N-1} points, repeated periodically, for the detail part. The detail part is saved, the smooth part in V_{-1} is then subjected to the same

analysis all over again — further repeated till only detail coefficients remain. Given the surviving detail coefficients, the whole procedure can be undone to recover the original data stream.

In practice now, the detail coefficients falling below certain thresholds are discarded (set equal to zero). Since the data stream reconstructed from the suppressed detail stream will bear a close resemblance to the original, we have achieved a data compression of sorts. Section 4 describes the results of several experiments along these lines.

The procedures just described are particularly simple to carry out for a compactly supported wavelet (only finitely many of the c_v s different from zero), and are encoded readily into a straightforward computer algorithm, all described in greater detail in Section 4 of this report. The reader should note a slight change of scale in the fundamental constants $\{c_v\}$.

The periodic repetition of the data stream is reflected in the stepping to the right (end around) of the rows of the matrix effecting the transform at any particular level of the algorithm. It is to be noted, however, that periodic repetition of the data stream introduces unnatural and undesirable end effects (as in the DFT for example), so it is worth improvising some minor modification of the DWT that avoids end around effects as much as possible. A brief appendix, Section 4.9, describes a relatively straightforward cut at this problem.

In case the wavelet is not compact, the construction of the linear transformation required to give the smooth and detail parts of a data stream in-

volves various infinite sums of the c_vs. These could be computed once and for all for a given data stream width, and thence for all its divisors. The numerical problems are avoided to a large degree when the Fourier series $\sum c_v e^{ivx}$ is known explicitly; all computations are then carried out conveniently on the Fourier side. Again, the reader will find a more detailed description again in Section 4.

There are, of course, well-known procedures for data compression using Fourier techniques. These are explored experimentally, for purpose of contrast with the experimental results already obtained for wavelet compression, in Section 5.

It is perhaps useful to make a few remarks about sampling rates for analog waveforms for input to the discrete wavelet transform. The correct sampling rate does, of course, depend on the choice of wavelet, but how? It is possible to give a preliminary evaluation that is relatively satisfactory. We begin by inquiring what would have happened if we had sampled at twice the selected rate. Would we have found that the doubling led to a data stream with very little first-order detail structure, so that its smooth part was essentially the original stream? The easiest way to answer this question is to find the doubled data stream with no first-order detail structure.

Let a_v be the original data stream "corresponding" to a wavelet expansion in V_0: $f(x) = \sum a_v \phi(x - v)$. Since $\phi(x - v) = \sum c_k \phi(2x - 2v - k)$, we have, in V_1, $f(x) = \sum d_\ell \phi(2x - \ell)$, where $d_\ell = \sum_v a_v c_{\ell - 2v}$. The d_ℓ stream is the one that projects to the a_v stream with no fine structure (the scalings are correct). So we must compare the d_ℓ stream with the analog signal sampled

at twice the chosen rate to compute a squared deviation. This need not be carried all the way through, only partly into the d stream.

It is interesting to note that if we were choosing Haar wavelets and the original stream were $a_1, a_2, a_3, \ldots$ etc., the d stream would be $a_1, a_1, a_2, a_2, a_3, a_3, \ldots$ etc.

2.6 Wavelets and Partial Differential Equations

A good start has been made on adapting some of the familiar pseudo-spectral and Galerkin methods to wavelet expansions . AWARE Corporation is very active in this area, and their preliminary work suggests better stability properties in the presence of shock fronts — such as in Burger's Equation.

Yet the methods described to date hardly use the multiresolution features of wavelet analysis. They tend to stick to a single resolution and do no refining to get the smooth and detail parts — this will probably come later.

Some more detailed comments are the subject of Section 8.

2.7 Symmetric Wavelets

It is known that a symmetric wavelet, with exception of Haar wavelets, cannot be compactly supported. But by enlarging the affine group to include reflection (the improper affine group), it is possible by mimicry of the analysis of Mallat and Daubechies to get compactly supported symmetric wavelets. These may lead to very useful filters for signal processing. Readers will find the theory and construction described in Section 7.

2.8 Wavelets and Physics

We have prepared a wavelet primer, written by a physicist, for physicists. It is the subject of Section 3.

2.9 Wavelets and Speech Processing — Adaptive Wavelets

By their very nature, and by the nature of their perception by the ear, speech signals lend themselves to a wavelet analysis. The group at Yale, however, has gone well beyond a simple wavelet analysis. They have constructed a whole family of wavelets, called a wavelet packet for easy use by computer, and use an entropy measure to decide, on the fly, which of the wavelet expansions in the packet to use. Using lab quality speech, they can apparently, achieve compressions of 10^{-1} and get acceptable quality.

The idea of adaptively using wavelets is currently under investigation at MITRE also. Their goal is by parameterizing the space of wavelets, to move continuously in order to find the "best" wavelet for certain feature extraction problems.

2.10 Wavelets and Image Processing

Wavelets lend themselves to image processing as naturally as they do to speech. A comment on some of the research done will be found in Section 9.

We want to note additionally that for the purpose of edge detection in images, or sudden onset in signals, some researchers have returned to continuous affine transforms: $F(\sigma, \tau) = \sqrt{\sigma} \int_{-\infty}^{\infty} f(x) g(\sigma x - \tau) dx$.

With the choice of an analyzing function g as a derivative of the Gaussian, an integration by parts shows that $F(\sigma, \tau)$ is quite sensitive to the appearance of jumps (discontinuities) in f.

The results of several experiments on image compression are found in Section 4.

2.11 Wavelets and $1/f$ Processes

Classically, one models stationary processes as sums, with stochastic coefficients, of pure sinusoids. The theory never produces the $1/f$ spectrum,

which is ubiquitous.

Wornell and Oppenheim show, however, that with appropriately chosen stochastic coefficients, wavelet expansions can be adjusted to have, at least formally, spectra such as $1/f$, and even $\frac{1}{f^\lambda}$, for other values of λ. It is the self similarity of the functions in the wavelet basis that plays the crucial role here.

2.12 Wavelets and Fast Linear Algebra

This may very well turn out to be the most important consequence of wavelet theory, although it is now just a side issue. If one regards a matrix as an image, then the matrix may go sparse (as does an image itself) in a wavelet basis. For many matrices that occur in practice (discretization of certain integral operators) the sparse matrix is sparse in a highly structured way, which eases the numerical burden of inverting or multiplying two such matrices together.

Fast matrix multiply would affect all areas of numerical analysis. The description and results of some experiments we made are described in Section 4.

3 A WAVELET PRIMER: INTRODUCTION

The basic idea behind wavelets is to analyze according to scale. In the simplest case they involve decomposing a function in terms of a basis constructed by iterating translations ($W(x) \rightarrow W(x+1)$) and dilations ($W(x) \rightarrow W(2x)$) of a single function $W(x)$. In some cases this wavelet transform of a function can reveal structure that is not evident in other ways of presenting the function. In problems involving compression of speech or images the wavelet transform seems promising because its structure mimics the tendency of the human auditory and visual systems to process information according to scale (e.g., by octaves in the case of auditory information). Thus there is hope that one can manipulate the wavelet transform to keep just that information that is most important to human perception.

Current developments in wavelet theory can be traced back to work on seismic analysis, although similar ideas and techniques occur in a variety of other areas. Examples include scaling and renormalization group ideas in physics and the use of quadrature mirror filters in signal processing. Mathematical developments over the last five years have put wavelets on a more rigorous footing and at the same time have increased their flexibility, thus setting the stage for the current flurry of applications.

Readers should be forewarned that the author of this primer is no expert in wavelets. They should also be aware that there already exist introductions to wavelet theory of various degrees of sophistication. The papers by Gross-

mann, Kronland-Martinet, and Morlet, by Meyer, and by Daubechies [1] provide a good introduction to the field, as does the short review by Strang [2]. There is also a book which has just appeared by Meyer [3], one of the leading mathematicians in the field. These reviews tend to be oriented towards mathematicians or towards those acquainted with the ideas of signal processing. The goal in writing this primer is to make these ideas more widely known among physicists, partly in the hope that they might prove useful in problems where scaling plays an important role.

Although it would be inappropriate to make any attempt at a history of wavelets, it may be useful to mention a few highpoints in their development. The first mention of wavelets appeared in an appendix to the thesis of A. Haar. These wavelets had compact support but were not continuous. The wavelet transform was proposed in the context of seismic analysis by A. Grossmann and J. Morlet [4]. Inspired in part by these results, Y. Meyer then constructed the first non-trivial wavelets [5]. Unlike the Haar wavelets, they are continuously differentiable. Also unlike the Haar wavelets, they do not have compact support, but rather fall off at infinity faster than the inverse of any polynomial. Wavelets with exponential decay were subsequently constructed by Lemarié and Battle [6]. The wavelets of Daubechies [7] are perhaps the most elegant from a mathematical point of view. She constructed an infinite family of wavelets W_n^D having compact support of order n and having roughly $n/2$ continuous derivatives. All of these constructions were understood within a general framework called multi-resolution analysis developed by S. Mallat [8] and Y. Meyer. Both the theory and applications of wavelets are undergoing rapid development and it would be impossible to

write a complete treatment of the subject that would not soon be out of date. We hope the material covered here is sufficient to make the current literature on wavelets accessible to the dedicated reader.

3.1 Some Wavelets

Before digging into the theory let us first meet some wavelets. For now a wavelet orthonormal basis for square integrable functions of one variable, ($\mathcal{L}^2(R)$), is a set of functions labeled by two integers, W_{jk}, obtained by rescaling by powers of two and translating by integers a single function $W(x)$ termed the mother function or *analyzing wavelet*,

$$W_{jk} = 2^{j/2} W(2^j x - k), \qquad (3-1)$$

such that the resulting set of functions provides an orthonormal basis for $\mathcal{L}^2(R)$. Clearly for this to work the analyzing wavelet must be chosen with care. With a little thought one may happen across a simple solution known as the Haar wavelet and shown in Figure 3-1.

In equations we can write it suggestively as $W(x) = \phi(2x) - \phi(2x-1)$ where $\phi(x)$ is the box function,

$$\phi(x) = \begin{cases} 1 & 0 < x \leq 1 \\ 0 & \text{otherwise} \end{cases} . \qquad (3-2)$$

The orthonormality of the Haar wavelets $W_{jk}(x)$ is obvious, as is the fact that they provide a basis, at least modulo any mathematical niceties. [1]

[1] Actually, the fact that they provide a basis may seem a bit odd unless a certain mathematical nicety is appreciated. Namely, the W_{jk} all have $\int W_{jk}(x)dx = 0$ so one

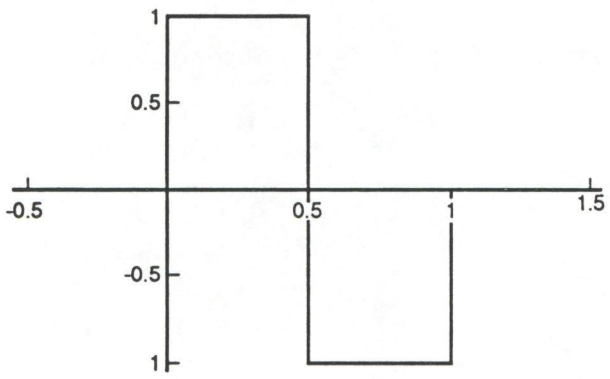

Figure 3-1. The Haar wavelet.

The Haar wavelet shows that analyzing wavelets exist, but it has some obvious faults. In particular, it is not smooth, and this gives rise to problems in applications where one wants to approximate smooth functions. We would like to do better. Smoother analyzing wavelets exist but are not so easy to find, and it will take a while before we understand the details of their construction.

---

might be tempted to think functions with $\int f(x)dx \neq 0$ cannot be expanded in terms of them. This is not true. For example, consider the box function. As far as $\mathcal{L}^2(R)$ is concerned we can replace this with a function defined by taking the limit $\epsilon \to 0$ of a function that is the same as the box function for $x < 1$ and is equal to $-\epsilon$ for $1 < x < 1/\epsilon$ and has a vanishing integral. It is instructive to verify that the expansion of the box function in terms of the W_{jk} is well behaved and relies on the identity $\sum_{i=N}^{\infty} 2^{-i} = 2^{-N+1}$.

$\phi(x)$ normalized so that $\int \phi(x)dx = 1$ and obeying the *scaling equation*

$$\phi(x) = \sum_k c_k \phi(2x - k) \qquad (3-3)$$

where the c_k are a fixed set of coefficients called the *wavelet coefficients.* Assume that only N of the c_k with $k = 0, \cdots, N-1$ are non-zero with N an even integer. Next, impose the following two conditions on the coefficients:

$$\sum_{k=0}^{N-1} c_k = 2, \qquad (3-4)$$

$$\sum_{k=0}^{N-1} c_k c_{k+2l} = 2\delta_{l,0}. \qquad (3-5)$$

The first of these just corresponds to the arbitrary normalization we have chosen for the integral of ϕ, as can be easily checked using the scaling equation. The second is less trivial and is crucial for the orthonormality of the wavelets. Finally, construct the analyzing wavelet as

$$W(x) = \sum_{k=-1}^{N-2} (-1)^k c_{k+1} \phi(2x + k). \qquad (3-6)$$

This analyzing wavelet has compact support in $[1 - N/2, N/2]$ and the set of wavelets $W_{jk}(x)$ provide an orthonormal basis for $\mathcal{L}^2(R)$. This is not obvious. For $N = 2$ the conditions Equations (3–4) and (3–5) give

$$c_0 + c_1 = 2, \qquad c_0^2 + c_1^2 = 2, \qquad (3-7)$$

with the solution $c_0 = c_1 = 1$. The scaling function is just the box function defined above and the corresponding wavelet is the Haar wavelet. So far so good.

The case $N = 4$ is more interesting. We now need to solve the equations

$$c_0 + c_1 + c_2 + c_3 \quad = 2,$$

$$\begin{aligned} c_0^2 + c_1^2 + c_2^2 + c_3^2 &= 2, \\ c_0 c_2 + c_1 c_3 &= 0. \end{aligned} \tag{3-8}$$

Setting

$$x = c_0 + c_1, \qquad y = c_0 - c_1, \tag{3-9}$$

$$w = c_2 + c_3, \qquad z = c_2 - c_3, \tag{3-10}$$

these equations reduce to

$$(y+z)^2 = 0, \qquad x + w = 2, \tag{3-11}$$

and

$$(w-1)^2 + y^2 = 1. \tag{3-12}$$

$$\begin{aligned} c_0 &= (1 - \cos\theta + \sin\theta)/2, \\ c_1 &= (1 - \cos\theta - \sin\theta)/2, \\ c_2 &= (1 + \cos\theta - \sin\theta)/2, \\ c_3 &= (1 + \cos\theta + \sin\theta)/2. \end{aligned} \tag{3-13}$$

As a check we note that for $\theta = \pi/2$ we recover the Haar wavelet.

What do these look like for other values of θ? We might try to impose some natural condition on the wavelet in order to pick out a unique solution. Since the wavelet already satisfies $\int W(x)dx = 0$ as a consequence of $y+z = 0$ it is natural to try to make higher moments vanish as well. In our case we can impose $\int xW(x)dx = 0$, which leads to the additional equation

$$-c_2 + 2c_1 - 3c_0 = 0. \tag{3-14}$$

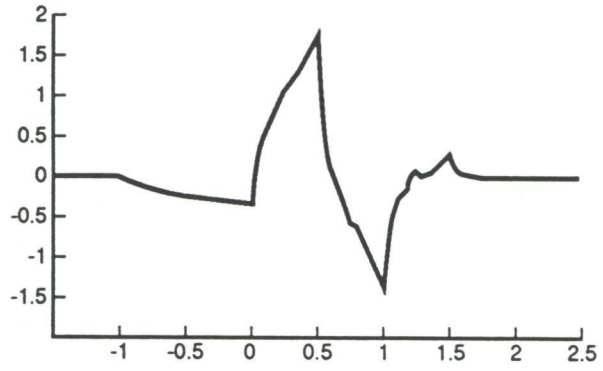

Figure 3-2. Daubechies wavelet W_4 (χ).

The unique solution with this further condition is then

$$c_0 = \frac{1+\sqrt{3}}{4}, \qquad c_1 = \tfrac{3+\sqrt{3}}{4}, \qquad (3\text{-}15)$$
$$c_2 = \frac{3-\sqrt{3}}{4}, \qquad c_3 = \tfrac{1-\sqrt{3}}{4}.$$

The resulting analyzing wavelet is denoted W_4 and was first constructed by Daubechies as the second wavelet in an infinite family starting with the Haar wavelet (W_2) and having an increasing number of vanishing moments. W_4 is shown in Figure 3-2.

The scaling function $\phi(x)$ that corresponds to $W_4(x)$ is shown in Figure 3-3 (the scaling function related to $W_n(x)$ is often called $D_n(x)$).

It may not be clear how Figures 3-2 and 3-3 were produced, since so far we have discussed only the scaling equation and not its solution. However,

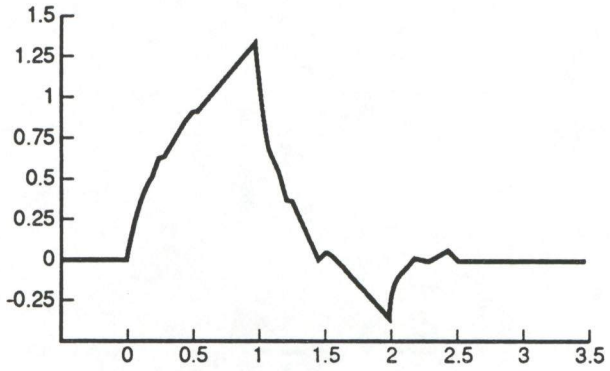

Figure 3-3. Daubechies scaling function D_4 (χ).

the scaling equation itself gives us a recursive procedure for calculating the scaling function and hence the wavelet. Simply start with the box function as a first guess, $\phi_0(x)$, and for the next guess use the scaling equation:

$$\phi_1(x) = \sum_k c_k \phi_0(2x - k). \qquad (3-16)$$

Continuing this procedure quickly gives the scaling function to any desired accuracy. Two useful facts follow immediately from this procedure. The first is that the scaling function ϕ has support in $[0, N-1]$ if the non-zero coefficients are $c_0, \cdots c_{N-1}$. The second is that ϕ is orthogonal to its integer translates. To see this, note that it is obviously true for the box function, and this property is preserved by the recursion using Equation (3-5).

Many of the properties of wavelets are most easily understood in terms

of the discrete Fourier transform of the coefficients c_k:

$$H(\omega) = \frac{1}{2}\sum_k c_k e^{ik\omega}. \qquad (3-17)$$

For example, the Fourier transform of the scaling equation gives

$$\hat{\phi}(2\omega) = H(\omega)\hat{\phi}(\omega) \qquad (3-18)$$

where $\hat{\phi}(\omega)$ is the Fourier transform of $\phi(x)$ and the conditions (Equations (3–4) and (3–5)) become

$$|H(0)| = 1, \qquad (3-19)$$

$$|H(\omega)|^2 + |H(\omega+\pi)|^2 = 1. \qquad (3-20)$$

The further condition (Equation (3–14)) that ensures the vanishing of the first two moments of $W(x)$ is, in the Fourier domain, the statement that $H(\omega)$ has a zero of order two at $\omega = \pi$.

Note also that $H(0) = 1$ as a consequence of Equation (3–4) so that iterating Equation (3–18) gives

$$\hat{\phi}(\omega) = \prod_{i=1}^{\infty} H\left(\frac{\omega}{2^i}\right) \qquad (3-21)$$

and we can thus calculate the Fourier transform of the scaling function directly in terms of $H(\omega)$.

We can construct wavelets with other desired properties by imposing conditions on $H(\omega)$ whether or not they lead to wavelets with compact support. For example, the wavelet of Lemarié and Battle [6] corresponds to putting conditions on the spline approximation of the wavelet transform. The resulting $H(\omega)$ is given by

$$H(\omega) = \sqrt{\frac{\Sigma_8(\omega)}{2^8\Sigma_8(2\omega)}} \qquad (3-22)$$

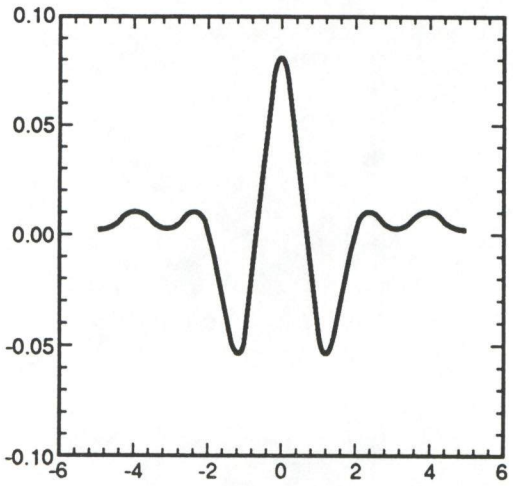

Figure 3-4. Wavelet of Lemarié and Battle.

where

$$\Sigma_8(\omega) = \sum_{k=-\infty}^{\infty} \frac{1}{(\omega + 2\pi k)^8}. \qquad (3-23)$$

The resulting analyzing wavelet is shown in Figure 3-4.

Note that in return for giving up compact support we have gained a smoother wavelet. This is a general theme in wavelet theory: larger support means smoother wavelets. On the other hand, while this wavelet does not have compact support, it does have exponential fall off. From a practical point this may be all one really needs.

Having met some wavelets the reader undoubtedly has many questions. The description of wavelets seems rather roundabout and the wavelets themselves have a rather strange fractal appearance. Why is this so? Why do the above constructions work? What other wavelets exist? Is it necessary to

scale by powers of two or will other multiples work as well? Can wavelets be extended to higher dimensions? Can wavelet theory be put in a more general mathematical context? Since wavelets form an orthonormal basis, are they eigenfunctions of some differential operator or perhaps some more general class of operators? And finally, what are they good for?

Wavelets based on rescalings by powers other than two do exist, but the theory is less well developed and so will not be discussed in this primer. In addition, scaling by powers of two is particularly well adapted to computer implementation of the discrete wavelet transform. Higher-dimensional versions of wavelets do exist and may be useful in image compression. The simplest examples are tensor products of one-dimensional wavelets. Other less trivial examples exist, but again the theory is not yet fully developed. Whether wavelets are related to some type of operator in a natural way seems to be a deep open question. Many physical applications of the Fourier transform are based on the fact that it diagonalizes derivative operators. With the wavelet transform this is no longer true, and there do not seem to be any natural operators that are diagonalized by the wavelet transform. However, many interesting operators may become "almost" diagonal, meaning that their matrix elements have fast decay away from the diagonal. For numerical purposes this may be sufficient to make the wavelet transform a useful tool in the solution of partial differential equations.

The next section will discuss a more general mathematical context for wavelets involving the theory of coherent states. We will discuss continuous Gabor and wavelet transforms and then discuss their discrete versions. The

third section will explain why the above construction works and describe how larger classes of wavelets can be constructed. This involves the concept of a multi-resolution analysis introduced by Mallat and Meyer and is closely related to the concept of quadrature mirror filters in signal processing. The final section will attempt to give some flavor for the possible applications of wavelets.

3.2 Coherent States

In this section we will be concerned with coherent states for two groups, the Weyl-Heisenberg (WH) group and the affine group. Coherent states for the WH group are the familiar coherent states associated with the quantum-mechanical simple harmonic oscillator. They appear in signal processing in connection with the Gabor transform and also play an important role in the design of radar signals. Affine coherent states are perhaps less familiar. They underlie the theory of wavelets; the theory of the continuous wavelet transform (based on continuous rescaling and translation) is basically the theory of affine coherent states. Both the continuous WH coherent states and the continuous affine coherent states provide an overcomplete basis for $\mathcal{L}^2(R)$. A fundamental difference appears when we try to obtain an orthonormal basis by choosing a discrete subset of these coherent states. In the WH case there are strong constraints on one's ability to do this, and the theory becomes rather unpleasant. In contrast, the affine case leads to an elegant theory: the discrete wavelets discussed in the introduction.

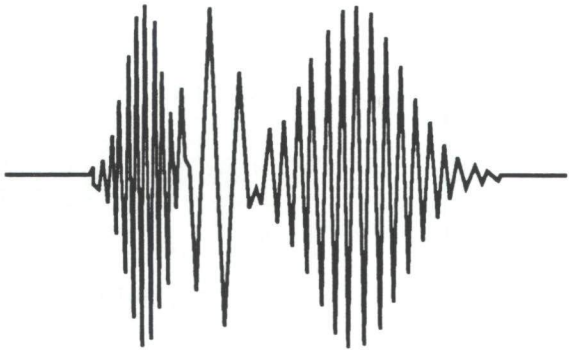

Figure 3-5. A signal with both frequency and time localization.

To motivate the rest of this section we start by describing two common problems in signal processing. Suppose we have a signal $f(t)$, which has components that are localized both in frequency and in time. As a simple example the signal in Figure 3-5 consists of three different frequencies, each within an envelope that localizes the time at which the frequency occurs. Straightforward Fourier analysis of such a signal will of course give peaks at these frequencies but with non-zero width and additional structure needed to accommodate the overlap regions. In other words, the Fourier transform is not much simpler than the original signal despite the relative simplicity of the signal. A more effective approach would be to try to carry out Fourier analysis that is local in time by Fourier analyzing only within some "window." For example, we might choose a function $g(t)$ that has support only in some

finite window and compute a windowed Fourier transform of the signal as

$$\hat{f}(\omega,\tau) = \int_{-\infty}^{+\infty} e^{i\omega t} f(t) g(t-\tau) dt \qquad (3-24)$$

where τ labels the location of the window. A suitable choice for $g(t)$ that has good localization in both the time and frequency domains would be $g(t) = e^{-t^2/2}$. The idea here is to calculate the overlap of the signal with translated and frequency shifted versions of the basic window function $g(t)$. A careful study of such transforms, studied in the context of radar by Gabor [10], leads to the theory of WH coherent states.

An alternate method of localizing a signal in both frequency and time is given by the continuous wavelet transform. In this case we compute the overlap of the signal with dilated and translated versions of some window $g(t)$: [2]

$$\check{f}(a,b) = \int_{-\infty}^{+\infty} f(t) a^{1/2} g(\frac{t-b}{a}) dt. \qquad (3-25)$$

Again a good choice for g will have good localization in both time and frequency. In this case the mathematical formalism is that of affine coherent states.

A second problem in signal processing where the WH and affine groups play an important role is the design of radar or sonar signals. A classic problem in radar (or sonar) is to identify the velocity and range of a target in the presence of noise. One wishes to design the outgoing radar signal in order to minimize the uncertainty in whatever combination of range and velocity is appropriate to the problem at hand (for example, in police radars the accuracy in velocity is crucial, while the accuracy in range is immaterial).

[2] This notation for the wavelet transform is not standard.

The basic tool utilized in the design of radars is the radar ambiguity function, first introduced for narrow-band signals by Woodward and closely related to the Wigner-Ville distribution and the theory of WH coherent states.

Let $s(t)$ be the outgoing signal, propagating with velocity c. A target at range R moving with radial velocity component v will cause an echo $r(t)$ given, in the absence of noise, by

$$r(t) = As(at + \tau) \qquad (3-26)$$

where A represents the reduction in energy of the echo,

$$a = \frac{c - v}{c + v} \qquad (3-27)$$

gives the Doppler shift of the signal, and

$$\tau = \frac{2R}{c + v} \qquad (3-28)$$

is the signal time delay at time $t = 0$. It is convenient to normalize the signals to have unit energy

$$\int_{-\infty}^{+\infty} |s(t)|^2 dt = 1. \qquad (3-29)$$

With this convention we write the received signal as

$$r(t) = \frac{1}{\sqrt{a}} s(at + \tau). \qquad (3-30)$$

We thus see that the effect of the Doppler shift is to give a dilated and translated version of the original signal. So far this is for general (broad-band) signals. In radar one often deals with narrow-band signals. For a narrow-band signal centered at frequency f,we have

$$s(at + \tau) \sim e^{2\pi i \delta f t} s(t + \tau) \qquad (3-31)$$

where $\delta f = f(a-1)$. So for narrow-band signals the effect of the Doppler shift is to give a translated and frequency shifted version of the original signal. In both of these examples it is clear that there is an underlying group structure. In the Gabor transform and narrow-band radar signals the underlying group is the WH group. The action of this group on functions is given by

$$U_{WH}(0,\omega,\tau)g(t) = e^{i\omega t}g(t-\tau) \qquad (3-32)$$

where U_{WH} is a representation of the WH group that acts on square integrable functions as

$$U_{WH}(z,\omega,\tau)g(t) = ze^{i\omega\tau}e^{i\omega t}g(t-\tau) \qquad (3-33)$$

with $|z| = 1$ and obeys the composition law

$$U_{WH}(z_1,\omega_1,\tau_1)U_{WH}(z_2,\omega_2,\tau_2) = U_{WH}(e^{i(\omega_1\tau_2-\omega_2\tau_1)}z_1z_2,\omega_1+\omega_2,\tau_1+\tau_2). \qquad (3-34)$$

The phase part of U_{WH} (i.e., multiplication by z) is needed only to have a simple group structure and is immaterial in what follows. For the wavelet transform and the analysis of broad-band signals the underlying group is the affine group, which acts on $f \in \mathcal{L}^2(R)$ as

$$U_A(a,b)f(t) = f(\frac{t-b}{a}) \qquad (3-35)$$

where $U_A(a,b)$ gives a representation of the affine, or $ax+b$, group and obeys the composition law

$$U_A(a_1,b_1)U_A(a_2,b_2) = U_A(a_1a_2, a_2b_1+b_2). \qquad (3-36)$$

After this motivation we now turn to a description of the coherent states for these two groups. Let us start with the more familiar case of WH coherent states. In quantum mechanics these states occur as follows.

Start with the Hamiltonian for a harmonic oscillator in one dimension

$$H = \frac{P^2}{2m} + \frac{m\omega^2 Q^2}{2}, \qquad (3-37)$$

with Q and P the position and momentum operators satisfying the canonical commutation relation $[P, Q] = -i\hbar$. To simplify the analysis set $\hbar = m = \omega = 1$ henceforth. The standard method for studying the spectrum of H is to introduce creation and annihilation operators

$$a = \frac{1}{\sqrt{2}}(Q + iP), \qquad a^\dagger = \frac{1}{\sqrt{2}}(Q - iP), \qquad (3-38)$$

obeying the commutation relations

$$[a, a] = [a^\dagger, a^\dagger] = 0, \qquad [a, a^\dagger] = 1, \qquad (3-39)$$

with H then written as

$$H = (N + 1/2) \qquad (3-40)$$

with $N = a^\dagger a$ the number operator. The eigenstates of H with eigenvalue $(n + 1/2)$ are then given by

$$|n\rangle = \frac{1}{(n!)^{1/2}}(a^\dagger)^n |0\rangle \qquad (3-41)$$

with $|0\rangle$ the ground state satisfying $a|0\rangle = 0$. In a coordinate basis with Q acting as multiplication by q and P as $-id/dq$, the ground state is given by

$$\psi_0(q) = \langle q|0\rangle = e^{-q^2/2}. \qquad (3-42)$$

The set of eigenstates $|n\rangle$ form a basis for the Hilbert space of square integrable wave functions, $\mathcal{H} = \mathcal{L}^\epsilon(\mathcal{R})$; thus any function in $\mathcal{H}$ can be expanded as

$$f = \sum_n f_n |n\rangle \qquad (3-43)$$

with $f_n = \langle f|n\rangle$ and the projection operator

$$\sum_n |n\rangle\langle n| = 1 \qquad (3-44)$$

with 1 the identity operator.

One way of introducing coherent states is as eigenstates of the annihilation operators. Thus consider the coherent state

$$|z\rangle = e^{za-z^*a^\dagger}|0\rangle = e^{-\frac{1}{2}|z|^2}e^{za^\dagger}|0\rangle \qquad (3-45)$$

with z a complex number. This state obeys $a|z\rangle = z|z\rangle$, which is most easily checked using the representation $a = d/da^\dagger$.

From a practical point of view, these coherent states are useful in the discussion of the classical limit of quantum mechanics. The reason is that these coherent states are minimum uncertainty states that saturate the uncertainty relation

$$\Delta P \Delta Q \geq \frac{1}{2}, \qquad (3-46)$$

and furthermore the time evolution of these states corresponds to the classical equation of motion for a harmonic oscillator. These states are thus as classical as a quantum mechanical state can get.

The coherent states $|z\rangle$ do not, however, provide an orthonormal basis for $\mathcal{H}$. It is easy to see that coherent states corresponding to different values of z are not orthogonal. In particular

$$\langle z_2|z_1\rangle = e^{\frac{1}{2}|z_2|^2-\frac{1}{2}|z_1|^2+z_2^*z_1}. \qquad (3-47)$$

They also form an overcomplete set, since using Equation (3–24) we have

$$\int d^2z|z\rangle\langle z| = \pi 1. \qquad (3-48)$$

More generally the above equation says that the coherent states give a resolution of the identity that allows us to reconstruct a function in terms of its overlap with the coherent states $|z\rangle$

$$f = \frac{1}{\pi}\int d^2 z \langle f|z\rangle\langle z|. \qquad (3-49)$$

A group theoretical point of view is also useful. We introduce the Weyl operator

$$U(p,q) = e^{i(pQ-qP)}, \qquad (3-50)$$

which acts as a translation operator for Q and P in the sense that

$$U^\dagger(p,q)QU(p,q) = Q + q\,. \qquad (3-51)$$

These operators obey the composition law

$$U(p_2,q_2)U(p_1,q_1) = e^{i(q_1p_2-p_1q_2)}U(p_2+p_1, q_2+q_1). \qquad (3-52)$$

Using Equation (3–38) we can write

$$U(p,q) = e^{za^\dagger - z^* a} \qquad (3-53)$$

with $z = (q-ip)/\sqrt{2}$, which shows that the coherent states can be written as

$$|z\rangle = |p,q\rangle = U(p,q)|0\rangle. \qquad (3-54)$$

We can thus think of these states as resulting from the action of the Weyl operator $U(p,q)$ on the particular state $|0\rangle$. The set of coherent states $\{|p,q\rangle\}$ for all p,q defines the orbit of the Weyl-Heisenberg group acting on the state $|0\rangle$. In general we can take any square integrable function $g(q)$ and define a set of coherent states as the orbit of g under the action of the WH group:

$$|p,q\rangle_g = U(p,q)g(q). \qquad (3-55)$$

The affine group does not play such a fundamental role in quantum mechanics, but we can define coherent states for this group in a similar way. The general setup is as follows.

We start with a Hilbert space $\mathcal{H}$ (in our case $\mathcal{L}^2(R)$) and an irreducible representation U of a locally compact group $\mathcal{G}$. If $d\mu$ is the left-invariant Haar measure on $\mathcal{G}$ then we say that $g \in \mathcal{H}$ is an admissible vector for U if

$$c_g = ||g||^{-2} \int d\mu(y) |\langle g, U(y)g \rangle|^2 < \infty. \qquad (3-56)$$

Given an admissible vector g we can define coherent states for $\mathcal{G}$ as the orbit of g under the action of $U(y)$. We then have a resolution of the identity given by

$$\int d\mu(y) U(y)|g\rangle\langle g|U(y)^* = c_g 1. \qquad (3-57)$$

For the WH group any $g \in \mathcal{L}^2(R)$ is an admissible vector and the above precision is unnecessary. This is not true for the affine group. In general, if a group is unimodular (that is, it has equal left- and right-invariant measures) then the existence of one admissible vector implies that all vectors in $\mathcal{H}$ are admissible. However, the affine group is not unimodular. With the representation given above, that is

$$U(a,b)f(x) = |a|^{-1/2} f(\frac{x-b}{a}), \qquad (3-58)$$

the left-invariant measure is $dadb/a^2$ while the right-invariant measure is $dadb/|a|$. The admissibility condition for the affine group then reads

$$c_g = 2\pi \int dk |k|^{-1} |\hat{g}(p)|^2 < \infty \qquad (3-59)$$

with $\hat{g}(p)$ the Fourier transform of $g(x)$. Given such a g we then construct affine coherent states as

$$|a,b\rangle_g = U(a,b)g \qquad (3-60)$$

and we have a resolution of the identity given as

$$\int a^{-2} da db |a,b\rangle_{gg}\langle a,b| = c_g 1. \qquad (3-61)$$

Since the coherent states for both the WH and affine groups give an overcomplete set, it is natural to ask whether some discrete subset of the coherent states could form a basis. For the WH group a natural discretization consists of dividing phase space up into a lattice of points of the form (mp_0, nq_0) with m, n integer. It is known that the set of functions

$$|mp_0, nq_0; 0\rangle \equiv U(mp_0, nq_0)|0\rangle \qquad (3-62)$$

is not even dense in $\mathcal{H}$ unless $p_o q_o \leq 2\pi$ [11]. At the critical density $p_0 q_0 = 2\pi$ the resulting lattice is called a von Neumann lattice. Unfortunately, it is possible to show that this set of functions is *not* a basis for H. In fact, even more is true. A set of functions need not form a basis in order to be a useful tool for analyzing elements of H. If we have a set of functions $\{g_i\}$ that is dense in $\mathcal{H}$ all we really need is to be able to extract an arbitrary element f of $\mathcal{H}$ from its expansion in terms of the g_is. That is, given the set of overlaps $\langle g_i|f\rangle$ we must be able to reconstruct f. This will be the case as long as the projection operator

$$P = \sum_i |g_i\rangle\langle g_i| \qquad (3-63)$$

can be inverted or, equivalently, its spectrum is bounded away from zero. From a calculational point of view it can still be difficult to carry out the

inversion of P. These problems do not arise if one has what is called a tight frame for which P is a multiple of the identity operator $P = c1$ with c a constant.

Thus we could ask whether the set of coherent states $|mp_0, nq_0; 0\rangle$ at least gives a frame or a tight frame for H. The answer again is no, and one method of proof is to show explicitly that the spectrum of the corresponding projection operator includes zero [12].

In order to construct a frame, tight frame, or basis out of a discrete set of coherent states it is necessary either to relax the restriction that $p_0 q_0 = 2\pi$ and consider higher densities in phase space or to consider the action of $U(p, q)$ on functions other than the harmonic oscillator ground state $0\rangle$. The possibilities are limited by a theorem due to Balian and Low [13]. This theorem states that with $p_0 q_0 = 2\pi$ the set of coherent states given by the action of $U(mp_0, nq_0)$ on a function $f(x) \in \mathcal{L}^2(R)$ can be a frame only if either the expectation value of P^2 or the expectation value of Q^2 diverges, i.e., the state corresponding to f has infinite uncertainty in the sense that $\Delta P \Delta Q = \infty$.

If we consider the action of U on $\psi_0(q)$ but use a higher density of points in phase space then it is possible to construct a frame. For example, if we choose the density so that $p_0 q_0 = \pi$ then the resulting set of coherent states forms a frame but not a tight frame. From a computational point of view, tight frames have a great advantage. In order to construct tight frames it is necessary to consider more general functions for U to act on, and by the Balian-Low theorem these functions must have slow fall-off in either

the spatial or Fourier domain. Although the discrete sets of WH coherent states and the corresponding discrete Gabor transform can still be useful in practical applications, it is disappointing to be unable to construct an orthonormal basis with good localization in both time and frequency, and in fact before the advent of wavelets no such orthonormal basis for $\mathcal{L}^2(R)$ was known.

In order to define a discrete version of the affine or wavelet transform we need to choose an appropriate discretization of the parameter space (a, b) and an appropriate admissible vector g for the corresponding discrete affine group elements to act on. We can identify the parameter space for the affine group with the upper half plane

$$H = (a, b); \qquad a, b \in R, \qquad a \geq 0,$$

with the hyperbolic metric given by the left-invariant Haar measure for the affine group. We now have to decide how to choose a discrete set of points in this space. It is natural to think that the hyperbolic geometry should play a central role in the choice of discretization. Two natural choices of discretization that come to mind are to take a point and its orbit under a discrete subgroup of $SL(2, R)$, for example $SL(2, Z)$, or to take a discrete set of points so that the corresponding affine group elements are a discrete subgroup of the affine group. In fact neither of these corresponds to what is actually used. The standard discretization used in the literature is to take a lattice with

$$a_n = a_0^n, \qquad b_{mn} = m b_0 a_0^n$$

with a_0 and b_0 some fixed numbers. Note that with the hyperbolic metric

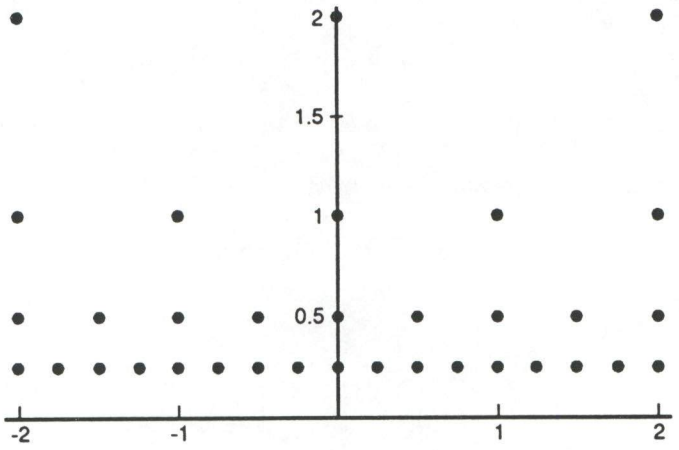

Figure 3-6. Lattice of affine group elements.

the cells in this lattice all have equal area. The simplest choice is given by $a_0 = 2$ and $b_0 = 1$. Part of the corresponding lattice is shown in Figure 3-6.

One can show that a frame can be constructed for *any* $a_0 > 0$ and $b_0 > 0$. Even if b_0 is fixed to equal 1, there is still no sharp value for a_0 that divides frames from non-frames. For details see [14]. Although the theory of the discretization of the parameter space in its present state (or at least the author's understanding of it) is somewhat unsatisfactory, the surprising fact is that there do exist discretizations that yield orthonormal bases for $\mathcal{L}^2(R)$ with the function g having good localization in both time and frequency. The construction of these bases is the subject of the following section.

3.3 Multi-Resolution Analysis

We now describe a formalism that allows one to obtain concrete constructions of wavelets. This formalism, known as multi-resolution analysis, is one of those happy examples where a slight amount of mathematical formalism yields a handsome dividend in insight and ease of calculation. A more precise description of what follows, along with proofs, can be found in [8].

We want to formalize the idea of making successively better approximations to a function based on scaling by factors of two. If $f(t)$ is our original function we would like a sequence of approximations $f_i(t)$ with the "resolution" increasing for increasing i. The approximation $f_i(t)$ will live in a subspace V_i of $\mathcal{L}^2(R)$. We would like to obtain the approximation f_i by the application of some linear "smoothing" operator P_i on the original function $f(t)$. We would also like to demand that further application of P_i not change the resolution; thus, P_i should be a projection operator, $P_i P_i f(t) = P_i f(t) = f_i(t)$. Finally, we would like to be able to recover the approximation f_i from any finer approximation f_j with $j < i$, and we would also like to build some translation invariance into the formalism. We thus have the following.

Definition

A multi-resolution analysis of $\mathcal{L}^2(R)$ consists of a sequence of closed subspaces $V_m \subset \mathcal{L}^2(R)$ with

$$\cdots \subset V_{-1} \subset V_0 \subset V_1 \subset V_2 \subset \cdots \qquad (3-64)$$

that satisfies the following conditions:

1. As the resolution becomes infinite we should recover the original function; as the resolution becomes infinitely bad the approximation approaches zero. Symbolically this means

$$\bigcup_{j\in Z} V_j \quad \text{is dense in } \mathcal{L}^2(R), \qquad \bigcap_{j\in Z} V_j = 0. \tag{3-65}$$

2. If $f_i(t)$ belongs to V_i, then $f_i(2t)$ belongs to V_{i+1}.

3. If $f_0(t)$ belongs to V_0 then its integer translates do also, $f_0(t-k) \in V_0$.

4. There exists a function $\phi(t)$ in V_0 such that the set of functions $\phi(t-k)$ is a Riesz basis for V_0.

This last condition just means that any function f in V_0 can be uniquely written as $\sum_k c_k\phi(t-k)$ with $\sum_k |c_k|^2$ finite. The $\phi(t-k)$ are not automatically orthonormal, but if they are not one can construct from them an orthonormal set with the same span. From now on we assume this has been done. The resulting $\phi(t)$ will turn out to be the scaling function mentioned in the introduction. If we define $\phi_{mn}(t) = 2^{-m/2}\phi(2^{-m}t - n)$ then the above suffices to show that the ϕ_{mn} form a basis for V_m. Thus, once we form a basis at a certain fixed resolution V_0, the multi-resolution analysis gives us a basis in terms of iterated scalings and translations of ϕ for all other resolutions. The ϕ_{mn} for fixed m can be assumed to be orthonormal since if they are not, one can always choose new linear combinations that will be orthonormal. However these are not yet wavelets: the ϕ_{mn} for different m are not orthogonal, since the spaces V_m for different m are not orthogonal.

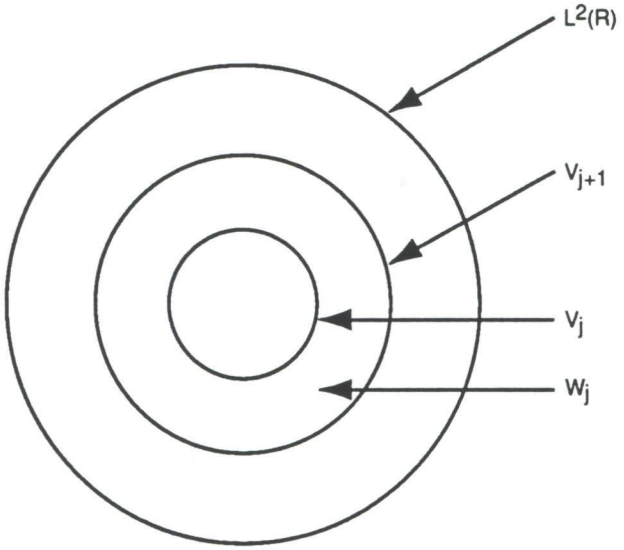

Figure 3-7. Embedding of spaces in multiresolution analysis.

To remedy this and construct wavelets ψ_{mn} that will be orthogonal for different n and m we focus on the orthogonal complements of the V_i. In particular, let W_i by the orthogonal complement of V_i in V_{i+1}. In equations,

$$V_{i+1} = V_i \oplus W_i, \qquad W_i \perp V_i. \tag{3-66}$$

The "bullseye" in Figure 3-7 gives a schematic picture of the multi-resolution analysis and the spaces W_i.

We can project a function $f \in \mathcal{L}^2(R)$ into W_i by the projection operator $Q_i = P_{i+1} - P_i$. Now something very pretty happens. The W_i are related by scaling as were the V_i. Namely, if $f(t) \in W_i$ then $f(2t) \in W_{i+1}$. Thus the W_i are related by scaling to W_0 just as the V_i were related to V_0. Furthermore, just as the integer translates of ϕ provided a basis for V_0, there is a function ψ, which is the wavelet we are after, whose integer translates provide a basis

for W_0. Thus the ψ_{mn} for fixed m are a basis for W_m, but since the spaces W_m are orthogonal for different m and sum to $\mathcal{L}^2(R)$,

$$\mathcal{L}^2(R) = \oplus_{m\in Z} W_m, \tag{3-67}$$

the ψ_{mn} for different m are also orthogonal!

The remaining problem is actually to construct the functions ϕ and ψ whose integer translates provide a basis for V_0 and W_0 respectively. This is where the scaling equation appears. Since $\phi \in V_0 \subset V_1$ and since the functions $\phi(2t-n)$ form a basis for V_1 we must have

$$\phi(t) = \sum_n c_n \phi(2t-n) \tag{3-68}$$

for some constants c_n. This is just the scaling equation of the introduction. Once such a ϕ is constructed, the wavelet ψ is easily constructed as

$$\psi(t) = \sum_n (-1)^n c_{n+1} \phi(2t+n). \tag{3-69}$$

The basic condition on the coefficients

$$\sum_k c_k c_{k-2m} = 2\delta_{0m} \tag{3-70}$$

just comes from demanding orthogonality of the $\phi(t-n)$.

This discussion has been rather formal. To understand how it all works it may be useful to consider an explicit example. The simplest example is the Haar wavelet, which although trivial in many ways, still contains all the essential features.

To define the multi-resolution analysis associated with the Haar wavelet

we start with the subspaces V_i defined as

$$V_i = \{f \in \mathcal{L}^2(R); \quad \text{f constant on the interval } [2^m n, 2^m(n+1)] \text{ for all } n \in Z\}. \tag{3-71}$$

It should be clear that this satisfies conditions 1–3. The function ϕ we just take to be the box function

$$\phi(x) = \begin{cases} 1, & 0 \leq x < 1 \\ 0, & \text{otherwise} \end{cases}. \tag{3-72}$$

The projection operator P_i just replaces f by its average on each subinterval,

$$P_i f|_{[2^{-i}n, 2^{-i}(n+1)]} = 2^i \int_{2^{-i}n}^{2^{-i}(n+1)} f(t)dt. \tag{3-73}$$

This makes it clear that the projections of f onto the subspaces V_i do correspond to increasing resolution as i increases.

Our final task in this section will be to relate multi-resolution analysis to quadrature mirror filters and finally to a fast algorithm for the actual computation of the wavelet transform of a finite data sample. We start by taking the Fourier transform of the scaling equation. With $\hat{\phi}(\omega) = \int \phi(t)e^{i\omega t}dt$ this reads

$$\hat{\phi}(\omega) = H(\omega/2)\hat{\phi}(\omega/2) \tag{3-74}$$

with

$$H(\omega) = \frac{1}{2}\sum_k c_k e^{ik\omega}. \tag{3-75}$$

Condition 4 of the definition then implies that

$$|H(\omega)|^2 + |H(\omega+\pi)|^2 = 1, \tag{3-76}$$

and condition 1 implies that

$$|H(0)| = 1. \tag{3-77}$$

Now the wavelet ψ whose integer translates provide a basis of W_0 satisfies $\psi(x) \in W_0 \subset V_1$ and therefore its Fourier transform can be written as

$$\hat{\psi}(2\omega) = G(\omega)\hat{\phi}(\omega) \tag{3-78}$$

for some 2π-periodic function $G(\omega)$. Furthermore, since V_0 is the direct sum of V_{-1} and W_{-1}, the Fourier transform of any $f \in V_0$ can be written as

$$\hat{f}(\omega) = a(\omega)\hat{\phi}(\omega) = b(\omega)\hat{\phi}(2\omega) + c(\omega)\hat{\psi}(2\omega), \tag{3-79}$$

which, using Equation (3–77) and Equation (3–81), implies that

$$a(\omega) = b(\omega)H(\omega) + c(\omega)G(\omega). \tag{3-80}$$

In order for this orthogonal decomposition to hold for any $f \in V_0$ and hence for any $a(\omega)$, we must have

$$\begin{aligned} |H(\omega)|^2 + |G(\omega)|^2 &= 1, \\ H(\omega)G^*(\omega) + H(\omega+\pi)G^*(\omega+\pi) &= 0, \end{aligned} \tag{3-81}$$

which is equivalent to the statement that

$$\begin{pmatrix} H(\omega & G(\omega) \\ H(\omega+\pi) & G(\omega+\pi) \end{pmatrix} \tag{3-82}$$

is a unitary matrix. One common choice is to take

$$G(\omega) = e^{-i\omega}H^*(\omega+\pi). \tag{3-83}$$

The pair of functions $H(\omega), G(\omega)$ are known in the signal processing literature as *quadrature mirror filters* and play an important role in the implementation of the discrete wavelet transform.

Suppose we have a function $f(x)$ sampled at discrete points x_n with $f_n \equiv f(x_n)$ and let $f(\omega)$ be the corresponding Fourier series. We wish to

construct two sequences, $\{f_n^l\}$ and $\{f_n^h\}$, each having half as many samples and containing the low and high frequency parts of f respectively. The decomposition Equation (3–82) allows us to do this by convolving f with H (the low-pass filter) and keeping half the elements of the resulting sequence to obtain f^l; and by convolving f with G (the high-pass filter) and again keeping half the elements to obtain f^h. This process can be continued to obtain the full wavelet decomposition of the original sequence $\{f_n\}$.

To be completely concrete, start with the original sequence $\{f_n^0\}$. From this we compute two sequences (calling f^h d for notational simplicity)

$$\begin{aligned} f_k^1 &= \sum_n h(n-2k) f_n^0 \\ d_k^1 &= \sum_n g(n-2k) f_n^0 \end{aligned} \tag{3-84}$$

or symbolically,

$$\begin{aligned} f^1 &= H f^0 \\ d^1 &= G f^0. \end{aligned} \tag{3-85}$$

f^1 represents a smoothed or blurred version of f^0 at the next lowest resolution, while the sequence d^1 contains the difference in information between f^0 and f^1. Continuing this process at the jth level we have

$$\begin{aligned} f^j &= H f^{j-1} \\ d^j &= G f^{j-1}. \end{aligned} \tag{3-86}$$

Suppose that the original sequence contains N samples with N a power of two. We can continue this procedure until only a small number (usually four) of "smoothed" components remain. After j steps we have a decomposition of the original signal into d^1 ($N/2$ entries), d^2 ($N/4$ entries), $\cdots$, d^j ($N/2^j$ entries) and f^j ($N/2^j$ entries) for a total of N entries.

It is just as easy to reconstruct the original signal from its decomposition at some step using the relation

$$f^{j-1} = H^* f^j + G^* d^j. \qquad (3-87)$$

This kind of pyramidal or tree scheme is fast and easy to implement numerically.

The previous discussion shows that the wavelet can be usefully studied in terms of the function $H(\omega)$. Most of the known wavelets were discovered by imposing suitable conditions on H and then solving for the wavelet itself. We have already seen how the simple Haar wavelet provides an example of a multiresolution analysis. For this example we have $H(\omega) = e^{-i\omega/2}cos(\omega/2)$. There are close links between the behavior of $H(\omega)$, the falloff of $\phi(x)$ and its Fourier transform $\hat{\phi}(\omega)$, and the regularity of $\phi(x)$, which can be used to design wavelets with various properties. For a detailed description see [7].

Although the multi-resolution approach provides a flexible framework for constructing wavelets, it does not address the question of how many or what types of wavelets exist. In this regard, wavelets are very different from the usual orthonormal bases such as Fourier series, which are more or less unique given certain defining properties. There seem to be few uniqueness theorems for wavelets. On the other hand, this is also a strength since it opens up the possibility of designing wavelets for particular applications. Some work has been done in this area, but the situation is not yet well understood.

3.4 Applications

Since wavelets provide an orthonormal basis with good localization in both time and frequency, and since they analyze according to scale, it is natural to hope that they will find application in areas where these aspects are particularly important. The areas of most immediate application seem to be those of signal and image compression when "natural" sounds and images are involved. The transmission of HDTV signals and of CD quality digital radio signals will require progress in precisely such areas. Wavelets may also be useful in a variety of other numerical problems such as the solution of partial differential equations. In physics their use has been suggested in the analysis of data from turbulent systems and in the analysis of dynamical systems that exhibit chaotic behavior. They have also been used in proofs in constructive quantum field theory. Other proposed uses include the generation of musical sounds, the analysis of speech, the analysis of seismic signals, the performance of fast linear algebra, and signal recognition. This ignores their possible uses in pure mathematics. Quite likely the most interesting applications of wavelets have yet to be discovered. Given the rapid pace of development, I will briefly summarize some of these areas and provide a few references for those who are interested in pursuing particular areas. Some of these applications are discussed in more detail in subsequent sections of this report.

Signal Processing

Many of the basic ideas behind wavelets have their counterpart in tech-

niques of signal processing. The idea of combining low- and high-pass filters in such a way that the original signal can be reconstructed from its processed version leads to Equation (3–84), which defines a pair of quadrature mirror filters. The utility of the wavelet transform depends of course on the type of signal being analyzed and on the information about the signal that is desired. Speech and natural images are two examples where the signal has structure on many scales and one often wants to compress the signal in a way that preserves the information most important to human perception. In comparing wavelets with existing techniques it is important to remember that the existing techniques have undergone many small improvements to make them more efficient. While wavelet techniques may be more efficient in the long run, they have not yet reached the same level of sophistication.

Speech Compression

Since human speech has both frequency and time localization and structure on many scales, it seems like an ideal subject for the application of wavelet techniques. One particularly interesting advance here is the development of a library of wavelets for use in speech compression. This work and references to some earlier literature can be found in [20].

Image Processing

Wavelets appear promising in the compression and processing of images for a variety of reasons. For example, one may wish to construct an index of images that has only the largest scale structure, something that could be easily accomplished using the wavelet transform. Wavelets have also proved

to be a useful tool in edge detection. Some of the earliest work on the use of wavelets for image processing can be found in the work of Mallat [16]. Work on image enhancement related to wavelets can be found in [18].

Fractal Processes

Many physical systems exhibit structure on many scales and can often be characterized in terms of their fractal or multifractal structure. The wavelet transform provides a natural tool for the visualization of such processes [1]. Examples of such a use of wavelets can be found in [19], where wavelets are used to analyze turbulence through the study of wind-tunnel velocity fields, and in [20], where wavelets are used to characterize the fractal structure of diffusion-limited aggregates, a simple model of pattern formation and growth processes. It seems fair to say that so far wavelets have been more useful in this area as a tool for data analysis than as an analytical tool.

Other Applications

A number of other applications have been suggested for wavelets. In some problems of linear algebra or the solution of partial differential equations the wavelet transform may be of some utility. Although it does not diagonalize standard operators, in certain cases of interest it "almost" diagonalizes them in that the resulting operator has fast falloff away from the diagonal. Much work remains to see if wavelets can compete with well-established techniques in these areas. Other applications include computer generation of sound, where one needs to produce complex sounds with fast algorithms, and seismic analysis, where wavelets first originated. Combes et

al. (1989) has a number of articles discussing various applications of wavelets.

3.5 Discussion

Wavelets are a new and elegant mathematical tool that have found application in a variety of fields. Both the mathematical formalism and its applications are still undergoing rapid development. On the mathematical side, the general framework still seems unclear. Wavelets are a set of discrete coherent states for the affine group, but there does not seem to be a general understanding of precisely what types of wavelets are allowed, or whether there are other groups for which discrete coherent states would have such nice properties. In applications it seems that so far wavelets have led to quantitative but not qualitative changes. They may eventually lead to faster solutions to a variety of signal processing problems, but they have not yet opened up radically new directions. Since wavelets are still in their infancy, this situation may soon change.

REFERENCES

1. *Wavelets, Time-Frequency Methods and Phase Space*, J.M. Combes, A. Grossmann, and Ph. Tchamitchian eds. Springer Verlag (1989).
2. G. Strang, *SIAM Review*, Vol. 31, No. 4 (1989) 614.
3. Meyer, Y., *Ondelettes et Opérateurs*, Hermann, Paris.
4. Grossmann, A., and J. Morlet, *SIAM J. Math.* 15(1984) 723.
5. Meyer, Y., Principe d'incertitude, bases hilbertiennes et algèbres d' opérateurs, Bourbaki Seminar, 1985 no. 662.
6. P. G. Lemarié, Journ. de Math. Pures et Appl. Semi G. Battle, *Comm. Math. Phys.* 110 (1987) 610.
7. I. Daubechies, *Comm. Pure Appl. Math.*, 41 (1988) 909.
8. S. G. Mallat, *Trans. Amer. Math. Soc.*, 315 (1989) 69.
9. Y. Meyer, Ondelettes et fonctions splines, Seminaire EDP, École Polytechnique, Paris, France, December 1986.
10. D. Gabor, Theory of communication, *J. Inst. Electr. Engin.* (London) 93 (III) (1946) 429.
11. V. Bargmann, P. Butera, L. Girardello, and J.R. Klauder, *Rep. Math. Phys.* 2 (1971) 221; A. M. Perelomov, *Teor. Mat. Fiz.* 6 (1971) 213.
12. I. Daubechies, A. Grossmann, and Y. Meyer, J. *Math. Phys.* 27 (1986) 5 and references therein.
13. R. Balian, C.R. Acad. Sci. Paris 292 (1981) 1357; F. Low, Complete sets of wave packets, *A Passion for Physics - Essays in Honor of Geoffrey Chew*, C. DeTar et al. eds., World Scientific, Singapore (1985).
14. I. Daubechies, *The Wavelet Transform, Time-Frequency Localization and Signal Analysis*, (1987).
15. A. Grossman, *Wavelet Transforms and Edge Detection, Stochastic Processes in Physics and Engineering*, (1988) 147.
16. S.G. Mallat, *IEEE*, Vol.37 #12 (1989).
17. L. Rudin and S. Osher, Caltech preprint CS-TR-89-25.
18. F. Argoul, A. Arneodu, G. Grasseau, Y. Gagne, E.J. Hopfinger and U. Frisch, *Nature* 338 (1989) 51.
19. F. Argoul, A. Arneodo, J. Elezgaray, G. Grasseau, and R. Murenzi.
20. R. Coifman, Y. Meyer, and M.V. Wickerhauser, *Signal Compression with Wave Packets*, Yale preprint (1990).

4 THE DISCRETE WAVELET TRANSFORM: A PRIMER

Like the fast Fourier transform (FFT), the discrete wavelet transform (DWT) is a fast, linear operation that operates on a data vector whose length is an integer power of two, transforming it into a numerically different vector of the same length. Also like the FFT, the wavelet transform is invertible and (in fact) orthogonal – the inverse transform, when viewed as a big matrix, is simply the transpose of the transform. Both FFT and DWT, therefore, can be viewed as a rotation in function space, from the input space (or time) domain, where the basis functions are the unit vectors $\mathbf{e}_i$ – Dirac delta functions in the continuum limit–, to a different domain. For the FFT, this new domain has basis functions that are, of course, the familiar sines and cosines. In the wavelet domain, the basis functions are somewhat more complicated and have been given the fanciful names "mother functions" and "wavelets." Below, we will see what these look like.

Of course there is an infinity of possible bases for function space, almost all of them uninteresting! What makes the wavelet basis interesting is that, *unlike* sines and cosines, individual wavelet functions are quite localized in space; simultaneously, *like* sines and cosines, individual wavelet functions are quite localized in frequency or (more precisely) characteristic scale. As we will see below, the particular kind of dual localization achieved by wavelets renders large classes of functions and operators sparse, or sparse to some high accuracy, when transformed into the wavelet domain. Analogously to

the Fourier domain, where a class of computations, such as convolutions, become computationally fast, there is a large class of computations — those which can take advantage of sparsity — that become computationally fast in the wavelet domain.

Unlike sines and cosines, which define a unique Fourier transform, there is not one single unique set of wavelets; in fact, there are infinitely many possible sets. Roughly, the different sets of wavelets make different trade-offs between how they are localized in space and how smooth they are. (There are also further fine distinctions.) In this section we will principally consider two sets of wavelets, which are at nearly opposite poles of this trade-off. The so-called "Daubechies-4", D_4, or DAUB4 wavelets are about as compact in space as wavelets can be; by contrast, the "Lemarié cubic spline wavelets" are about as smooth as wavelets can usefully be. (Much of the original mathematics, and literature, on wavelets is French. The Lemarié wavelets is so smooth as to have been called "la reine des ondelettes" – the queen of wavelets.)

To get more specific, we need to introduce some further machinery. A particular set of wavelets is determined by a particular set of numbers, called *wavelet filter coefficients*. In the case of DAUB4, there are only four coefficients, $c_0, \ldots, c_3$. For the moment we specialize to this case for ease of notation.

4.1 Daubechies Wavelet Filter Coefficients

Consider the following transformation matrix acting on a column vector of data to its right:

$$\begin{bmatrix} c_0 & c_1 & c_2 & c_3 & & & & & & & & \\ c_3 & -c_2 & c_1 & -c_0 & & & & & & & & \\ & & c_0 & c_1 & c_2 & c_3 & & & & & & \\ & & c_3 & -c_2 & c_1 & -c_0 & & & & & & \\ \vdots & \vdots & & & & & \ddots & & & & & \\ & & & & & & & c_0 & c_1 & c_2 & c_3 & \\ & & & & & & & c_3 & -c_2 & c_1 & -c_0 & \\ c_2 & c_3 & & & & & & & & c_0 & c_1 & \\ c_1 & -c_0 & & & & & & & & c_3 & -c_2 & \end{bmatrix} \tag{4-1}$$

Here blank entries signify zeroes. Note the structure of this matrix. The first row generates one component of the data convolved with the filter coefficients $c_0, \ldots, c_3$. So do the third, fifth, and other odd rows. If the even rows followed this pattern, offset by one, then the matrix would be a circulant, that is, an ordinary convolution that could be done by FFT methods. (Note how the last two rows wrap around like convolutions with periodic boundary conditions.) Instead of convolving with $c_0, \ldots, c_3$, however, the even rows perform a *different* convolution, with coefficients $c_3, -c_2, c_1, -c_0$. The action of the matrix, overall, is thus to perform two related convolutions, then to decimate each of them by half (throw away half the values), and interleave the remaining halves.

It is useful to think of the filter $c_0, \ldots, c_3$ as being a smoothing filter, call it H, something like a moving average of four points, even though the cs are

not all positive. Then, because of the minus signs, the filter $c_3, -c_2, c_1, -c_0$, call it G, is *not* a smoothing filter. (In signal processing contexts, H and G are called *quadrature mirror filters.*) In fact, the cs are chosen so as to make G yield, insofar as possible, a *zero* response to a sufficiently smooth data vector. This is done by requiring the sequence $c_3, -c_2, c_1, -c_0$ to have a certain number of vanishing moments. When this is the case for p moments (starting with the zeroth), a set of wavelets is said to satisfy an "approximation condition of order p." This results in the output of H, decimated by half, accurately representing the data's "smooth" information. The output of G, also decimated, is referred to as the data's "detail" information.

For such a characterization to be useful, it must be possible to reconstruct the original data vector of length N from its $N/2$ smooth or s-components and its $N/2$ detail or d-components. That is effected by requiring the matrix (4–1) to be orthogonal, so that its inverse is just the transposed matrix

$$\begin{bmatrix}
c_0 & c_3 & & & \cdots & & & & & c_2 & c_1 \\
c_1 & -c_2 & & & \cdots & & & & & c_3 & -c_0 \\
c_2 & c_1 & c_0 & c_3 & & & & & & & \\
c_3 & -c_0 & c_1 & -c_2 & & & & & & & \\
 & & & & \ddots & & & & & & \\
 & & & & & c_2 & c_1 & c_0 & c_3 & & \\
 & & & & & c_3 & -c_0 & c_1 & -c_2 & & \\
 & & & & & & & c_2 & c_1 & c_0 & c_3 \\
 & & & & & & & c_3 & -c_0 & c_1 & -c_2
\end{bmatrix} \qquad (4-2)$$

One sees immediately that matrix Equation (4–2) is inverse to matrix

Equation (4–1) if and only if these two equations hold,

$$\begin{aligned} c_0^2 + c_1^2 + c_2^2 + c_3^2 &= 1 \\ c_2 c_0 + c_3 c_1 &= 0. \ ^{1} \end{aligned} \tag{4-3}$$

If additionally we require the approximation condition of order $p = 2$, then two additional relations are required, [1]

$$\begin{aligned} c_3 - c_2 + c_1 - c_0 &= 0 \\ 0c_3 - 1c_2 + 2c_1 - 3c_0 &= 0. \end{aligned} \tag{4-4}$$

Equations (4–3) and (4–4) are four equations for the four unknowns $c_0, \ldots, c_3$, first recognized and solved by Daubechies. The unique solution (up to a left-right reversal) is

$$\begin{array}{llll} c_0 = (1+\sqrt{3})/4\sqrt{2} & c_1 = (3+\sqrt{3})/4\sqrt{2} \\ c_2 = (3-\sqrt{3})/4\sqrt{2} & c_3 = (1-\sqrt{3})/4\sqrt{2}. \end{array} \tag{4-5}$$

In fact, DAUB4 is only the most compact of a sequence of wavelet sets: if we had six coefficients instead of four, there would be three orthogonality requirements in Equation (4–3) (with offsets of zero, two, and four), and we could require the vanishing of $p = 3$ moments in Equation (4–4). In this case, DAUB6, the solution coefficients can also be expressed in closed form,

$$\begin{array}{ll} c_0 = (1+\sqrt{10}+\sqrt{5+2\sqrt{10}})/16\sqrt{2} & c_1 = (5+\sqrt{10}+3\sqrt{5+2\sqrt{10}})/16\sqrt{2} \\ c_2 = (10-2\sqrt{10}+2\sqrt{5+2\sqrt{10}})/16\sqrt{2} & c_3 = (10-2\sqrt{10}-2\sqrt{5+2\sqrt{10}})/16\sqrt{2} \\ c_4 = (5+\sqrt{10}-3\sqrt{5+2\sqrt{10}})/16\sqrt{2} & c_5 = (1+\sqrt{10}-\sqrt{5+2\sqrt{10}})/16\sqrt{2}. \end{array} \tag{4-6}$$

[1] There is a change of of scale here from usage in other parts of this report

For higher p, up to 10, Daubechies (1988) has tabulated the coefficients numerically. The number of coefficients increases by two each time p is increased by one.

4.2 Discrete Wavelet Transform

We have not yet defined the DWT, but we are almost there: the DWT consists of applying a wavelet coefficient matrix such as (4–1) *hierarchically*, first to the full data vector of length N, then to the "smooth" vector of length of $N/2$, then to the "smooth-smooth" vector of length $N/4$, and so on until only a trivial number of "smooth-...-smooth" components (usually four) remain. The procedure is sometimes called a *pyramidal algorithm*, for obvious reasons. The output of the DWT consists of these remaining components and all the "detail" components that were accumulated along the way. A diagram should make the procedure clear:

$$\begin{bmatrix} y_1 \\ y_2 \\ y_3 \\ y_4 \\ y_5 \\ y_6 \\ y_7 \\ y_8 \\ y_9 \\ y_{10} \\ y_{11} \\ y_{12} \\ y_{13} \\ y_{14} \\ y_{15} \\ y_{16} \end{bmatrix} \underset{\longrightarrow}{\text{DAUB}} \begin{bmatrix} s_1 \\ d_1 \\ s_2 \\ d_2 \\ s_3 \\ d_3 \\ s_4 \\ d_4 \\ s_5 \\ d_5 \\ s_6 \\ d_6 \\ s_7 \\ d_7 \\ s_8 \\ d_8 \end{bmatrix} \underset{\longrightarrow}{\text{permute}} \begin{bmatrix} s_1 \\ s_2 \\ s_3 \\ s_4 \\ s_5 \\ s_6 \\ s_7 \\ \underline{s_8} \\ d_1 \\ d_2 \\ d_3 \\ d_4 \\ d_5 \\ d_6 \\ d_7 \\ d_8 \end{bmatrix} \underset{\longrightarrow}{\text{DAUB}} \begin{bmatrix} S_1 \\ D_1 \\ S_2 \\ D_2 \\ S_3 \\ D_3 \\ S_4 \\ \underline{D_4} \\ d_1 \\ d_2 \\ d_3 \\ d_4 \\ d_5 \\ d_6 \\ d_7 \\ d_8 \end{bmatrix} \underset{\longrightarrow}{\text{permute}} \begin{bmatrix} S_1 \\ S_2 \\ S_3 \\ \underline{S_4} \\ D_1 \\ D_2 \\ D_3 \\ \underline{D_4} \\ d_1 \\ d_2 \\ d_3 \\ d_4 \\ d_5 \\ d_6 \\ d_7 \\ d_8 \end{bmatrix} \underset{\longrightarrow}{\text{DAUB}} \begin{bmatrix} \mathcal{S}_1 \\ \underline{\mathcal{S}_2} \\ \mathcal{D}_1 \\ \underline{\mathcal{D}_2} \\ D_1 \\ D_2 \\ D_3 \\ \underline{D_4} \\ d_1 \\ d_2 \\ d_3 \\ d_4 \\ d_5 \\ d_6 \\ d_7 \\ d_8 \end{bmatrix}$$

$$(4-7)$$

If the length of the data vector were a higher power of 2, there would be more stages of applying DAUB4 (or any other wavelet coefficients) and permuting. The endpoint will always be a vector with two Ss and a hierarchy of $\mathcal{D}$s, Ds, ds, etc. Notice that once ds are generated, they simply propagate through to all subsequent stages.

A value d_i of any level is termed a "wavelet coefficient" of the original data vector; the final values $\mathcal{S}_1, \ldots, \mathcal{S}_4$ should strictly be called "mother-function coefficients," although the term "wavelet coefficients" is often used loosely for both ds and final $\mathcal{S}$s. Since the full procedure is a composition of orthogonal linear operations, the whole DWT is itself an orthogonal linear operator.

To invert the DWT, one simply reverses the procedure, starting with

the smallest level of the hierarchy and working (in Equation 4–7) from right to left. The inverse matrix Equation (4–2) is of course used instead of the matrix Equation (4–1).

Here is a routine that performs the pyramidal algorithm (or its inverse if `isign` is negative) on some data vector `a(1..n)` for a given routine `wtstep` that does a single application of the wavelet filter and a permutation:

```
      subroutine wt1 (a,n,isign, wttep)
      real a(n)
      if (n.lt.4) return
      if (isign.ge.0) then
           nn=n
1           if (nn.ge.4) then
                call wtstep(a,nn,isign)
                nn=nn/2
           goto 1
           endif
      else
           nn=4
2           if (nn.le.n) then
                call wtstep(a,nn,isign)
                nn=nn*2
           goto 2
           endif
      endif
      return
      end
```

Here, as a specific instance of `wtstep`, is a routine for the DAUB4 wavelets:

```
      SUBROUTINE daub4(a,n,isign)
      INTEGER n,isign,NMAX
      REAL a(n),C3,C2,C1,C0
      PARAMETER (C3=-0.1294095225512604,C2=0.2241438680420134,
     *     C1=0.8365163037378079,C0=0.4829629131445341,NMAX=1024)
      REAL wksp(NMAX)
      INTEGER nh,nh1,i,j
      if(n.lt.4)return
```

```
nh=n/2
nh1=nh+1
if (isign.ge.0) then
      i=1
      do j=1,n-3,2
           wksp(i)=C0*a(j)+C1*a(j+1)+C2*a(j+2)+C3*a(j+3)
           wksp(i+nh)=C3*a(j)-C2*a(j+1)+C1*a(j+2)-C0*a(j+3)

           i=i+1
      enddo
      wksp(i)=C0*a(n-1)+C1*a(n)+C2*a(1)+C3*a(2)
      wksp(i+nh)=C3*a(n-1)-C2*a(n)+C1*a(1)-C0*a(2)
else
      wksp(1)=C2*a(nh)+C1*a(n)+C0*a(1)+C3*a(nh1)
      wksp(2)=C3*a(nh)-C0*a(n)+C1*a(1)-C2*a(nh1)
      j=3
      do i=1,nh-1
           wksp(j)=C2*a(i)+C1*a(i+nh)+C0*a(i+1)+C3*a(i+nh1)

         wksp(j+1)=C3*a(i)-C0*a(i+nh)+C1*a(i+1)-C2*a(i+nh1)
           j=j+2
      enddo
endif
do i=1,n
      a(i)=wksp(i)
enddo
return
END
```

4.3 Wavelet Filters in the Fourier Domain; Lemarié Wavelets

The Fourier transform of a set of wavelet coefficients c_j is given by

$$H(\omega) = \sum_j c_j e^{ij\omega}. \qquad (4-8)$$

Here H is a function periodic in 2π, and it has the same meaning as before: it is the wavelet filter, now written in the Fourier domain. A very useful fact is that the orthogonality conditions for the cs (e.g., Equation 4–3 above) collapse to two simple relations in the Fourier domain,

$$\frac{1}{2}|H(0)|^2 = 1 \qquad (4-9)$$

$$\frac{1}{2}\left[|H(\omega)|^2 + |H(\omega+\pi)|^2\right] = 1. \qquad (4-10)$$

Likewise the approximation condition of order p (e.g., Equation 4–4 above) has a simple formulation, requiring that $H(\omega)$ have a pth order zero at $\omega = \pi$, or (equivalently)

$$H^{(m)}(\pi) = 0 \qquad m = 0, 1, \ldots, p-1. \qquad (4-11)$$

It is thus relatively straightforward to invent quadrative mirror filter sets in the Fourier domain. You simply invent a function $H(\omega)$ satisfying Equations (4-9) - (4-11). To find the actual C_js applicable to a data (or s-component) vector of length N, and with periodic wrap-around as in matrices (4-7) and (4-2), you invert Equation (4-8) by the discrete Fourier transform

$$C_j = \frac{1}{N}\sum_{k=0}^{N-1} H(\frac{2\pi k}{N})e^{-2\pi ijk/N} = \sum_{v=j+kN} c_v. \qquad (4-12)$$

The quadrature mirror filter G (reversed c_js with alternating signs), incidentally, has the Fourier representation

$$G(\omega) = e^{-i\omega} H^*(\omega + \pi) \qquad (4-13)$$

where the asterisk denotes complex conjugation.

In general the above procedure will *not* produce wavelets with compact support. The Daubechies wavelets, or other wavelets with compact support, are specially chosen so that $H(\omega)$ is a trigonometric polynomial with only a small number of Fourier components, guaranteeing that there will be only a small number of nonzero c_js.

On the other hand, there is often no particular reason to demand compact support. Giving it up in fact allows the ready construction of relatively smoother wavelets (higher values of p). Even without compact support, the convolutions implicit in the matrix Equation (4–1) can be done efficiently by FFT methods.

Lemarié's wavelet ("la reine," recall) has $p = 4$, does not have compact support, and is defined by the choice of $H(\omega)$,

$$H(\omega) = \left[2(1-u)^4 \frac{315 - 420u + 126u^2 - 4u^3}{315 - 420v + 126v^2 - 4v^3} \right]^{1/2} \qquad (4-14)$$

where

$$u \equiv \sin^2 \frac{\omega}{2} \qquad v \equiv \sin^2 \omega. \qquad (4-15)$$

It is beyond our scope to explain where Equation (4–14) comes from. An informal description is that the quadrature mirror filter $G(\omega)$ deriving from Equation (4–14) has the property that it gives identically zero when applied

to any function whose odd-numbered samples are equal to the cubic spline interpolation of its even-numbered samples. Since this class of functions includes many very smooth members, it follows that $H(\omega)$ does a very good job of truly selecting a function's smooth information content. (Below we will see what practical good this does.)

The following routine, which implements one step of the Lemarié wavelet (as another instance of `wtstep` for use by the DWT routine `wt1`), has some rather tricky manipulations of Fourier coefficients. The wavelet filter coefficients c_j are never calculated; rather, their Fourier transform is calculated and stored. Equation (4–13) is used to get the quadrature mirror filter. The real input array is Fourier transformed by use of the standard routine `realft`.

The decimation of the convolution by half is performed without actually throwing away (or unnecessarily computing) any values. One can readily verify that the *even* components of the convolution of two N-vectors a_i and b_i (whose Fourier transforms are denoted A_i and B_i) are obtained by an inverse FFT of length $N/2$ acting on the combination $A_iB_i + A_{i+N/2}B_{i+N/2}$ rather than on the usual product A_iB_i.

As if the routine were not already impenetrable enough, complex arithmetic is written out by real and imaginary components, yielding greater computational efficiency.

```
subroutine lemarie(q,nn,isign)
parameter (NNMAX=2048)
real c(NNMAX/2),q(nn)
double precision wr,wi,wpr,wpi,wtemp,theta
save nnsav,c
```

```
data nnsav /0/
if (nn.lt.4) return
n2=nn/2
if (nnsav.lt.nn) then
      do j=1,n2
           ang=3.141592653589793*(j-1)/float(n2)
           y=cos(ang/2.)**2
           x=1.-y
           v=4.*x*y
        c(j)=sqrt(2.*y**4*(315.+x*(-420.+x*(126+x*(-4.)))))/

*                 (315.+v*(-420.+v*(126+v*(-4.)))))
      enddo
      nnsav=nn
endif
if (isign.lt.0) call shuff(q,nn)
call realft(q,n2,1)
nnn=n2+2
theta=-3.141592653589793d0/dble(n2)
wpr=-2.0d0*dsin(0.5d0*theta)**2
wpi=dsin(theta)
wr=(1.0D0+wpr)/dble(n2)
wi=wpi/dble(n2)
n4=nnsav/4+1
en2=1./float(n2)
zi=2.*q(nnn-1)*c(n4)
q(nnn)=2.*q(nnn)*c(n4)*en2
if (isign.ge.0) then
      zr=q(1)*c(1)
      q(nnn-1)=-q(2)*c(1)*en2
      kinc=nnsav/nn
      k=1+kinc
else
      zr=q(2)*c(1)
      q(nnn-1)=q(1)*c(1)*en2
      kinc=-nnsav/nn
      k=nnsav/2+1+kinc
endif
q(1)=zr*en2
q(2)=zi*en
do j=2,nn/4
      j2=2*j-1
      j3=2*(nnn-j)-1
      k1=nnsav/2+2-k
      zr=q(j2)*c(k)+q(j3)*c(k1)
      zi=q(j2+1)*c(k)-q(j3+1)*c(k1)
      yr=q(j2)*c(k1)-q(j3)*c(k)
      yi=q(j2+1)*c(k1)+q(j3+1)*c(k)
      q(j3)=(yr*sngl(wr)-yi*sngl(wi))
      q(j3+1)=(yr*sngl(wi)+yi*sngl(wr))
      q(j2)=zr*en2
```

```
        q(j2+1)=zi*en2
        wtemp=wr
        wr=wr*wpr-wi*wpi+wr
        wi=wi*wpr+wtemp*wpi+wi
        k=k+kinc
      enddo
      nnn=(3*nn)/2+4
      do j=n2+4,(3*nn)/4,2
        zr=q(j-1)
        zi=q(j)
        q(j-1)=q(nnn-j-1)
        q(j)=q(nnn-j)
        q(nnn-j-1)=zr
        q(nnn-j)=zi
      enddo
      call realft(q,nn/4,-1)
      call realft(q(n2+1),nn/4,-1)
      if (isign.lt.0) call shuff(q,nn)
      return
      end
```

The referenced routine **shuff**, for performing the required reverse permutation without additional workspace, is

```
      SUBROUTINE SHUFF(A,N)
C Perfect shuffle an array N whose size is a power of 2
      DIMENSION A(N)
      L=N/4
1       IF(L.GE.1)THEN
          DO I=0,N-1,4*L
            IL=I+L
            ILL=IL+L
            DO J=1,L
              SWAP=A(J+IL)
              A(J+IL)=A(J+ILL)
              A(J+ILL)=SWAP
            ENDDO
          ENDDO
          L=L/2
      GOTO 1
      ENDIF
      RETURN
      END
```

Figure 4-1 shows the absolute value of the wavelet coefficient filter H in the Fourier domain for both the Lemarié and DAUB4 wavelets. One sees that DAUB4 ($p = 2$) has only a quadratic zero at $\pm\pi$, while Lemarié ($p = 4$) is quartic. The symmetry implied by Equation (4–10) is hinted at, but would become obvious if $|H|^2$ were plotted instead of $|H|$.

4.4 What Do Wavelets Look Like?

We are now in a position to actually see some "wavelets," but they are not really the continuum wavelets of the usual theory. They are for us simply the vectors that are the building blocks of the DWT; i.e., the initial vectors that map down after the DWT to the unit vectors in the coordinate directions, and that are readily produced by applying the inverse DWT to each of the coordinate unit vectors.

The discrete wavelets bear a superficial resemblance to the continuum wavelets and share some important features. After all, for example, $\mathbf{e_5}$ (unit vector with 1 in fifth coordinate) came from an initial vector, roughly speaking, which consisted of the coefficients in the expansion of $2^{-N/2}\psi(\frac{x}{2^N})$ in terms of integral translates of $\phi(x)$, and so is something of same shape. Owing to the end around features of the DWT, the superficial resemblance is further muddied. But for our purposes, these discrete wavelets are the ones that matter, and when we refer in this section to wavelets, we are generally talking about discrete wavelets.

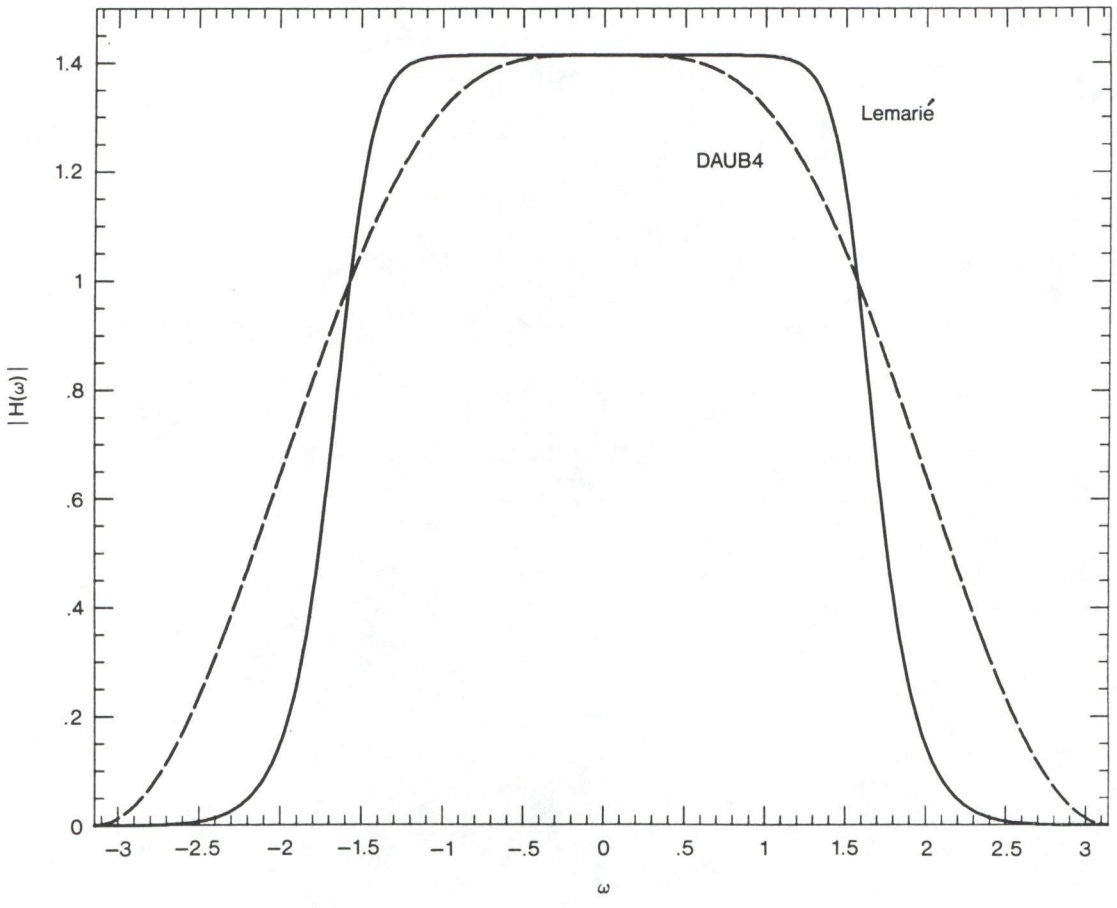

Figure 4-1.

The first wavelets (analogues of mother functions) are derived by running the unit vectors $\mathbf{e_5}$ through $\mathbf{e_8}$ through either of the above discrete wavelet transform, with **isign** negative, so that the inverse transforms is performed. These are wavelets of the largest spatial scale, and are shown in Figure 4-2. The top two panels show DAUB4 wavelets; the bottom two are Lemarie wavelets. The lower panel of each set simply redraws one of the wavelets without the confusion of the other three.

One sees that, for both examples, the individual wavelets are continuous. Lemarié wavelets also have continuous first and second derivatives. DAUB4 has the peculiar property that its derivative exists almost everywhere. Examples of points where the derivative fails to exist are $p/2^n$, with p and n integers; at such points, DAUB4 is left differentiable, but not right differentiable! This kind of discontinuity—at least in some derivative—is a necessary feature of wavelets with compact support, such as the Daubechies series. For every increase in the number of wavelet coefficients by two, the Daubechies wavelets gain about *half* a derivative of continuity. (But not exactly half; the actual orders of regularity are irrational numbers!) By contrast with DAUB4's left-right asymmetry, the Lemarié wavelets are left-right symmetric, as follows from their Fourier transform being real and even.

Wavelets then, especially those with compact support, are quite unlike other common basis functions. Paraphrasing Dorothy in Oz, we aren't in Kansas — or for that matter Fourier — anymore. Note that the fact that wavelets are not smooth does not prevent their having exact representations for some smooth functions, as demanded by their approximation order p. The

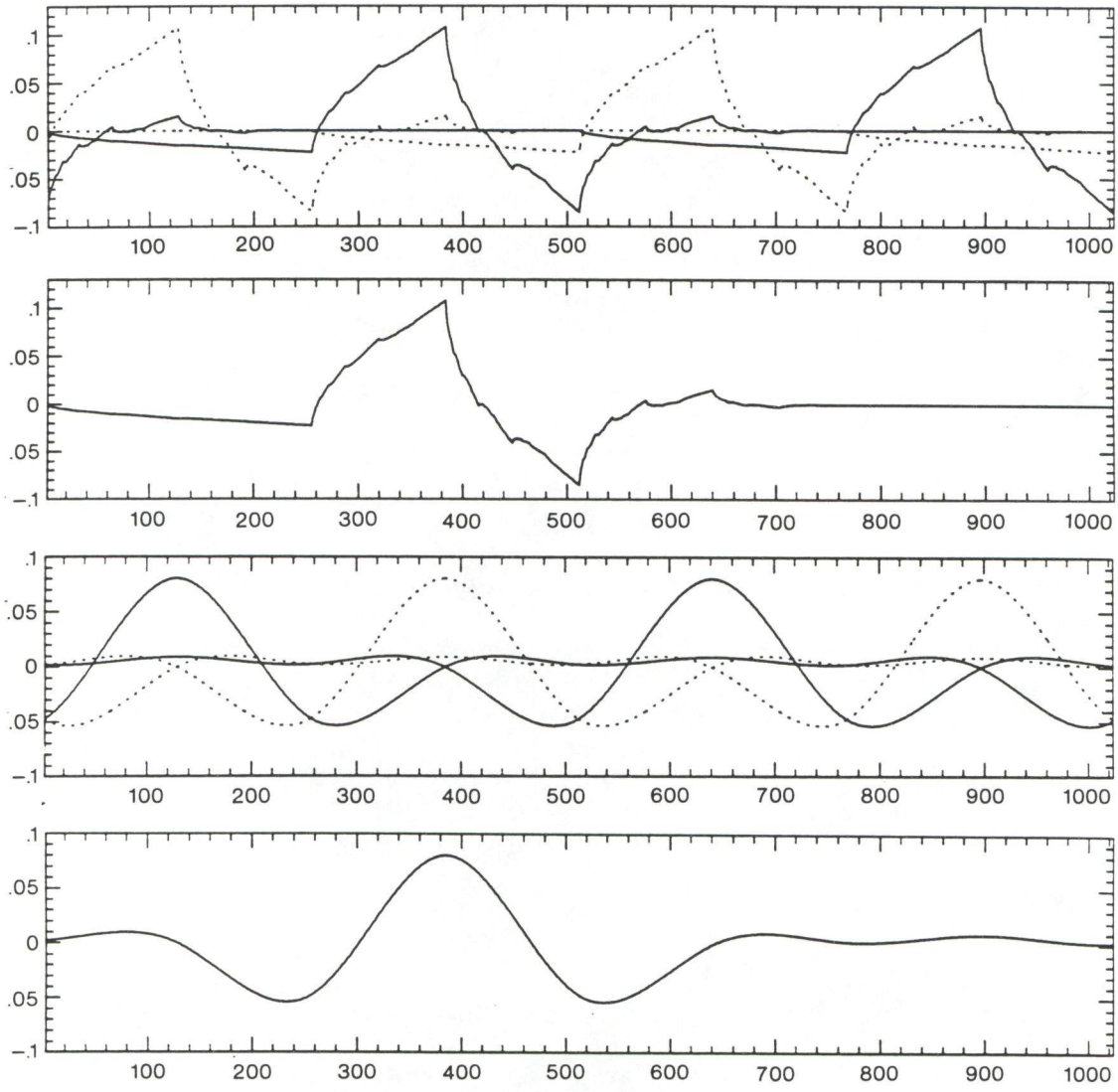

Figure 4-2.

continuity of a wavelet is not the same as the continuity of functions that a set of wavelets can represent. For example, DAUB4 can represent (piecewise) linear functions of arbitrary slope: in the correct linear combinations, the cusps all cancel out.

Figure 4-3 shows the result of performing the inverse DWT on the input vector $\mathbf{e}_{10} + \mathbf{e}_{58}$, again for the two different particular wavelets. Since 10 lies early in the hierarchical range of $9 - 16$, that wavelet lies on the left side of the picture. Since 58 lies in a later (smaller scale) hierarchy, it is a narrower wavelet; in the range of $33 - 64$ it is towards the end, so it lies on the right side of the picture. Note that smaller scale wavelets are taller, so as to have the same squared integral.

Finally, Figure 4-4 shows the scaling functions and first two mother wavelets that lie at the top of the wavelet hierarchy. With our conventions for DWTs, there are two scaling functions, obtained from basis vectors $\mathbf{e}_1, \mathbf{e}_2$, and two largest wavelets, obtained from basis vectors $\mathbf{e}_3, \mathbf{e}_4$. While the mother functions superficially resemble their "daughter" wavelets, they are different in detail. Note, for example that the mother functions have a vanishing integral over one period, while the scaling wavelets do not integrate to zero.

4.5 Truncated Wavelet Approximations

Most of the usefulness of wavelets rests on the fact that wavelet trans-

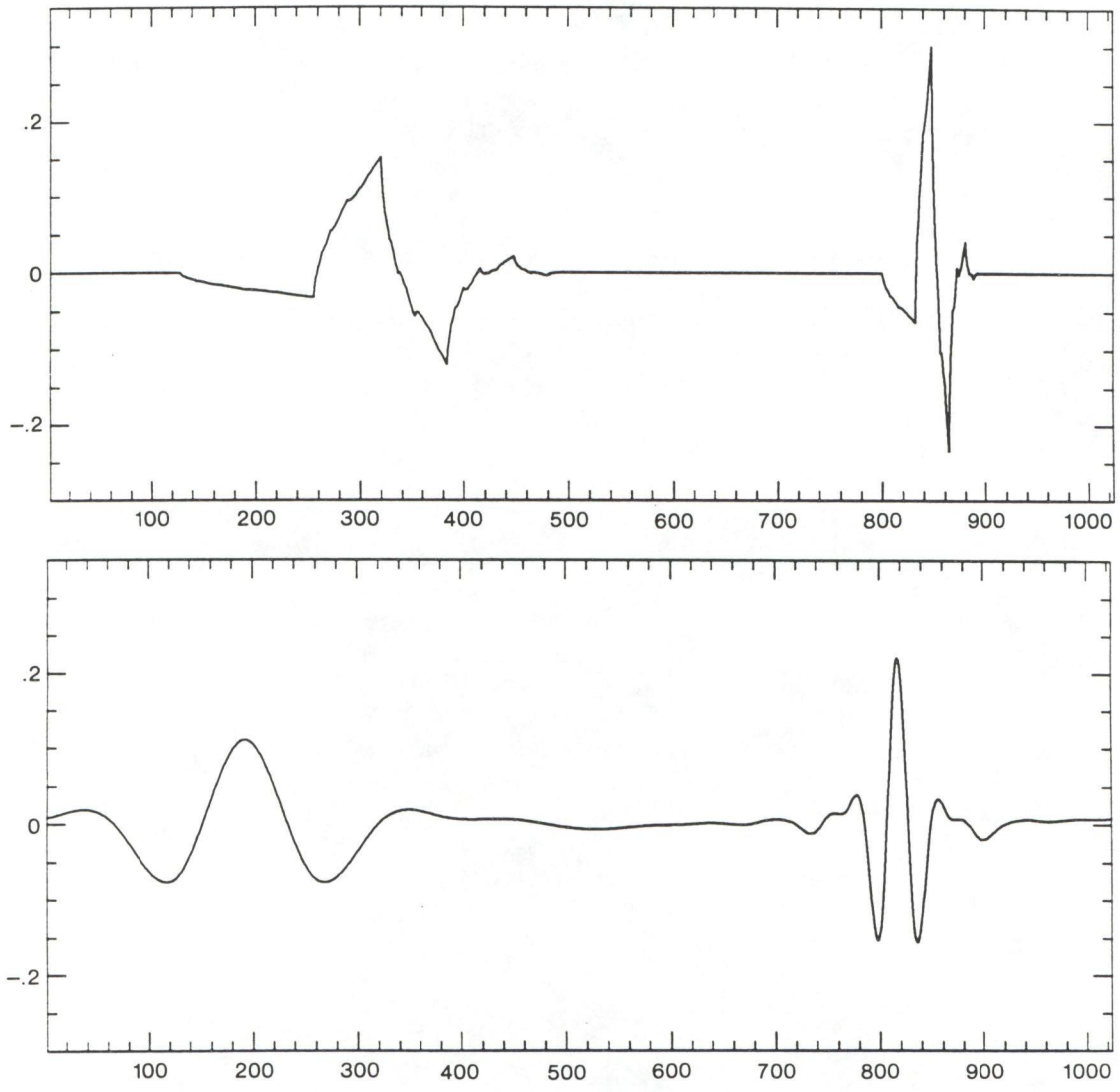
.2
0
−.2
100
200
300
400
500
600
700
800
900
1000
.2
0
−.2
100
200
300
400
500
600
700
800
900
1000

Figure 4-3.

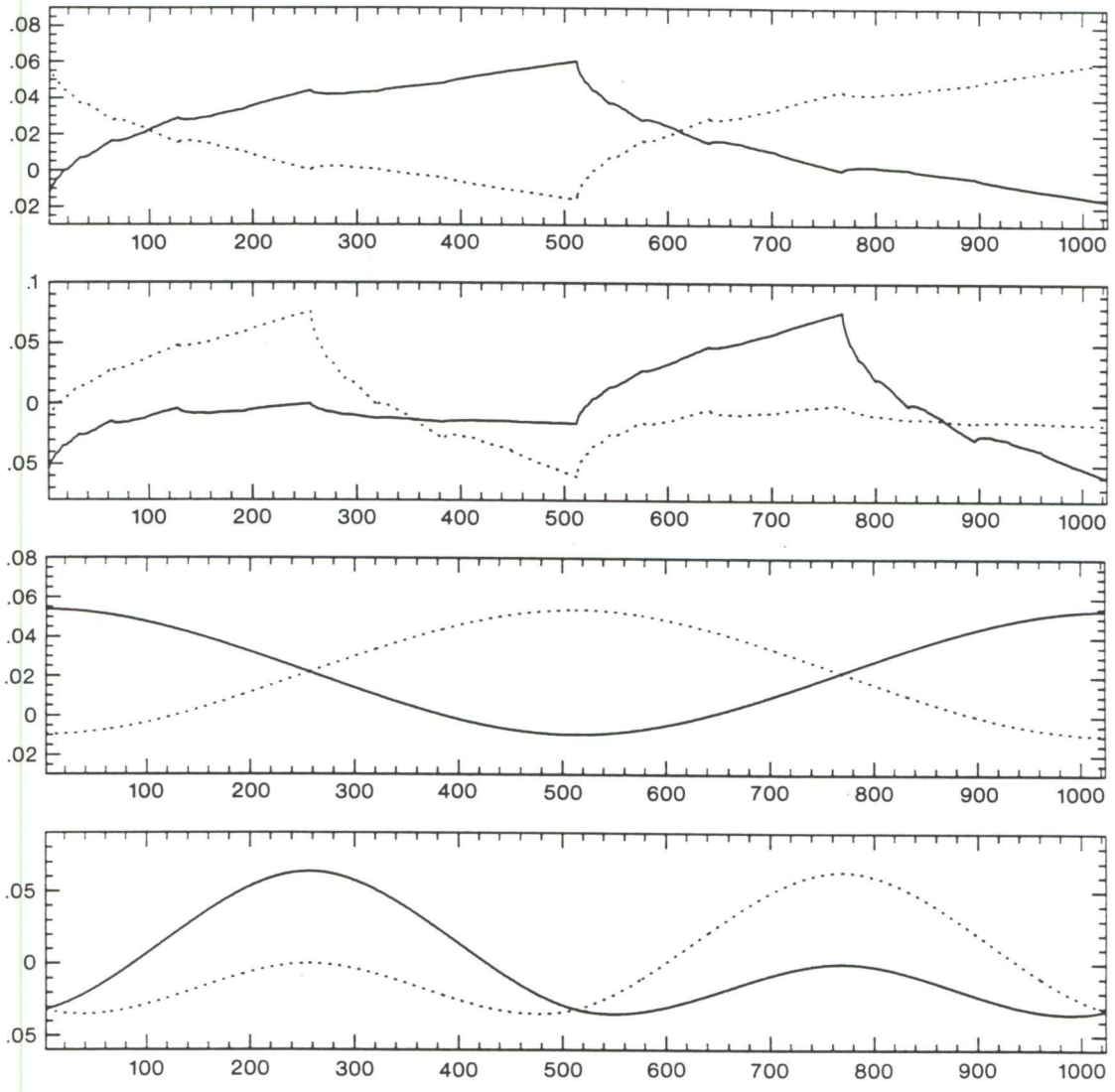
.08
.06
.04
.02
0
.02
100 200 300 400 500 600 700 800 900 1000
.1
.05
0
.05
100 200 300 400 500 600 700 800 900 1000
.08
.06
.04
.02
0
.02
100 200 300 400 500 600 700 800 900 1000
.05
0
.05
100 200 300 400 500 600 700 800 900 1000

Figure 4-4.

forms can usefully be severely truncated, that is, turned into sparse expansions. The case of Fourier transforms is different: FFTs are ordinarily used without truncation, to compute fast convolutions, for example. This works because the convolution operator is particularly simple in the Fourier basis. There are not, however, any standard mathematical operations that are especially simple in the wavelet basis.

To see how truncation works, consider the simple example shown in Figure 4-5. The upper panel shows an arbitrarily chosen test function, smooth except for a square-root cusp, sampled onto vector of length 2^{10}. The bottom panel (solid curve) shows, on a log scale, the absolute value of the vector's components after it has been run through the DAUB4 discrete wavelet transform. One notes, from right to left, the different levels of hierarchy, 513–1024, 257–512, 129–256, etc. Within each level, the wavelet coefficients are non-negligible only very near the location of the cusp, or very near the left and right boundaries of the hierarchical range (edge effects).

The dashed curve in the lower panel of Figure 4-5 plots the same amplitudes as the solid curve, but sorted into decreasing order of size. One can read off, for example, that the 140th largest wavelet coefficient has an amplitude less than 10^{-4} of the largest coefficient (power or square integral ratio less than 10^{-8}). Thus, the example function can be represented quite accurately by only 140, rather than 1024, coefficients — the remaining ones being set to zero. Note that this kind of truncation makes the vector sparse, but not shorter than 1024. It is very important that vectors in wavelet space be truncated according to the *amplitude* of the components, not their po-

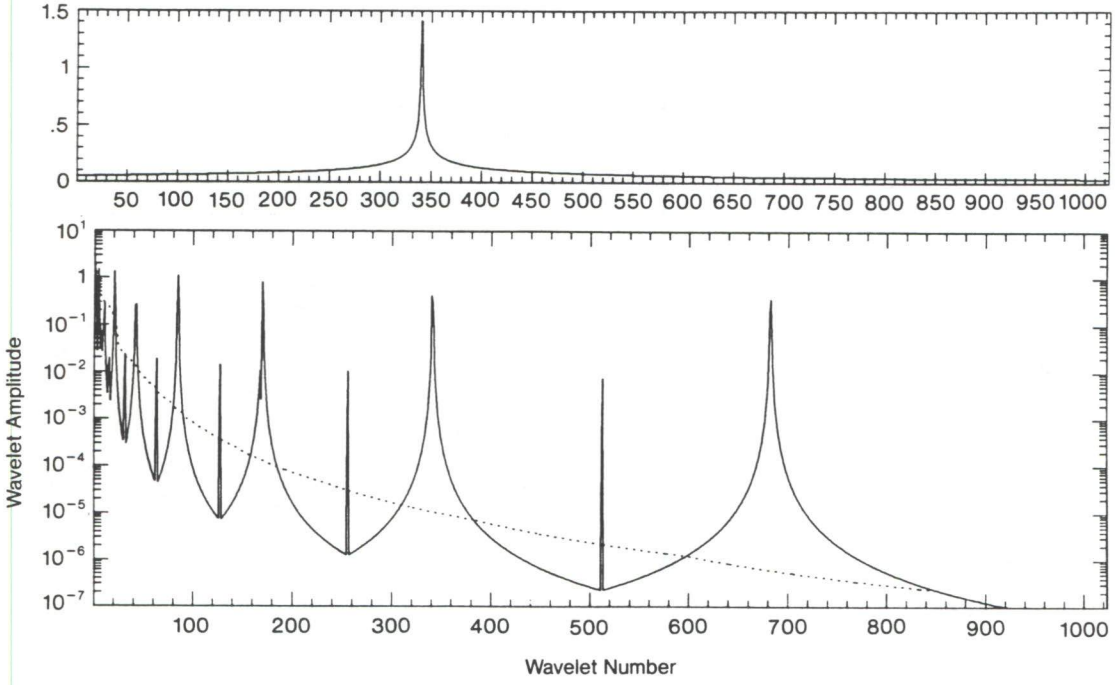
1.5
1
.5
0
50 100 150 200 250 300 350 400 450 500 550 600 650 700 750 800 850 900 950 1000
Wavelet Amplitude
10^{1}
1
10^{-1}
10^{-2}
10^{-3}
10^{-4}
10^{-5}
10^{-6}
10^{-7}
100 200 300 400 500 600 700 800 900 1000
Wavelet Number

Figure 4-5.

sition in the vector. Keeping the first 256 components of the vector (all levels of the hierarchy except the last two) would give an extremely poor, and jagged, approximation to the function. When you compress a function with wavelets, you have to record both the values *and the positions* of the non-zero coefficients.

Figure 4-6 is analogous to Figure 4-5, but shows the use of the Lemarié wavelets instead of DAUB4. Several differences are evident: for a given level of accuracy, more coefficients are required to take care of the edge effects. (DAUB4 is particularly good at edge effects because it has compact support.) At the position of the cusp in each hierarchy, Lemarié is less efficient than DAUB4 at achieving a low-accuracy representation ($\sim 10^{-2}$, say), but it becomes much more efficient as the level of accuracy is increased. Comparing the dotted curves, one sees that Lemarié is able to represent the function to machine accuracy using only about 325 coefficients, while DAUB4 requires essentially the whole vector of 2^{10}. (Incidentally, if the function were more finely sampled, say on 2^{15} points, the number of required coefficients for machine accuracy would still be only ~ 325, or increased by only a small logarithmic correction.)

Figures 4-5 and 4-6 together illustrate a general principle: compact (and therefore unsmooth) wavelets are better for lower accuracy approximation and for functions with discontinuities (such as edges), while smooth (and therefore noncompact) wavelets are better for achieving high numerical accuracy. This makes compact wavelets a good choice for image compression, for example, while it makes smooth wavelets ideal for fast solution of integral

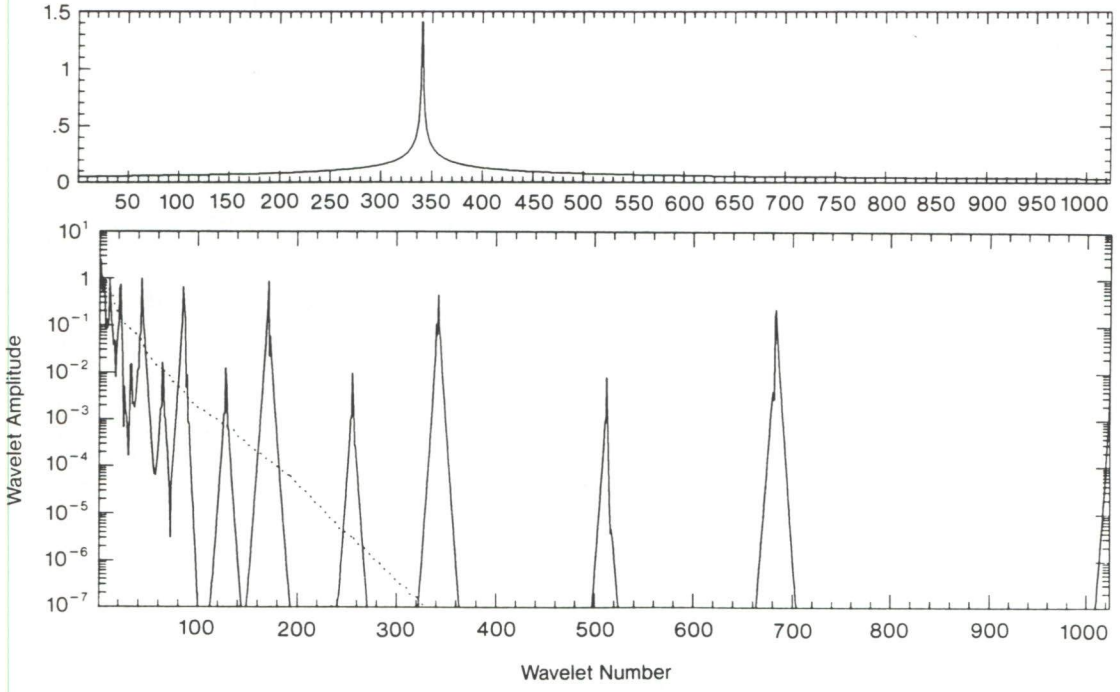
1.5
1
.5
0
50 100 150 200 250 300 350 400 450 500 550 600 650 700 750 800 850 900 950 1000
10^{1}
1
10^{-1}
10^{-2}
10^{-3}
10^{-4}
10^{-5}
10^{-6}
10^{-7}
Wavelet Amplitude
100 200 300 400 500 600 700 800 900 1000
Wavelet Number

Figure 4-6.

equations, as we will see below.

4.6 Wavelet Transform in Multidimensions

A wavelet transform of a d-dimensional array is most easily obtained by transforming the array sequentially on its first index (for all values of its other indices), then on its second, and so on. Each transformation corresponds to multiplication by an orthogonal matrix. By matrix associativity, the result is independent of the order in which the indices were transformed. The situation is exactly like that for multidimensional FFTs. A routine for effecting the multidimensional DWT can thus be modeled on a multidimensional FFT routine like *Numerical Recipes'* `fourn`:

```
      subroutine wtn(a,nn,ndim,isign,wtstep)
      parameter (NMAX=1024)
      real a(*),wksp(NMAX)
      integer nn(ndim)
      ntot=1
      do idim=1,ndim
           ntot=ntot*nn(idim)
      enddo
      nprev=1
      do idim=1,ndim
           write (*,*) 'Now doing dimension ',idim
           n=nn(idim)
           nnew=n*nprev
           if (n.gt.4) then
                do i2=0,ntot-1,nnew
                     do i1=1,nprev
                          write (*,*) 'origin is ',i1+i2
                          i3=i1+i2
                          do k=1,n
                               wksp(k)=a(i3)
                               i3=i3+nprev
                          enddo
                          if (isign.ge.0) then
                               nt=n
1                               if (nt.ge.4) then
```

```
                        call wtstep(wksp,nt,isign)
                        nt=nt/2
                             goto 1
                             endif
                        else
                             nt=4
2                             if (nt.le.n) then
                        call wtstep(wksp,nt,isign)
                        nt=nt*2
                             goto 2
                             endif
                        endif
                        i3=i1+i2
                        do k=1,n
                             a(i3)=wksp(k)
                             i3=i3+nprev
                        enddo
                    enddo
                enddo
            endif
            nprev=nnew
        enddo
        return
        end
```

Here, as before, `wtstep` is an individual wavelet step, either `daub4` or `lemarie`.

4.7 Compression of Images

An immediate application of the multidimensional transform `wtn` is to image compression. The overall procedure is to take the wavelet transform of a digitized image, and then to "allocate bits" among the wavelet coefficients in some highly nonuniform, optimized, manner. In general, large wavelet coefficients get quantized accurately, while small coefficients are quantized coarsely with only a bit or two—or else are truncated completely. If the

resulting quantization levels are still statistically nonuniform, they may then be further compressed by a technique such as Huffman coding.

While a more detailed description of the "back end" of this process, namely the quantization and coding of the image, is beyond our scope, it is quite straightforward to demonstrate the "front-end" wavelet encoding with a simple truncation: we keep (with full accuracy) all wavelet coefficients larger than some threshold, and we delete (set to zero) all smaller wavelet coefficients. We can then adjust the threshold to vary the fraction of preserved coefficients.

Figure 4-7 shows a sequence of images that differ in the number of wavelet coefficients that have been kept. The original picture (which is an official IEEE test image) has 256 by 256 pixels with 8-bit gray scale. Successive reproductions are reconstructed with 23 percent, 5.5 percent, 2.6 percent, and 0.9 percent of the 65,536 wavelet coefficients. The latter two, while so poor that they would probably not be useful images, best illustrate the kind of compromises made by the truncated wavelet representation. High contrast edges (such as the model's right cheek and hair highlights) are maintained at a relatively high resolution, while low contrast areas (such as the model's left eye and cheek) are washed out into what amounts to large constant pixels.

The way that an image degrades at high wavelet compression is quite different from other compression techniques. Figure 4-8 shows the same image reconstructed from its largest amplitude Fourier coefficients, keeping 5.5 percent and 2.4 percent of the original values (zeroing the rest). The splotchiness results from the nonlocality of the basis functions, so that errors

Figure 4-7a. 100%

Figure 4-7b. 23%

Figure 4-7c. 5.5%

Figure 4-7d. 2.6%

Figure 4-7e. 0.9%

Figure 4-8a. 5.5% FFT

Figure 4-8b. 2.4% FFT

at one part of the figure introduce random phase oscillations throughout.

(Not surprisingly, this is *not* the best way to use Fourier transforms to compress images. A much better method is to break up the image into small blocks of pixels, say 16 by 16, and then to take the cosine transform of the blocks one at a time. Bits are then nonuniformly allocated to the resulting 256 coefficients, with high spatial frequencies being quantized more coarsely than low frequencies.)

In Figure 4-9, every 4 by 4 block of original pixels has been replaced by its average value (with also some smoothing at the edges of the blocks). This figure therefore contains about 6 percent of the original's data. Comparing it to the corresponding wavelet reconstruction of 5.5 percent, and to the Fourier reconstruction at 5.5 percent leaves not much doubt as to the advantages of the wavelet scheme.

Figures 4-10 and 4-11 show a series of reconstructions of black and white target patterns. When the orientation of the lines is at 90 degrees, the wavelets' exceptional performance is in part due to the image itself being a separable product of x and y. However, even when the pattern is at 45 degrees, the wavelet reconstruction at about 5 percent retained coefficients is very much better than the corresponding Fourier reconstruction.

4.8 Fast Solution of Linear Systems

One of the most interesting, and promising, wavelet applications is linear

Figure 4-9. 6%

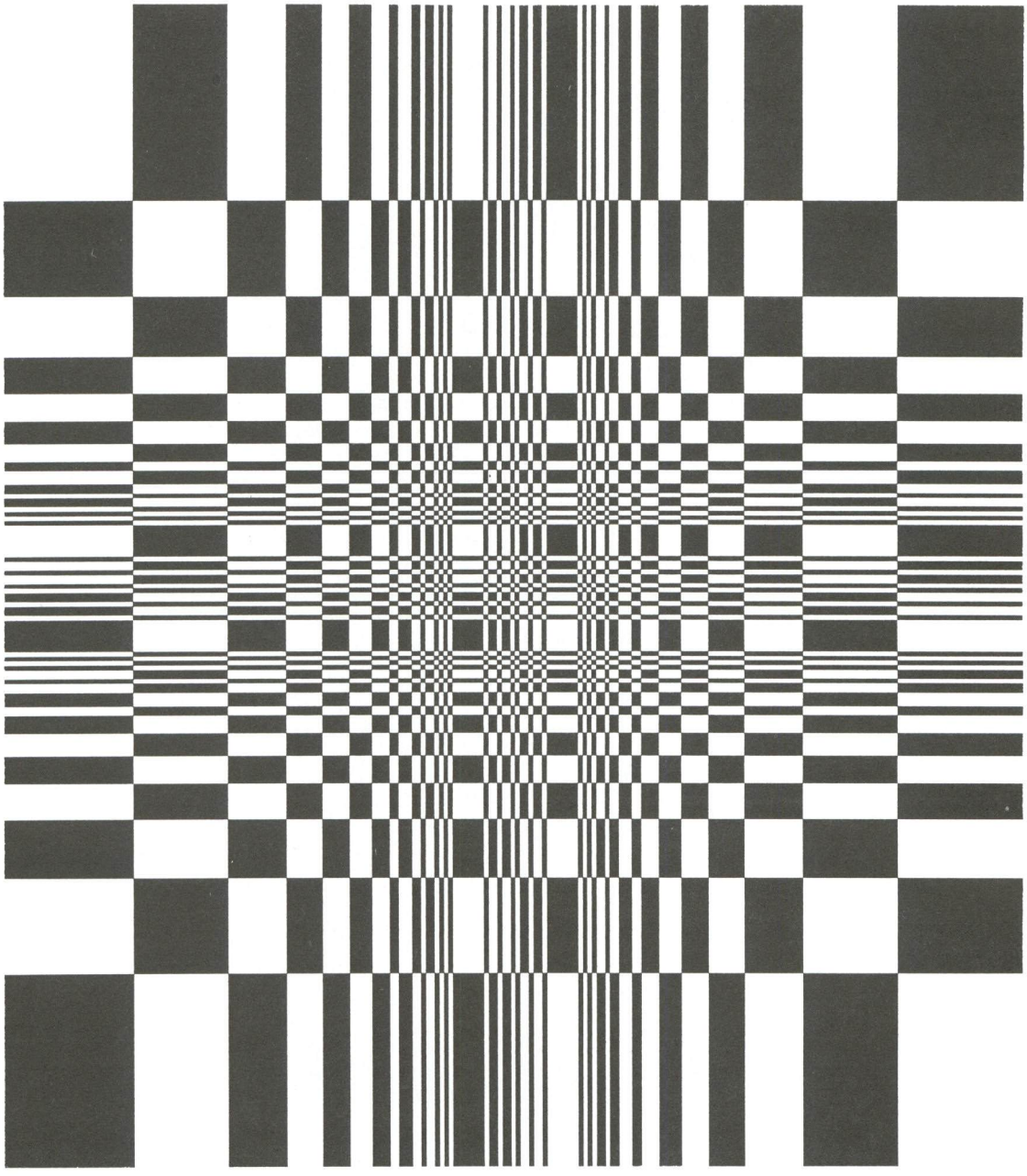

Figure 4-10a.

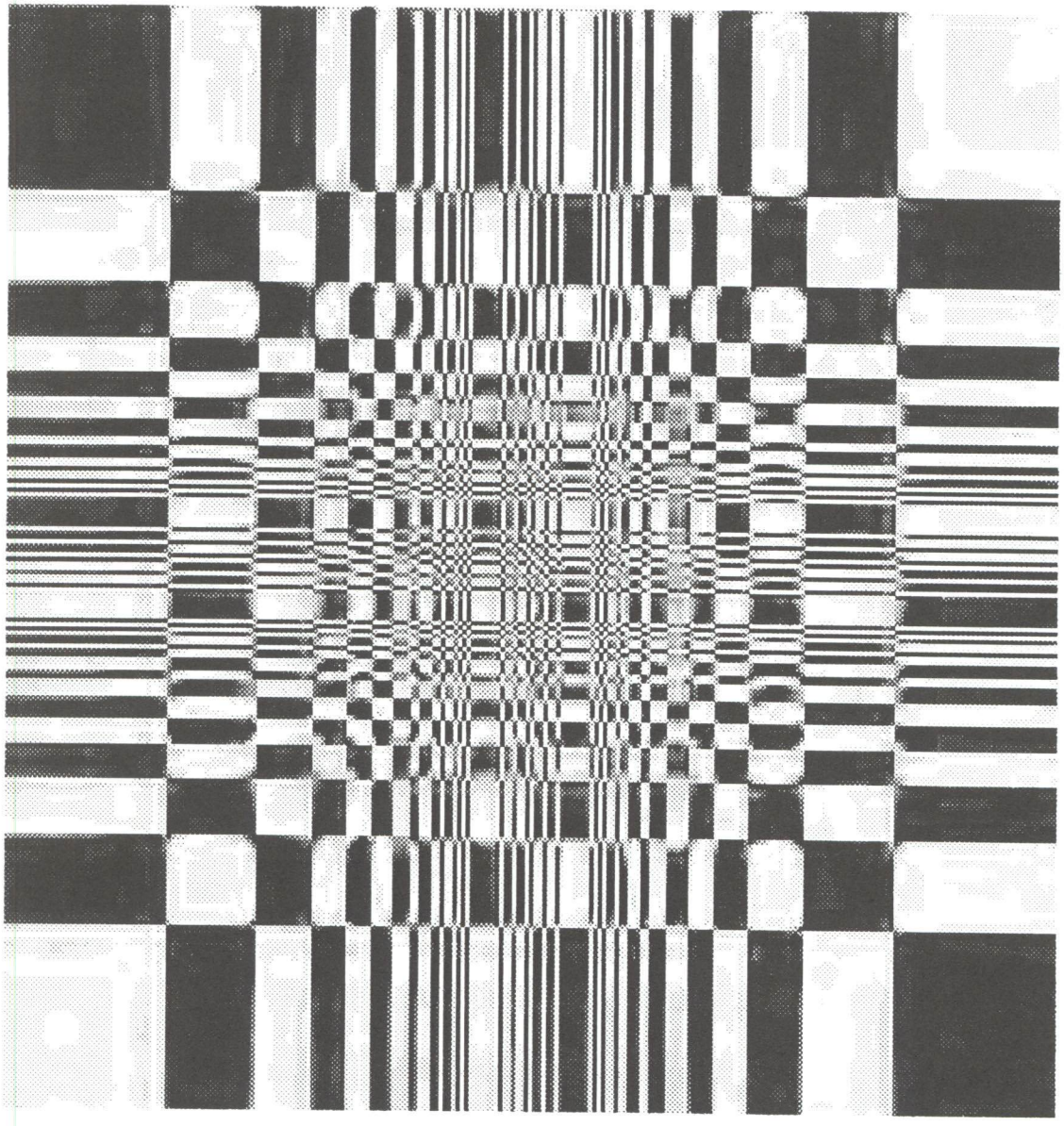

Figure 4-10b. 5.5%

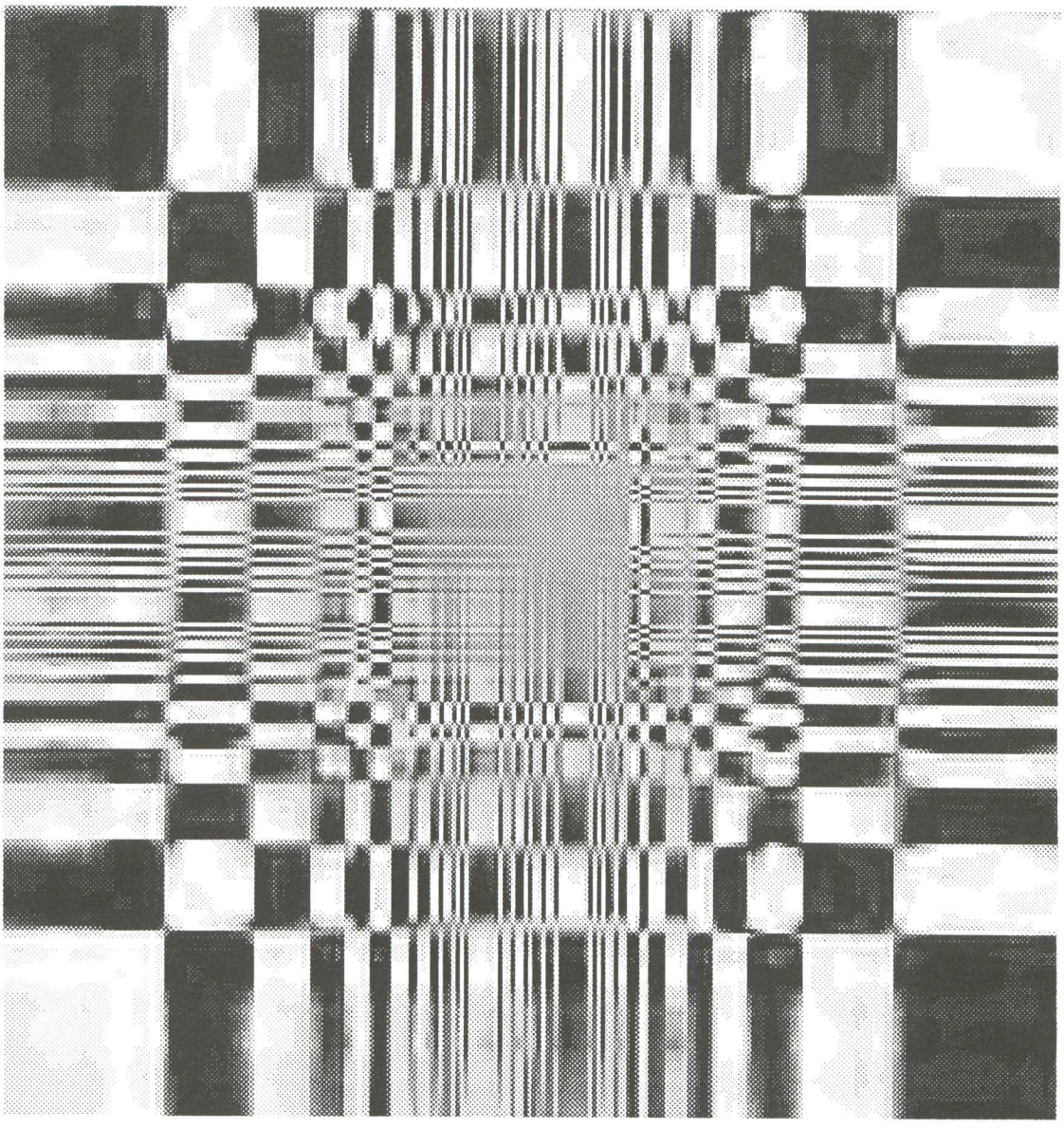

Figure 4-10c. 1.5%

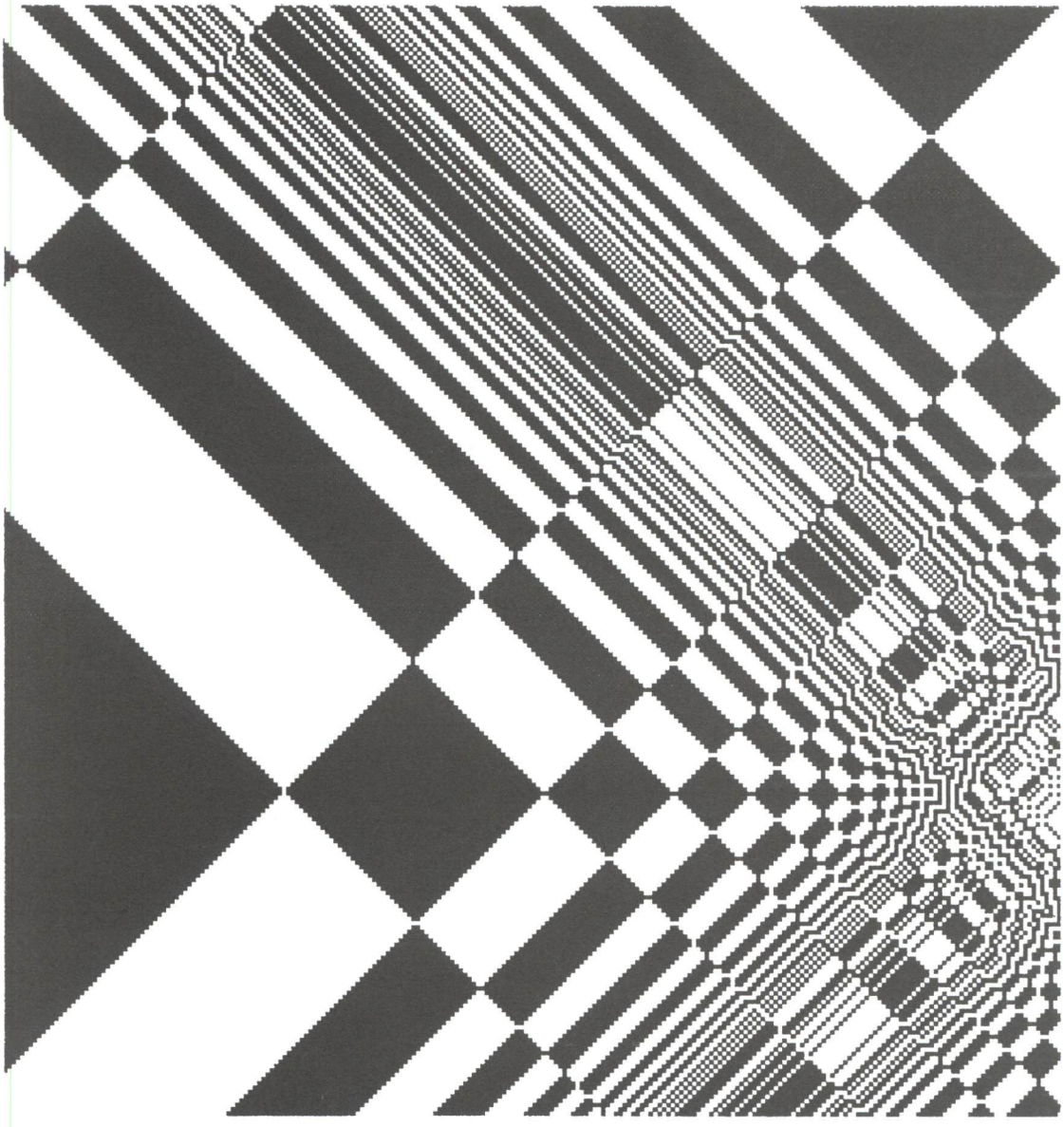

Figure 4-11a. 75% ≈ 100%

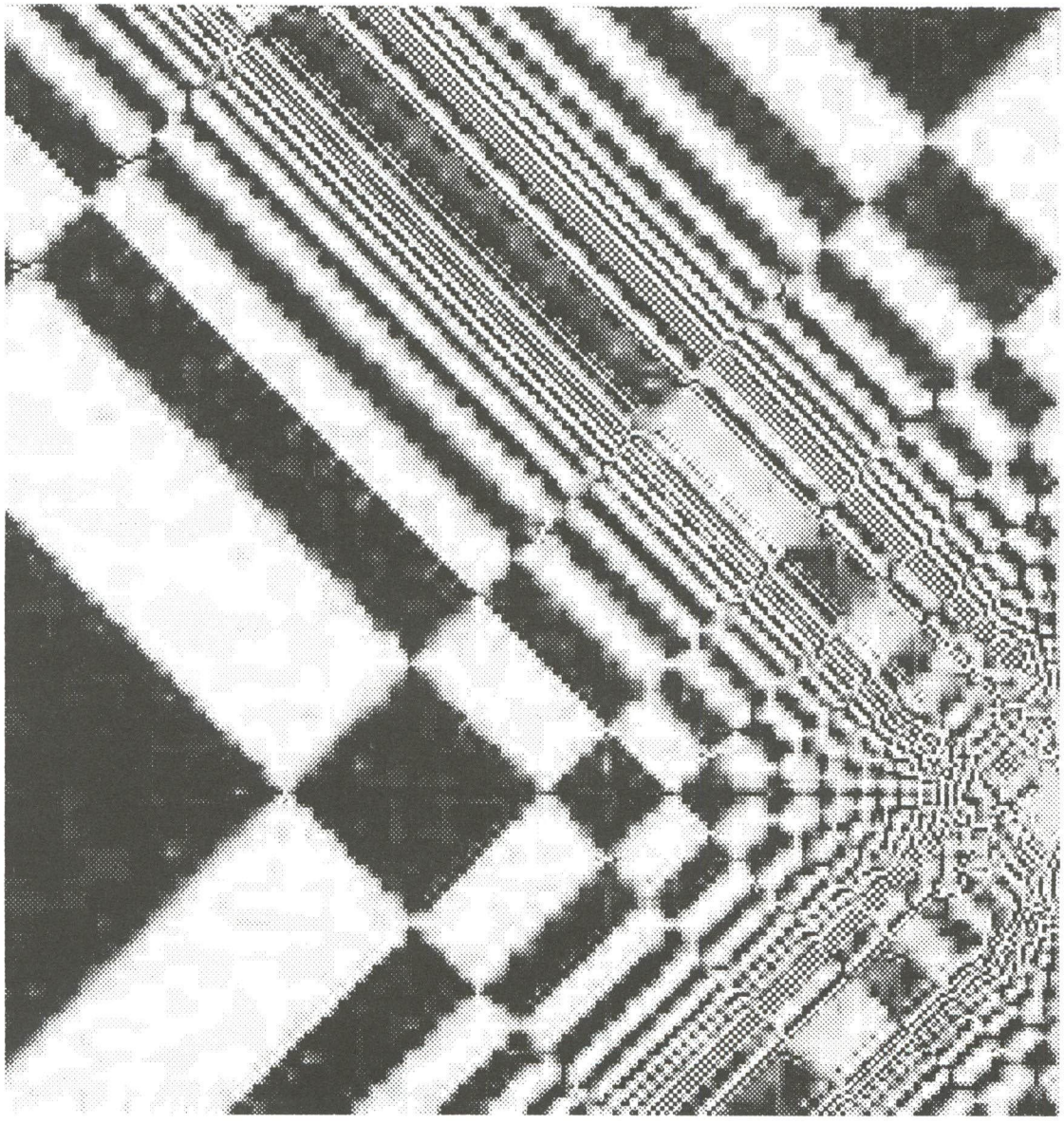

Figure 4-11b. 6.2%

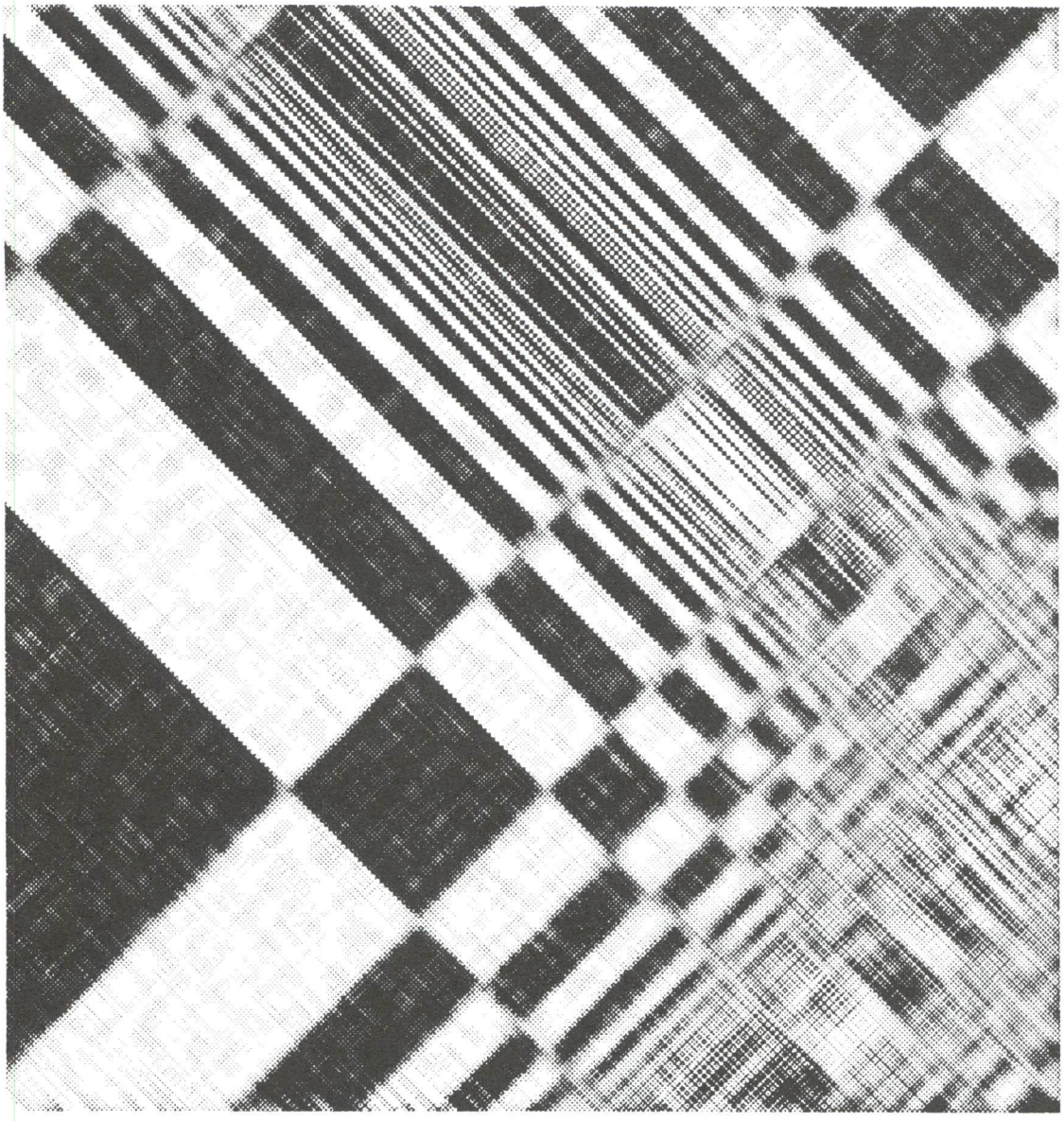

Figure 4-11c. 5.2% FFT

algebra. The basic idea is to think of an integral operator (that is, a large matrix) as a digital image. Suppose that the operator compresses well under a two-dimensional wavelet transform, i.e., that a large fraction of its wavelet coefficients are so small as to be negligible. Then any linear system involving the operator becomes a sparse system in the wavelet basis. In other words, to solve

$$\mathbf{A}\mathbf{x} = \mathbf{b} \tag{4-16}$$

we first wavelet-transform the operator $\mathbf{A}$ and the right-hand side $\mathbf{b}$ by

$$\tilde{\mathbf{A}} \equiv \mathbf{W}\mathbf{A}\mathbf{W}^T, \quad \tilde{\mathbf{b}} \equiv \mathbf{W}\mathbf{b}, \tag{4-17}$$

where $\mathbf{W}$ represents the one-dimensional wavelet transform, then solve

$$\tilde{\mathbf{A}}\mathbf{x} = \tilde{\mathbf{b}} \tag{4-18}$$

and finally transform the answer by the inverse wavelet transform

$$\mathbf{x} = \mathbf{W}^T\mathbf{x}. \tag{4-19}$$

(Note that the routine `wtn` does the complete transformation of $\mathbf{A}$ into $\tilde{\mathbf{A}}$.)

A typical integral operator that compresses well into wavelets has arbitrary (or even nearly singular) elements near to its main diagonal, but becomes smooth away from the diagonal. An arbitrary example might be

$$A_{ij} = \begin{cases} -1 & \text{if } i = j \\ |i-j|^{-1/2} & \text{otherwise.} \end{cases} \tag{4-20}$$

Figures 4-12 a, b, and c show a graphical representation of the wavelet transform of this matrix, where i and j range over $1 \ldots 256$, for three different wavelet families of differing smoothness: DAUB4, DAUB12 and DAUB20.

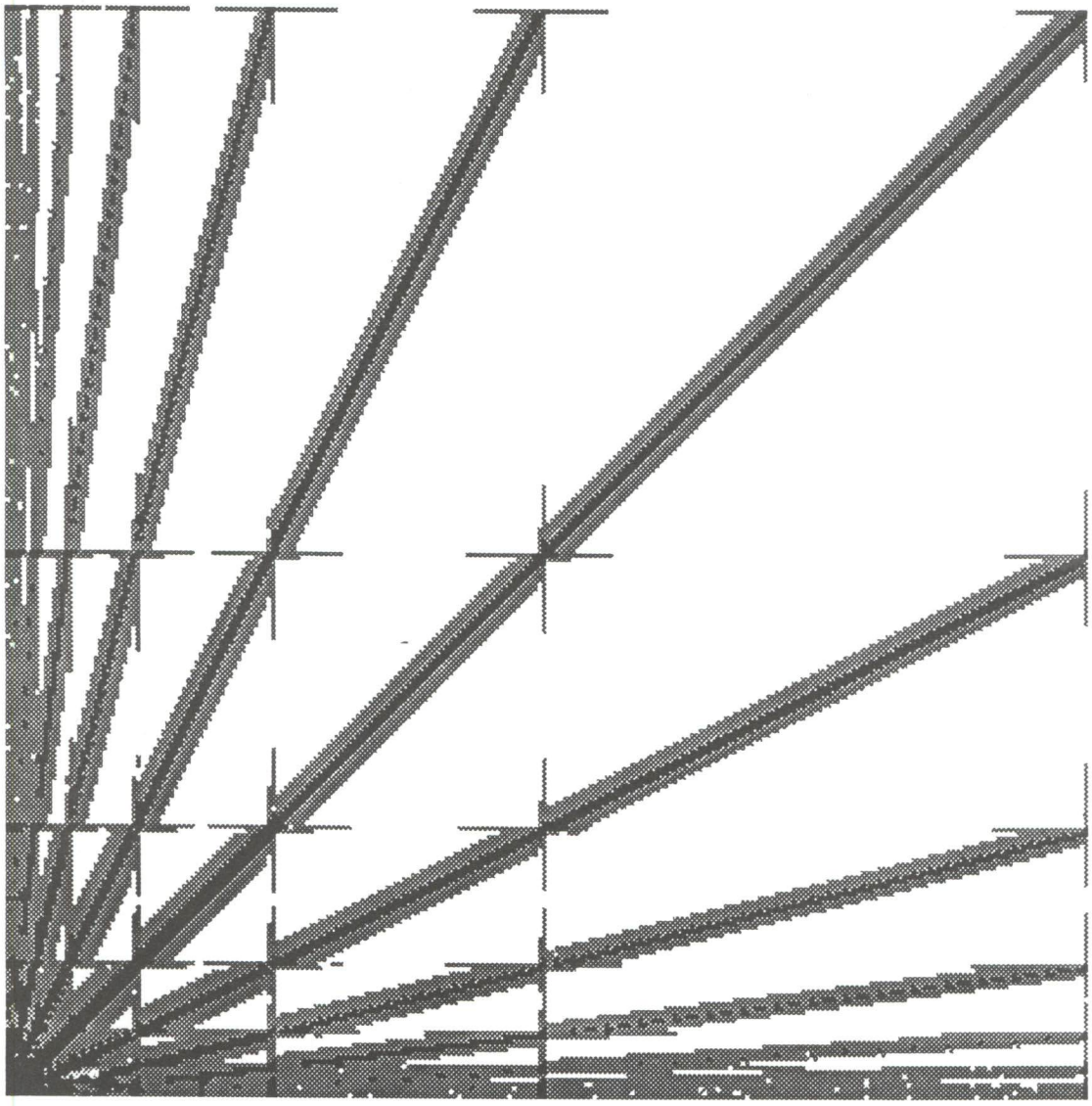

Figure 4-12a.

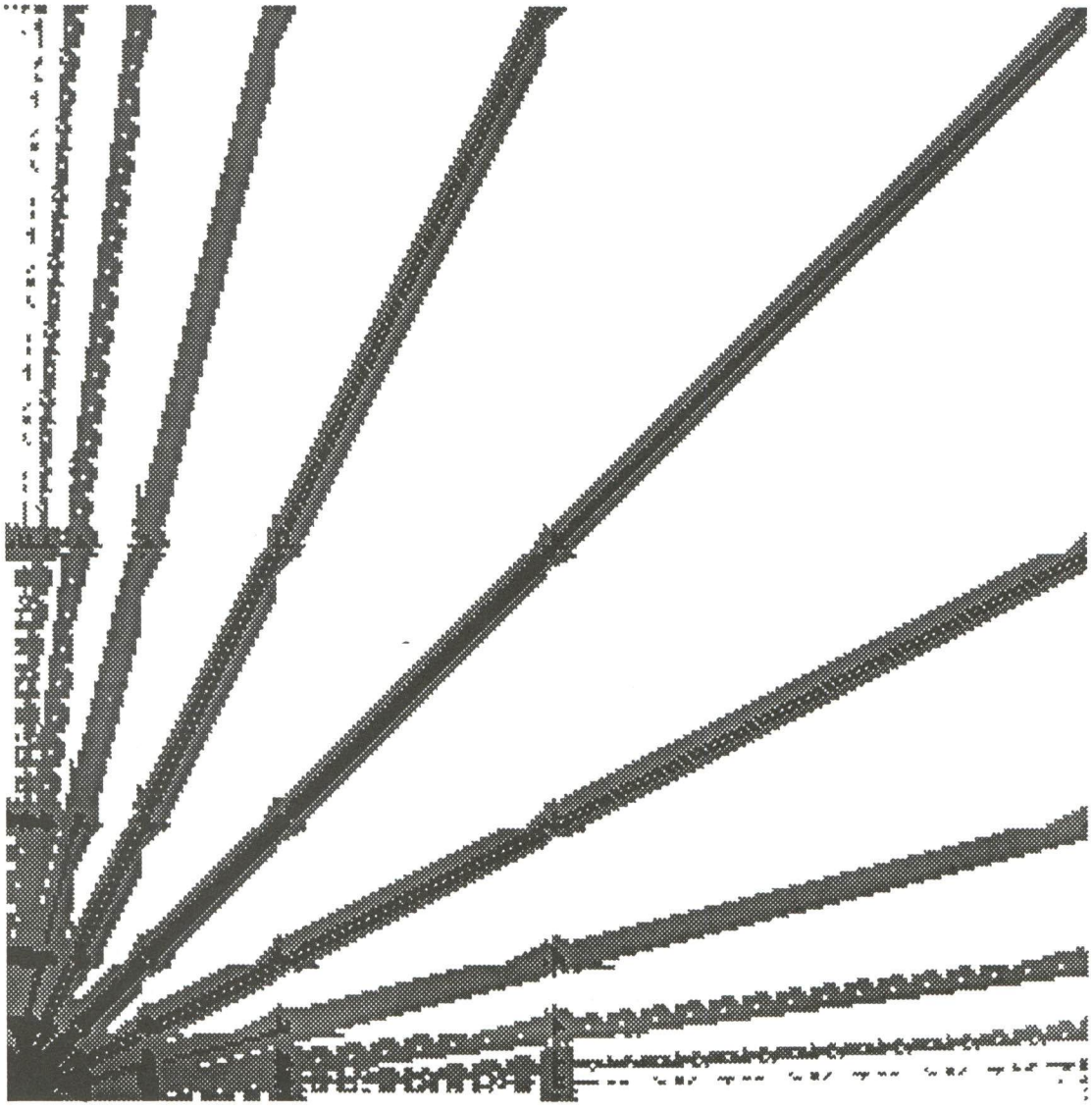

Figure 4-12b.

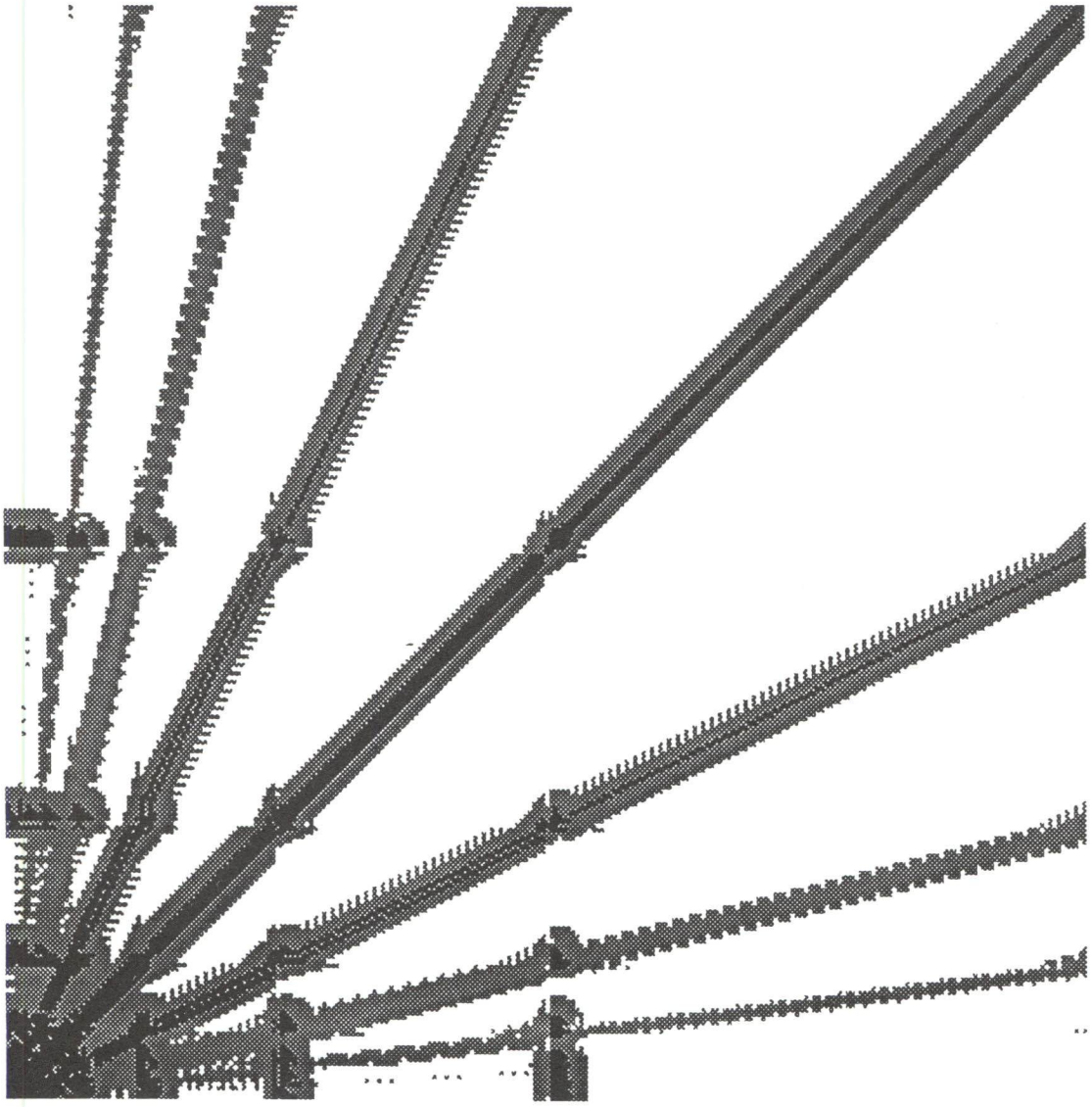

Figure 4-12c.

Elements larger in magnitude than 10^{-3} times the maximum element are shown as black pixels, while elements between 10^{-3} and 10^{-6} are shown in gray. White pixels are $< 10^{-6}$. The indices i and j each number from the lower left.

In the figures, one sees the hierarchical decomposition into power-of-two sized blocks. At the edges or corners of the various blocks, one sees edge effects caused by the wrap-around wavelet boundary conditions. Apart from edge effects, within each block, the nonnegligible elements are concentrated along the block diagonals. This is a statement that, for this type of linear operator, a wavelet is coupled mainly to near neighbors in its own hierarchy (square blocks along the main diagonal) and near neighbors in other hierarchies (rectangular blocks off the diagonal).

Comparing Figures 4-12a, 4-12b, and 4-12c, one sees that the principal effects of going to smoother wavelets are (1) to decrease the couplings among more distant hierarchical levels (bands become sparser the further they are from the main diagonal), but (2) to increase the bandwidth of the remaining bands. In fact, for the accuracy level shown, the number of nonnegligible elements is about the same in the three figures. As higher and higher accuracies are required, the picture for less-smooth wavelets will fill in and become non-sparse.

The number of nonnegligible elements in a matrix such as that in Figure 4-12 scales only as N, the linear size of the matrix; as a rough rule of thumb it is about $10N \log_{10}(1/\epsilon)$, where ϵ is the truncation level, e.g., 10^{-6}. For a 2000 by 2000 matrix, then, the matrix is sparse by a factor on the order of

30.

Various numerical schemes can be used to solve sparse linear systems of this "hierarchically band-diagonal" form. Coifman and Rokhlin make the interesting observations that (1) the product of two such matrices is itself hierarchically band-diagonal (truncating, of course, newly generated elements that are smaller than the predetermined threshold ϵ); and moreover that (2) the product can be formed in order N operations. This can be seen by sliding any of the Figures 4-12 across any other one, and noting that "black times black is at most black and at least gray."

Fast matrix multiplication makes it possible to find the matrix inverse by Newton's rule (in this context also called Schultz's method or Hotelling's method [see Pan and Reif, Proc. 17th ACM Symposium on Theory of Computing, 1985]). The basic iteration, which converges *quadratically*, is

$$\mathbf{A}_{n+1}^{-1} = 2\mathbf{A}_n^{-1} - \mathbf{A}_n^{-1}\mathbf{A}\mathbf{A}_n^{-1} \qquad (4-21)$$

resulting in $\mathbf{A}_n^{-1} \rightarrow \mathbf{A}^{-1}$ as $n \rightarrow \infty$. Schultz's method will always converge from a starting value

$$\mathbf{A}_0^{-1} = \mathbf{A}^T / \|\mathbf{A}^T\mathbf{A}\| \qquad (4-22)$$

(see Pan and Reif, reference above).

Other schemes are also possible for fast solution of hierarchically band-diagonal forms. For example, one can use the conjugate gradient method with operator splitting. The natural operator to split off for direct solution is the main diagonal band. Convergence of the full solution is then quite rapid.

4.9 Truncation of Wavelet Matrices

The matrix Equation (4-1) represents the basic DAUB4 matrix. More generally, if the same basic form is observed but the non-zero entries of the rows alternate between $c_0, \ldots, c_{2n-1}$ and $c_{2n-1}, -c_{2n-2}, \ldots, -c_0$ (reading cyclicly), we have a basic DAUB$-2n$ matrix M_{2n}. Orthogonality of M_{2n} is implied by n equations of the form

$$\begin{aligned} \sum_i c_i \, c_i &= 1, \qquad \text{and} \\ \sum_i c_i \, c_{i+2k} &= 0, \qquad 1 \leq k \leq n-1. \end{aligned} \tag{4-23}$$

Additionally, n-moment conditions may be reinforced

$$\sum_i (-1)^{i+1} \, i^k \, c_i = 0, \quad 0 \leq k \leq n-1. \tag{4-24}$$

We think of M_{2n} as a $2^N \times 2^N$ matrix where $2^N >> n$. When $2^N \leq 4n$ our truncation procedure $M_{2n} \rightarrow M'_{2n}$ does not work, but in this regime far from diagonal entries are of little consequence so we simply set M'_{2n} equal to M_{2n}.

Notice the cyclical pattern of non-zero entries in M. This is an undesirable consequence of the algebra used to find wavelets. It derives from translation invariance and corresponds to taking "wrap-around" boundary conditions on the data vector being sent into wavelet space (using the procedure explained by Equation (4–7)). Two consequences of this cyclic symmetry are undesirable. Most importantly, wrapping up the data vector is not physical in most applications. This means that the data will look less sparse than it should in wavelet space. To recover the input accurately many wavelet coefficients near the edge will be needed to beat down Gibbs-like effects. A

second problem is the computational annoyance and cost of manipulating not-quite-band-diagonal matrices.

To resolve these difficulties, we describe a method of truncating M_{2n} to a purely band-diagonal $2^N \times 2^N$ matrix M'_{2n} that agrees with M_{2n} except in the first n and last n rows.[2] The procedure requires the "orthogonality relations" Equation (4–23) to hold for M_{2n} but makes no use of the moment conditions Equation (4–24). (If the moment conditions are satisfied on the rows of M_{2n} they will, in general, fail for the $2n$ new rows of M'_{2n}. This is a "cost" of avoiding more serious edge effects.)

For ease of description we henceforth assume n=odd. The case n=even is nearly identical. Before we start, let us revise, slightly, the form of the basic wavelet matrix M_{2n}. Let us cycle the columns $n-1$ steps so that the non-zero entries are roughly centered on the diagonal and the pattern of non-zero entries is (roughly):

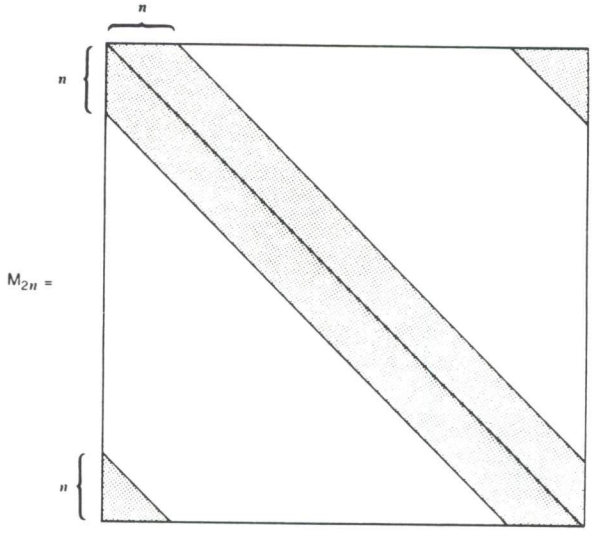

$(4-25)$

[2]If n is odd, due to the staircase pattern of non-zero entries in M_{2n} only the first and last n-1 rows are actually changed.

First, the picture is now symmetrical. But more importantly, when the procedure Equation (4–7) which produces wavelet coefficients, is executed, the "edge effects" — that is, the mixing of data obtained from opposite ends of the interval — will fall only at the last possible moment (rather than repeatedly) on data from the middle of the measurement stream.

The first unbroken row of M_{2n} (see Equation (4–25)) is the n^{th} when n=odd, the $n+1^{\text{st}}$ when n is even (due to the staircase form near the diagonal). The "intact" rows of M_{2n}:

$$\begin{aligned}
r_n &= c_0, \quad \dots \quad c_{2n-1}, \quad 0, \quad 0, \quad \dots \\
r_{n+1} &= c_{2n-1}, -c_{2n-2}, \quad \dots \quad -c_0, \quad 0, \quad 0, \quad \dots \\
r_{n+2} &= 0, \quad 0, \quad c_0, \quad \dots \quad c_{2n-1}, \quad \dots \\
r_{n+3} &= 0, \quad 0, \quad c_{2n-1}, -c_{2n-2}, \quad \dots, \quad -c_0, \quad \dots \\
&\vdots \\
r_{2^N-n+1} &= 0, \quad \dots, c_{2n-1}, -c_{2n-2}, \dots, -c_0
\end{aligned} \tag{4-26}$$

span the "central" subspace $C \subset V$, where V is the underlying vector space on which M_{2n} operates.

Here is the algorithm for writing down M'_{2n}. The first and last $n-1$ rows are broken into "left" and "right" pieces by a sea of 0-entries.

Geometrically speaking (and ignoring the staircase effect) these non-zero entries break up into two trapezoids and two triangles:

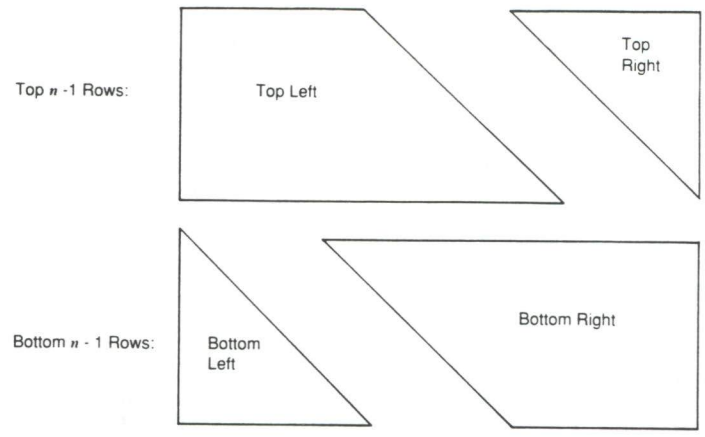

$(4-27)$

Call the $4(n-1)$ vectors represented by the rows of these figures $\{v_i^{t,\ell},\ v_i^{t,r},\ v_i^{b,\ell},\ v_i^{b,r}; 0 \leq i \leq n-1\}$ where t = top, b = bottom, ℓ = left, and r = right.

To construct the first $n-1$ rows of M'_{2n}, follow these steps. Place "bottom-left" on top of "top-left" to form a $2(n-1) \times 2(n-1)$ triangle. Select every other row of this triangle to form an $(n-1) \times 2(n-1)$ triangle of rows. These rows are:

$$v_2^{b,\ell},\ v_4^{b,\ell},\ \ldots,\ v_{n-1}^{b,\ell},\ v_2^{t,\ell},\ v_4^{t,\ell},\ \ldots,\ v_{n-1}^{t,\ell}. \qquad (4-28)$$

Starting with the shortest, apply the Gram-Schmidt orthnormalization to obtain another $(n-1) \times 2(n-2)$ triangle of rows $w_1^t,\ \ldots,\ w_{n-1}^t$. Insert these as the first $(n-1)$ rows of M'_{2n}.

The middle rows of M'_{2n} agree with those of M_{2n}. The last $n-1$ rows of M'_{2n} are made by applying Gram-Schmidt (in reverse order, starting with the shortest rows) to:

$$v_2^{b,r},\ v_4^{b,r},\ \ldots,\ v_{n-1}^{b,r},\ v_2^{t,r},\ v_4^{t,r},\ \ldots,\ v_{n-1}^{t,r} \qquad (4-29)$$

The non-zero entries of M'_{2n} are indicated below. In particular M'_{2n} is

band-diagonal with no increase in band width over the central portion of M_{2n}.

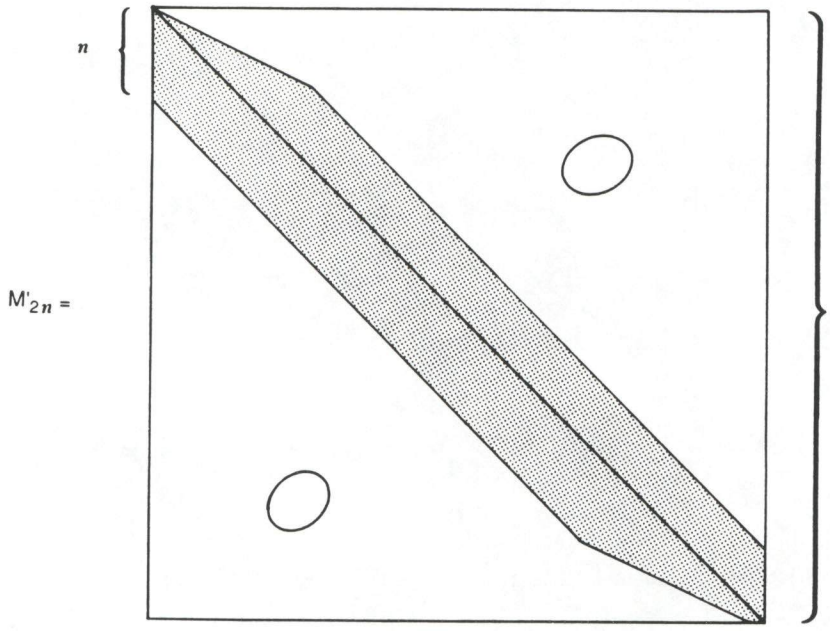

(4 – 30)

We must now explain why M'_{2n} is an orthogonal matrix. Let $C^{\perp}$ denote the subspace of vectors in V that are perpendicular to C. Since M_{2n} is orthogonal the $2(n-1)$ rows of M_{2n} $\left\{v_i^{t,\ell} + v_i^{t,r},\ v_i^{b,\ell} + v_i^{b,r};\ \ i \leq i \leq n-1\right\}$ span $C^{\perp}$. Thus

$$\{ \quad v_1^{b,\ell},\ \ldots,\ v_{n-1}^{b,\ell},\ v_1^{t,\ell},\ \ldots,\ v_{n-1}^{t,\ell}\}$$

and

$$\{ \quad v_1^{b,r},\ \ldots,\ v_{n-1}^{b,r},\ v_1^{t,r},\ \ldots,\ v_{n-1}^{t,r}\} \qquad (4\text{-}31)$$

together with span $C^{\perp}$. Also the geometry of the matrix, when $n << 2^N$, implies that any vector in the upper brace of Equation (4–31) is perpendicular to any vector in the lower brace. Thus it suffices to verify that the span of the even-numbered vectors in each brace contains the odd-numbered vectors

in that brace. In fact we will show using the orthogonality relations Equation (4–23) that:

the $(2k+1)^{\text{st}}$ and $(2k+2)^{\text{nd}}$ vectors in either brace

are dependent modulo the shorter vectors in that brace.

Because of the symmetry we only consider the first brace, which we write out below:

$$
\begin{array}{lcccccc}
\text{row } 1 & c_{2n-2} & c_{2n-1} & & & & \\
\text{row } 2 & c_1 & -c_0 & & & & \\
\text{row } 3 & c_{2n-4} & c_{2n-3} & c_{2n-2} & c_{2n-1} & & \\
\text{row } 4 & c_3 & -c_2 & c_1 & -c_0 & & \\
\text{row } 5 & c_{2n-6} & c_{2n-5} & c_{2n-4} & c_{2n-3} & c_{2n-2} & c_{2n-1} \\
\text{row } 6 & c_5 & -c_4 & c_3 & -c_2 & c_1 & -c_0 \\
\vdots & \vdots & & & & & \\
\text{Row } 2n-2 & c_{2n-3} & \cdots & & & \cdots & -c_0
\end{array}
\tag{4-32}
$$

The two-term relation in Equation (4–23) implies the first two rows are colinear.

Clearly row 4 is perpendicular to $\alpha = (0, 0, c_0, c_1)$ and $\beta = (c_0, c_1, c_2, c_3)$. Row 3 is also perpendicular to α and β, using the two- and four-term relations Equation (4-23). Since row 2 is also perpendicular to α and β, rows 2, 3, and 4 span only a two-dimensional space. Since row 2 is colinear with neither row 3 nor row 4, it follows that rows 3 and 4 are dependent modulo row 2.

Similarly, rows 5 and 6 both lie in the three-dimensional subspace perpendicular to $\alpha' = (0, 0, 0, 0, c_0, c_1)$, $\beta' = (0, 0, c_0, c_1, c_2, c_3)$, and $\gamma' = (c_0, c_1, c_2, c_3, c_4,$

c_5). Also in this subspace are rows 2 and 4. Since row 2 and row 4 are independent of each other and of rows 5 and 6, it follows that rows 5 and 6 are dependent modulo rows 2 and 4.

Continuing in this way we see that row $2k+1$ and row $2k+2$ are dependent modulo the shorter even-numbered rows, establishing (*).

It should be remarked that the truncation $M_{2n} \rightarrow M'_{2n}$ can be made directly applicable to image (or higher dimensional data) processing by using the "tensorial" or "product" wavelet decompositions on a rectangle (or multi-rectangle). For other more subtle wavelets based in dimension 2 and higher, analogues of this truncation exist. It is not known if the details of these will prove as elegant — for example, some coarsening of the band of non-zero entries may be expected in certain places — but the existence of a truncation is assured by a general theory for modifying the topology of the "control" space of an orthogonal transformation. This section, dealing, as it does, with the passage from circular control to interval control, is a first case of a rather flexible theory.

5 COMPARISON OF WAVELET AND FOURIER COMPRESSION

In this section, we look at the following items:

- How well do truncated wavelet transforms work in representing some waveforms? These include artificial waveforms, as in Section 4, as well as a signal from a familiar chaotic system, the Lorenz attractor. The latter is characteristic of many complex waveforms encountered in practice. It also provides a test of how well a linear transform method works on an essentially nonlinear signal.

- How well do wavelet transforms compare to Fourier transforms? Of course, we do not have a complete answer to this (if one exists) but we can directly compare the truncated wavelet transforms to truncated Fourier transforms on the same time trace.

- In representing an observed time series $f(t)$ by an expansion in some basis $\psi_k(t)$ by

$$f(t) = \sum_k a_k \psi_k(t), \qquad (5-1)$$

it is natural to ask *how many* terms a_k one needs to model the signal. We explore an answer that depends on an information theoretic result, which requires a penalty for too many coefficients and makes a clear choice of the "best" number balancing the cost of the coefficients against the accuracy of the approximation.

In the first part of this section we take the programs given in the discrete wavelet primer for the compact D4 wavelet and for the Lemarié wavelet and apply them to three different waveforms. The first waveform is the square root singularity discussed elsewhere, so this may repeat some material in the Primer. The waveform is

$$f(j) = \frac{1}{\sqrt{j + 1/2 - n}}, \qquad (5-2)$$

which for fixed N (here taken to be $N = 1024$) is shown in Figure 5-1. Now this waveform is transformed using the D4 wavelets with the wavelet coefficients which result shown in Figure 5-2. In Figure 5-3 we see the number of wavelet coefficients greater than a given size ϵ as a function of ϵ. As indicated in the primer, one wants to truncate the coefficients by their size, not simply cut off the series expansion of the waveform. This form of cutoff is closely related to a decision about the accuracy with which one wants the expansion to reproduce one's original waveform. In Figure 5-3 we see that the number of wavelet coefficients depends quite strongly on the accuracy one dictates. Choosing $\epsilon = 0.0001$ or one part in 10^4 we read off that 137 wavelets are required in the sum. These are **not** the first 137 in the series $f(t) = \sum_k a_k \psi_k(t)$ (Equation (5-1)), but are those greater than a certain magnitude. In Figure 5-4 we show the truncated square root waveform created from the 137 wavelet coefficients and their wavelet functions. So far this precisely reflects the information shown in various figures in the primer, Section 4.

Next we turn to a slightly different, but useful, question about the wavelet expansion. The basis for this question is the idea that we are making models of the process creating the waveform and want to know how many

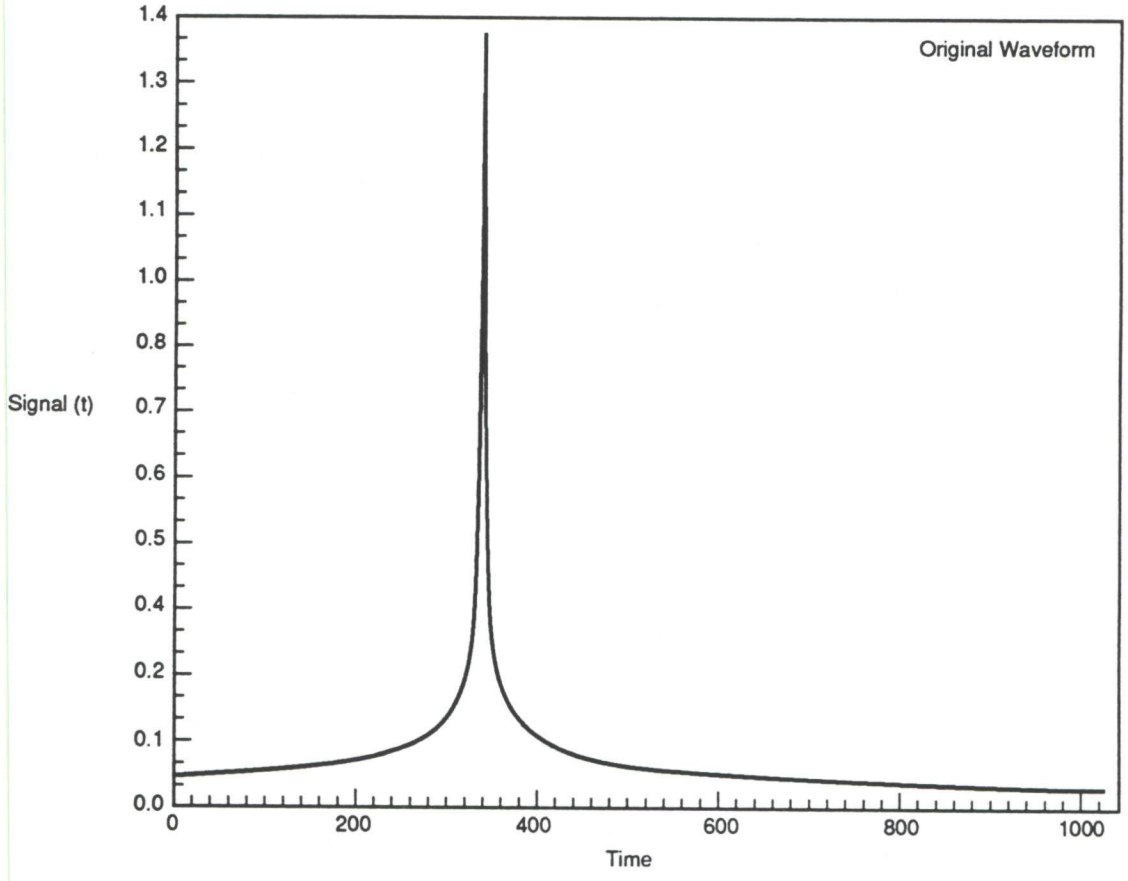
Original Waveform
Signal (t)
1.4
1.3
1.2
1.1
1.0
0.8
0.7
0.6
0.5
0.4
0.2
0.1
0.0
0
200
400
600
800
1000
Time

Figure 5-1.

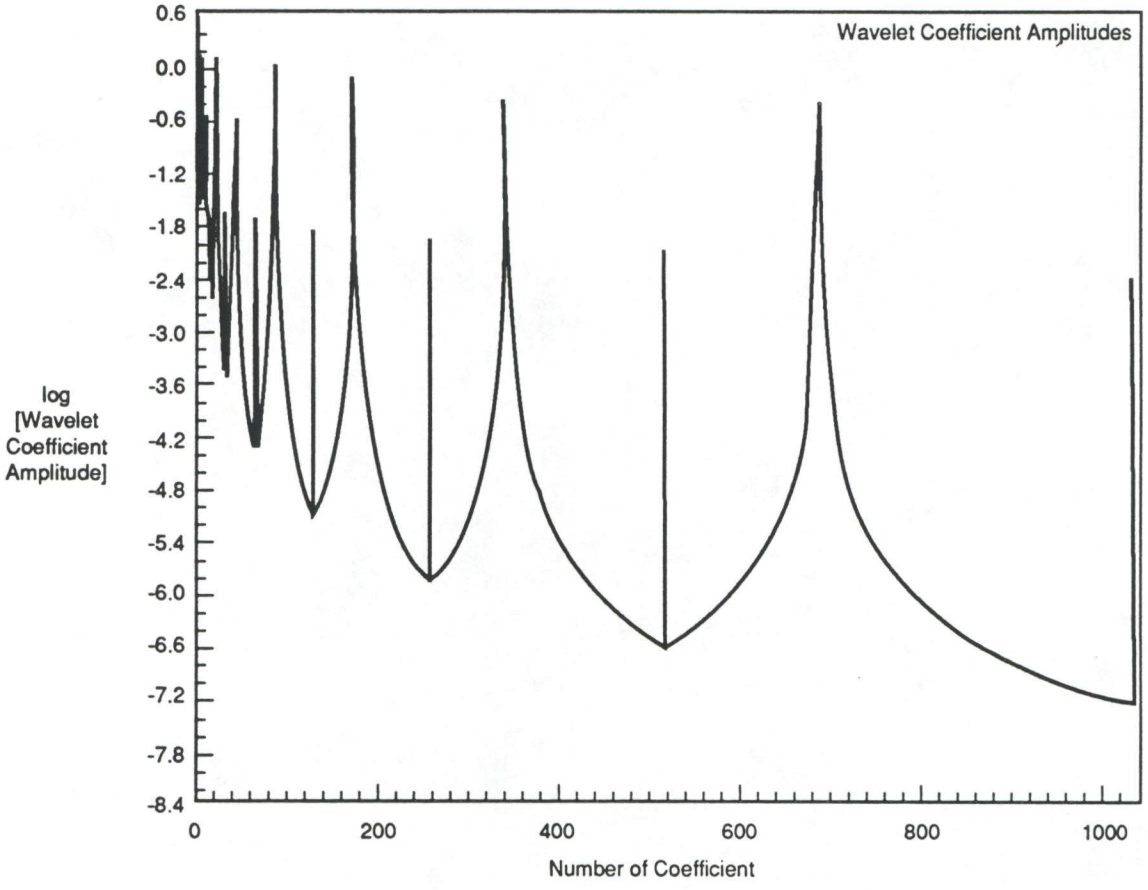
Wavelet Coefficient Amplitudes
log
[Wavelet
Coefficient
Amplitude]
0.6
0.0
-0.6
-1.2
-1.8
-2.4
-3.0
-3.6
-4.2
-4.8
-5.4
-6.0
-6.6
-7.2
-7.8
-8.4
0
200
400
600
800
1000
Number of Coefficient

Figure 5-2.

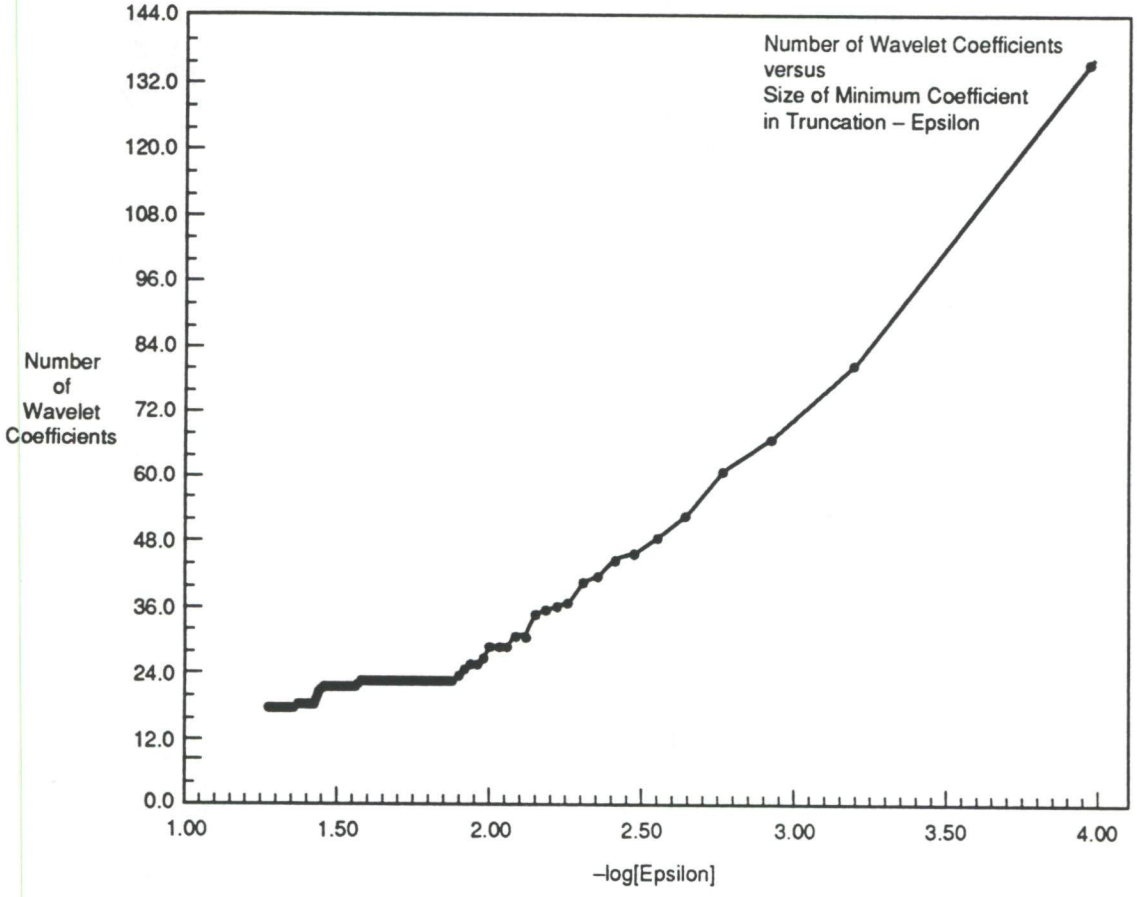
Number of Wavelet Coefficients
versus
Size of Minimum Coefficient
in Truncation – Epsilon
Number
of
Wavelet
Coefficients
144.0
132.0
120.0
108.0
96.0
84.0
72.0
60.0
48.0
36.0
24.0
12.0
0.0
1.00
1.50
2.00
2.50
3.00
3.50
4.00
–log[Epsilon]

Figure 5-3.

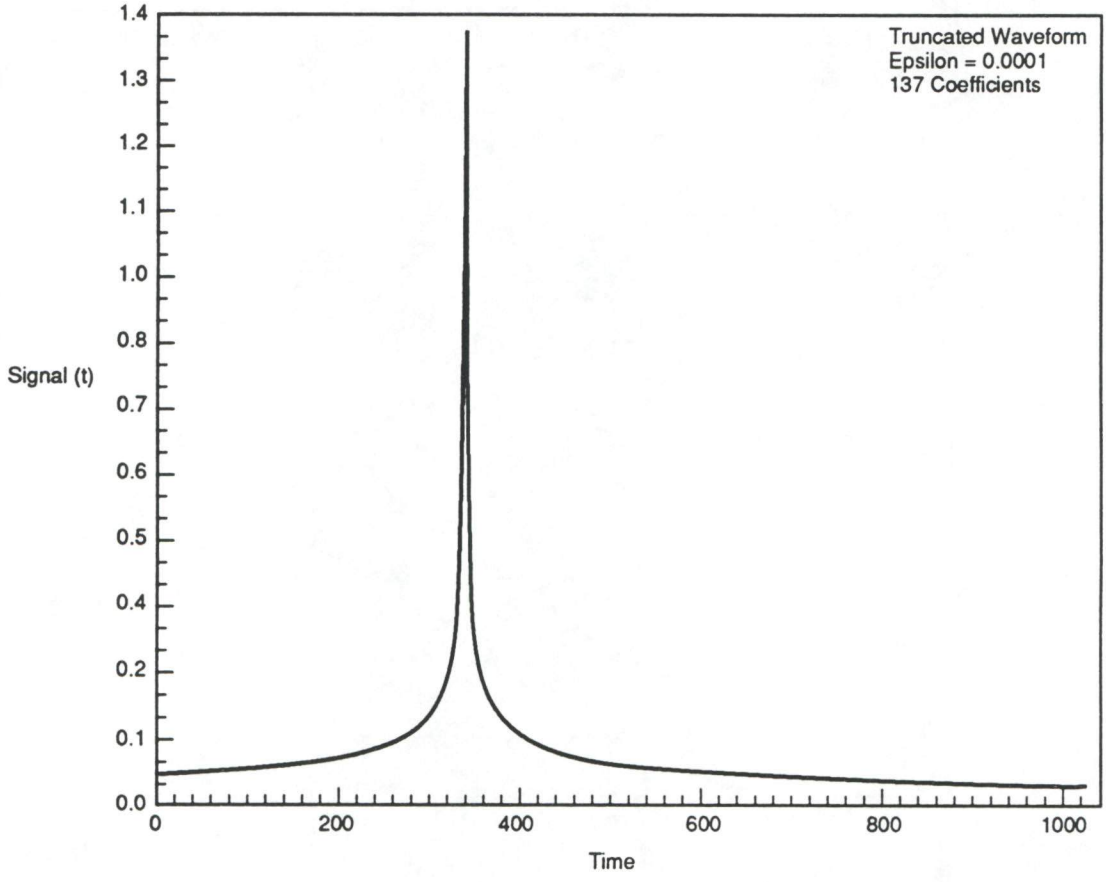
Truncated Waveform
Epsilon = 0.0001
137 Coefficients
Signal (t)
1.4
1.3
1.2
1.1
1.0
0.8
0.7
0.6
0.5
0.4
0.2
0.1
0.0
0
200
400
600
800
1000
Time

Figure 5-4.

coefficients are required to describe the data **best** in terms of the model we are using. The idea is that if we are given N pieces of time series data $f(j); j = 1, 2, ..., N$ we can always fit this data with a polynomial in "time" j

$$f(j) = \sum_{k=1}^{N} c_k \psi_k(j), \qquad (5-3)$$

using N terms in the sum. We are simply translating N pieces of data in 'time' j to N pieces of data c_k, and have neither made a model, really, nor learned anything about the data. One would like to use fewer than N coefficients to represent the data, and then, based on whatever interpretation one gives of the basis functions $\psi_k(j)$, we can interpret the model in some physical sense.

A usual criterion for the quality of the fit is least squares or equivalently maximum likelihood on the assumption of Gaussian statistics for the errors in making the model. If we think of the distribution of the error over the whole time series

$$E_K = \frac{1}{N} \sum_{j=1}^{N} [f(j) - f_K(j)]^2, \qquad (5-4)$$

where $f(j)$ is the original time series, and $f_K(j)$ is the reconstructed time series with a truncation of the expansion coefficients at K in number, then it is natural to assume that this quantity is distributed as

$$p(E_K) = \frac{\exp[-\frac{1}{2\sigma} E_K^2]}{\sqrt{\pi\sigma}}. \qquad (5-5)$$

The information required to encode the time series in terms of entropy contained in this model is –log[$p(E_K)$], and minimizing this is the familiar least squares criterion. The entropy is proportional to $\frac{E_K^2}{\sigma}$.

In making a model one should pay some price for the addition of extra coefficients, since we have seen by a simple argument that using N coefficients for N pieces of data is not useful. The price to pay is suggested by the information theoretic arguments of Rissanen [1]. The error associated with N measurements is of order $\frac{1}{\sqrt{N}}$ for large N, and if we have K independent quantities that are determined to this accuracy, then the entropy of this is $-k\log(1\sqrt{N})$ or $\frac{K}{2}$ log (N). The arguments of Rissanen then tell us that if we add to the cost of the maximum likelihood of the model this cost for parameters and **minimize** with respect to the number of parameters, we will realize the model in the class being considered—here Gaussian errors—that has the shortest code length, or equivalently the most efficient model in terms of the data presented. The code length has been called the Minimum Description Length or MDL. For our case this MDL(K) is

$$\text{MDL(K)} = \frac{E_K^2}{\sigma} + \frac{K}{2}\log(N), \qquad (5-6)$$

and we are instructed to minimize this over K.

In our way of truncating wavelet coefficients we use as a criterion not just the number of coefficients but the size of the coefficients, which we choose to be larger than some ϵ we select. In Figure 5-5 we display MDL(K) for the D4 wavelet expansion of the square root singularity waveform as a function of the number of wavelet coefficients as chosen on the basis of coefficient size ϵ. The minimum near 25 coefficients tells us that the best model, in terms of length of description of the data, comes by using about 25 coefficients. Going back to Figure 5-3 we see that means that the best model description comes at an accuracy of $\epsilon \approx 0.01$ for this wavelet basis with this data.

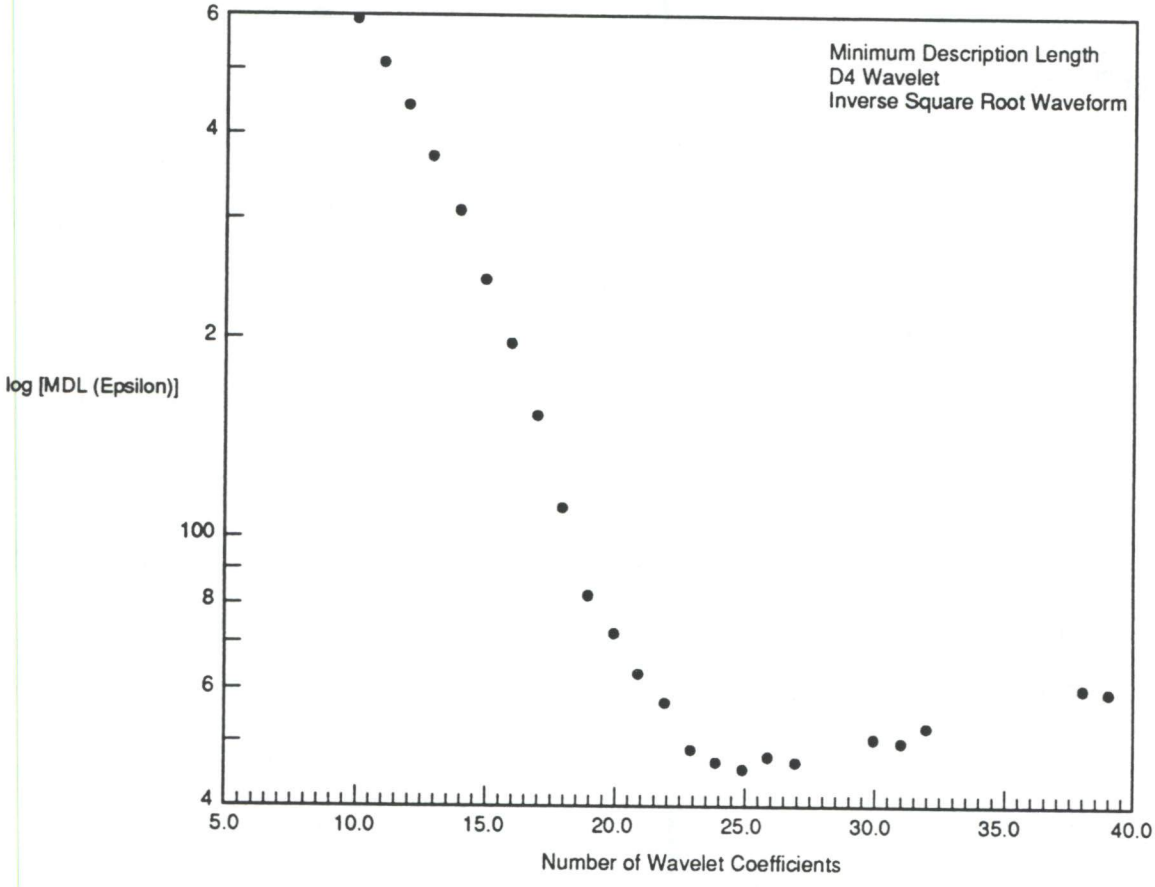
Minimum Description Length
D4 Wavelet
Inverse Square Root Waveform
log [MDL (Epsilon)]
6
4
2
100
8
6
4
5.0
10.0
15.0
20.0
25.0
30.0
35.0
40.0
Number of Wavelet Coefficients

Figure 5-5.

If we choose to use more wavelet coefficients we can, of course, improve the **fit** to the data—we can make ϵ smaller. There is a cost for doing this in the transmission of the "model" for the data that results: namely, we will require a larger number of bits to send the representation of the data with more coefficients, and the accuracy with which we are reproducing the waveform is offset by the amount of information we require to create this waveform; that is, the cost of transmitting the coefficients themselves. If very high accuracy is required, that cost may be acceptable, but one must then begin to ask whether it would not be more practical simply to transmit the original waveform instead of fussing around with wavelet bases or other bases. To put it in other words, in data compression, which is a goal of projecting waveforms into various bases, one must account for the cost of the expansion coefficients as well as for the quality of the fit to the data.

Next we return to a more familiar question for the data, and ask the same questions for Fourier expansions of our square root waveform. In Figure 5-6 we show the number of Fourier coefficients required to produce a specified accuracy ϵ in the reproduction of the waveform in Figure 5-1. For accuracy $\epsilon = 0.005$, about half of what we asked of the wavelet basis, we see that 984 Fourier coefficients are required, and in Figure 5-7 we see the waveform that results from using that number of Fourier terms. There is no question that the Fourier representation is less attractive than the D4 expansion with only 14% of the number of coefficients, and we would say that we have thus captured the square root waveform better with a D4 basis with fewer coefficients. Perhaps one could well expect this for a waveform with such high derivatives, since many Fourier coefficients are natural to capture the

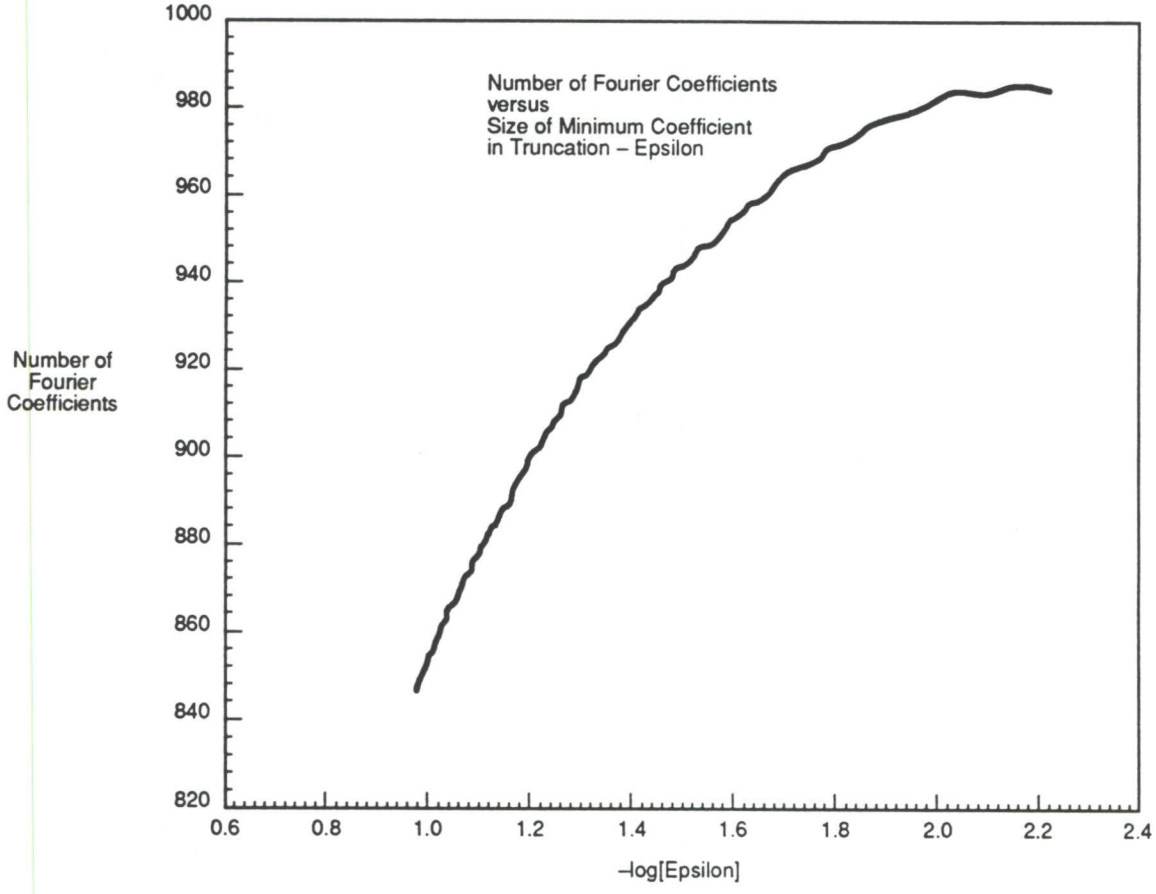
Number of Fourier Coefficients
versus
Size of Minimum Coefficient
in Truncation – Epsilon
Number of
Fourier
Coefficients
1000
980
960
940
920
900
880
860
840
820
0.6
0.8
1.0
1.2
1.4
1.6
1.8
2.0
2.2
2.4
–log[Epsilon]

Figure 5-6.

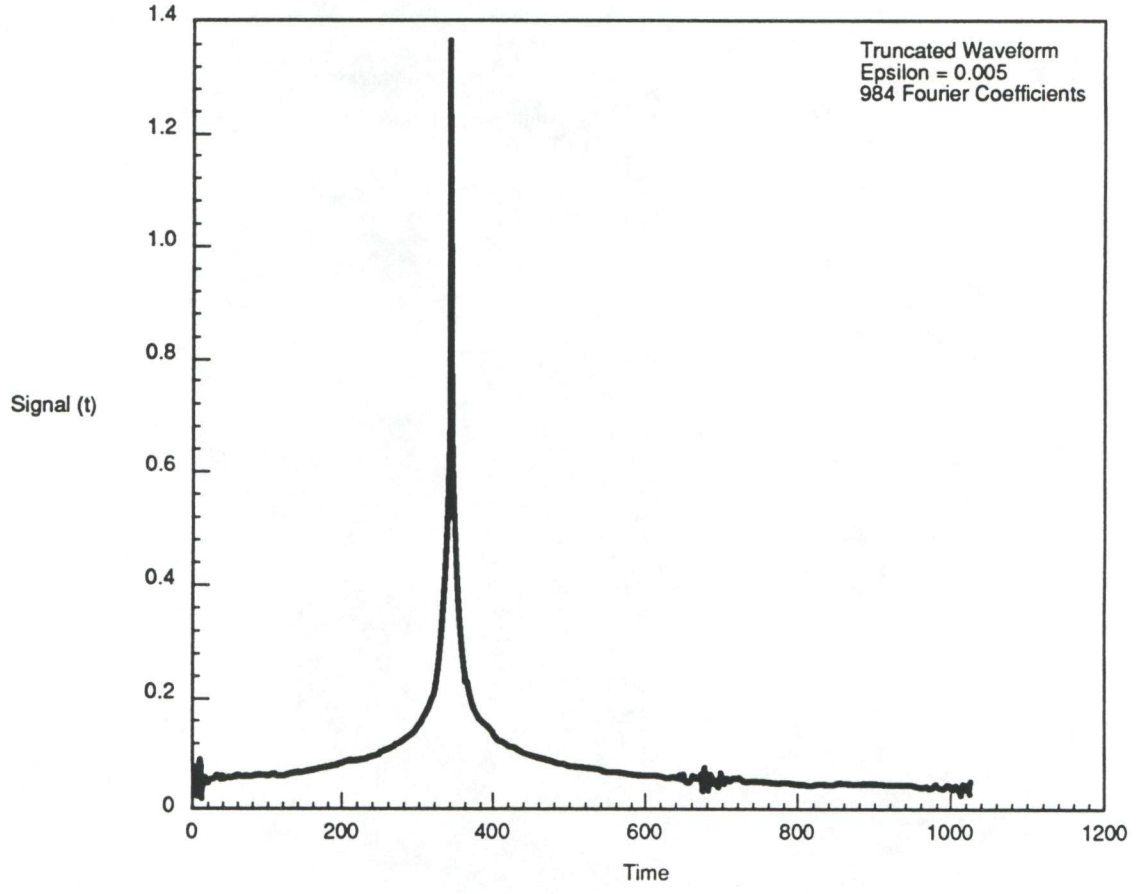
Truncated Waveform
Epsilon = 0.005
984 Fourier Coefficients
Signal (t)
1.4
1.2
1.0
0.8
0.6
0.4
0.2
0
0
200
400
600
800
1000
1200
Time

Figure 5-7.

short wave lengths in the wave.

Next we perform the same set of operations using the D4 basis on the signal shown in Figure 5-8. This time series comes from one of the variables in the Lorenz system of three ordinary differential equations

$$\begin{aligned} \frac{dx_1}{dt}(t) &= \sigma[x_2(t) - x_1(t)] \\ \frac{dx_2}{dt}(t) &= -x_1(t)x_3(t) - rx_1(t) - x_2(t) \\ \frac{dx_3}{dt}(t) &= x_1(t)x_2(t) - bx_3(t) \end{aligned} \tag{5-7}$$

where we take $\sigma = 16, b = 4$, and $r = 45.92$. This set of equations is chosen since it is well studied, is known to be a paradigm for chaotic behavior—namely complex time series, and is easy to compute. The first time series as shown in Figure 5-8 is very sparsely sampled in time, so high frequencies are filtered out. In Figure 5-9 we see the number of wavelet coefficients required to achieve a specified accuracy ϵ, and choosing $\epsilon = 0.005$ we show in Figure 5-10 the resulting reconstructed waveform from 64 wavelet coefficients. The shape of the truncated waveform is now seen to be much rougher where the original had high derivatives.

In Figure 5-11 we show the same time series for the Lorenz model with a much higher sampling rate in time. Now, as seen in Figure 5-12, we need nearly an order of magnitude more wavelet coefficients to capture the same accuracy (0.005) as with the less well sampled version of the time series. With 545 wavelet coefficients (out of a possible 1024) we show the truncated waveform in Figure 5-13. For this same time series, we have asked how

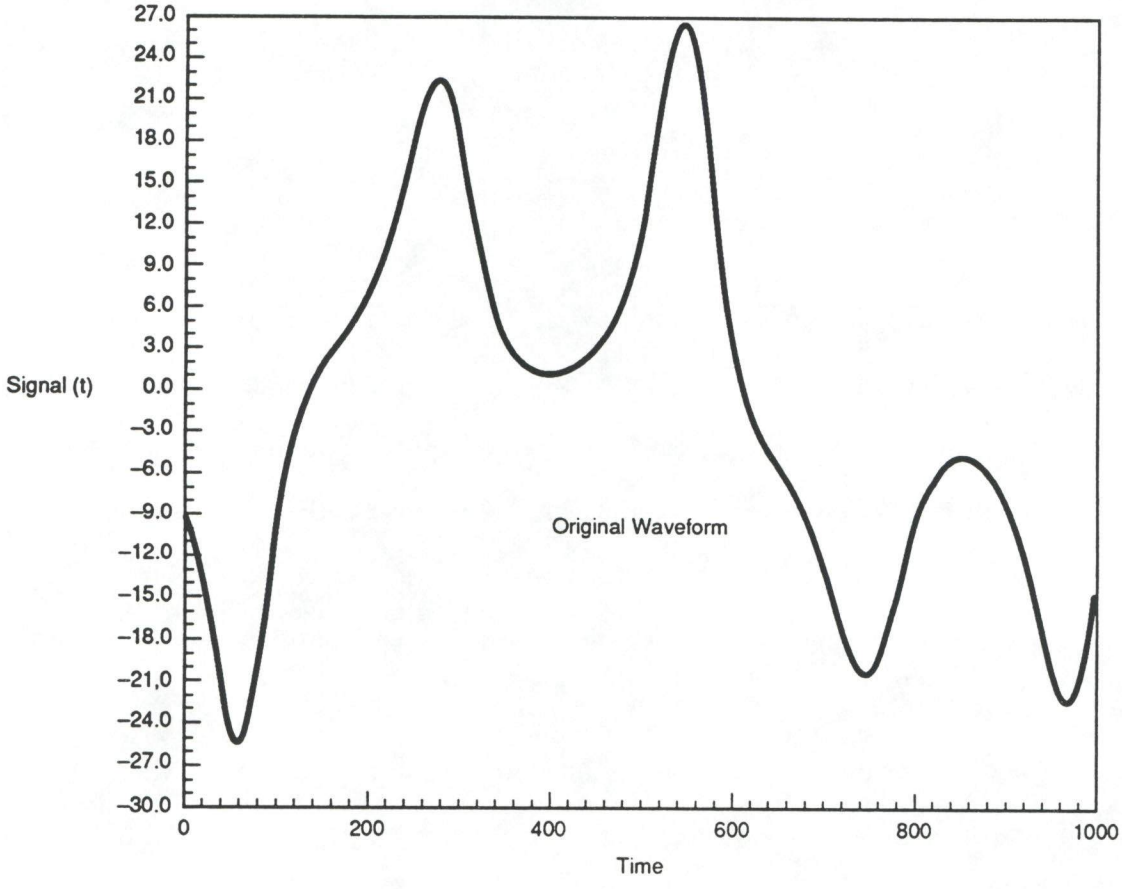
27.0
24.0
21.0
18.0
15.0
12.0
9.0
6.0
3.0
0.0
-3.0
-6.0
-9.0
-12.0
-15.0
-18.0
-21.0
-24.0
-27.0
-30.0
Signal (t)
Original Waveform
0
200
400
600
800
1000
Time

Figure 5-8.

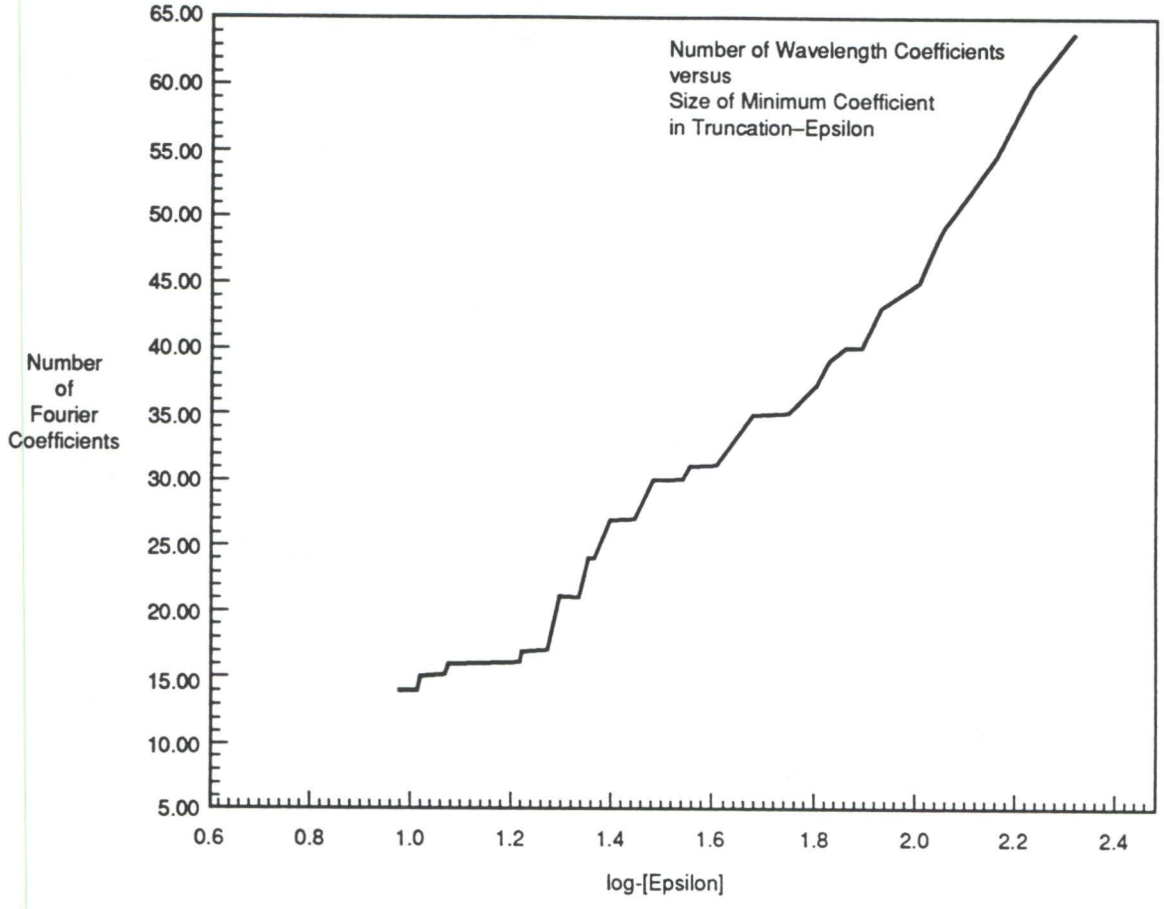
Number of Wavelength Coefficients
versus
Size of Minimum Coefficient
in Truncation–Epsilon
Number
of
Fourier
Coefficients
65.00
60.00
55.00
50.00
45.00
40.00
35.00
30.00
25.00
20.00
15.00
10.00
5.00
0.6
0.8
1.0
1.2
1.4
1.6
1.8
2.0
2.2
2.4
log-[Epsilon]

Figure 5-9.

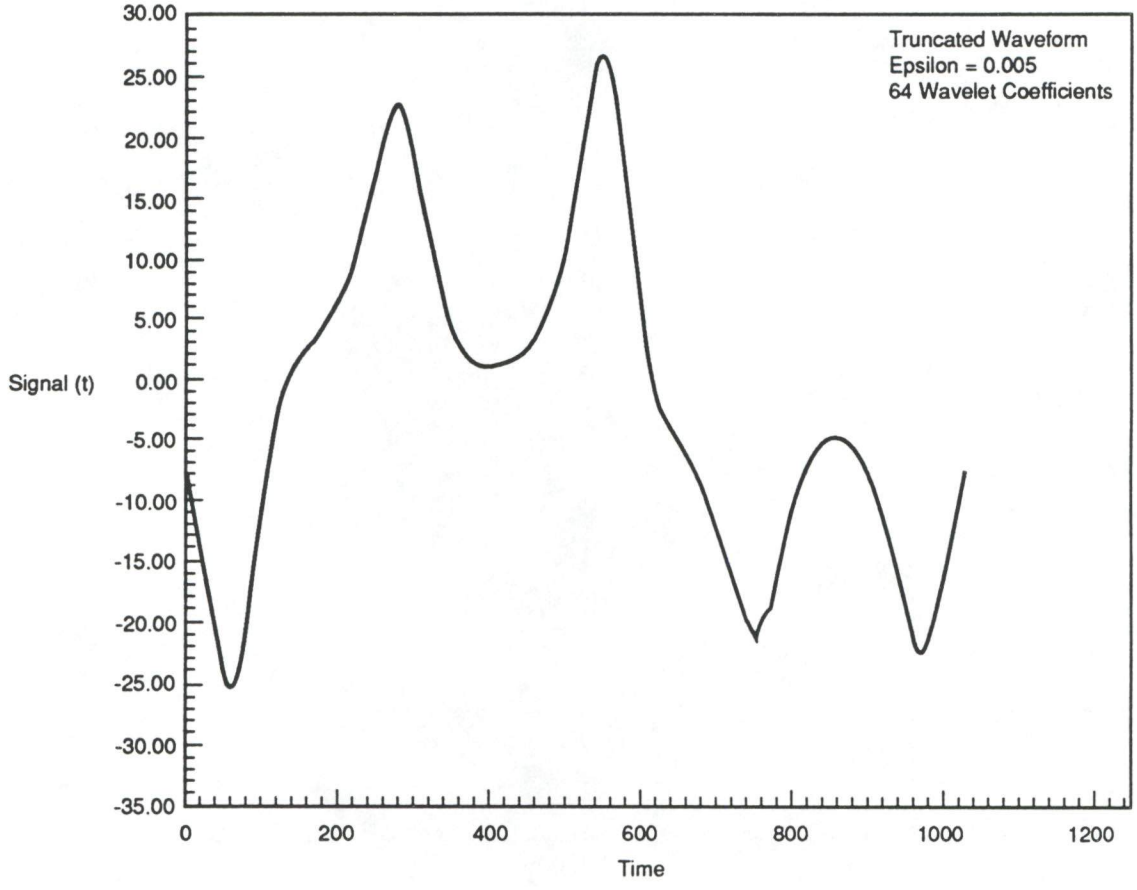
Truncated Waveform
Epsilon = 0.005
64 Wavelet Coefficients
Signal (t)
30.00
25.00
20.00
15.00
10.00
5.00
0.00
-5.00
-10.00
-15.00
-20.00
-25.00
-30.00
-35.00
0
200
400
600
800
1000
1200
Time

Figure 5-10.

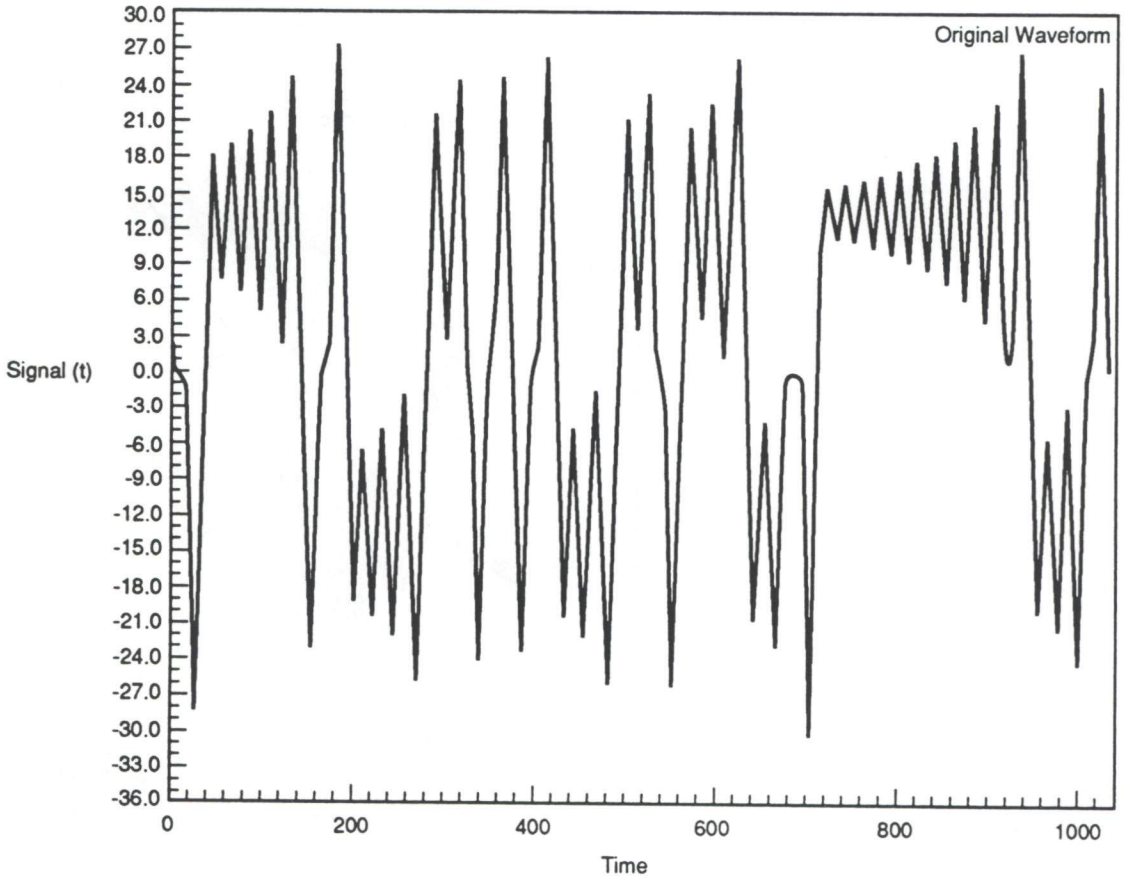
Original Waveform
Signal (t)
30.0
27.0
24.0
21.0
18.0
15.0
12.0
9.0
6.0
3.0
0.0
-3.0
-6.0
-9.0
-12.0
-15.0
-18.0
-21.0
-24.0
-27.0
-30.0
-33.0
-36.0
0
200
400
600
800
1000
Time

Figure 5-11.

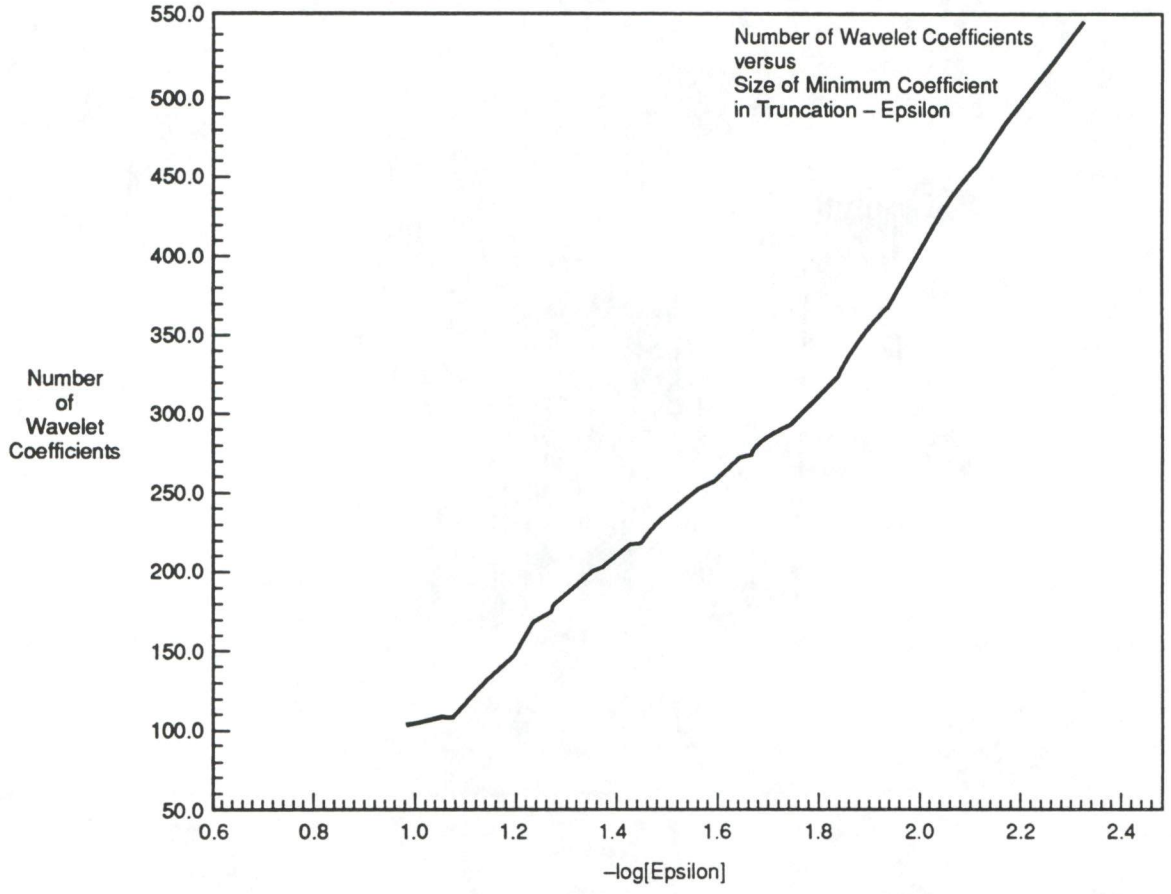
Number of Wavelet Coefficients
versus
Size of Minimum Coefficient
in Truncation – Epsilon
Number
of
Wavelet
Coefficients
550.0
500.0
450.0
400.0
350.0
300.0
250.0
200.0
150.0
100.0
50.0
0.6
0.8
1.0
1.2
1.4
1.6
1.8
2.0
2.2
2.4
–log[Epsilon]

Figure 5-12.

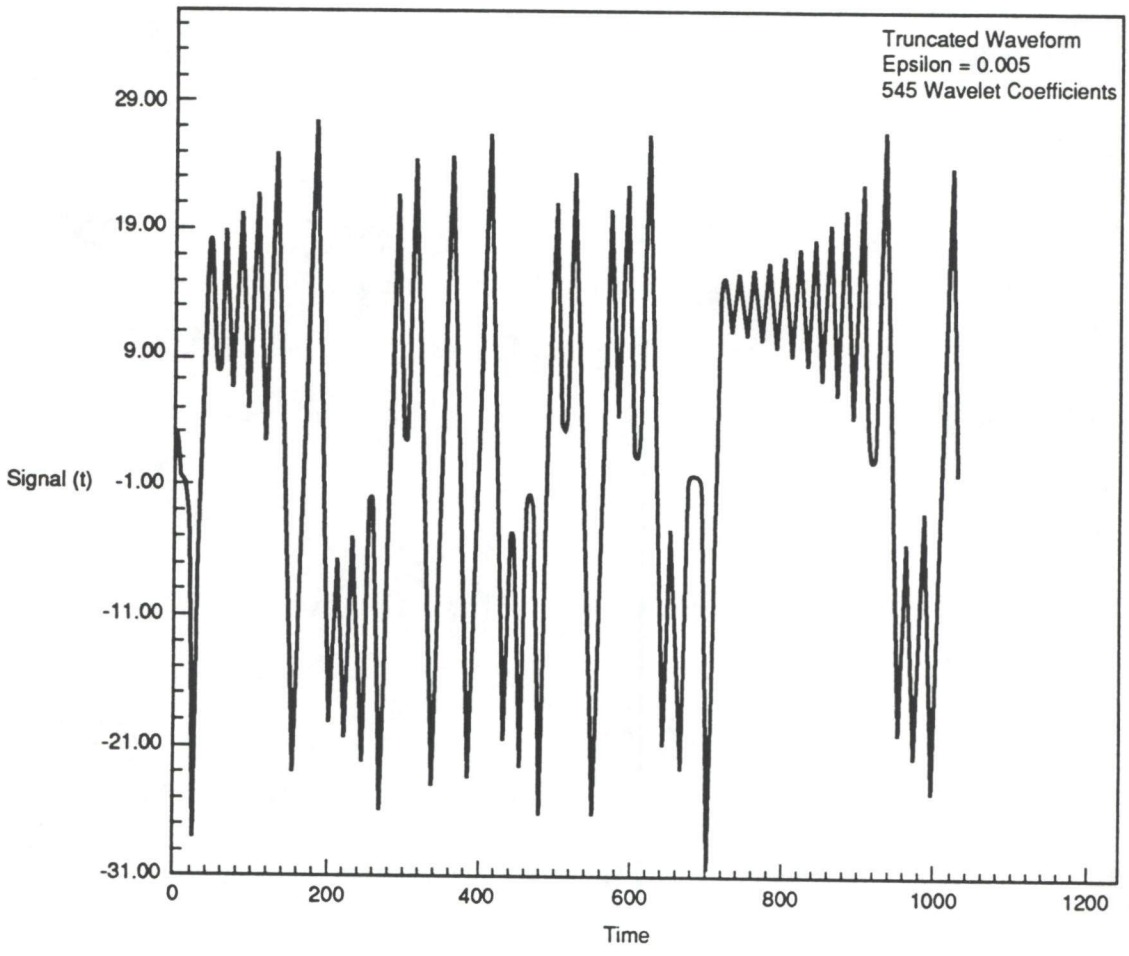
Truncated Waveform
Epsilon = 0.005
545 Wavelet Coefficients
29.00
19.00
9.00
-1.00
-11.00
-21.00
-31.00
Signal (t)
0
200
400
600
800
1000
1200
Time

Figure 5-13.

well a Fourier representation would do. In Figure 5-14 we show the plot of the number of required Fourier coefficients needed to achieve an accuracy ϵ. This is actually similar to that for the square root waveform and reflects the presence of high frequency components, just as the need for many more wavelet coefficients reflects the presence of detail at smaller scales. Figure 5-15 is the truncated waveform coming from using 983 Fourier coefficients to achieve an accuracy $\epsilon \approx 0.005$.

Our final set of pictures concerns the use of the Lemarié wavelet basis a basis with smoother members — to represent the square root waveform and the highly sampled Lorenz waveform. In Figure 5-16 we see the number of Lemarié coefficients required to achieve accuracy ϵ, and in Figure 5-17 we see the waveform reconstructed to accuracy ≈ 0.005, coming from the use of 61 Lemarié coefficients. Figure 5-18 is the MDL for this basis, and it indicates that one would do well to choose about 45 Lemarié wavelet coefficients in modeling the data of the square root waveform if encoding and transmission were the issue. At 45 Lemarié coefficients, the accuracy of the truncated waveform would be reduced to ≈ 0.015, which is quite adequate for most purposes. If one demands higher accuracy, it costs!

In our final three figures we show the capability of the Lemarié wavelet basis to capture the highly sampled Lorenz waveform. Figure 5-19 shows the time series reproduced by 339 wavelet coefficients, which we have determined are required for accuracy of ≈ 0.005, and in Figure 5-20 we see the reproduction using the 670 Lemarié coefficients required for an accuracy of ≈ 0.00005! Finally, we have performed the MDL analysis on the Lemarié wavelet basis

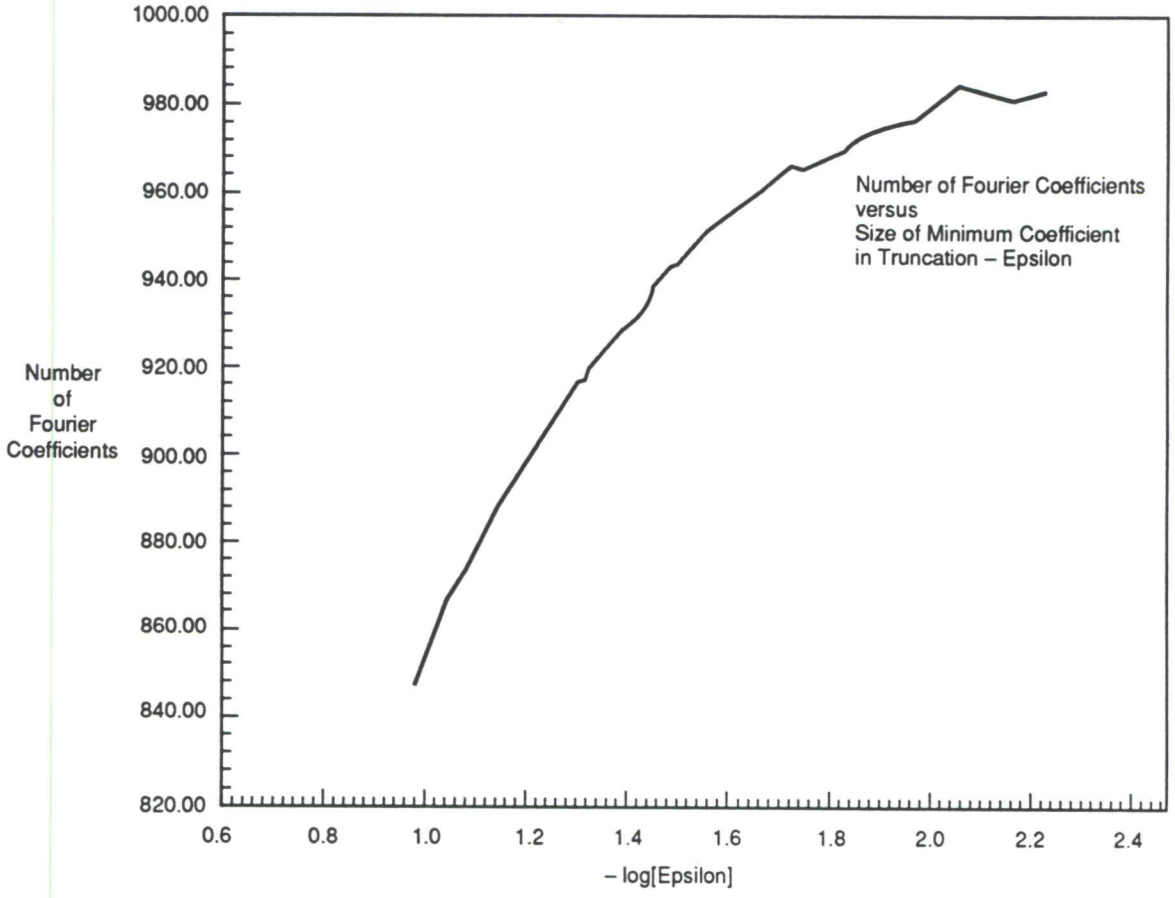
1000.00
980.00
960.00
940.00
920.00
900.00
880.00
860.00
840.00
820.00
Number
of
Fourier
Coefficients
Number of Fourier Coefficients
versus
Size of Minimum Coefficient
in Truncation – Epsilon
0.6
0.8
1.0
1.2
1.4
1.6
1.8
2.0
2.2
2.4
– log[Epsilon]

Figure 5-14.

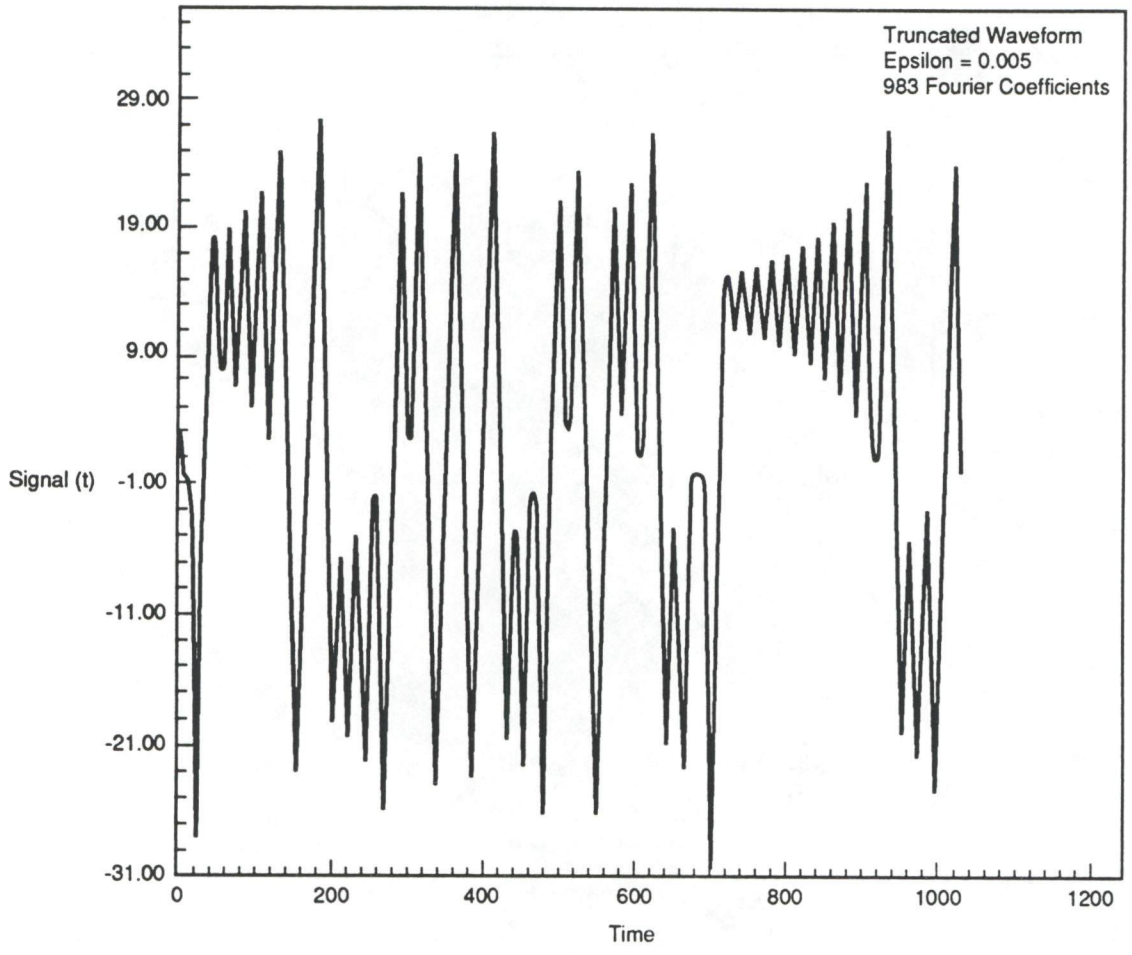
Truncated Waveform
Epsilon = 0.005
983 Fourier Coefficients
29.00
19.00
9.00
-1.00
-11.00
-21.00
-31.00
Signal (t)
0
200
400
600
800
1000
1200
Time

Figure 5-15.

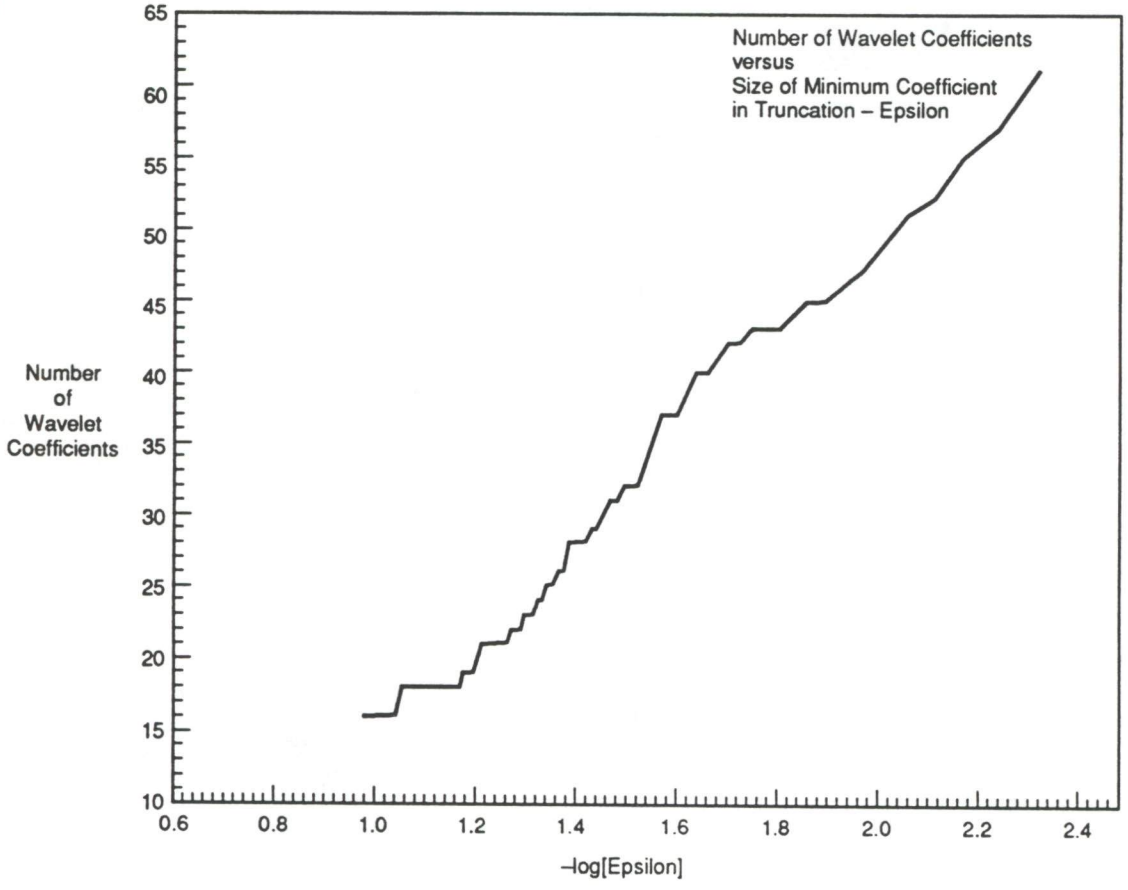
Number of Wavelet Coefficients
versus
Size of Minimum Coefficient
in Truncation – Epsilon
Number
of
Wavelet
Coefficients
65
60
55
50
45
40
35
30
25
20
15
10
0.6
0.8
1.0
1.2
1.4
1.6
1.8
2.0
2.2
2.4
–log[Epsilon]

Figure 5-16.

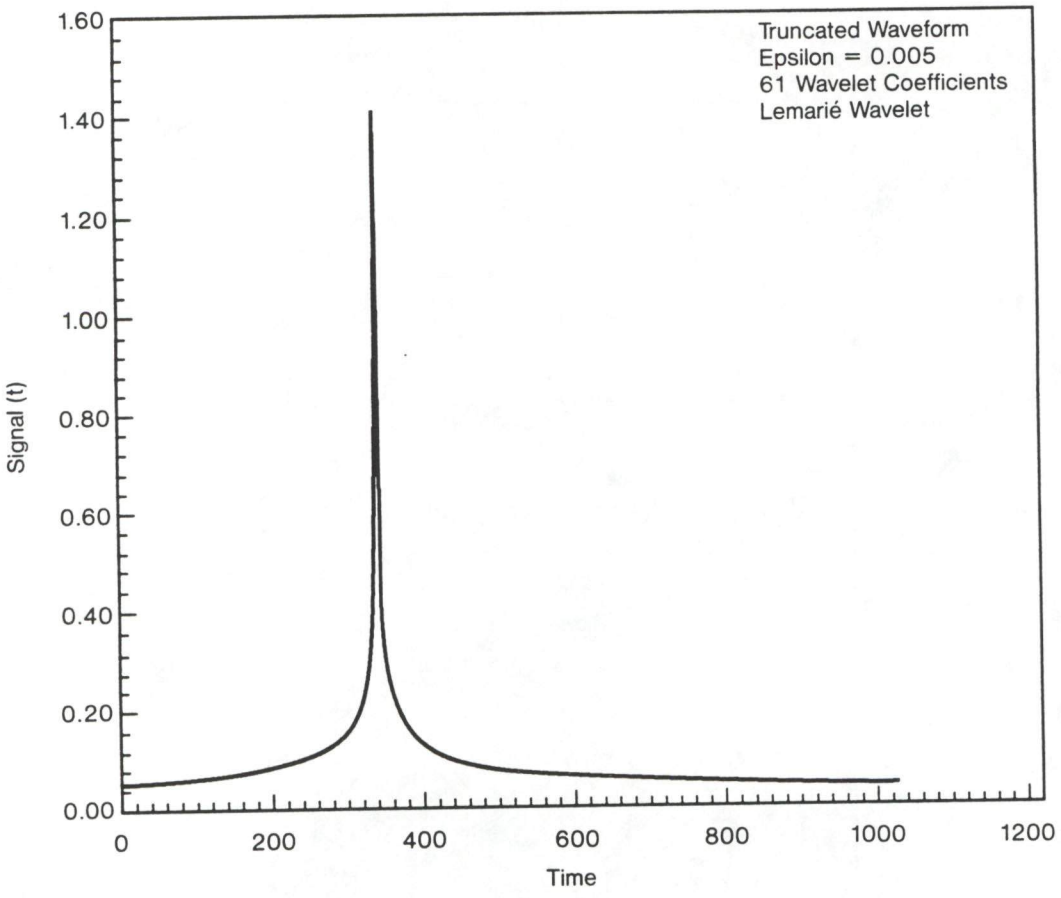
Truncated Waveform
Epsilon = 0.005
61 Wavelet Coefficients
Lemarié Wavelet
Signal (t)
1.60
1.40
1.20
1.00
0.80
0.60
0.40
0.20
0.00
0
200
400
600
800
1000
1200
Time

Figure 5-17.

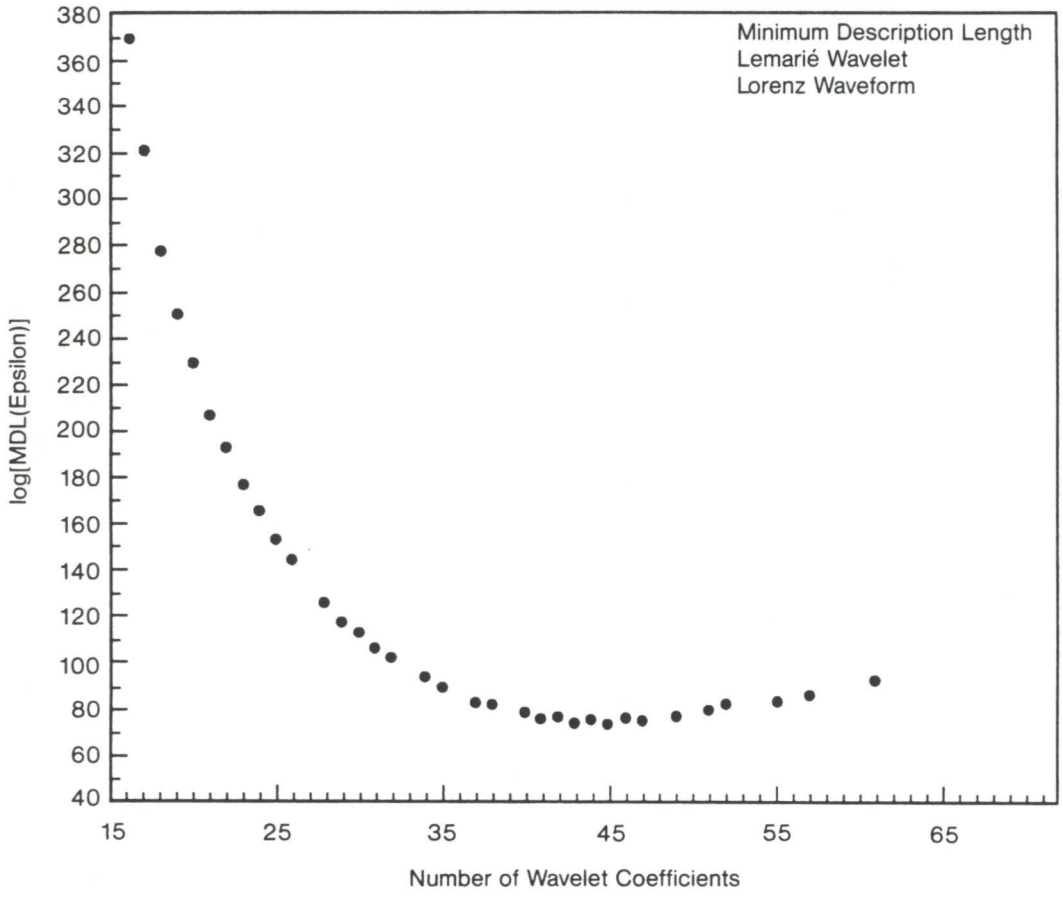
Minimum Description Length
Lemarié Wavelet
Lorenz Waveform
log[MDL(Epsilon)]
380
360
340
320
300
280
260
240
220
200
180
160
140
120
100
80
60
40
15
25
35
45
55
65
Number of Wavelet Coefficients

Figure 5-18.

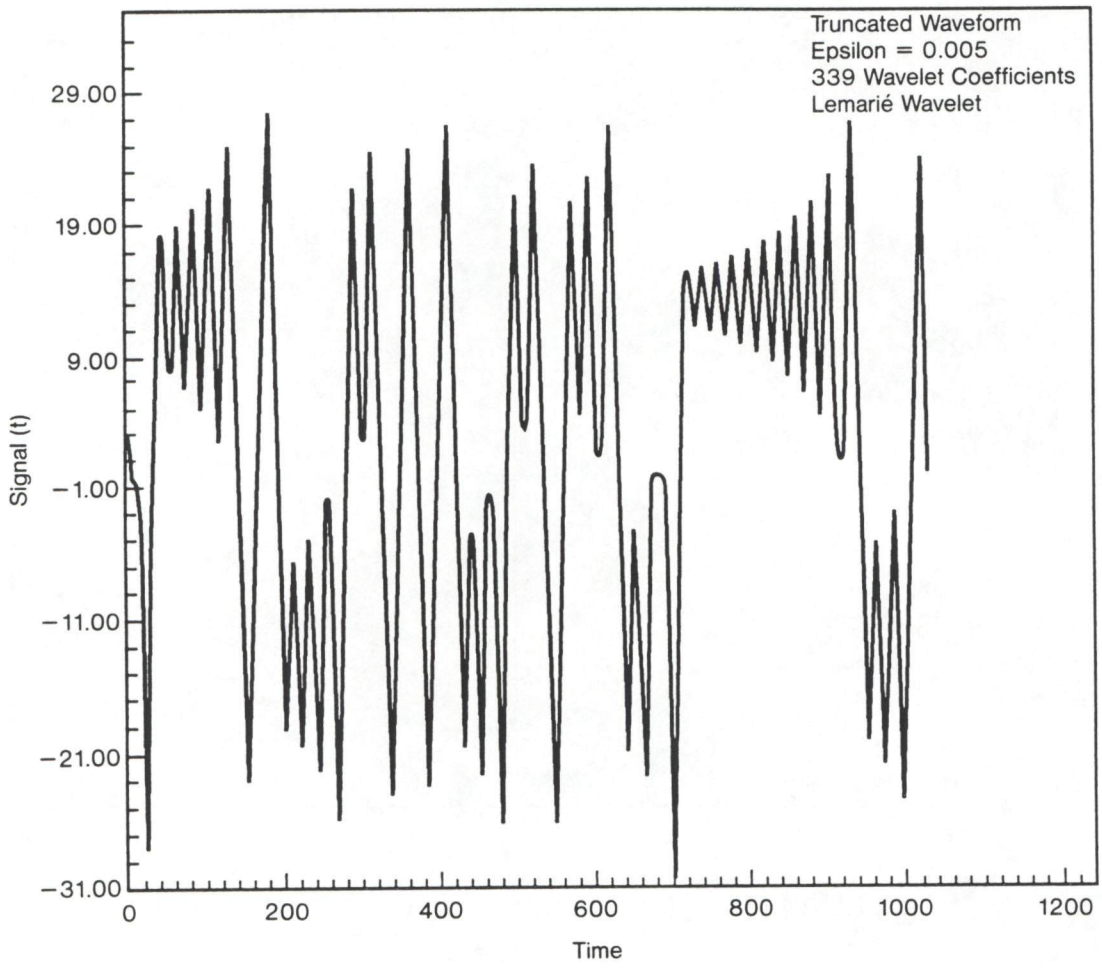
Truncated Waveform
Epsilon = 0.005
339 Wavelet Coefficients
Lemarié Wavelet
29.00
19.00
9.00
−1.00
−11.00
−21.00
−31.00
Signal (t)
0
200
400
600
800
1000
1200
Time

Figure 5-19.

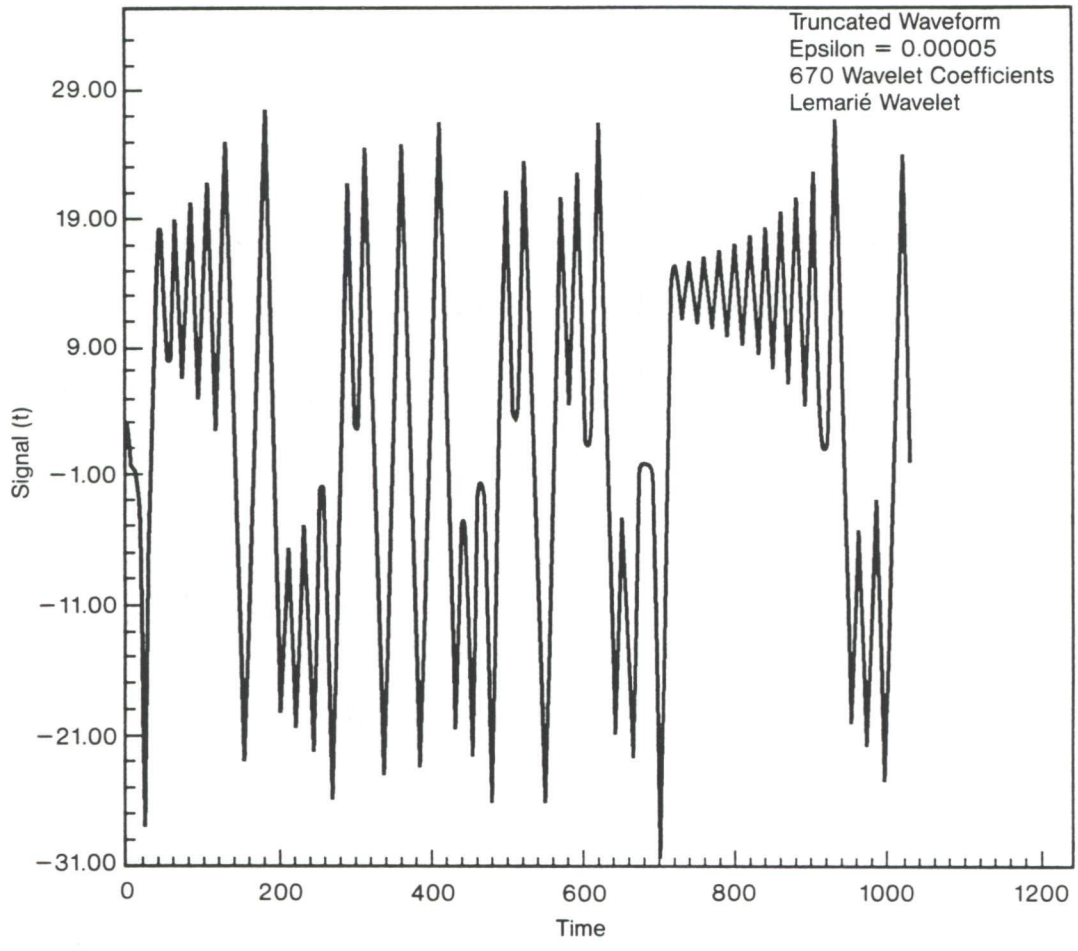
Truncated Waveform
Epsilon = 0.00005
670 Wavelet Coefficients
Lemarié Wavelet
29.00
19.00
9.00
−1.00
−11.00
−21.00
−31.00
Signal (t)
0
200
400
600
800
1000
1200
Time

Figure 5-20.

working on the highly sampled Lorenz data. Figure 5-21 indicates that using more than 540 or so wavelet coefficients is unattractive from the point of view we have described. At 550 wavelet coefficients we achieve an accuracy of $\approx 3 \times 10^{-4}$, which means we are unlikely to be constrained by this information theoretic criterion in the transmission of this waveform, if we can accept the cost of decreased accuracy.

As an attachment we reproduce the wavelet driver program that reads the waveform from an external file and performs the analysis described in this section.

The results here were all produced quite rapidly on a PC. This means that questions regarding the combination of accuracy, waveform reproduction, and information theoretic criterian on encoding can be asked accurately and quickly once the waveform and an expansion basis are given. The combination of the answers to use for a given problem is user dependent, but the collection of answers will prove useful as a part of a wavelet (or Fourier) toolkit.

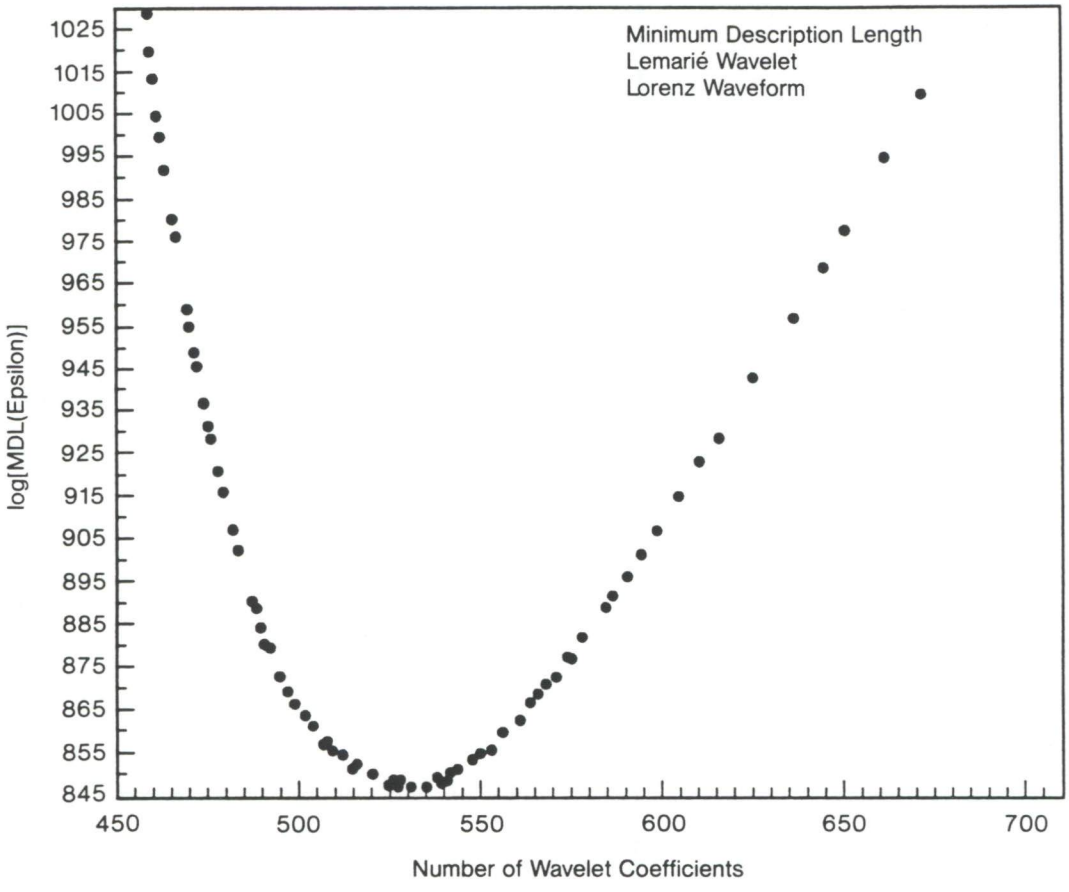
Minimum Description Length
Lemarié Wavelet
Lorenz Waveform
log[MDL(Epsilon)]
1025
1015
1005
995
985
975
965
955
945
935
925
915
905
895
885
875
865
855
845
450
500
550
600
650
700
Number of Wavelet Coefficients

Figure 5-21.

```
program wdriv
      parameter (NM=1024)
      real a(NM),b(NM),c(NM), x(5000)
C      b is orgin fn; c are log10 of wavelet coefficients
C      a is reconstr fn to acuracy eps; d is sorted c
      external daub4
      open(unit=23,file='waveform.dat',status='unknown')
      open(unit=24,file='wvcoeff.dat',status='unknown')
      open(unit=25,file='trunc.dat',status='unknown')
      open(unit=26,file='mdl.dat',status='unknown')
      open(unit=30,file='nc.dat',status='unknown')
      open(unit=2,file='lorx.dat',status='unknown')

      do 207 m=1,3000
      read(2,*) x(m)
207     continue

      pip = 4.0*atan(1.0)
      sigma = 1.d-6
      do j=1,NM
c           a(j)=0.
c           a(j)=1./sqrt(abs(j-NM/3+0.5)
c           a(j)=sin((j-1)*3.14159/NM).
           a(j)=sin((j-1)*3.14159/NM)**2
           a(j)=x(j+1400)
           b(j)=a(j)
      write(23,*),j,b(j)
      enddo
c     b(j) is now original data
14     format(i5,2x,f96.6)
      mmax=100
      do 101 mm=1,mmax
      eps=0.005 + (mm-1)*0.1/(float(mmax-1))
      do 907 m=1,NM
      a(m) = b(m)
907     continue

c     we place the orignial waveform b in a, then transform
c     again for a new eps

      call wt1(a,NM,1,daub4)
c     a(j) is now the full set of wavelet coefficients.

      amax=0.

      do j=1,NM,
            if(abs(a(j)).gt.amax)amax=abs(a(j))
      enddo

      nc=0
c     this is the count on the number of coefficients
```

```
      do j=1,NM
            c(j)=alog10(abs(a(j))+1.e-8)
            if(abs(a(j)).lt.eps*amax)then
                  a(j)=0.
8                  else
                  nc=nc+1
            endif
            if(mm.eq.1)write(24,*)j, c(j)
      enddo

c     c is now log10 of ALL the wavelet coefficients
c     a now the truncated set of nc wavelet
c      coefficient of size > eps*maximum of |a|

      write (30,*)-alog10(eps),nc
c      write(6,*) 'eps and number of coeff', -alog(eps),nc
      call wt1(a,NM,-1,daub4)
c      in a is now the RECONSTRUCTED WAVEFORM with nc coeff
      sum=0.0
      do j=1,NM
            if(mm.eq.1)write (25,*)j,a(j)
c      this is the reconstructed, truncated waveform
      sum=sum + (b(j)-a(j))**2

      enddo

      write(6,*' eps and mdl',-alog10(eps),sum/float(NM)*sigma) +
     1      (nc/2)*alog10(float(NM))
      write(26,* nc,sum/sigma*float(NM))
     1      +(nc/2)*alog10(float(NM))
101     continue
15     format(f9.5,ex,e9.5)
      end

      subrountine wt1(a,n,isign,wtstep)
      real a(n)
      if (n.lt.4) return
      if (isign.ge.0) then
            nn=n
            if (nn.ge.4) then
                  call wstep(a,nn,isign)
                  nn=nn/2

            goto 1
            endif
      else
            nn=4
            if (nnlle.n) then
                call wtstep(a,nn,isign)
                nn=nn*2
            goto 2
```

```
      endif
endif
return
end
INCLUDE'daub4.for'
```

REFERENCES

1. Rissanen, J. *Stochastic Complexity in Statistical Inquiry*, World Scientific (1989).

2. Lorenz, E. N. "Deterministic Nonperiodic Flow," *J. Atmos. Sci.* **20**, 130 (1963). In his "Irregularity: A Fundamental Property of the Atmosphere," *Tellus* **36 A**, 98-110 (1984) there is a delightful description of how he came to consider this model. He was concerned with linear prediction of nonlinear models and used this three degrees of freedom model as a testing ground for this study. He concluded that the idea of linear prediction for this kind of system would not do.

6 WAVELETS IN SEISMOLOGY

6.1 Introduction

A seismologist and two mathematicians (Goupillaud, Grossmann, and Morlet, 1984/85) started the modern era of wavelet analysis with the publication of their paper "Cycle-octave and Related Transforms in Seismic Signal Analysis." In retrospect it is clear that the authors did not anticipate future reaction to their ground-breaking work. First, they published in a journal obscure even to geophysicists: *Geoexploration*. Secondly, they neglected to tie their analysis to the long history of the use of wavelets in seismology, even though the seismologist, Goupillaud, was intimately familiar with the literature. This inadvertent lapse clouded the early history of the subject and led to misconceptions as to the origin of the term "wavelet."

In this section, we first review the early use of wavelets in seismology and describe the physical setting in which wavelets were initially proposed. We next briefly describe our understanding of how the term wavelet has flowed across the Atlantic and back. An orthogonal expansion in wavelets, the Gram-Charlier series, is then developed in order to illustrate certain of the problems dealt with in exploration seismology. Finally, we briefly consider the application of modern wavelet theory to seismology.

6.2 Origin of the Term "Wavelet"

Ricker (1940) seems to have been the first to use the term "wavelet" in a scientific setting. In subsequent years, seismic wavelet analysis, along the lines described above, became the standard fare for books on geophysical data analysis (Robinson and Treitel, 1980; Kanasewick, 1981; Claerbout, 1976). The lead author of the seminal paper on wavelets, Goupillaud, had contributed over the years to the seismic theory of wavelets (see Goupillaud, 1961, published when the author was with Continental Oil Company in Ponca City, Oklahoma).

After publication of Goupillaud et al. (1984/85), a group of French mathematicians led by Yves Meyer rapidly deepened and extended the subject. In French, *wavelets* translates to *ondelettes*. The work on ondelettes traveled across the Atlantic to be taken up by American mathematicians and others who converted ondelettes back into wavelets, believing that ondelettes had started life in France. While the origin of the term is not of any importance, the history of the evolution of ideas in a subject is of interest.

6.3 The Ricker Wavelet

A basic problem in exploration seismology is determining the depth to various layers, or beds, of sedimentary deposits (usually rock). The acoustic impedance mismatch between different layers leads to a reflection of sound

energy that is propagated downwards after being generated by some source at the surface. Observations of the two-way travel time between the generation of the sound and the return of the reflected signal provide estimates of the depths to various discontinuities. Although the acoustic velocity of rocks varies, the variation is not great: the historical problem in the subject has been to unravel the complicated nature of the return signal as recorded at the surface receiver. All inhomogeneities in the underlying rocks will result in reflections with varying amplitudes, leading to a highly complex recorded waveform.

The description of seismic recording given above can be quantified. A dynamite explosion (an early sound source that has largely been replaced by a variety of sources, including those producing coded signals) produces a disturbance, which reflects from an inhomogeneity below. This reflected disturbance arrives at the detector (geophone) and produces a displacement $a_i F(t - t_i)$ on the sensor recording system. The time of arrival, the critical parameter in seismic exploration, is designated by t_i. The function $F(t)$ describes the shape of the pulse, and this shape is assumed to be the same for all arrivals (normal incidence reflection). The amplitudes a_i of the wavelets arriving at time t_i are assumed to be random variables because the distribution of the various layers is not known a priori. The record as observed at the surface is a sum of the wavelets $F(t)$ translated in time by t_i, with each wavelet having an amplitude a_i.

Ricker (1940) first postulated that a seismogram was made up of a sum of wavelets. In Ricker's model, the shape of the wavelets is determined by the

explosive source, as smoothed out by the attenuation of the high-frequency components of the outgoing wave. Ricker examined numerous seismograms of waves propagated in homogeneous materials. On the basis of this evidence, he suggested that the waveform of the shape shown in Figure 6-1 could be the basis for further analysis. This waveform has the functional characteristics of the second derivative of the error function

$$\phi^{(2)}(x) = \frac{d^2}{dx^2}\left[\frac{e^{-x^2/2}}{(2\pi)^{\frac{1}{2}}}\right].$$

Ricker's idea was pursued by numerous investigators, who looked at various possible functional forms for a wavelet that could be used to construct the observed seismograms. Later, Ricker (1953) noted that a seismogram is an elaborate wavelet complex and that analysis consists of breaking it down into the wavelet components. In the wavelet complex, constituent wavelets can be contracted or expanded (dilation), a concept that is fundamental to modern wavelet theory.

Robinson (1957), in his MIT doctoral thesis, made a major advance in wavelet analysis that has since had a major influence on the exploration industry. He used the observed time series to obtain the wavelet shape rather than assuming some functional form a priori. On the basis of this wavelet shape, Robinson then calculated the strength of the impulses. The seismic trace x_t at a time t is made up of a sum of wavelets of the form

$$x_t = b_o\epsilon_t + b_1\epsilon_{t-1} + \cdots = \sum_{s=0}^{\infty} b_s\epsilon_{t-s},$$

where the wavelets all have the same shape b_s but are weighted by the respective strengths ϵ_t. Taking the autocorrelation of the seismic trace removes the random, uncorrelated elements ϵ_t, but preserves the dynamic wavelet shape

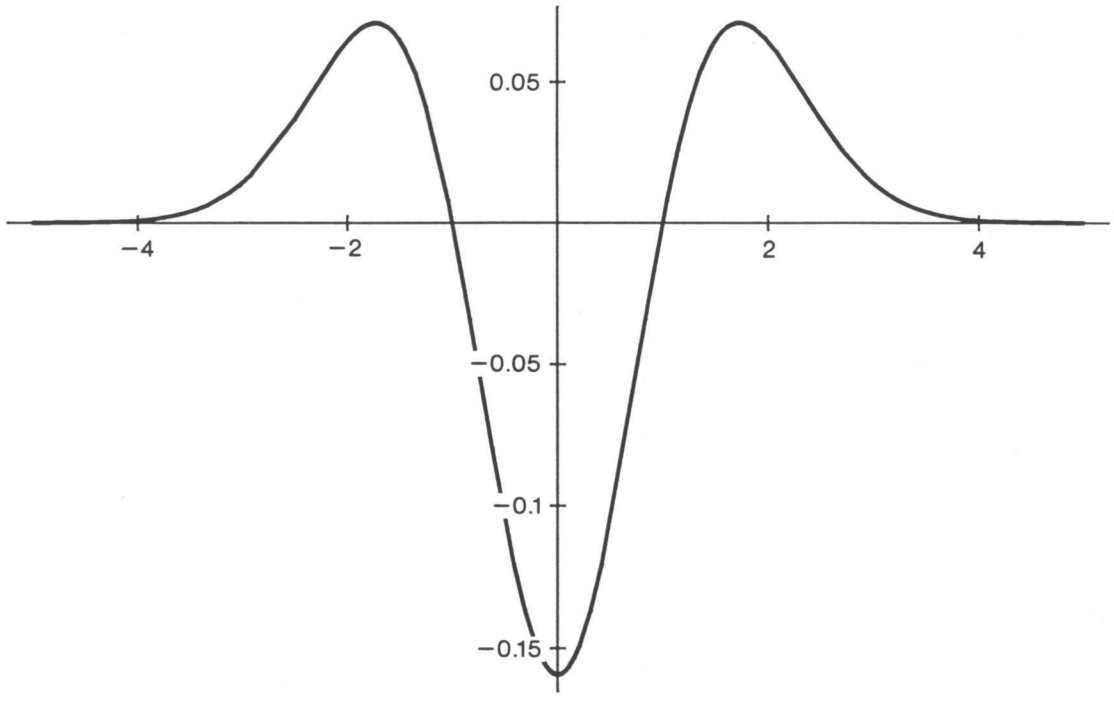

Figure 6-1. Ricker wavelet, $\frac{1}{2}\frac{d^2}{dx^2}\left[\exp\left(\frac{-x^2}{2}\right) / (2\pi^{1/2})\right]$.

b_t in the form of the autocorrelation of the wavelet b_t. Because phase information is lost in the autocorrelation, an infinite number of waveforms can have the same autocorrelation and power spectrum.

Some assumption must be made about the phase of the wavelet in order for the analysis to proceed. A common assumption is that of minimum phase, which means that the maximum of the wavelet is at its leading edge, but other assumptions have been applied. Once the wavelet shape is determined, the wavelet can be removed from x_t by filtering with the inverse wavelet. The filtering process then leads to the determination of ϵ_t, the amplitudes of the wavelets at times t. This procedure is basically an implementation of the Wold (1938) decomposition theorem, which states that the inverse wavelet shape is the optimum least squares predictor operator.

6.4 Gram-Charlier Series

Following Ricker's introduction of his wavelet (the second derivative of the error functions), various other derivatives were used in attempts to model seismograms (Horton, 1955). The subject can be brought together by considering a Gram-Charlier expansion (Cramér, 1946) of the form

$$x(t) = C_o\phi(t) + C_1\,\phi'(t) + \frac{C_2}{2!}\,\phi''(t) + \cdots + \frac{C_n}{n!}\,\phi^n(t) + \cdots, \qquad (6-8)$$

where the C_n are constant coefficients and $\phi^n(t)$ is the nth derivative of the error function

$$\phi^n(t) = \frac{1}{\sqrt{2\pi}}\,\frac{d^n}{dt^n}\,e^{-\frac{t^2}{2}}. \qquad (6-9)$$

The functions are localized in time, as illustrated by Figures 6-2 - 6-4, which show normalized $\phi^0(x)$ to $\phi^8(t)$, and by Figures 6-5 and 6-6, which illustrate normalized $\phi^{30}(t)$ and $\phi^{100}(t)$, respectively. The wavelets $\phi^n(t)$ are also localized in frequency because the Fourier transform of $\phi^0(t)$ is

$$\hat{\phi}(\omega) = \frac{1}{\sqrt{2\pi}} \int_{-\infty}^{\infty} e^{i\omega t - \frac{t^2}{2}}\, dt = e^{-\frac{\omega^2}{2}}, \qquad (6-10)$$

while the Fourier transfrom of the nth derivative of $\phi(t)$ is

$$\hat{\phi}^n(\omega) = (-i\omega)^n e^{-\frac{\omega^2}{2}}. \qquad (6-11)$$

The maximum of $|\hat{\phi}^n(\omega)|$ is at $\omega = n^{\frac{1}{2}}$, so the higher derivatives of $\phi(t)$ are required to capture the higher frequency components in a function $x(t)$ (see Figures 6-7 and 6-8).

The Gram-Charlier expansion of $x(t)$ is an orthogonal expansion because the Hermite polynomials $H_n(t)$ are defined by the relations

$$\frac{d^n}{dt^n}\, e^{-\frac{t^2}{2}} = (-1)^n\, H^n(t)\, e^{-\frac{t^2}{2}}. \qquad (6-12)$$

$H^n(t)$ is a polynomial of degree n, with the first few polynomials defined by

$$\begin{aligned} H_0(t) &= 1, H_1(t) = t, \quad H_2(t) = t^2 - 1, \\ H_3(t) &= t^3 - 3t, \quad H_4(t) = t^4 - 6t^2 + 3 \qquad (6-13) \\ H_5(t) &= t^5 - 10t^3 + 15t, \quad H_6(t) = t^6 - 15t^4 + 45t^2 - 15. \end{aligned}$$

By partial integration, we obtain relation

$$\frac{1}{(2\pi)^{1/2}} \int_{-\infty}^{\infty} H_m(t)\, H_n(t)\, e^{-\frac{t^2}{2}}\, dx = n! \text{ for } m = n \qquad (6\text{-}14)$$

$$= 0 \text{ for } n \neq m. \qquad (6\text{-}15)$$

The function $\frac{1}{(n!)^{\frac{1}{2}}}\, H_n(x)$ thus forms an orthonormal set of polynomials associated with the error function. The coefficients C_n in the Gram-Charlier

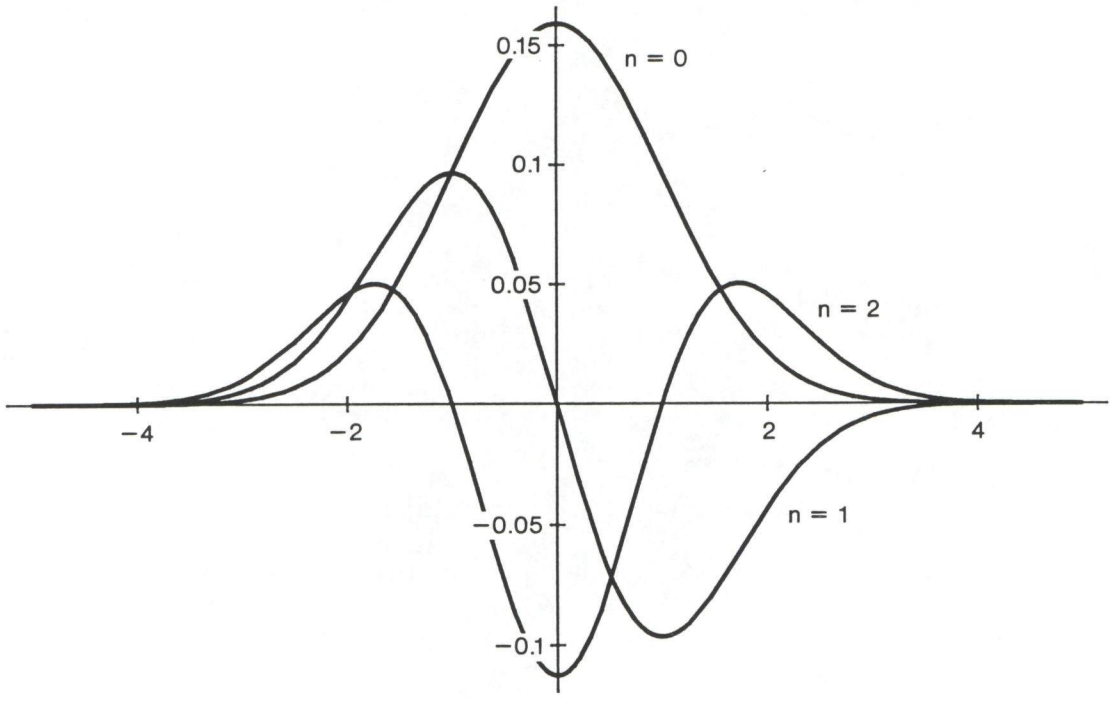

Figure 6-2. The error function $\vartheta(t) = \frac{1}{\sqrt{2\pi}} e^{-t^2/2}$ and its first five derivatives $\frac{1}{(2\pi)^{1/2}} \frac{d^2}{dt} (e^{-t^2/2})$ and $\frac{1}{(2\pi 21)^{1/2}} \frac{d^2}{dt^2} (e^{-t^2/2})$.

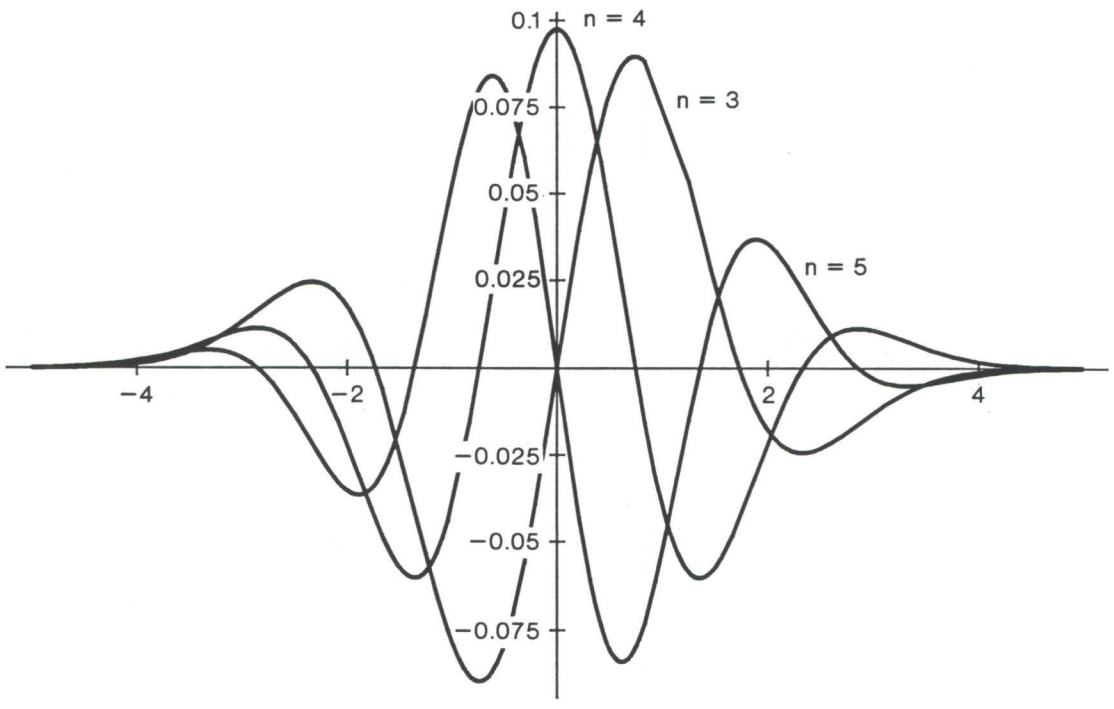

Figure 6-3. Normalized derivatives of the error function, $\frac{1}{(2\pi n!)^{1/2}} \frac{d^n}{dt^n} (e^{-t^2/2})$ box n = 3, 4 and 5.

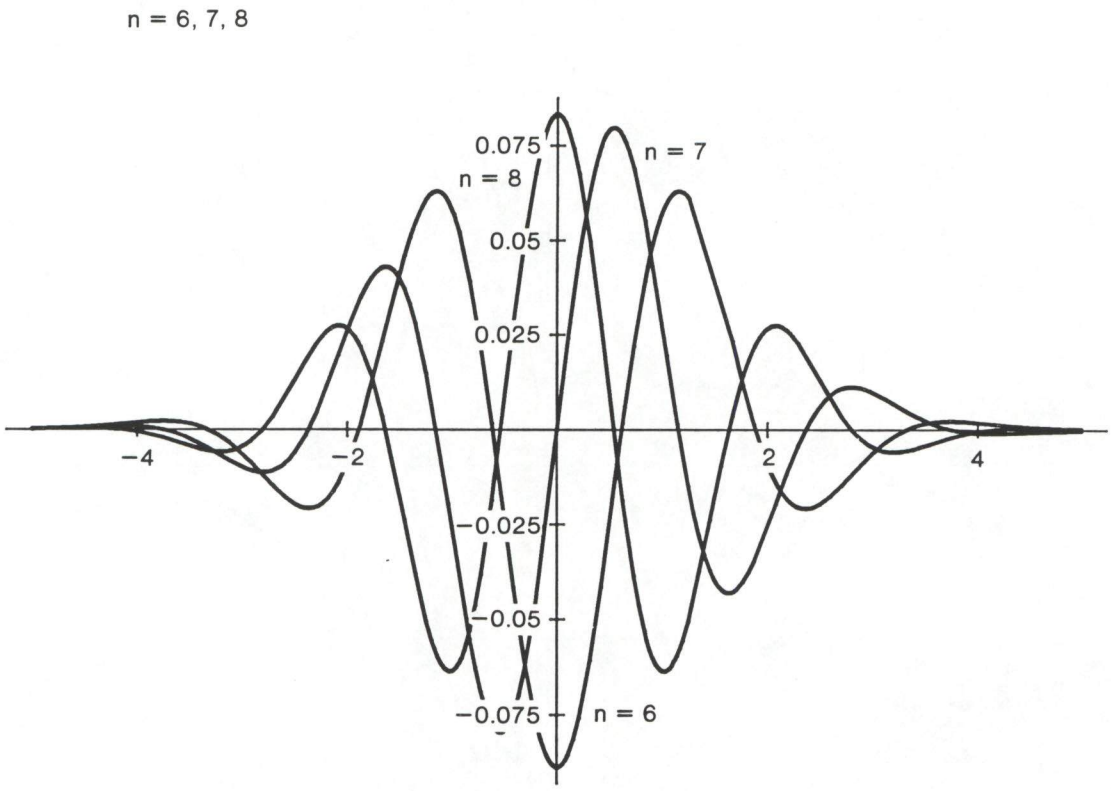

Figure 6-4. Normalized derivatives of the error function, $\frac{1}{(2\pi n!)^{1/2}} \frac{d^n}{dt^n} (e^{-t^2/2})$ box n = 6, 7 and 8.

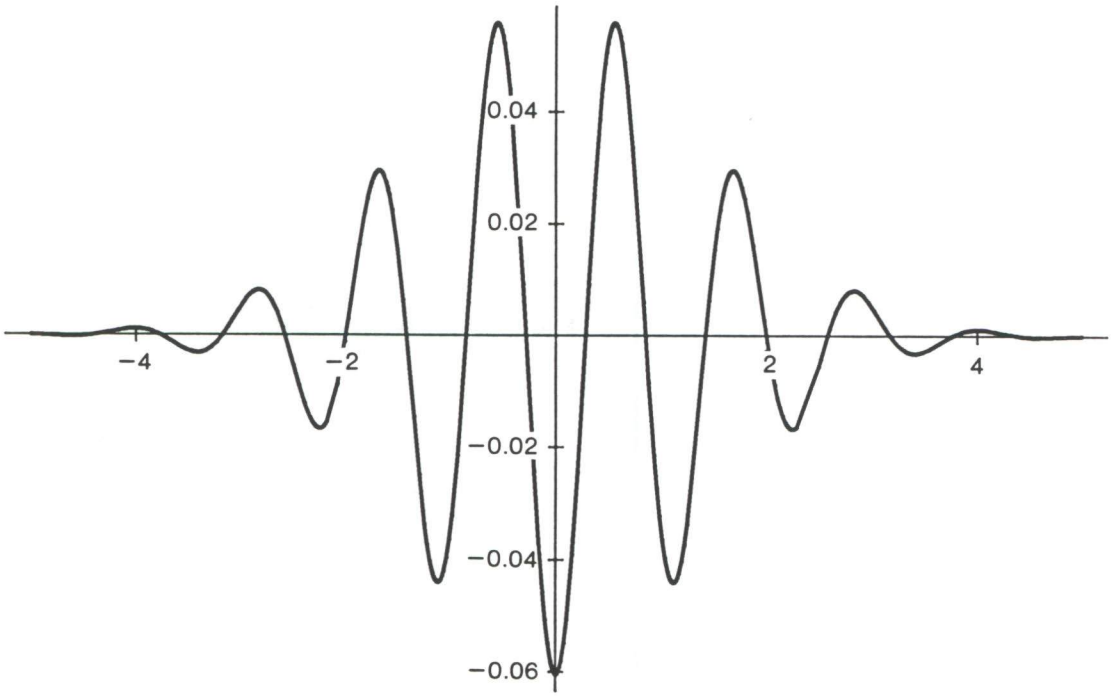

Figure 6-5. Normalized derivative of the error function, $\frac{1}{(2\pi n!)^{1/2}} \frac{d^n}{dt^n} (e^{-t^2/2})$, box n = 30.

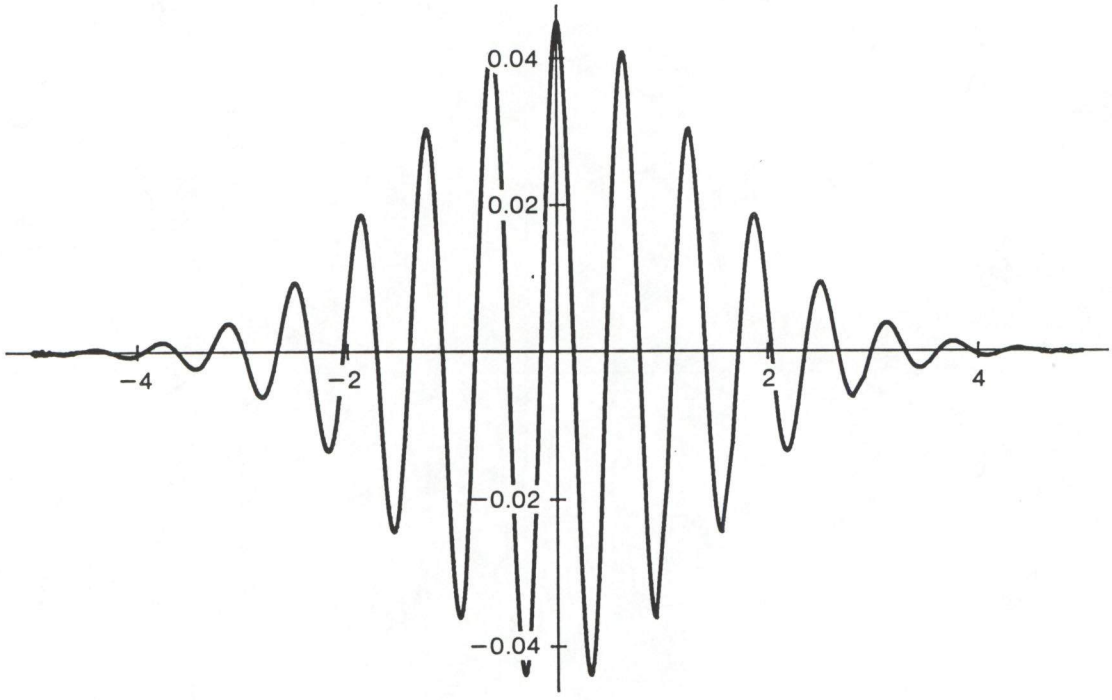

Figure 6-6. Normalized derivative of the error function, $\frac{1}{(2\pi n!)^{1/2}} \frac{d^n}{dt^n} (e^{-t^2/2})$, box n = 100.

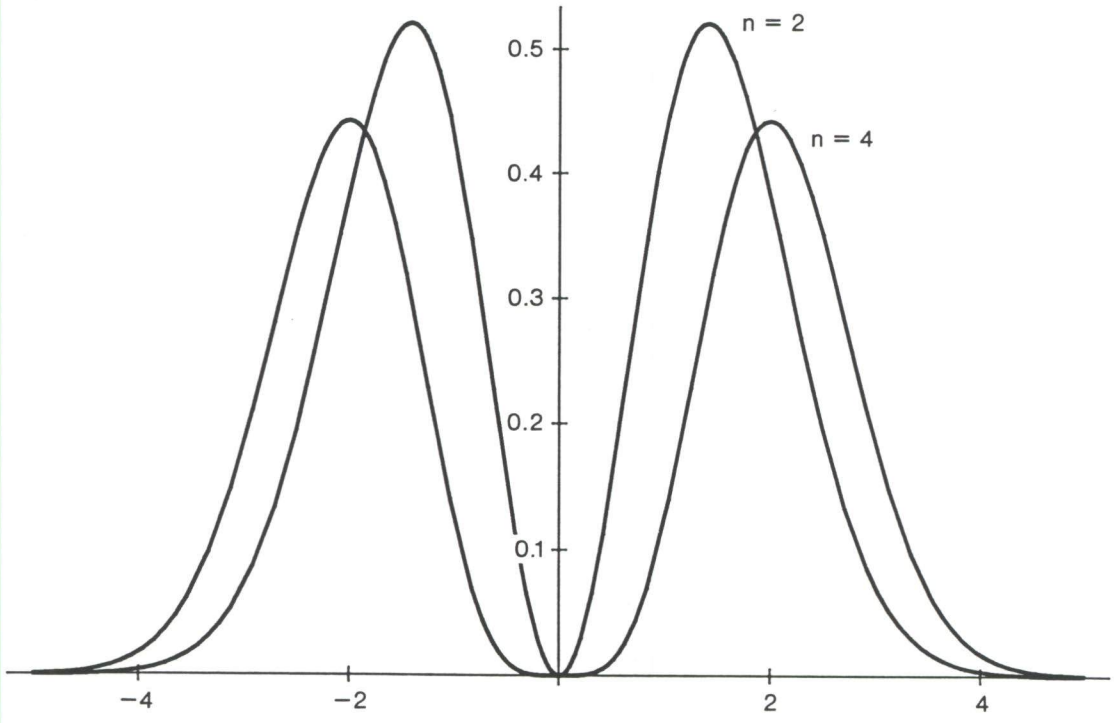

Figure 6-7. The normalized absolute value of Fourier transform of the n derivative of the error function, $|\hat{\alpha}^n(\omega)| = \frac{|(-i)^k \omega^n e^{-\omega 2/2}|}{(n!)^{1/2}}$ for n = 2 and 4. The case for n = 2, represents five Fourier transforms of the Ricker wavelet (see Figure 6-1).

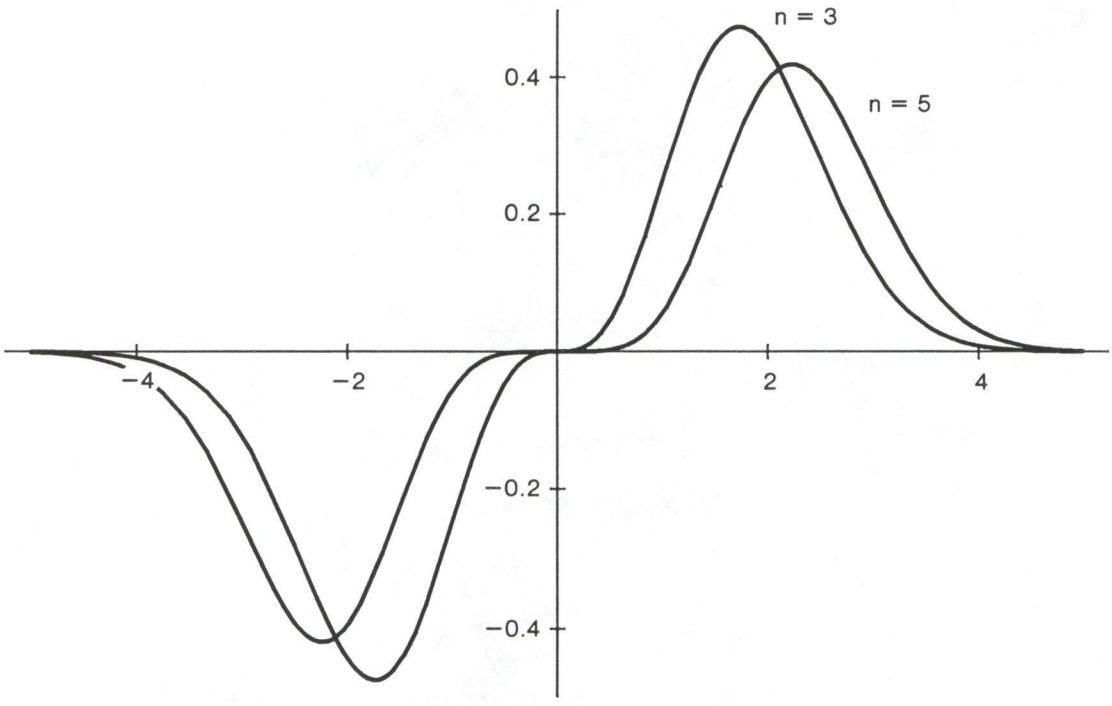

Figure 6-8. The normalized Fourier transform of the nth derivative of the error function, $\hat{\alpha}^n(\omega) = \frac{(-i\omega)^n e^{-\omega 2/2}}{(n!)^{1/2}}$ for n = 3, 5. For odd n, the transform is purely imaginary.

expansion of $(x)t$ are then determined by

$$C_n = (-1)^n \int_{-\infty}^{\infty} H_n(t)\, x(t)\, dt. \qquad (6-16)$$

Dilation and translation are achieved by the familiar statistical transformation

$$t = \frac{t-m}{\sigma}.$$

Higher time resolution is achieved through setting σ to a small number that is less than unity. The resulting Fourier transform of $\phi^n(t)$ after transformation is

$$|\sigma| e^{im\omega} \hat{\phi}^n(\sigma\omega).$$

The uncertainty principle is clearly at work here, with increased time resolution gained at the sacrifice of frequency resolution.

As noted above, the autocorrelation function of the seismogram is used to obtain the shape of the wavelet. The power spectrum of $\phi^n(t)$ is

$$S^n(\omega) = \omega^{2n} e^{-\omega^2},$$

which on cosine transformation yields the autocorrelation function

$$B^n(\tau) = \pi^{\frac{1}{2}}\, 2^{-n-1}\, e^{-\frac{\tau^2}{4}}\, H_{2n}\, (\frac{\tau}{\sqrt{2}}).$$

The autocorrelation function for the Ricker wavelet (see Figure 6-1) is shown in Figure 6-9.

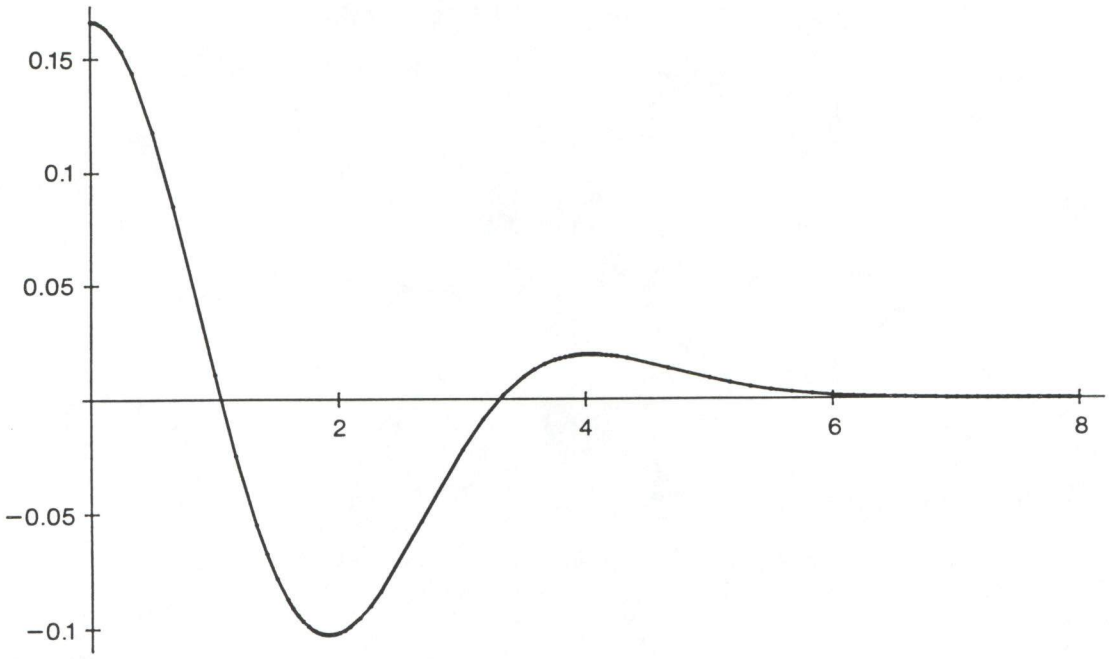

Figure 6-9. The autocorrelation function for the Richer wavelet shown in Figure 1.

6.5 Application of Modern Wavelet Theory to Seismology

Developments of the past few years have greatly advanced the analysis of wavelets from their rudimentary beginning in seismology. Concepts such as compact support of wavelets, orthogonality of translates, dilations of wavelets, and the understanding of conditions of differentiability have opened up a new chapter in harmonic analysis. However, there have been no applications of this new theory in seismology, despite its origins in the subject. The reason for this surprising development is not that seismologists are not aware of wavelets', they definitely are. In the exploration business, small advantages in reading seismograms can reap companies economic rewards that are measured in billions of dollars. Any advance in signal analysis is rapidly adopted by the industry because it may affect the bottom line. Yet modern wavelets have not been taken up.

The lack of application of modern wavelet analysis to seismology most likely derives from the fact that, in seismology, time resolution is the whole game. For almost all seismic problems, frequency resolution is not critical; it is the times of signal arrivals that determine the depths of reflections. Frequency becomes important if attempts are made to identify strata on the basis of attenuation characteristics, but these techniques are not standard in most exploration programs. Modern wavelet analysis has high applicability to problems in which high resolution is desirable in both frequency and time. At present the seismic community sees no advantage in this property, and

appears ready to continue to use old-style wavelets.

REFERENCES

1. Claerbout, J. (1976) *Fundamentals of Geophysical Data Processing*, McGraw-Hill, New York

2. Cramér, H. (1946) *Mathematical Methods of Statistics*, Princeton University Press, Princeton

3. Goupillaud, P. (1961) An approach to the inverse filtering of near-surface layer effects from seismic records, *Geophysics*, **26**, 754-760

4. Goupillaud, P., A. Grossmann and J. Morlet (1984/85) Cycle-octave and related transforms in seismic signal analysis, *Geoexploration*, **23**, 85-102

5. Horton, C. (1955) The structure of the noise background of a seismogram, *Geophysics*, **20**, 565-584

6. Kanasewick, E. (1981) *Time Sequence Analysis in Geophysics*, 3rd ed., University of Alberta Press, Edmonton

7. Ricker, N. (1940) The form and nature of seismic waves and the structure of seismograms, *Geophysics*, **5**, 348-366

8. Ricker, N. (1953) Wavelet contraction, wavelet expansion, and the control of seismic resolution, *Geophysics*, **18**, 769-792

9. Robinson, E. (1957) Predictive decomposition of seismic traces, *Geophysics*, **22**, 767-778

10. Robinson, E. and S. Treitel (1980) *Geophysical Signal Analysis*, Prentice-Hall, Englewood Cliffs, N.J.

11. Wold, H. (1938) *A Study in the Analysis of Stationary Time Series*, Almquist and Wiksells, Uppsala

7 WAVELETS AND LATTICE SHINGLING

We restrict attention to a lattice $L \subset R^M$ and the construction of associated wavelet bases for $L^2(R^M)$. More precisely, let L' be a sublattice of L and τ an endomorphism of L not necessarily preserving L'. A *lattice shingling* of R^M is made by finding a closed set $S \subset R^M$ such that: (1) $\{\ell S, \ell \in L'\}$ covers R^M, and (2) almost every point in R^M lies in exactly δ shingles ℓS where δ is the *depth*. Suppose $det(\tau) = k$ is an integer greater than one and that $\tau(S)$ is an (almost) disjoint union of k shingles $\tau(S) = \ell_1(S) \cup \ldots \cup \ell_k(S), \ell_i \in L'$. In this case we say the shingling admits the expansion τ.

We say a shingling *underlies* a wavelet basis if the interior of the shingles on a given scale constitutes the supports of the wavelet basis functions on that scale. For example, Figures 7-2 and 7-3 of "Wavelet incorporating reflection" show the shingling pattern underlying the recursive construction of $D4$ and $D6$.

In higher dimensions, shingles typically assume a fractal shape,[1] however, there are interesting classes where the shingles are the rectangular solids $1 \times \sqrt{2}$ (in the plane), $1 \times 2^{1/3} \times 2^{2/3}$ (in 3-space), and $1 \times \ldots \times 2^{M-1/M}$ (in R^M). The lattice L is the integral span of $2^{i/M} e_i, i = 0, \ldots, M-1$ and set $L' = \text{span}\{e_0, (2N-1)2^{1/M} e_1, \ldots, (2N-1)2^{M-1/M} e_{M-1}\}$. The endomorphism τ cyclicly permutes the axes and expands uniformly by $2^{1/M}$. For simplicity we consider the first interesting case not on the line, $M = N = 2$.

[1] W. Thurston, "Groups, Tilings and Finite State Automata," Center for Geometry and Computing, Univ. of Minn. (Math. Dept.), Preprint, 1990.

The basic shingle S_o is shown in Figure 7-1.

The shingle S_0 and its integral horizontal translates S_1, S_2, and S_3 together cover $\tau(S_0)$. We consider a ϕ with support on $\tau(S_0)$. The formula

$$\phi(x) = \sum c_i \phi(f_i(x)), \qquad (7-1)$$

where $f_i : S_i \to \tau(S_0)$ is $S_i \overset{+(-i,0)}{\to} S_0 \overset{\tau}{\to} \tau(S_0)$, can be used to define a scaling function ϕ at the points $a = (2, 2\sqrt{2}), b = (4, 2\sqrt{2}), c = (2, \sqrt{2})$ and $d = (4, \sqrt{2})$ provided an eigenvalue condition is (uniquely) satisfied.

From line (1) we get a generalized ϕ satisfying:

$$\begin{aligned} \phi(a) &= c_0\phi(b) + c_1\phi(d) \qquad (7\text{-}2) \\ \phi(b) &= c_2\phi(b) + c_3\phi_3(d) \\ \phi(c) &= c_0\phi(a) + c_1\phi(c) \\ \phi(e) &= c_2\phi(a) + c_3\phi_3(c). \end{aligned}$$

The eigenvalue condition to solve for $\vec{\phi} = \begin{pmatrix} \phi(a) \\ \phi(b) \\ \phi(c) \\ \phi(d) \end{pmatrix}$ is that:

$$\begin{vmatrix} -1 & c_0 & 0 & c_1 \\ 0 & c_2 - 1 & 0 & c_3 \\ c_0 & 0 & c_1 - 1 & 0 \\ c_2 & 0 & c_3 & -1 \end{vmatrix} = 0. \qquad (7-3)$$

The other orthogonality equations for the overlapping translates of ϕ are:

$$\begin{aligned} c_0^2 + c_1^2 + c_2^2 + c_3^2 &= 1 \text{ and} \qquad (7\text{-}4) \\ c_0c_2 + c_1c_3 &= 0. \end{aligned}$$

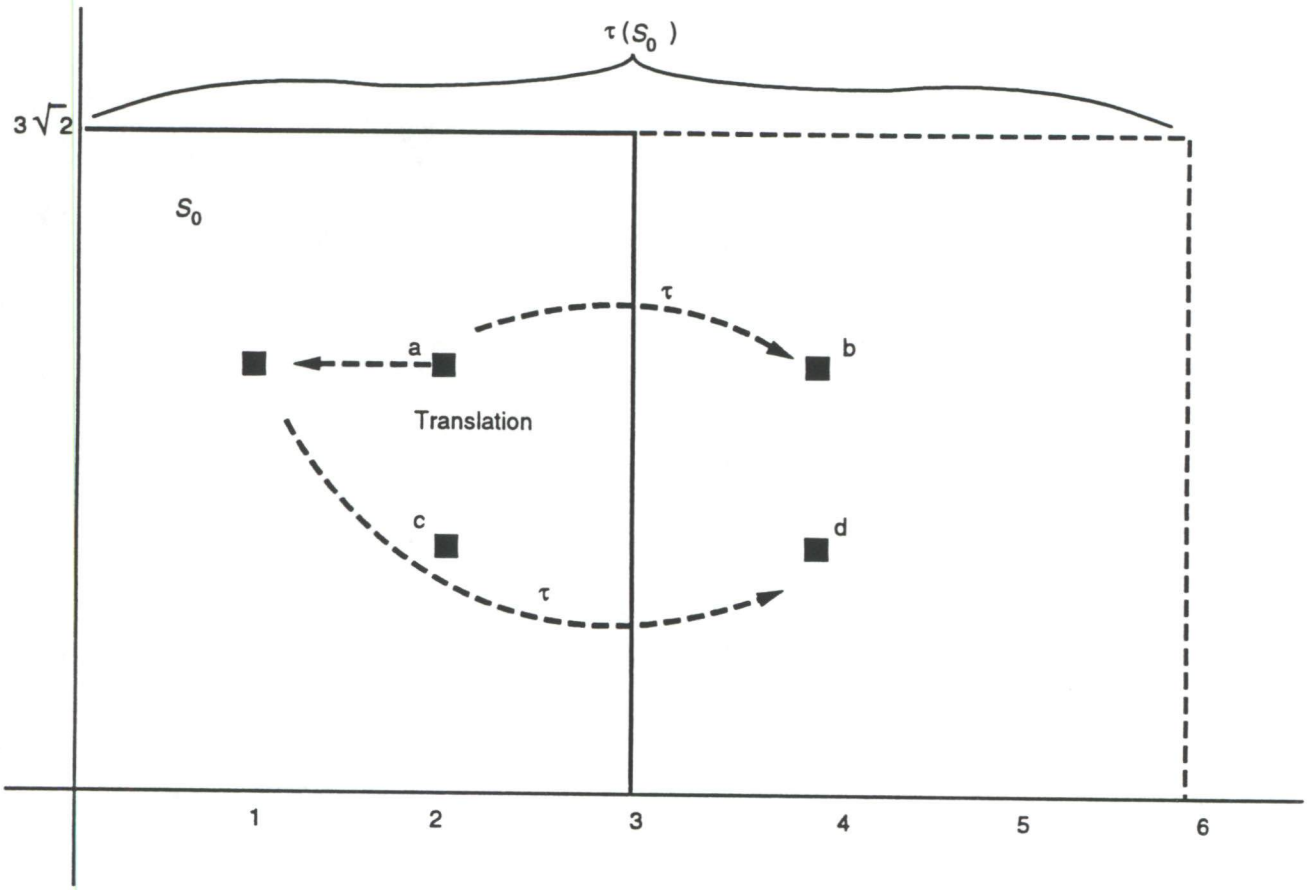

Figure 7-1. Basic Shingle S_0

The differentials of the three left-hand sides of (7-3) and (7-4) at the solution $(c_0, c_1, c_2, c_3) = (1, 0, 0, 1) = x$ are:

$$\begin{array}{lll} -3dc_0 & -1dc_1 - 3dc_2 & 3dc_3 \\ -2dc_0 & & +2dc_3 \\ & dc_1 + dc_2 & . \end{array} \qquad (7-5)$$

Since these differentials are independent, the implicit function theorem guarantees a smooth arc β of solutions running through $x = (1, 0, 0, 1) \in R^4$.

The point x corresponds to a Haar solution, but away from x along β the solutions are more interesting. If $2N$ is increased from 4 to 6 a similar analysis shows that the 0^{th} moment of the coefficients can also be killed along a one-dimensional family. Presumably as N increases, additional moments may also be killed. A similar pattern is expected for M-dimensional generalization of this construction. To check these speculations requires rather tedious and piecemeal calculations or some algebraic geometric insight into the relevant solution spaces of "varieties."

Constructions of bases for L^2 (hyperbolic plane) or L^2 (symmetric space) may be pursued by considering lattice shinglings in these geometries. Unfortunately we know of no signal processing motivation for studying these function spaces.

In another direction, some extension of wavelets adapted to non-lattice, but self-similar, shinglings could be interesting. How this might have been done and what use these might be deserves further thought.

Finally, a very interesting problem is how self-similarity might be sac-

rificed near domain boundaries to reduce "Gibbs effects" while retaining orthonormality. This problem is analyzed in Section 4.5.

7.1 Wavelets Incorporating Reflection

Daubechies's construction of compactly supported wavelets based on scale and translation has an analogue based on scale, translation and reflection. That is, the wavelet functions ψ at any given scale alternate between being translates ψ_i and reflected translates $\tilde{\psi}$: of a basic ψ_0. This example is pursued primarily to indicate the flexibility of wavelets. However, this style of wavelet might have utility. It is a consequence of orthogonality to translates that no "mother" wavelet ϕ except a Haar function and no wavelet ψ can be symmetric. If in some applications this is perceived as a fault, it may be partially redressed by interspersing reflected copies $\tilde{\psi}$ of the basic wavelet.

In speech, for example, consonants commence with a sharp attack and gradually tail off, so the time series will not be similar to its reversal. Here, perhaps, wavelet asymmetry could actually be useful. In other situations, e.g., Hamiltonian systems, time reversal is intrinsic and reflected wavelets might be appropriate.

We begin with quick picture of $D4$, the simplest interesting wavelet. When we attempt to introduce reflections to make a $D4'$, this "fails": the wavelet degenerates back to the Haar wavelet. Next we stick reflections into $D6$ to make a family $D6'$. This family contains several easy-to-spot Haar

wavelets and a linear analysis around one of these shows that it is part of a nontrivial continuous family. Thus the construction of a $D6'$ "succeeds." As in Daubechies's work, once a nontrivial solution exists it is possible to tune them to maximize approximation properties (i.e., killing moments), smoothness, or other criteria. We have not carried this forward, but suspect a small price is necessary for including reflections. That is, a couple of additional coefficients will be required to kill a given number of moments or achieve a given smoothness.

Daubechies begins with the dilation equation:

$$\phi(x) = \sum_{i=0}^{2N-1} c_i \, \phi(2x - i)$$

and defines

$$\psi(x) = \sum_{i=0}^{2N-1} (-1)^i \, c_i \phi(2x - (2N-1) + i).$$

Assume that the functions $\{\phi(x-k)\}$ are orthonormal. When $N = 2$ the result is:

$$c_0^2 + c_1^2 + c_2^2 + c_3^2 = 2 \qquad (7-6)$$

and

$$c_0 c_2 + c_1 c_3 = 0. \qquad (7-7)$$

The most elementary approximation condition, that is, constants $\subset$ span $\{\psi(x-k)\}$, implies the vanishing of the zero$^{\text{th}}$ moment:

$$c_0 - c_1 + c_2 - c_3 = 0. \qquad (7-8)$$

Add twice (7-2) to (7-1) to find that $(c_0 + c_2)^2 + (c_1 + c_3)^2 = 2$. By (7-3) $(c_0 + c_2) = (c_1 + c_3)$ so $(c_0 + c_2) = 1 = (c_1 + c_3)$. This gives the usual

(but redundant) normalization:

$$c_0 + c_2 + c_1 + c_3 = 2. \qquad (7-9)$$

Setting $c_2 = 1 - c_0$ and $c_3 = 1 - c_1$, Equation (7–1) becomes

$$\left(c_0 - \frac{1}{2}\right)^2 + \left(c_1 - \frac{1}{2}\right)^2 = \frac{1}{2}, \qquad (7-10)$$

the circle of radius $\sqrt{2}/2$ about $(\frac{1}{2}, \frac{1}{2})$. Any point on this circle gives a wavelet. The points (0,1), (1,1), (1,0) give Haar wavelets. Daubechies imposes the vanishing of an additional moment:

$$-c_1 + 2c_2 - 3c_3 = 0 \qquad (7-11)$$

or

$$c_0 - c_1 = \frac{1}{2}. \qquad (7-12)$$

This places $f(x) = x$ in span $(\psi_i's)$. To see this consider the i^{th} coefficient $= a_i = \int x\psi(x-i)dx = \int (y+i)\psi(y)dy = 1+m$, where $m = \int y\psi(y)dy$. Since ψ has compact support

$$\left(\int_{-M}^{M} x dx - \int_{-M}^{M} \sum a_i \psi(x-i)dx\right)$$

is bounded as $m \to \infty$ if and only if $x \in$ span $(\psi(x-i))$.

This implies $m = 0$. But $m = \int x\psi(x)dx = \int x \sum (-1)^i\ c_{2N-1-i}\phi(2x - i)dx = \sum \int (\frac{y}{2}+\frac{1}{2})(-1)^i c_{2N-1-i}\phi(y)\frac{dy}{2} = \frac{1}{4}\sum i(-1)^i c_{2N-1-i} + \frac{1}{4}\sum\ i(-1)^i c_{2N-1}m$. Thus $m = 0$ implies line (7–6).

The conditions of Equations (7–5) and (7–6) together may be pictured as shown in Figure 7-2.

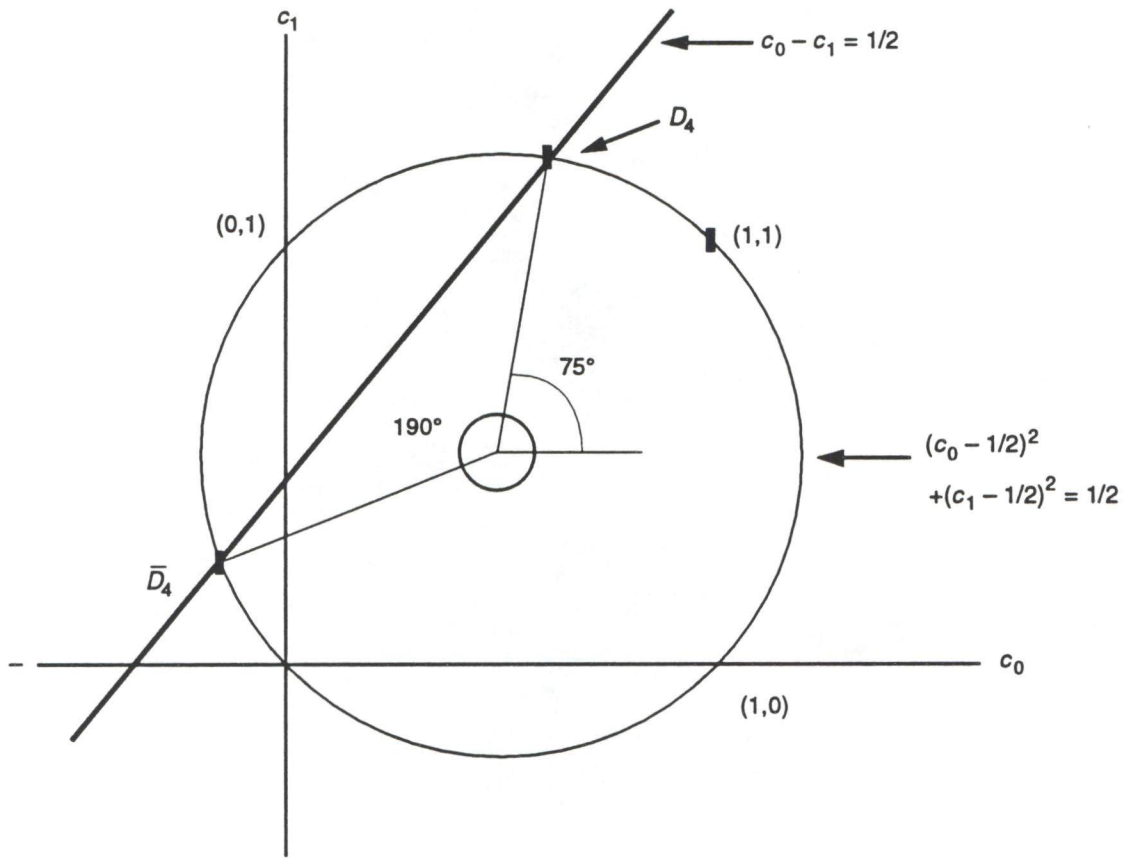

Figure 7-2.

For $D4$ $c_0 = \frac{1}{4}(1+\sqrt{3}), c_1 = \frac{1}{4}(3+\sqrt{3}), c_2 = \frac{1}{4}(3-\sqrt{3})$, and $c_3 = \frac{1}{4}(1-\sqrt{3})$. (For $\bar{D}_4 \bar{c}_0 = c_2, \bar{c}_2 = c_0, \bar{c}_1 = c_3, \bar{c}_3 = c_1$.)

Now let us attempt to incorporate reflections into the "dilation equation." Write:

$$\phi(x) = c_0\phi(2x) + c^0\phi(-2x+4) + c_1\phi(2x-2) + c^1\phi(-2x+6). \quad (7-13)$$

Since we are looking for a ϕ with support $(\phi) = [0,3]$ the above equation can be visualized as based on a "shingling" pattern on the line in which the intervals (shingles) of length $1\frac{1}{2}$ are expanded and matched to [0,3]. The matching preserves (reverses) orientation for solid (dashed) shingles.

On the lattice points 1 and 2, the recursion (7-8) stipulates:

$$\begin{aligned} \phi(1) &= c_0\phi(2) + c^0\phi(2) \text{ and} \\ \phi(2) &= c_1\phi(2) + c^1\phi(2). \end{aligned} \quad (7\text{-}14)$$

The new version of orthogonality is that ϕ should have norm = 1, be orthogonal to its even integer translates and be orthogonal to the reflection of its odd integer translates ($\int \phi(x)\phi(-x+2k)dx = 0$; the $2k$ is explained by recalling that support ϕ has odd length). It is easily verified (superimpose Figure 7-3 on a reflected copy of itself shifted to [1,4] and observe that reflection reverses solid and dashed lines) that these new orthogonality conditions simply give us:

$$\begin{aligned} c_0^2 + c^{0^2} + c_1^2 + c^{1^2} &= 2 \text{ and} \\ c_1 c^1 &= 0. \end{aligned} \quad (7\text{-}15)$$

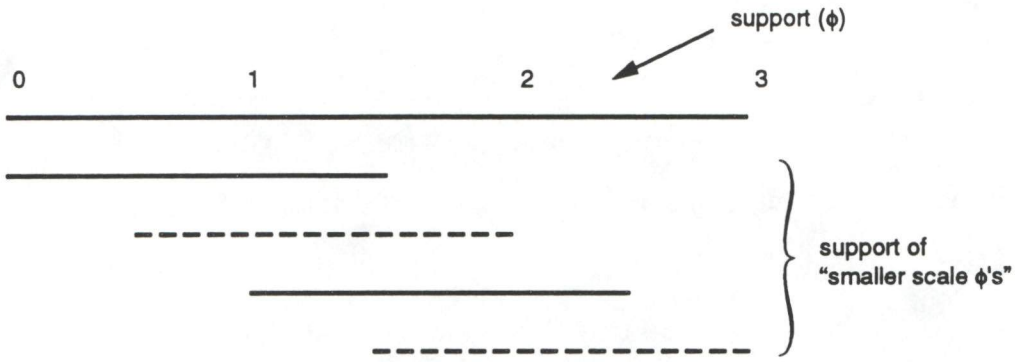

Figure 7-3. Shingling on [0,3]

The 0^{th} moment condition says

$$c_0 + c^0 = c_1 + c^1 \qquad (7-16)$$

and line (7–9) implies

$$c_1 + c^1 = 1. \qquad (7-17)$$

The only solutions are Haar wavelets (e.g., $c_0 = 0, c_1 = 1, c^0 = 0, c_1 = 1$). Other solutions exist if Equation (7–11) is dropped, but since this is undesirable, we investigate next the possibility of inserting reflection into the construction of $D6$.

Now we are looking for a ψ with support [0,5] and the shingling pattern indicated in Figure 7-4. Again the solid shingles of length $2\frac{1}{2}$ are identified with [0,5], preserving orientation, and the dashed shingles are reversed. The "dilation" equation becomes

$$\begin{aligned} \phi(x) &= c_0\phi(2x) + c_1\phi(2x-2) + c_2\phi(2x-4) \\ &\quad + c^0\phi(-2x+6) + c^1\phi(-2x+8) + c^2\phi(-2x+10). \end{aligned} \qquad (7\text{-}18)$$

The new orthogonality conditions are:

$$\begin{aligned} c_0^2 + c_1^2 + c_2^2 + c^{0^2} + c^{1^2} + c^{2^2} &= 2 \qquad (7\text{-}19) \\ c_1 c^2 + c_2 c^1 &= 0 \\ c_2 c_0 + c^2 c^0 &= 0. \end{aligned}$$

The vanishing of the 0^{th} moment requires

$$c_0 + c_1 + c_2 = c^0 + c^1 + c^2 \qquad (7-20)$$

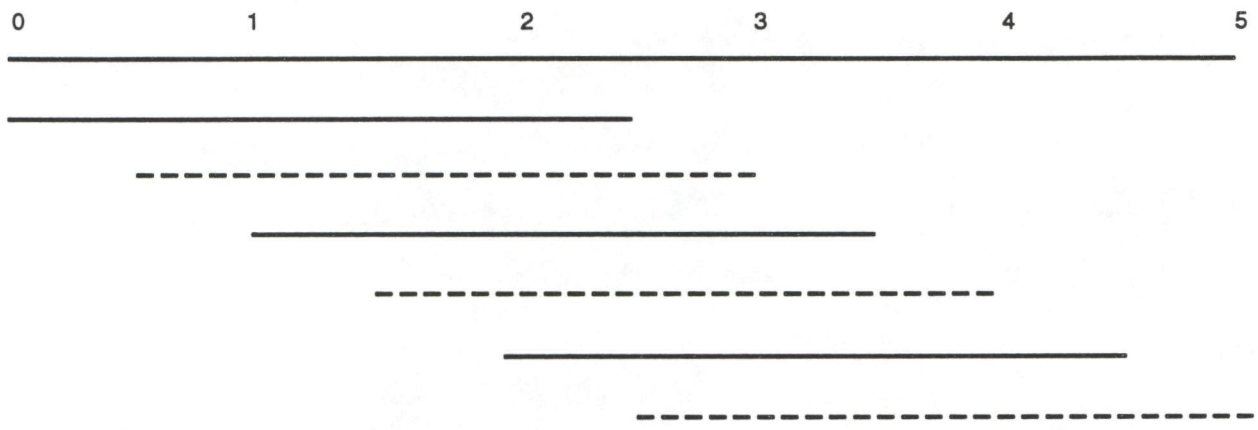

Figure 7-4. Shingling on [0,5]

and finally to define ϕ at integer values a certain determinant (line (7–16)) must vanish.

Once ϕ is defined on the even integers recursive application of line Equation (7–12) defines ϕ on all dyadic rationals.

From Equation (7–12) we see that $(\phi(2), \phi(4))$ must satisfy

$$\begin{vmatrix} c_1 + c^0 & c_0 + c^1 \\ c^2 & c_2 \end{vmatrix} \begin{pmatrix} \phi(2) \\ \phi(4) \end{pmatrix} = \begin{pmatrix} \phi(2) \\ \phi(4) \end{pmatrix}. \qquad (7-21)$$

The condition for solving Equation (7–15) is that 1 be a characteristic root of the above matrix:

$$c_1 c_2 - c^2 c^1 + c^0 c_2 - c_0 c^2 - c_2 - c_1 - c^0 + 1 = 0. \qquad (7-22)$$

Equations (7–13), (7–14), and (7–16) admit a Haar solution:

$$c_0 = c^2 = 1, \text{ and } c_1 = c_2 = c^0 = c^1 = 0. \qquad (7-23)$$

Computing the differentials of the five functions $f_i, i = 1, \ldots, 5$, from line Equations (7–13), (7–14), and (7–16), which vanish at the point x given on line Equation (7-17), we get:

$$\begin{aligned} df_1(x) &= 2dc_0 + 2dc^2 \qquad (7\text{-}24) \\ df_2(x) &= dc_1 \\ df_3(x) &= dc_2 + dc^0 \\ df_4(x) &= -dc^1 - dc_0 - dc^2 \\ df_5(x) &= dc_0 + dc_1 + dc_2 - dc^0 - dc^1 - dc^2. \end{aligned}$$

In matrix form, the coefficients of Equation (7–18) are:

$$\left|\begin{array}{cccccc} 2 & & & & & 2 \\ & 1 & & & & \\ & & 1 & 1 & & \\ -1 & & & & -1 & -1 \\ 1 & 1 & 1 & -1 & -1 & -1 \end{array}\right|. \qquad (7-25)$$

It is easily checked that this matrix has rank = 5. It follows immediately from the implicit function theorem that the locus of solutions to $f_1, \ldots, f_5$ in some neighborhood of $x = (c_0, c_1, c_2, c^1, c^1, c^2) = (1, 0, 0, 0, 0, 1) \in R^6$ consists of a smoothly embedded one-dimensional arc α.

This arc α and the entire one-dimensional irreducible variety that contains it form an interesting class of wavelets incorporating reflections. Because this family is one-dimensional it is natural to attempt to impose an additional condition or optimize for some desired quality, but this has not been tried. Numerical computation of nontrivial coefficients in this family would also be of interest.

A quick comment on the group theoretic setting is in order. The affine group of the line A is the matrix group on the upper $\frac{1}{2}$-plane $\left\{\left|\begin{array}{cc} a & b \\ 0 & 1 \end{array}\right|, a > 0\right\}$ restricted to the line $y = 1$. If orientation reversing transformations are admitted we obtain $\bar{A} = \left\{\left|\begin{array}{cc} a & b \\ 0 & 1 \end{array}\right|, a \neq 0\right\}$. $\bar{A}$ is a split extension of Z_2 by A.

$$0 \to A \to \bar{A} \to Z_2 \to 0 \qquad (7-26)$$

A (and $\bar{A}$) has left-invariant volume $\frac{dadb}{a^2}$ and right-invariant volume $\frac{dadb}{a}$. The left (right)-invariant metrics are $ds^2 = (da/a)^2 + (db/a)^2$ (and $ds^2 = (da/a)^2 + (db)^2$). Both of these define a geometry on A isometric to

the hyperbolic plane (and $g \mapsto g^{-1}$ is the isometry between the two). In fact if $g = \begin{vmatrix} a & b \\ 0 & 1 \end{vmatrix}$ a basis of left (right)-invariant forms will consist of the first row of $g^{-1}dg = (da/a, db/a)$ (first row of $dgg^{-1} = (da/a, -(b/a)da + db)$). Wedging these forms gives the claimed left (right)-invariant volume element.

The set of linear scalings considered by Daubechies $\{y = 2^i x + k, j, k\}$ integers form a lattice L in the right-invariant geometry on A. This means that these rescalings $\phi(y)$ of a function $\phi(x)$ are no more and no less "independent" if the variable x is affinely transformed $x' = ax+b, y' = 2^j(ax+b)+k$. It is this lattice property that makes the set $\{y_{j,k}\}$ natural. Similarly the rescalings implied by line Equation (7–12) $\{y = 2^j x + 2k$ and $\tilde{y} = -2^j x + 2k, j, k$ integers$\}$ is a lattice on $\bar{A}$ with respect to its right-invariant metric.

A word of caution. One should not become too attached to the hyperbolic plane (= Poincaré disk) for signal processing, isometries that move ∞ to scramble high and low frequency wavelets and should therefore be excluded.

7.2 Construction of Symmetric Wavelets

The previous subsection has laid out the basic idea of how to construct systems of compactly supported wavelets that, unlike those of Daubechies, incorporate reflection symmetry. In this subsection we shall pursue this idea further and derive the conditions on the coefficients of these wavelet systems. We shall also construct the four simplest such wavelet systems. They will turn out to be analogous to the lowest order Daubechies wavelet systems, but

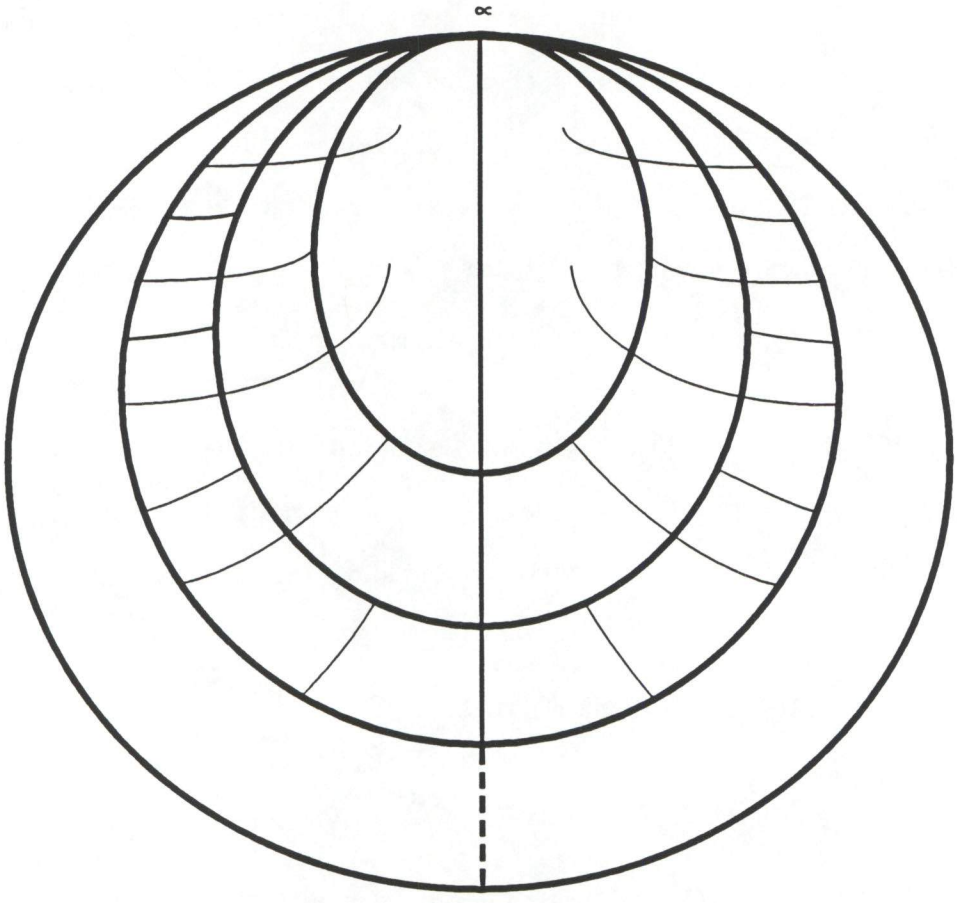

Figure 7-5.

different in detail. They appear to be the beginning of a whole new series of compactly supported wavelet systems. The full exploration of this new series of wavelet systems is beyond the scope of this report, but will be reported elsewhere.

As Daubechies does, we begin with the scaling function $\phi(x)$ and its recurrence relations:

$$\phi(x) = \sum_k c_k \phi(2x - k) + \sum_k b_k \phi(k - 2x). \qquad (7-27)$$

Here the $\{c_k\}$ are one finite set of real coefficients, and the $\{b_k\}$ are a different such set. The index k runs over some finite range of integers to be specified below. The $\{c_k\}$ tell how the scaling function depends on the half scale copies of itself, following Daubechies. The new wrinkle here is the $\{b_k\}$, which tell how it depends on the half scale, *reflected,* copies of itself. A full set of scaling functions at a given scale consists of all the integer translates, and their reflections, of the scaling function,

$$\{\phi(x - m), \phi(m - x) \mid \text{integer } m\}.$$

Figure 7-6 shows the supports of such a full set of scaling functions. The solid, right-pointing arrows are the supports of the $\phi(x - m)$, while the dashed, left-pointing arrows are the supports of the $\phi(m - x)$. Note that this subsection pursues a slightly different scheme than the previous subsection; here, the dashed supports overlay the solid supports, while previously, the dashed supports were interleaved among the solid supports.

The orthogonality relations on the scaling function are now

$$\delta_{0m} = \int dx\, \phi(x)\phi(x - m), \text{ integer } m, \qquad (a) \qquad (7\text{-}28)$$

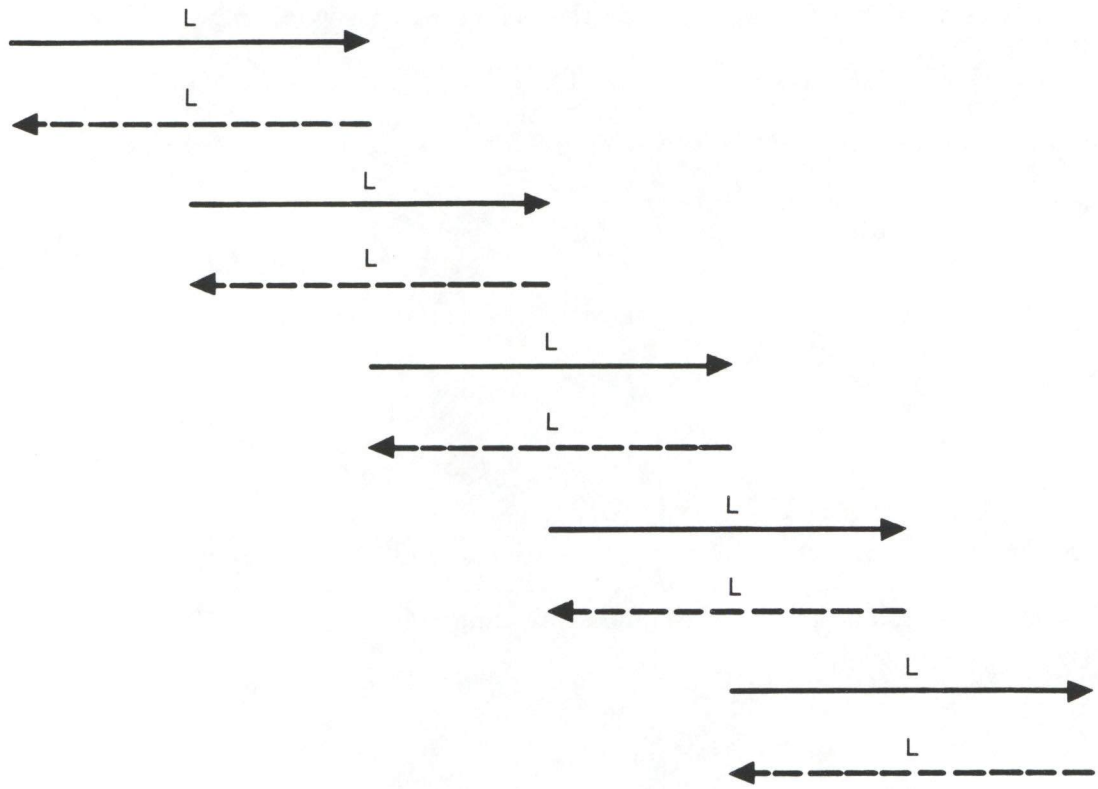

Figure 7-6. Supports of the translations and reflections of scaling function ϕ (x). Solid, right-pointing arrows are supports of the translated functions ϕ (x-m) , while dashed, left-pointing arrows are supports of the reflected and translated functions ϕ (m-x); here m is any integer. The supports step across the real line with unit stride; each support is of integer length L; the supports have been spread out vertically for clarity. Note that each dashed support is congruent with a corresponding solid support.

$$0 = \int dx\, \phi(x)\phi(m-x), \text{ integer } m. \qquad (b)$$

These orthogonality relations must be consistent with the recurrence relations, Equation (7–27), and so the coefficients $\{c_k, b_k\}$ must obey some equations

$$\begin{aligned} 2\delta_{0m} &= \sum_k c_k c_{k-m} + \sum_k b_k b_{k-m}, \text{ even } m \geq 0, \quad (a) \\ 0 &= \sum_k c_k b_{m-k}, \qquad (b) \end{aligned} \qquad (7\text{-}29)$$

In Equation (7–29a), m omits negative values because m and $-m$ lead to the same equation, following a redefinition of k in the sum. For compactly supported wavelets, the coefficients $\{c_k, b_k\}$ must form a finite set and must satisfy Equations (7–29) and must also satisfy the "normalization" conditions

$$\begin{aligned} \text{even}_k c_k + \text{even}_k b_k &= 1, \quad (a) \\ \text{odd}_k c_k + \text{odd}_k b_k &= 1, \quad (b) \end{aligned} \qquad (7\text{-}30)$$

to be derived presently. Actually Equations (7–29) and (7–30) are not all independent, as squaring and adding Equations (7–30 a,b) leads to a linear combination of Equations (7–28 a,b) for various m. There seems to be only this single redundancy in this set of equations. Furthermore we will impose some moment conditions below, which amount to requiring that polynomials in x up to some order P can be written as sums of scaling functions.

To organize our study of these equations in this report, we consider some fixed number N of coefficients

$$\{c_k | k = 0, 1, \ldots, N-1\}, \text{ fixed positive integer } N, \qquad (7-31)$$

along with an equal number N of coefficients

$$\{b_k | k = N + M - 1, N + M, \ldots, 2N + M - 2\}, \text{ fixed nonnegative integer } M. \tag{7-32}$$

The total number of coefficients is thus $2N$. Sums such as those in Equations (7–27), (7–29), and (7–30) will be understood to run only over ks consistent with Equations (7–31) and (7–32). The second number M specifies a kind of offset between the unreflected and reflected contributions to Equation (7–27). Negative Ms lead to systems that are just trivial reflections of systems for positive Ms and need not be considered separately. Taking the c_ks to start at c_0 is likewise an inessential restriction, because a different starting point would just lead to a trivially spatially translated system. One could in addition consider systems of coefficients in which the number of c_ks differs from the number of b_ks — indeed, taking the number of b_ks to be zero leads to Daubechies wavelets — but our preliminary work suggests that the most interesting cases are those of equal numbers, to which this report will confine itself, and Daubechies's case of vanishing b_ks.

A glance at the scaling-functional recurrence relation, Equation (7–27), reveals that the length L of the support of $\phi(x)$ is

$$L = \frac{2N + M - 2}{2}, \tag{7-33}$$

since the left endpoint of the support is delimited by the first term involving c_0, while the right endpoint is delimited by the last term involving $b_{(2N+M-2)}$. The support of $\phi(x)$ is thus

$$\text{Supp } \phi(x) = [0, 2L].$$

A generic point x of the real line is covered by $2L$ such supports at various translations, half non-reflected (solid arrows in Figure 7-6) and half reflected (dashed arrows in Figure 7-7). Here we are assuming that the support has only one component, a hypothesis that is supported by all the numerical evidence to be presented below.

Now consider allowable values of N. The case $N = 1$ leads immediately to the Haar wavelets, the only previously known system of compactly supported wavelets that admits reflection symmetry. The case $N = 3$ is found to reduce, after some calculations starting from Equations (7–29) and (7–30), to the case $N = 2$. We believe it likely that the cases of all higher odd-N cases reduce to the next lower even-N case; at any rate we will restrict ourselves henceforth to even integers $N > 0$.

Now consider allowable values of M, for a given even N. If M is odd, the two even choices $m = N + M - 1$ and $m = 3N + M - 3$ in Equation (7–29b) give sums that collapse ominously to single terms, leading to two equations

$$\begin{aligned} c_0 b_{N+M-1} &= 0, \quad (a) \\ c_{N-1} b_{2N+M-2} &= 0, \quad (b) \end{aligned} \tag{7-34}$$

that force two end coefficients to vanish and that therefore drop us down to a lower case in N. Therefore we restrict ourselves to even $M \geq 0$ henceforth.

Let us now count unknowns and equations, given an even $N > 0$ and an even $M \geq 0$. There are $2N$ unknowns $\{c_k, b_k\}$ — see Equations (7–31 and 7–32). In Equation (7–29a), $m \geq 0$ can take even values $\{0, 2, 4, \ldots, N - 2\}$

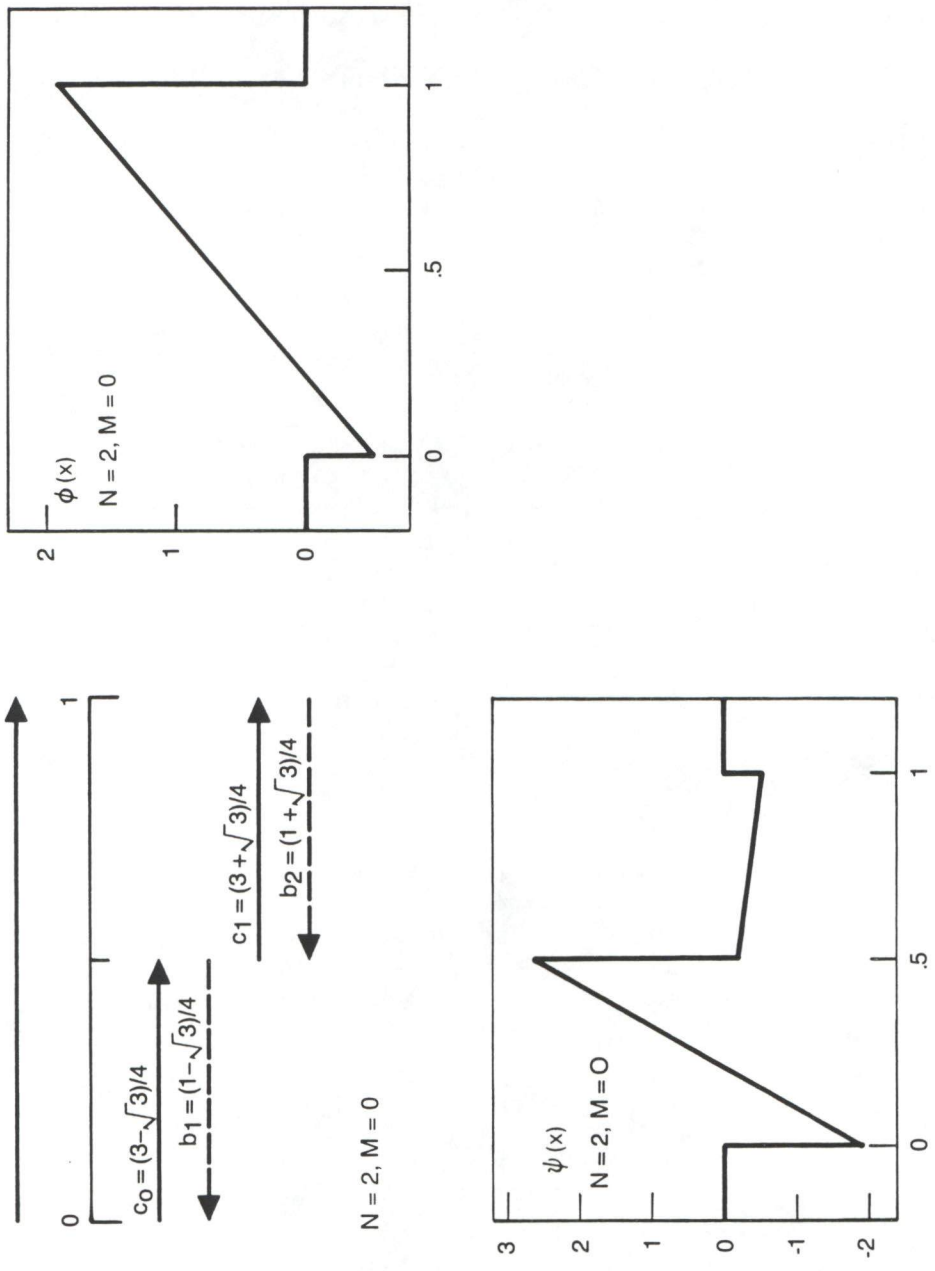

Figure 7-7. The case N = 2, M = 2. Shown at upper left are the supports of half scale functions feeding into the scaling function ϕ (x) in the recurrence relation equation (7-27), along with the coefficient $\{c_k, b_k\}$ belonging to each; symbolism is as in the previous figure. At upper right the scaling function ϕ (x) is graphed, and at lower left the analyzing function ψ (x) is graphed. Their support is [0,1]. These functions are piecewise linear, discontinuous, in this case.

so as to give $\frac{1}{2}N$ equations. In Equation (7–29b), m can take even values $\{N+M, N+M+2, \ldots, 3N+M-4\}$, so as to give $N-1$ equations. In Equations (7–29 a,b) there are two more equations, only one of which, as noted above, is independent of the previous ones. Thus the total number of equations that the $2N$ unknowns must satisfy is

$$\frac{3}{2}N.$$

We have not shown that these equations are actually all independent, but they are in fact independent for all the cases we detail below. Assuming independence, we have $\frac{1}{2}N$ more unknowns than equations, so we expect to be able to impose $\frac{1}{2}N$ more equations. These, following Daubechies, will be moment equations.

The master moment equation — an appellation to be justified soon — asserts that x^P (integer $P > 0$) is in the span of the full set of scaling functions,

$$x^P = \sum_n F_P(n)\phi(x-n) + \sum_n (-1)^P F_P(-n)\phi(n-x), \qquad (7-35)$$

where, throughout, sums on n run over all the integers. Here $F_P(n)$ is a real P^{th} degree polynomial in n, with coefficients to be determined. The structure of the second sum [specifically the factor of $(-1)^P$, and the sign flip of n inside $F_P(-n)$] has been chosen so as to make the entire equation invariant under the reflection map $\{x \to -x, n \to -n\}$. By forming differences of the master moment equation in x and its various translates in $(x+j)$ (j an integer), we obtain a subsidiary moment equation that asserts that $x^{(P-1)}$ is likewise in the span of the full set of scaling functions. Repeating the trick recursively shows that all powers x^l from $l = P$ down to $x = 0$ are likewise in the span.

Thus it suffices to impose the master moment equation, in order to put all P^{th} degree polynomials in x into the span.

To impose the master moment equation on the unknowns $\{c_k, b_k\}$, substitute the recurrence relations, Equation (7–27), into Equation (7–35), to yield a formula expressing x^P in terms of translates and reflections of $\phi(2x)$. Alternatively, replacing x by $2x$ in Equation (7–35) gives a different formula for $2^P x^P$ in terms of translates and reflections of $\phi(2x)$. These two formulas must be the same by orthonormality, up to the factor of 2^P, and equations relating the $\{c_k, b_k\}$ to the polynomial $F_P(n)$ result:

$$2^{-P} F_P(2n) = \sum_{\text{even } k} c_k F_P(n-k) + (-1)^P \sum_{\text{even } k} b_k F_P(-n-k), \quad (a) \quad (7\text{-}36)$$

$$2^{-P} F_P(2n) = \sum_{\text{odd } k} c_k F_P(n-k) + (-1)^P \sum_{\text{odd } k} b_k F_P(-n-k). \quad (b)$$

Since the polynomial $F_P(n)$ is of degree P, it has $(P+1)$ coefficients, which we treat as unknowns. There are $2(P+1)$ equations in Equations (7–36) when we impose them order by order in n. That is, n is a formal variable in Equations (7–36). In particular, the two equations for n^P have already been imposed as Equations (7–30). Thus, when we impose the master moment equation for degree P, we are imposing a net number P of new relations upon the original unknowns $\{c_k, b_k\}$. These equations involve sums like $\text{even}_k k^l c_k$ and $\text{odd}_k k^l b_k$ for $k = 0, 1, \ldots, P$ and similar sums for the $\{b_k\}$. Since we want to impose $\frac{1}{2}N$ more equations, we want to choose

$$P = \frac{1}{2}N. \qquad (7-37)$$

Turn now to the analyzing function, or mother wavelet function $\psi(x)$.

It is to be orthogonal to all the translations and reflections of the scaling function $\phi(x)$,

$$\begin{aligned} 0 &= \int dx\, \phi(x)\psi(x-m), \text{ integer } m, \quad (a) \\ 0 &= \int dx\, \phi(x)\psi(m-x), \text{ integer } m, \quad (b) \end{aligned} \tag{7-38}$$

and orthonormal to the set of all its own translations and reflections,

$$\begin{aligned} \delta_{0m} &= \int dx\, \psi(x)\psi(x-m), \text{ integer } m, \quad (a) \\ 0 &= \int dx\, \psi(x)\psi(m-x), \text{ integer } m. \quad (b) \end{aligned} \tag{7-39}$$

The analyzing function is to be constructed from the scaling function $\phi(x)$ by a relation parallel to Equation (7–27),

$$\psi(x) = \sum_k g_k \phi(2x-k) + \sum_k f_k \phi(k-2x), \tag{7-40}$$

where a new set of $2N$ unknown coefficients has been introduced,

$$\{g_k | k = 0, 1, \ldots, N-1\}, \text{ fixed positive integer } N, \quad (a) \tag{7-41}$$

$\{f_k | k = N+M-1, N+M, \ldots, 2N+M-2\}$, fixed nonnegative integer M (b),

parallel to Equations (7–31), where N and M are as above. Equations (7–38) – (7–41) entail a set of algebraic equations for these coefficients, namely

$$\begin{aligned} 0 &= \sum_k c_k g_{k-m} + \sum_k b_k f_{k-m}, \text{ even } m, \\ 0 &= \sum_k c_k f_{m-k} + \sum_k b_k g_{m-k}, \text{ even } m, \end{aligned} \tag{7-42}$$

and

$$\begin{aligned} 2\delta_{0m} &= \sum_k g_k g_{k-m} + \sum_k f_k f_{k-m}, \text{ even } m \geq 0, \quad (a) \\ 0 &= \sum_k g_k f_{m-k}, \text{ even } m. \quad (b) \end{aligned}$$

In general these equations do not seem to have a simple solution for the $\{g_k, f_k\}$. In the particular cases we examine below, these equations do have solutions for the $\{g_k, f_k\}$, although the solution is not unique. The support of $\psi(x)$ is

$$\text{Supp}\psi(x) = [0, 2L]$$

where L is given in Equation (7–33).

One interesting kind of non-uniqueness that occurs in all cases is as follows. If $\psi(x)$ itself is symmetric under reflection of x about the midpoint of its support, $x \rightarrow (2L - x)$, then we have constructed a symmetric wavelet. But say $\psi(x)$ is not symmetric. Then $\psi(x)$ and $\psi(2L - x)$ are linearly independent, and we can form even and odd linear combinations $\psi^{(+)}(x)$ and $\psi^{(-)}(x)$ on the same support that are respectively symmetric and antisymmetric under reflection. Thus, in the construction of a *system* of wavelets that is invariant under reflection, we can always obtain individual *wavelets* that are either symmetric or antisymmetric under reflection.

Finally, the orthonormal system of wavelets is defined as

$$\begin{aligned} \psi_{p,m,+}(x) &= 2^{-p/2}\psi((x-m)/2^p), \quad (a) \\ \psi_{p,m,-}(x) &= 2^{-p/2}\psi((m-x)/2^p), \quad (b) \end{aligned} \tag{7-43}$$

for integers m and p.

In a preliminary reconnaissance of the properties of symmetric wavelet systems, we have done some numerical constructions for $N = 2$ and $N = 4$. We proceeded as follows. Having fixed N, we found the $\{c_k, b_k\}$ by solving

Equations (7–29), (7–30) and (7–36) numerically for many values of M. For each N and M a discrete set of solutions $\{c_k, b_k\}$ was found, usually more than one solution. To obtain the analyzing-function coefficients $\{g_k, f_k\}$ we guessed the (non-obvious) solution

$$\begin{aligned} g_k &= \begin{cases} +c_{k+1}, & k \text{ even}, \\ -c_{k-1}, & k \text{ odd}, \end{cases} \quad (a) \\ f_k &= \begin{cases} -b_{k+1}, & k \text{ odd}, \\ +b_{k-1}, & k \text{ even}. \end{cases} \quad (b) \end{aligned} \tag{7-44}$$

While this guess is unlikely to be valid for the general case, we found it to be valid for the cases at hand involving $N = 2, 4$.

Having found the recursion coefficients $\{c_k, b_k\}$ we constructed the scaling function $\phi(x)$ by numerical iteration of Equation (7–27) on a finite mesh, starting more or less arbitrarily with a step function. The analyzing function $\psi(x)$ was then constructed with one application of Equation (7–40) from $\phi(x)$ and the $\{g_k, f_k\}$. The results were displayed graphically and the smoothest cases were selected by eyeball. Smoothness was used to select values of M within each N, and also to select among the discrete set of solutions for the coefficients that usually offered themselves. Here we present only the smoothest results; many more wild wavelets were produced as by-products.

The results are shown graphically in Figures 7-7 – 7-15 Interestingly, one analytic solution turned up: the piecewise linear discontinuous wavelet for $N = 2$, $M = 0$ shown in Figures 7-7 and 7-8. The coefficients happen to be a permutation of Daubechies's coefficients for her case $N = 4$. This

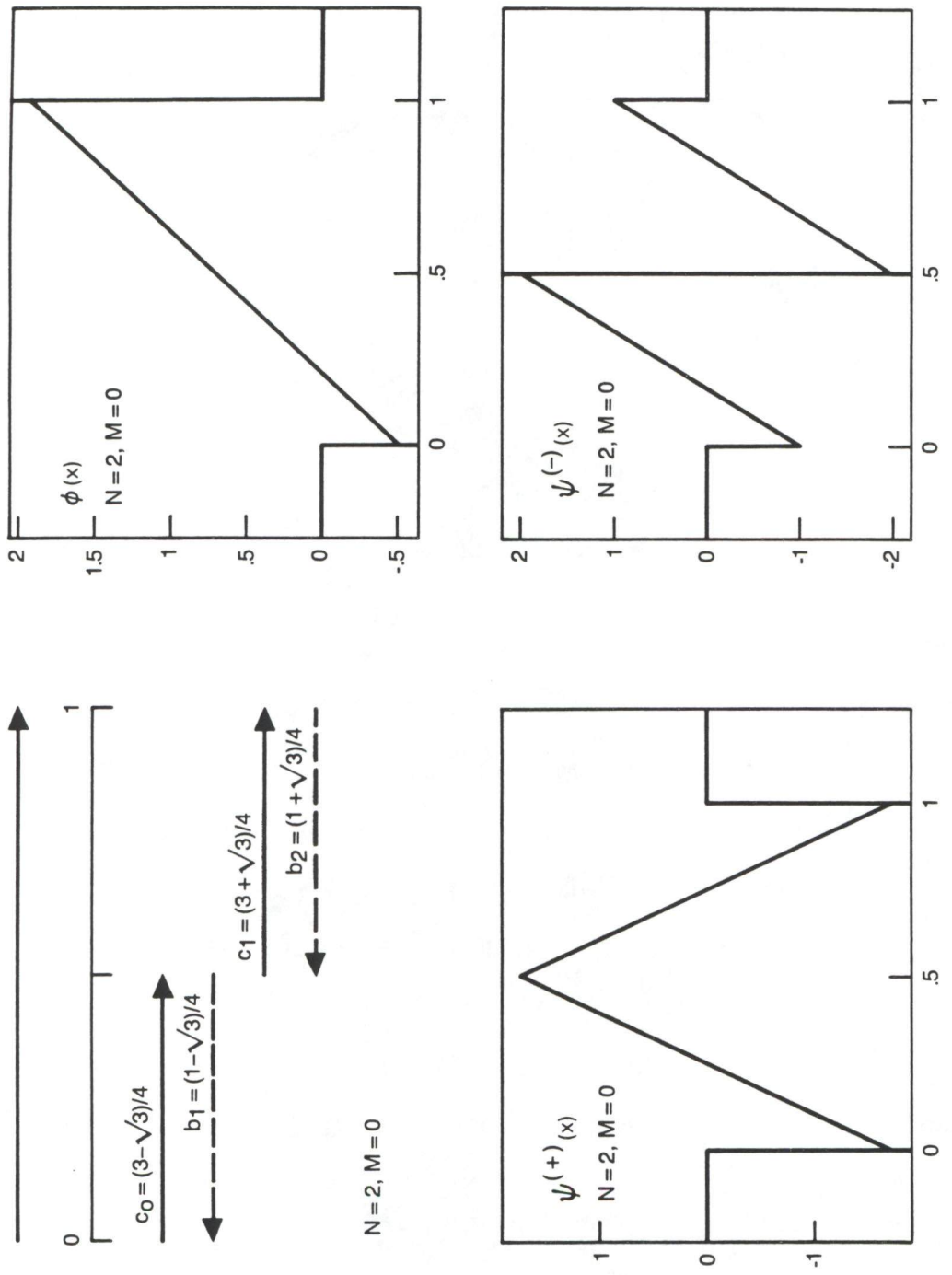

Figure 7-8. Same as the previous figure, except that the symmetric and antisymmetric analyzing functions ψ (±) (x) are graphed at lower left and right.

solution is supported on $[0,1]$ and is given by

$$\begin{aligned} \phi(x) &= (2\sqrt{3}x - \sqrt{3} + 1)/\sqrt{2}, \quad 0 \le x \le 1, \qquad (a) \qquad (7\text{-}45) \\ \psi(x) &= \begin{cases} ((6+4\sqrt{3})x - 1 - \sqrt{3})/\sqrt{2}, 0 \le x \le \frac{1}{2} \\ ((6-4\sqrt{3})x - 5 + 3\sqrt{3})/\sqrt{2}, \frac{1}{2} \le x \le 1. \quad (b) \end{cases} \end{aligned}$$

The choice $M = 2$ gives the smoothest wavelets of any M for $N = 2$. The coefficients are

$$\begin{aligned} c_0 &= (2 - \sqrt{7})/4, \quad (a) \qquad (7\text{-}46) \\ c_1 &= 3/4 \qquad (b) \\ b_3 &= 1/4, \qquad (c) \\ b_4 &= (2 + \sqrt{7})/4 \quad (d) \end{aligned}$$

and the scaling and analyzing functions are shown in Figures 7-9 and 7-10. Larger values of M give substantialy wilder functions; see $M = 4$ in Figure 7-11.

Now move to $N = 4$. Two values of M give about the same smoothness, namely $M = 4$ and $M = 6$ (along with discrete choices within each M, as noted above.) Coefficients and graphs are given in Figures 7-14. The next smoothest value of M is $M = 2$, as shown in Figure 7-15; other M give wilder results.

In summary, we have given the general equations that govern the construction of systems of compactly supported wavelets that admit reflection symmetry, and we have presented a selection of numerically derived examples of such systems. Clearly much remains to be done. A promising approach

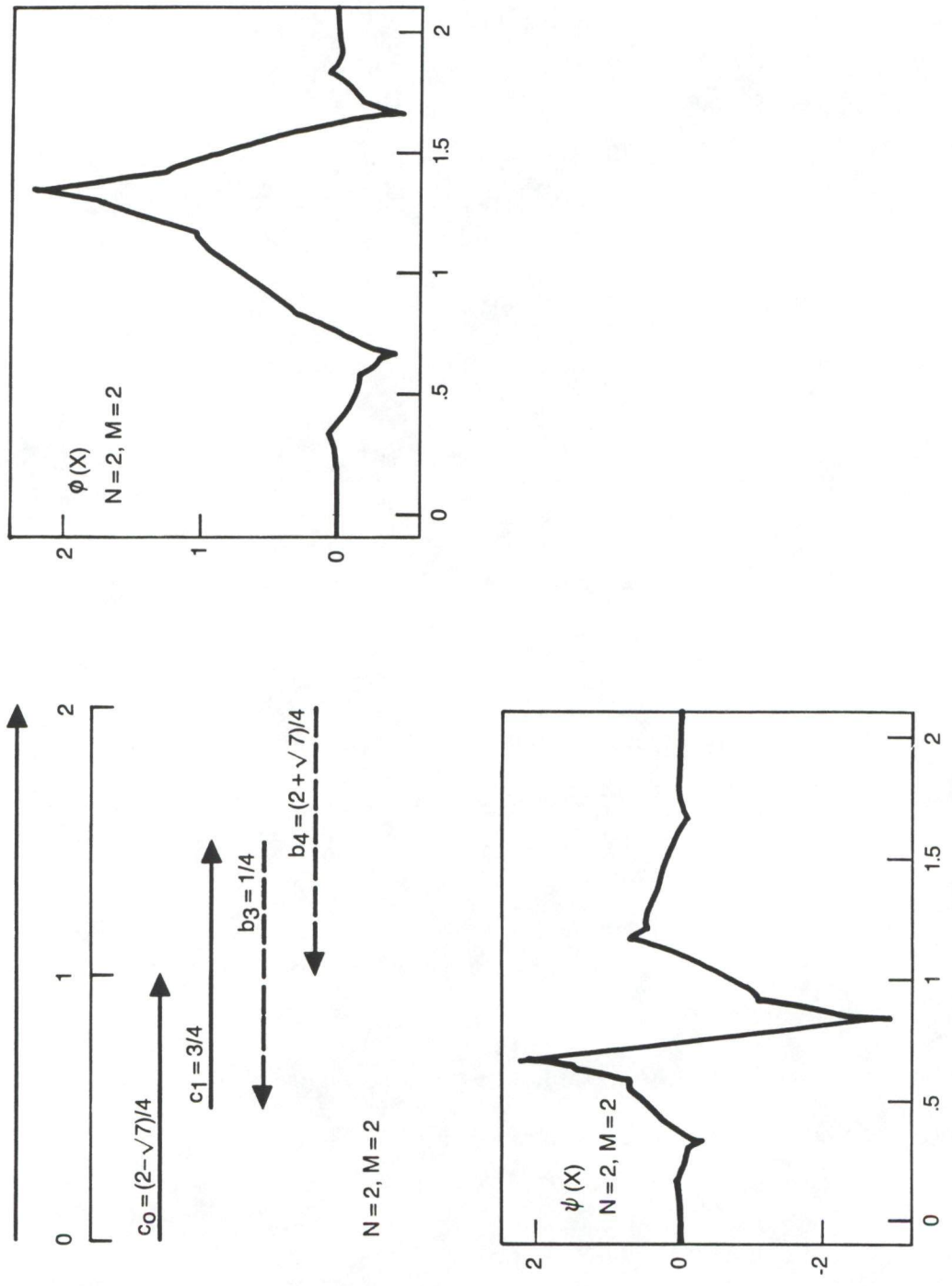

Figure 7-9. The case N = 2, M = 2. Display is otherwise the same as in Figure 7-7. The smoothness of the functions is somewhere between C^0 and C^1.

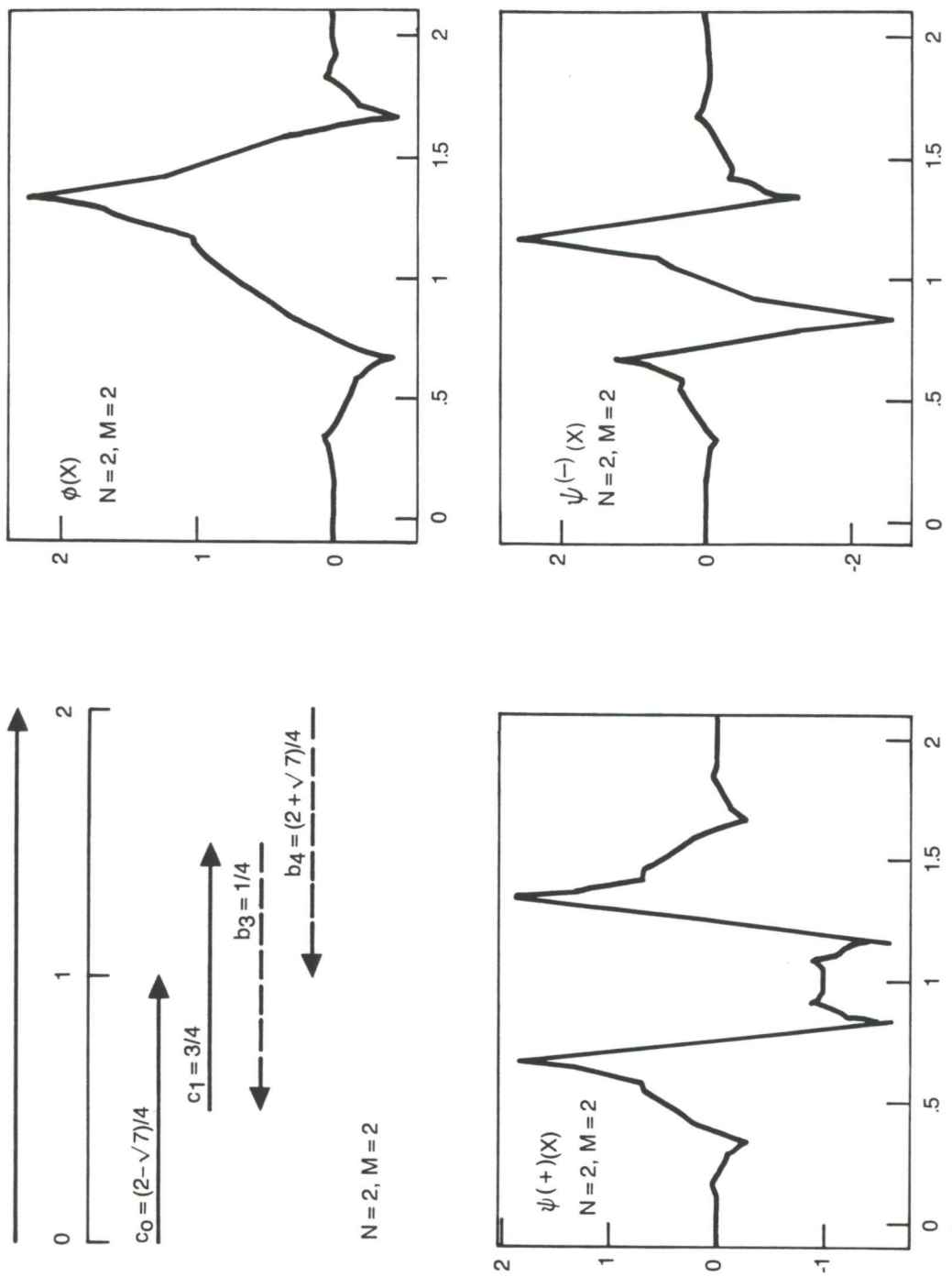

Figure 7-10. The same case N = 2, M = 2; displayed at lower left and right are the symmetric and antisymmetric analyzing functions ψ (±) (X).

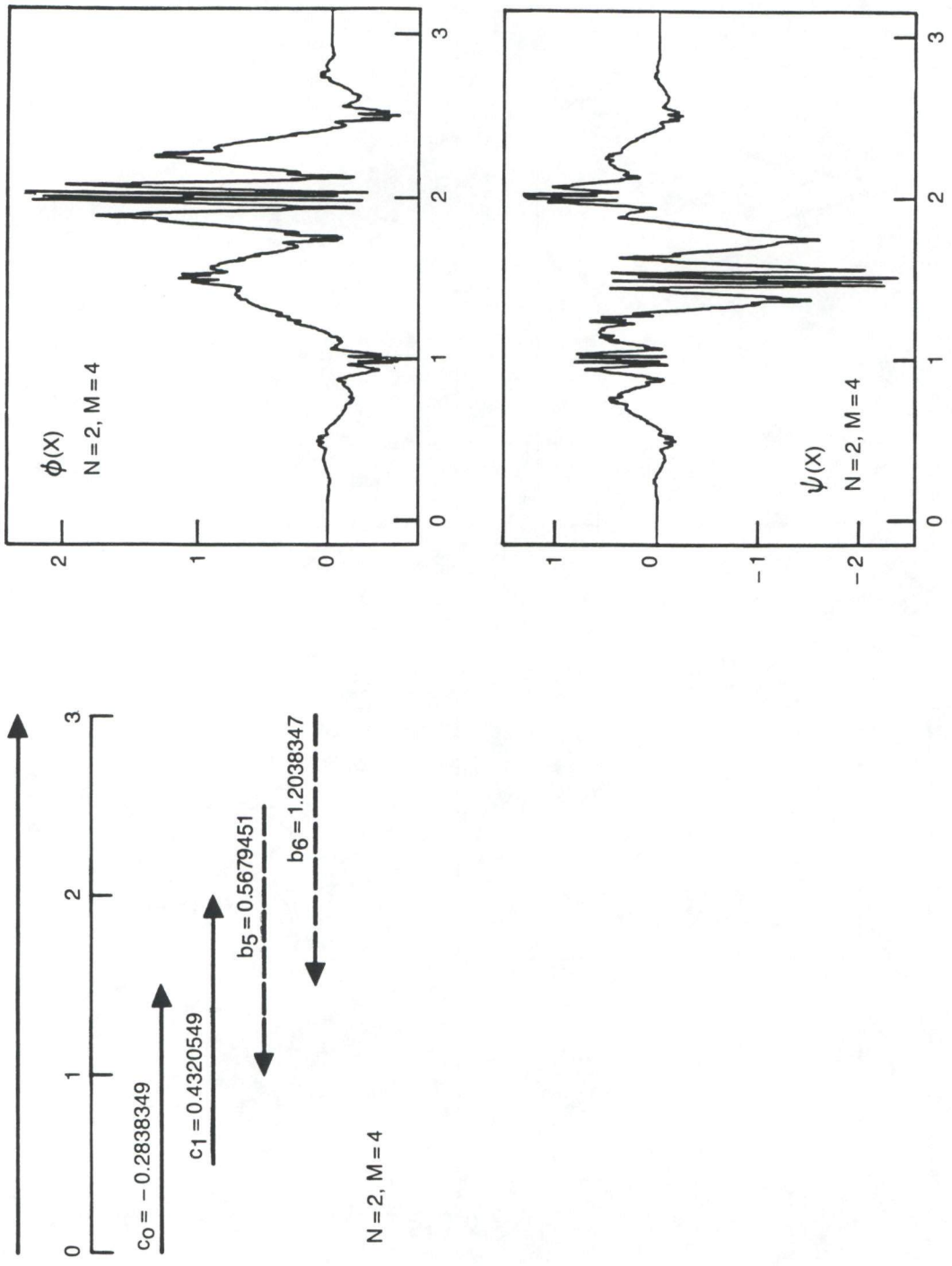

Figure 7-11. The case N = 2, M = 4; a rather wild wavelet, similar to many which were constructed but are not presented in this report.

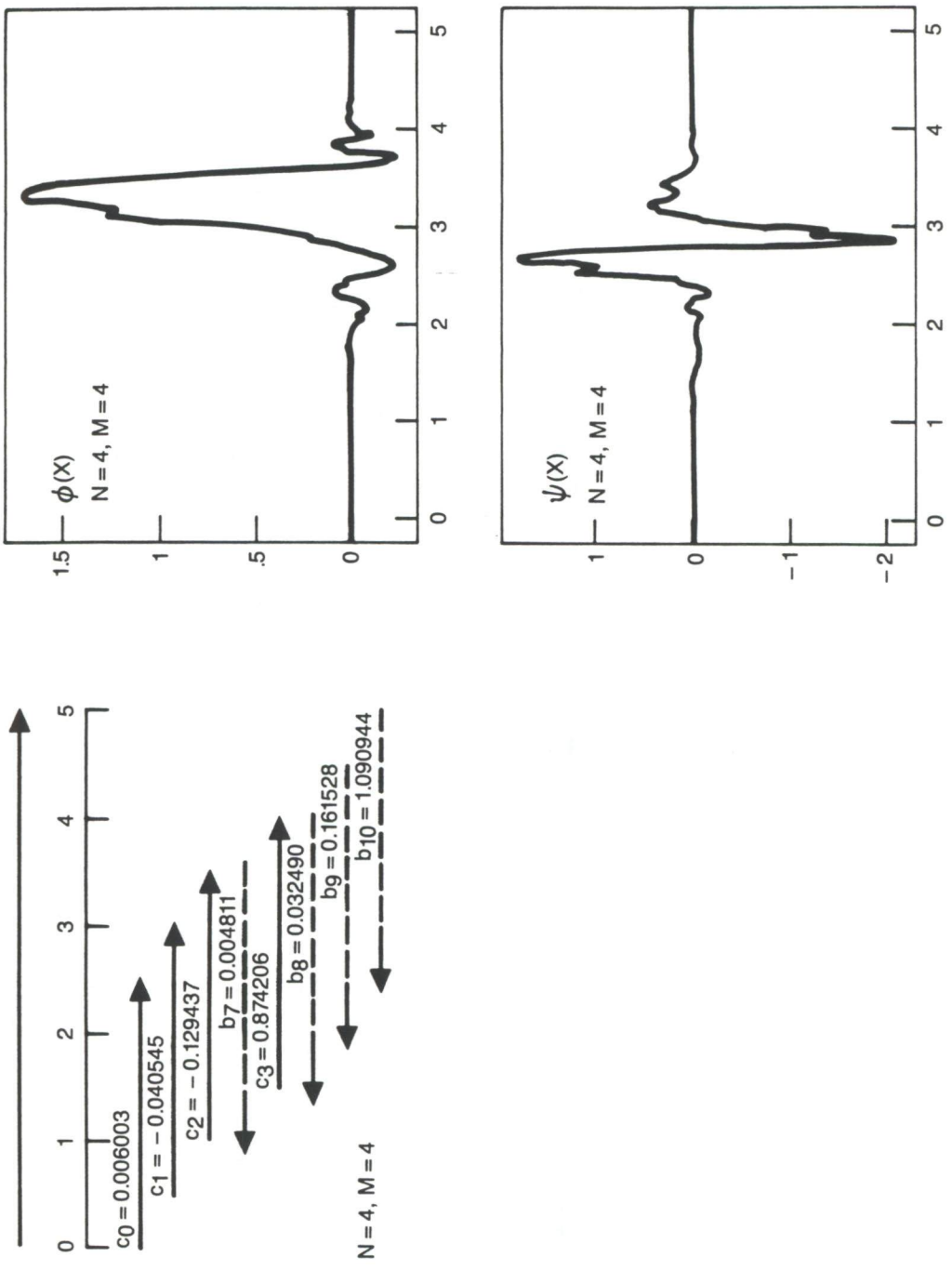

Figure 7-12. We now move to cases N = 4 with more coefficients. This the case N = 4, M = 4; a discrete choice among solutions for the coefficients has been made to optimize smoothness. Display is similar to Figure 7-8. Smoothness appears to be better than C^1 (not obvious, perhaps, on this figure, but plausible on blowups of it).

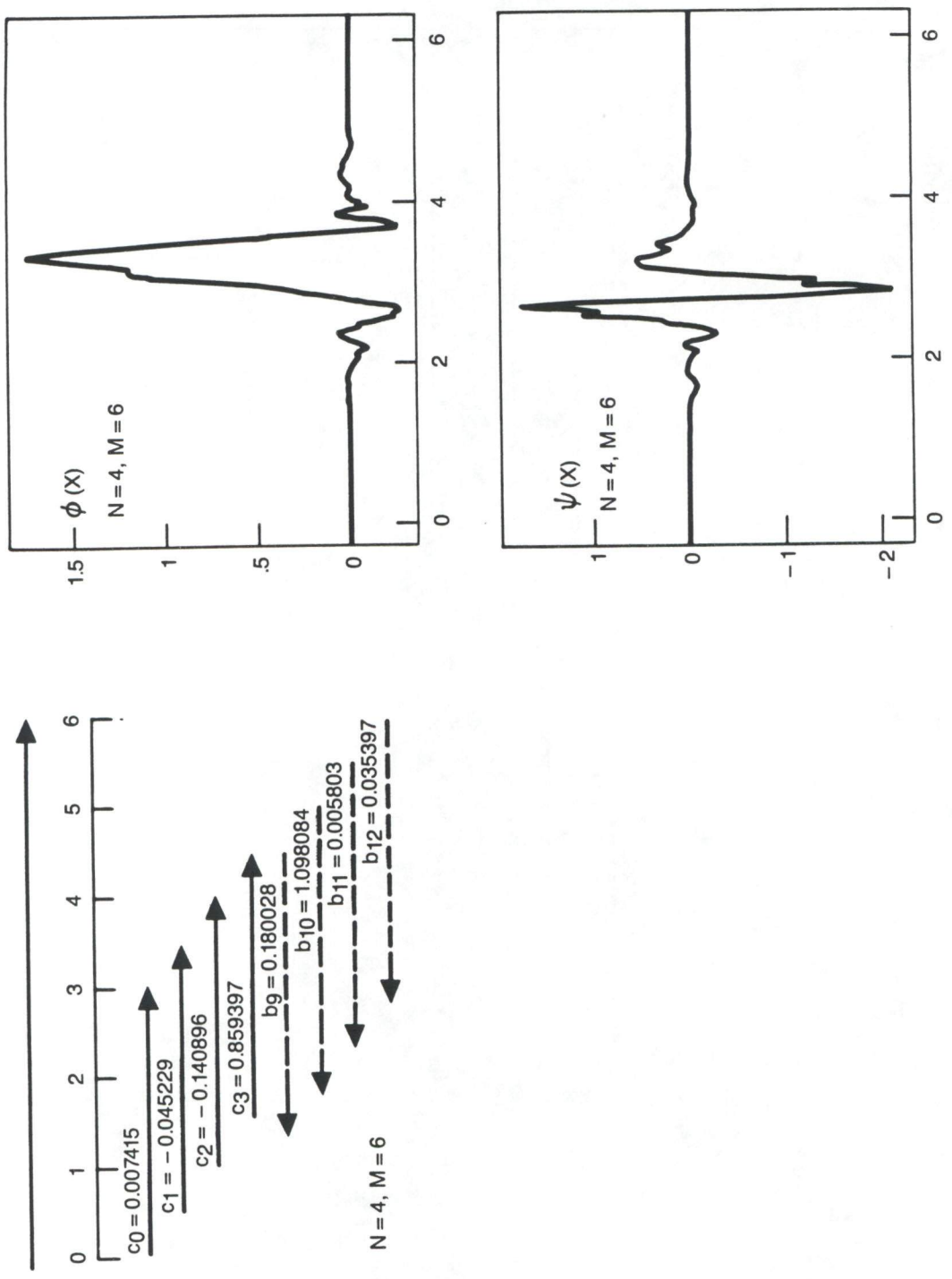

Figure 7-13. The case N = 4, M = 6. Display is similar to previous figures. Smoothness appears about the same as the previous figure, and in fact the shape of the graphs is surprisingly similar.

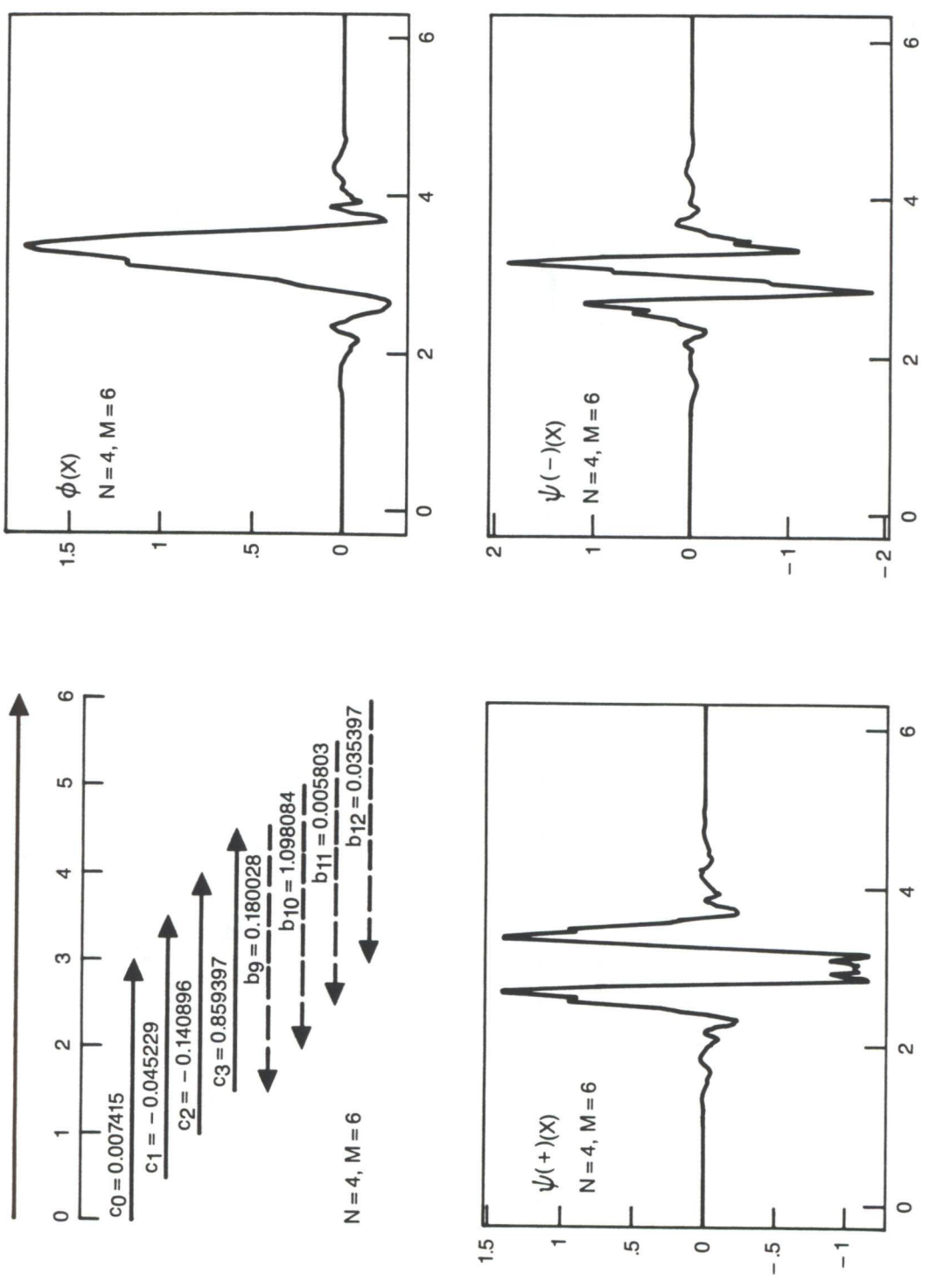

Figure 7-14. The case N = 4, M = 6 again, except now displaying the symmetric and antisymmetric wavelets at bottom left and right.

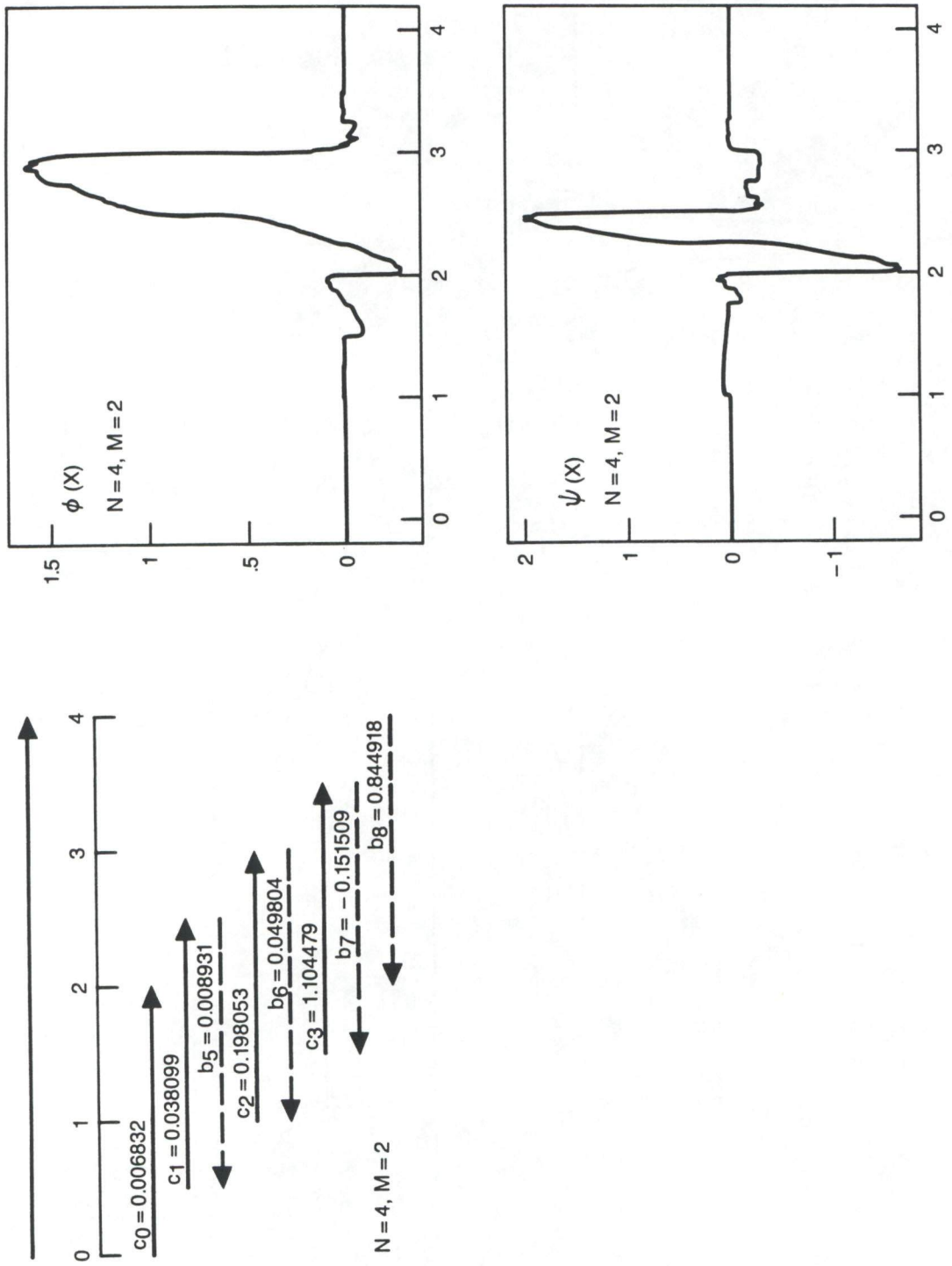

Figure 7-15. A somewhat less smooth case at N = 4: here M = 2.

for further progress is to investigate the harmonic polynomials

$$H(\omega) = \sum_k (c_k + ib_k)e^{ik\omega}$$

that encode the recursion coefficients. The examples already available here suggest that an infinite number of symmetric wavelet systems exist, with properties that are likely to be interesting and useful.

8 WAVELETS AND PARTIAL DIFFERENTIAL EQUATIONS

8.1 Introduction

The recent flurry of interest in wavelets has led to many suggestions for possible useful applications. One of these possibilities is the numerical solution of partial differential equations (PDEs). Some exploratory work (Aware, Inc.) on this has been done. However, researchers in the field seem so intent on generalizations and other applications that necessary detailed work has not been aggressively pursued.

The main problem is the following: with the introduction of wavelets, many different expansions for solutions of PDEs are suggested. In principle these all can lead to useful results. For practical purposes we must restrict ourselves to a finite number of terms. The real problem then is to determine what expansion choice leads to the smallest amount of calculation for a prescribed accuracy.

Corresponding problems for other methods of solving PDEs are well known. The question of the utility of finite element procedures as compared with spectral ones is well studied. For sufficiently regular geometry spectral methods work best. For sufficiently complicated geometry finite element methods are preferred.

Other important points concern the feasibility of wavelet methods in

dimensions higher than one and for complicated geometries. It is also important to note that there has been a huge investment in algorithms for solving PDEs. If this investment is to be thrown away there would need to be a very significant improvement in calculation efficiency.

8.2 A Brief Review

Both to have an agreed-upon notation and to see where there is freedom to make choices we here give a very abbreviated version of the voluminous literature.

With an element of the affine group

$$x \rightarrow x' = ax + b \qquad (8-1)$$

and a function $g(x)$ we associate a set of functions

$$g_{ab}(x) = |a|^{-1/2} g\left(\frac{x-b}{a}\right). \qquad (8-2)$$

If we let b vary over the real numbers and a over the nonzero real numbers we can readily show that (with mild requirements on g) a function $f \varepsilon L^2$ can be represented by the functions

$$(uf)(a,b) = < g_{ab}, f > = |a|^{-1/2} \int dx\, g\left(\frac{x-b}{a}\right) f(x). \qquad (8-3)$$

Notice the freedom of choice here:

1. We chose the affine group of Equation (8-1).

2. We could have restricted a to the positive real numbers. (This would put an additional constraint on g. Its Fourier transform cannot then have purely positive support.)

3. The set of functions $g_{ab}(x)$ is clearly overcomplete. For computation purposes it is necessary to restrict a, b so that the $g_{a,b}$ are a discrete set.

The most common choice seems to be the set

$$g_{j,k} = 2^{j/2} g(2^j x - k)$$

where j, k range over the integers. One major reason for this scaling by powers of 2 is that it is particularly well suited to digital computers. However, other choices can be made. In Resnikoff (1989) the situation for $2 \rightarrow m$ is discussed. No particular advantage is demonstrated. But for certain purposes there may be some.

The next specialization involves the choice of the $g(x)$. A very popular choice is one of the set of functions derived by Daubechies (1988). These are obtained as follows. Define $\phi(x)$ by the scaling relation

$$\phi(x) = \sum_k h(k) 2^{1/2} \phi(2x - k). \qquad (8-4)$$

Requiring $\phi(x)$ to have compact support leads to the condition that we have a finite sequence $h(0), \ldots h(2N-1)$ of nonzero coefficients.

Remark: Compactness can be a useful property. On the other hand there may be some situations where one might prefer great smoothness as compared with compactness.

For convenience we (can) choose

$$\int \phi(x)\, dx = 1, \tag{8-5}$$

which implies

$$\sum_k h(k) = \sqrt{2}. \tag{8-6}$$

If we demand that the translates of ϕ be orthonormal, i.e.,

$$\int \phi(x-\ell)\phi(x-m)dx = \delta_{\ell m}, \tag{8-7}$$

we obtain the conditions

$$\sum_k h(k+2\ell)h(k+2m) = \delta_{\ell m}. \tag{8-8}$$

With

$$P(\zeta) = \sqrt{2}\sum_k h(k)e^{ik\zeta} \tag{8-9}$$

we find for the Fourier transform of $\phi \equiv \hat{\phi}(\zeta)$

$$\hat{\phi}(\zeta) = \prod_{i=1}^{\infty} P\left(\frac{\zeta}{2^i}\right). \tag{8-10}$$

If we want the translates of $\phi(x)$ to reproduce the polynomials $1, x, \ldots x^{p-1}$ exactly we find $P(\zeta)$ must have a zero of order p at $\zeta = \pi$. Alternatively this implies

$$\sum_k (-1)^k k^m h(k) = 0, \ m = 0, 1, \ldots (p-1). \tag{8-11}$$

Parenthetically we remark that for $p \geq 1$ we have

$$1 = \sum_k \phi(x-k), \ \ k \varepsilon Z. \tag{8-12}$$

$\phi(x)$ is called the scaling function. Closely related is the wavelet defined by

$$\psi(x) = \sum_k g(k) 2^{1/2} \phi(2x - k) \qquad (8-13)$$

with

$$g(k) = (-1)^k h(1-k). \qquad (8-14)$$

The conditions of Equation (8 11) can be rewritten as

$$\sum_k g(k) k^m = 0, \qquad (8-15)$$

which implies

$$\int x^m \psi(x)\, dx = 0, \quad m = 0, 1, \ldots (p-1). \qquad (8-16)$$

Other orthogonality properties that follow from the conditions on $h(k)$ and the definition of $g(k)$ are

$$\begin{aligned} \int \psi(x)\, \phi(x-m)\, dx &= 0 \\ \int \psi(x)\, \psi(2x-m)\, dx &= 0 \\ \text{and } \int \psi(x)\, \psi(x-m)\, dx &= 0. \end{aligned} \qquad (8\text{-}17)$$

Remark: Daubechies has indicated how to construct an infinite sequence of scaling functions and associated wavelets that satisfy the above conditions.

We define scaled and translated versions of ϕ and ψ by

$$\phi_{jk}(x) = 2^{j/2} \phi(2^j x - k) \qquad (8-18)$$

and

$$\psi_{jk}(x) = 2^{j/2} \psi(2^j x - k) \qquad (8-19)$$

where j, k run through all the integers.

The main result on the completeness of these functions is the following. Let V_{j+1} be the spaced spanned by

$$\phi_{j+1,k}, \quad -\infty < k < \infty. \tag{8-20}$$

Then

$$V_{j+1} = V_j \oplus W_j \tag{8-21}$$

where W_j is the space spanned by the ψ_{jk}. We have

$$L^2(R) = V_n \oplus \sum_{j \geq n} \oplus W_j \tag{8-22}$$

for every integer n.

Note that by virtue of Equation (8–21) any $f(x) \varepsilon V_{n+1}$ can be expressed in the forms

$$\begin{aligned} f(x) &= \sum_k c_k \phi_{n+1,k} \\ &= \sum_k a_k \phi_{n,k} + \sum_k h(k) \psi_{n,k}. \end{aligned}$$

But by virtue of the recursion relations of Equations (8–4) and (8–13)

$$\begin{aligned} \phi_{nk} &= \sum_\ell h(\ell - 2k) \phi_{n+1,\ell} \\ \psi_{nk} &= \sum_\ell g(\ell - 2k) \phi_{n+1,\ell} \end{aligned}$$

and therefore

$$c(k) = \sum_j h(k - 2j) a(j) + \sum_j g(k - 2j) b(j). \tag{8-23}$$

(Note: This is known as the Mallat transform (Mallat, 1989).) We remark that this transform is readily inverted. Thus the orthonormal properties of

the ϕ and ψ are equivalent to

$$\begin{aligned}
\sum_{\ell} h(\ell - 2k)h(\ell - 2m) &= \delta_{km} \\
\sum_{\ell} h(\ell - 2k)g(\ell - 2m) &= 0 \\
\sum_{\ell} g(\ell - 2k)h(\ell - 2m) &= 0 \\
\sum_{\ell} g(\ell - 2k)g(\ell - 2m) &= \delta_{km}.
\end{aligned} \tag{8-24}$$

Therefore

$$\begin{aligned}
a(k) &= \sum_{j} h(j - 2k)c(s) \\
b(k) &= \sum_{j} g(j - 2k)c(s).
\end{aligned} \tag{8-25}$$

8.3 Applications to PDEs

To apply wavelets to PDEs we choose an appropriate basic scaling function and determine the wavelet. The desired solution is assumed expanded in terms of the scaled and translated functions. The coefficients of these functions then satisfy a set of algebraic equations that are to be solved.

If we follow the path outlined above we might choose some set of Daubechies coefficients, e.g., one of $D_4, D_6, D_8, D_{10}, \ldots$. After this choice the functions to be used in the expansions are known—at least recursively.

That there is considerable ambiguity remaining is readily seen.

1. From Equation (8-22) we see that we have different bases for each integer n.

2. Having fixed n we still have the problem of determining which finite number of the coefficients are to be nonzero. There are several ways to do this; which is best probably depends on the problem and the experience of the investigator.

   (a) Since

   $$\lim_{n\to\infty} V_n = L^2(R)$$

   we can choose some large n and use as basis the functions

   $$\phi_{n,k} \text{ for the fixed } n.$$

   The coefficients of $\phi_{n,k}$ are dropped when they are below a preset limit.

   (b) A general, if perhaps inefficient, method is to take $n = 0$ and choose a large number of ϕ_{jk}, ψ_{jk}, $j = 0, 1, 2, \ldots j$ as basis functions. Coefficients are put equal to zero when they fall below a certain limit. The problem here is that in the absence of insight into the nature of the solution one needs to start with an unnecessarily large number of terms to make sure significant basis functions have not been outlined.

   (c) An adaptive scheme (Aware, Inc.,) has been used. This assumes scaling and wavelet functions with $n_f \geq n \geq n_0$. One starts the calculation at the coarsest level using $\phi_{n_0,k}$, $\psi_{n_0,k}$. Having obtained a solution here one uses the Mallat transform [Equation (8–23)] to obtain a first approximation to the solution at level $n_0 + 1$. Iteratively one improves this. Then one can go back to level n_0 using the inverse transform [Equation (8–25)]. When satisfied

with the accuracy at level n_0 one then proceeds from level $n_0 + 1$ to level $n_0 + 2$ and repeats the procedure.

(d) A special trick can be applied [1c] when the solution is to be periodic. One can stick with the translates of the original scaling function. Keeping more and more translates increases the period. The effective result is higher and higher resolution. In Reference 1c this has been usefully employed to solve Burger's equation.

8.4 Conclusions

It is clear that wavelet expansions can be and indeed have been useful in solving PDEs. Important questions remain to be answered. There are many choices to be made before a given equation can be attacked. One needs to be able to decide for a given class of problems what the optimal choices are. Given the optimal choice one needs to know if the wavelet approach is then more efficient than other numerical algorithms.

We have also not touched on other questions that arise naturally when considering wavelets. Here we started with a unitary representation of the affine group. It was seen that this provides an overcomplete set of basis functions. While it is reassuring to reduce these to the familiar case of an orthonormal basis, this may not be the best thing to do. An overcomplete set, while not necessarily the most efficient, may perhaps lead to a more robust method of solution.

Both theory and many numerical experiments are needed to see which PDEs are best treated by wavelet expansions and how the results compare with more traditional methods.

REFERENCES

1. Aware, Inc. Reports

   (a) AD900307.1.2.

   (b) AD890527.1.

   (c) AD900615.1.

2. H., Resnikoff. Aware Inc. Report AD900701.

3. I. Daubechies (1988), *Comm. Pure. Appl. Math*, **41**, 909–996.

4. S. Mallat (1989), *IEEE Trans. Pattern Annual and Machine Intell.*, **11**, 674–693.

9 APPLICATION OF WAVELETS TO IMAGE PROCESSING

We heard a lucid discussion by Stéphane Mallat of the utility of wavelets for processing images. We also read a number of papers by Mallat and others on the processing of images, using either wavelets or other techniques. Competing techniques are Gabor transforms, Fourier cosine transforms with or without windows, and a great variety of wavelet transforms. The purpose of the processing is usually to compress the information contained in an image so that it can be transmitted over a limited bandwidth with minimal loss of essential detail. Objective assessment of the relative merits of different processes is difficult, because the meaning of the phrase "essential detail" is different in different contexts. Details that are essential for location of military targets in a landscape will be different from details that convey expression in a human face.

We saw evidence that wavelet processing has great promise as a fast and convenient technique for image compression. We did not see any systematic and objective comparison of the performance of wavelet and other processes applied to the same images with the same criteria of merit. Until such comparisons are made, we cannot be sure that wavelets have any substantial advantages over other methods.

The following are our conclusions and recommendations in the area of image processing.

1. A large volume of excellent work has been done in the commercial arena, exploring the applications of wavelets to image processing particularly to commercial videophone and high-definition television projects. This work does not depend on DARPA support. If it is supported, the support should not be biased toward wavelets but should be given to image processing technology in general. The commercial world will be the best judge of whether wavelets are cost-effective compared with other methods of image processing.

2. There is a need for careful and objective comparison of wavelets and other image processing algorithms for military applications to which commercial criteria do not apply. Such comparisons should be encouraged and supported by DARPA. Unless these comparisons show wavelets to have a substantial advantage, wavelets should be given no special preference in military programs.

3. Our preliminary judgement, based on (admittedly) inadequate evidence, is that wavelets will be advantageous for some purposes but will not have an overwhelming advantage. Their margin of superiority over other methods, if it exists, is more likely to be a factor of two than a factor of ten. A factor of two advantage may in the long run be important, but it cannot be quickly demonstrated. In the meantime, wavelets should be explored and exploited in parallel with other data processing techniques.

10 WAVELETS REFERENCE LIST

1. Aware Inc., "About AWARE, Inc.", Aware, MA, undated.

2. Aware, Inc., A packet of illustrations, undated.

3. Basdevant, C., M. Holschneider and V. Perrier, "Travelling Wavelets Method," *Comptes Rendus de L Academie des Sciences Serie I-Mathematique,* **310** (8), 647-652, 1990

4. Battle, Guy and Paul Federbush, "Ondelettes and Phase Cell Cluster Expansions, A Vindication," *Commun. Math. Phys.* **109**, 417-419, 1987.

5. Battle, Guy, "A Block Spin Construction of Ondelettes. Part I: Lemarie Functions," *Commun. Math. Phys.* **110**, 601-615, 1987.

6. Benedetto, John, Christopher Heil and David Walnut, "Remarks on the Proof of the Balian-Low Theorem," The MITRE Corporation, VA, undated.

7. Beylkin, G., R. Coifman and V. Rokhlin, "Fast Wavelet Transforms and Numerical Algorithms I," Yale Univ., December 1989.

8. Burt, Peter J., "Multiresolution Techniques for Image Representation Analysis, and 'Smart' Transmission," *SPIE Conf.* 1199, November 1989.

9. Coifman, Ronald R., and Yves Meyer, "Orthonormal Wave Packet Bases," undated.

10. Coifman, Ronald R., Yves Meyer, and M. Victor Wickerhauser, "Signal Compression with Wave Packets," NARG, New Haven, CT, April 5, 1990.

11. d'Alessandro, Christophe, "Time-Frequency Modifications Using an Elementary Waveform Speech Model," France, undated.

12. Daubechies, Ingrid and Thierry, Paul, "Time-Frequency Localisation Operators: a Geometric Phase Space Approach: II. The Use of Dilations," *Inverse Problems* 4, November 2, 1987.

13. Daubechies, Ingrid, A. Grossman and Y. Meyer, "Painless Nonorthogonal Expansions," *J. Math. Phys.* **27** (5), (1271-1283), May 1986.

14. Daubechies, Ingrid, "Orthonormal Bases of Compactly Supported Wavelets," *Commun. Pure & Appl. Math.* **XLI**, 909-996, 1988.

15. Daubechies, Ingrid, Stéphane Jaffard and Jean-Lin Journe, "A Simple Wilson Orthonormal Basis with Exponential Decay,"

16. Daubechies, Ingrid, "The Wavelet Transform, Time-Frequency Localization and Signal Analysis," IEEE Transactions on Information Theory, **36** 5, 961-1005, September 1990

17. Daubechies, Ingrid, "Time-Frequency Localisation Operators: A Geometric Phase Space Approach," *IEEE*, **34**, 4, July 1988.

18. Daubechies, I.D. and J.C. Lagarias, "Two-Scale Difference Equations: I. Global Regularity of Solutions," October 19, 1988.

19. Daubechies, Ingrid, and Jeffrey C. Lagarias, "Two-Scale Difference Equations: II. Local Regularity, Infinite Products of Matrices and Fractals," November 9, 1989.

20. Everson, R., L. Sirovich, and K. R. Sreenivasan, "Wavelet Analysis of the Turbulent Jet," *Phys. Lett.* A, **145**, 314-322, 1990.

21. Feichtinger, Hans G. and K.H. Groschenig, "Banach Spaces Related to Integrable Group Representations and Their Atomic Decompositions, I," *J. Funct. Analysis* **86**, 307-340, 1989.

22. Frazier, Michael and Bjorn Jawerth, "Decomposition of Besov Spaces," *Indiana Univ. Math. Journal*, **34**, 4, 1985.

23. Freysz, E., B. Pouligny, F. Argoul and A. Areneodo, "Optical Wavelet Transform of Fractal Aggregates," *Phys. Rev. Lett.* **4** (7), 745-748, 1990.

24. Ghez, J. M. and S. Vaienti, "On the Wavelet Analysis for Multifractal Sets," J. *Statist. Phys.* **57**, 415-420, 1989.

25. Glowinski, Roland, Wayne M. Lawton, Michel Ravachol and Eric Tenebaum, "Wavelet Solution of Linear and Nonlinear Elliptic, Parabolic and Hyperbolic Problems in One Space Dimension," AWARE, Inc., MA, 1989.

26. Goupillaud, P., A. Grossmann and J. Morlet, "Cycle-Octave and Related Transforms in Seismic Signal Analysis," Geoexploration, April 12, 1984.

27. Gröchenig, Karlheinz, "Describing Functions: Atomic Decompositions versus Frames," McMaster University, March 16, 1988.

28. Grossmann, A., and J. Morlet, *SIAM J. Math.* 15(1984) 723.

29. Grossman, A., "Wavelet Transforms and Edge Detection," *Stochastic Processes in Physics and Engineering*, 149-157, 1988.

30. Heil, Christopher and David Walnut, "Gabor and Wavelet Expansions," The MITRE Corporation, VA, 1989.

31. Heil, Christopher E. and David F. Walnut, "Continuous and Discrete Wavelet Transforms," *SIAM Review*, **31**, 4, 628-666, December 1989.

32. Heil, Christopher, "A Discrete Zak Transform," The MITRE Corporation, December 1989.

33. Heil, Christopher, "Uncertainty Principles and the Balian-Low Theorem," The MITRE Coporation, 1990.

34. Holschneider, M., "Wavelet Analysis on the Circle," *J. Math. Phys.*, **31** (1), 39-44, 1990.

35. Istas, J., "Wavelet Coefficients of a Gaussian Process," *Comptes Rendus de L' Académie des Sciencies Serie I-Mathématique* **312** (11), 893-896, 1991.

36. Jones, D. L. and R. G. Baraniuk, "Efficient Approximation of Continuous Wavelet Transforms," *Electronic Lett.* **27** (9), 748-750, 1991.

37. Kaiser, Gerald, "An Algebraic Theory of Wavelets. I. Operational Calculus and Complex Structure," University of Lowell, MA, April 1990.

38. Klauder, J. R. and R. F. Streater, "A Wavelet Transform for the Poincaré Group," *J. Math. Phys.* **32** (6), 1609-1611, 1991.

39. Kronland-Martinet, R., J. Morlet and A. Grossmann, "Analysis of Sound Patterns Through Wavelet Transforms," *Inter. J. Pattern Recognition & Artificial Intell.*, January 26, 1987.

40. Latto, Andy and Eric Tenebaum, "Compactly Supported Wavelets and the Numerical Solution of Brugers' Equation," AWARE, MA, 1990.

41. Lawton, W. M. "Necessary and Sufficient Conditions for Constructing Orthonormal Wavelet Bases," *J. Math. Phys.* **32** (1), 57-61, 1991.

42. Lemarié, P.G. and Y. Meyer, "The Discrete Wavelet Transform with Applications to the Symbolic Calculus for Algebras of Singular Integral Operators," Division of Math., U.A.M., June 16, 1986.

43. Lewis, A. S. and G. Knowles, "Video Compression Using 3D Wavelet Transforms," *Electronics Lett.,* **26** (6), 396-398, 1990.

44. Liandrat, J. and F. Moretbailly, "The Wavelet Transform – Some Applications to Fluid Dynamics and Turbulence," *European J. Mechanics B-Fluids,* **9** (1), 1-19, 1990.

45. Mallat, Stéphane G., "A Theory for Multiresolution Signal Decomposition: The Wavelet Representation," *IEEE Trans. Pattern Annual and Machine Intell*, **11**, 7, 674-693, July 1989.

46. Mallat, Stephane G., "Multifrequency Channel Decompositions of Images and Wavelet Models," *IEEE Trans. Pattern Annual and Machine Intell.*, **37**, 12, 674-693, December 1989.

47. Maday, Y., V. Perrier and J. C. Ravel, "Dynamical Adaptivity Using Wavelets Basis for the Approximation of Partial Differential Equations," *Comptes Rendus de L' Académie des Sciences Série I-Mathématique* **312** (5), 1991, 405-410.

48. Mehta, C. H., B.S. Goel, D.D. Bhatta and S. Radhakrishnan, "Minimum Phase Wavelet by Arma Factorization," *IEEE Trans. Signal Processing* **39** (2), 1991, 512-515.

49. Meneveau, C., "Dual Spectra and Mixed Energy Cascade of Turbulence in the Wavelet Representation," *Phys. Rev. Lett.* **66** (11), 1450-1453, 1991.

50. Meyer, Y., "Séminaire Equations aux Derivées Partielles 1986-1987," Centre de Mathematiques, France, December 16, 1986.

51. Meyer, Yves, "Les Ondelettes," Universitè de Paris, undated.

52. Meyer, Y., *Ondelettes et Opérateurs*, Hermann, Paris.

53. Meyer, Yves, "Principe d'Incertitude, Bases Hilbertiennes et Algébres d'opérateurs," Séminaire Bourbaki, February 1986.

54. Meyer, Yves, "Wavelets Viewed by a Mathematician," Universitè de Paris, undated.

55. Meyer, Yves, "Wavelets with Compact Supports," handwritten, undated.

56. Multipliers. *Electronics Lett,* **27** (2), 171-173, 1991.

57. Nautiyal, A., "Limitations in Recursive Wavefield Continuation with Spatial Wavelets," *IEEE Trans. Geoscience and Remote Sensing*, **28** (2), 272-274, 1990.

58. Orr, Richard S., "Application of Gabor Representations to Military Problems," Presentation to JASON Wavelets, May 21, 1990.

59. Ramanathan, J. and O. Zeitouni, "On the Wavelet Transform of Fractional Brownian Motion," The MITRE Corporation, MA, undated.

60. Resnikoff, H.L., "Foundations of Arithmeticum Analysis: Compactly Supported Wavelets and The Wavelet Group," Aware, MA, 1989.

61. Resnikoff, H.L., "Weierstrass Functions and Compactly Supported Wavelets," Aware, MA, 1990.

62. Rieder, A., " Approximation Properties of the Continuous Wavelet Transform," *Zeitschrift für Angewandte Mathematik und Mechanik*, **70** (6), 577-578, 1990.

63. Rieder, A., "The Wavelet Transform on Sobolev Spaces and Its Approximation Properties," *Numerische Mathematik* **58** (8), 875-894, 1991.

64. Rokhlin, V., "Rapid Solution of Integral Equations of Scattering Theory in Two Dimensions," *J. Comp. Phys.* 86, 2, February 1990.

65. Rudin, Leonid I. and Stanley Osher, "Feature-Oriented Image Enhancement with Shock Filters, I.," undated.

66. Schempp, Walter, "Radar Ambiguity Functions, The Heisenberg Group, and Holomorphic Theta Series," *Proc. Amer. Math. Soc.*, 92, 1, September 1984.

67. Slezak, E., A. Bijaoui, G. Mars, "Identification of Structures from Galaxy Counts – Use of the Wavelet Transform," *Astron. Astrophys.*, **227** (2), 301-316, 1990.

68. Stark, H. G., "Fractal Graphs and Wavelet Series," *Phys. Lett.* A. **143** (9), 443-447, 1990.

69. Strang, Gilbert, *SIAM Review*, Vol. 31, No. 4 (1989) 614.

70. Strang, Gilbert, "Wavelets and Dilation Equations: A Brief Introduction," *SIAM Rev.* 31, 4, 614-627, December 1989.

71. Torresani, B., "Wavelets Associated with Representations of the Affine Weyl-Heisenberg Group," *J. Math. Phys.* **32** (5), 1273-1279, 1991.

72. Vetterli, Martin and Cormac Herley, "Wavelets and Filter Banks: Relationships and New Results," Columbia Univ., NY, undated.

73. *Wavelets, Time-Frequency Methods and Phase Space*, Combes, J.M. , A. Grossmann, and Ph. Tchamitchian eds. Springer Verlag (1989).

74. Wells, Jr., Raymond O., "Parametrizing Smooth Compactly Supported Wavelets," Aware, MA, 1989.

75. Yamada M. and Ohkitani, "Orthonormal Wavelet Expansion and its Application to Turbulence," *Prog. Theoretical Physics,* **83** (5), 819-823, 1990.

DISTRIBUTION LIST

CMDR & Program Executive Officer
US Army/CSSD-ZA
Strategic Defense Command
PO Box 15280
Arlington, VA 22215-0150

Mr. John M. Bachkosky
Deputy DDR&E
The Pentagon, Room 3E114
Washington, DC 20301

Dr. Joseph Ball
Central Intelligence Agency
Washington, DC 20505

Dr. Arthur E. Bisson
DASWD (OASN/RD&A)
The Pentagon, Room 5C675
Washington, DC 20350-1000

Mr. Edward Brown
Assistant Director
Nuclear Monitoring Research Office/DARPA
3701 North Fairfax Drive
Arlington, VA 22203

Dr. Herbert L. Buchannan
Director
DARPA/DSO
3701 North Fairfax Drive
Arlington, VA 22203

Dr. Curtis G. Callan, Jr.
Physics Department
PO Box 708
Princeton, NJ 08544

Dr. Peter Carruthers
Dept of Physics
Physics Bldg
University of Arizona
Tucson, AZ 85721

Dr. Andy O'. Chadlick
Naval Air Warfare Center
Code 5024
Warminster, PA 18974

Dr. Ferdinand N. Cirillo, Jr.
Central Intelligence Agency
Washington, DC 20505

Brig Gen Stephen P. Condon
Deputy Assistant Secretary
Management Policy & Program Integration
The Pentagon, Room 4E969
Washington, DC 20330-1000

Ambassador Henry F. Cooper
Director
S D I O - D
The Pentagon, Room 1E1081
Washington, DC 20301-7100

D A R P A Library
3701 North Fairfax Drive
Arlington, VA 22209-2308

D T I C (2)
Defense Technical Info. Center
Cameron Station
Alexandria, VA 22314

Mr. John Darrah
Sr. Scientist & Technical Advisor
H Q A F S P A C O M / C N
Peterson A F B, CO 80914-5001

Dr. Gary L. Denman
Acting Director, DARPA/DIRO
3701 North Fairfax Drive
Arlington, VA 22203

DISTRIBUTION LIST

Col. Doc Dougherty
D A R P A / D I R O
3701 North Fairfax Drive
Arlington, VA 22203

Capt. Kirk Evans
Director Undersea Warfare
Space & Naval Warfare Sys Cmd
Code PD-80
Washington, DC 20363-5100

Mr. F. Don Freeburn
US Department of Energy
Code ER-33
Mail Stop G-236
Washington, DC 20585

Dr. David Goldshmidt
CCR East
Thanet Road
Princeton, NJ 08540

Dr. S. William Gouse
Sr Vice President & General
The MITRE Corporation
Mail Stop Z605
McLean, VA 22102

Dr. A. Hales
CCR West
4350 Executive Drive
La Jolla, CA 92037

Ltgen Robert D. Hammond
CMDR & Program Executive Officer
Strategic Defense Command
PO Box 15280
Arlington, VA 22215-0150

Mr. Thomas H. Handel
Office of Naval Intelligence
The Pentagon, Room 5D660
Washington, DC 20350-2000

Maj Gen Donald G. Hard
Director of Space & SDI Programs
Code SAF/AQS
Washington, DC 20330-1000

Dr. Helmut Helwig
AFOSR/CC
Building 410
Bolling Air Force Base
Washington, DC 20332

Dr. Robert G. Henderson
Director, JASON Program Office
The MITRE Corporation
7525 Colshire Drive, Z561
McLean, VA 22102

Dr. Barry M. Horowitz
President & Chief Exec. Officer
The MITRE Corporation
202 Burlington Road
Bedford, MA 01730-1420

Dr. William E. Howard (2)
Director for Space & Strat. Techn.
Office/Assistant Sec. of the Army
The Pentagon, Room 3E474
Washington, DC 20310-0103

Dr. Gerald J. Iafrate
US Army Research Office
PO Box 12211
Research Triangle NC 27709-2211

Jason Library (5)
The MITRE Corporation, W002
7525 Colshire Drive
McLean, VA 22102

Dr. George Jordy (25)
Director for Program Analysis
US Department of Energy
MS ER30 Germantown
Washington, DC 20585

DISTRIBUTION LIST

Dr. O' Dean P. Judd
Los Alamos National Lab
Mail Stop A-110
Los Alamos, NM 87545

Dr. Gordon J. Macdonald
Institute on Global Conflict
UCSD/0518
9500 Gilman Drive
La Jolla, CA 92093-0518

Mr. Robert Madden (2)
Department of Defense
National Security Agency
Attn R-9 (Mr. Madden)
Ft. George G. Meade, MD 20755-6000

Dr. Arthur F. Manfredi, Jr. (10)
OSWR
Central Intelligence Agency
Washington, DC 20505

Mr. Joe Martin
Director
OUSD(A)/TWP/NW&M
The Pentagon, Room 3D1048
Washington, DC 20301

Mr. Ronald Murphy
DARPA/ASTO
3701 North Fairfax Drive
Arlington, VA 22203-1714

Dr. Julian C. Nall
Institute for Defense Analyses
1801 North Beauregard Street
Alexandria, VA 22311

Dr. Gordon C. Oehler
Central Intelligence Agency
Washington, DC 220505

Dr. Peter G. Pappas
Chief Scientist
US Army Strategic Defense Cmd
PO Box 15280
Arlington, VA 22215-0280

Dr. Bruce Pierce
USD(A)/DS
The Pentagon, Room 3D136
Washington, DC 20301-3090

Mr. John Rausch (2)
Division Head 06 Department
NAVOPINTCEN
4301 Suitland Road
Washington, DC 20390

Records Resources
The MITRE Corporation, W115
7525 Colshire Drive
McLean, VA 22102

Dr. Keith Richey
Wright Laboratory
Wright-Patterson Air Force Base
Dayton, OH 45433

Dr. Oscar S. Rothaus
Math Department
Cornell University
Ithaca, NY 14853

Dr. Fred E. Saalfeld
Director
Office of Naval Research
800 North Quincy Street
Arlington, VA 22217-5000

Dr. Allan Schell
AFMC/CA
Wright-Patterson Air Force Base
Dayton, OH 45433

DISTRIBUTION LIST

Dr. John Schuster
Technical Director of Submarine
Department of the Navy OP-02T
The Pentagon, Room 4D534
Washington, DC 20350-2000

Dr. Barbara Seiders
Chief of Research
Office of Chief Science Advisor, AC&DA
320 21st Street NW
Washington, DC 20451

Dr. Philip A. Selwyn (2)
Director
Office of Naval Technology
Room 907
Arlington, VA 22217-5000

Superintendent
Code 1424
Attn Documents Librarian
Naval Postgraduate School
Monterey, CA 93943

Dr. George W. Ullrich (3)
Deputy Director
Defense Nuclear Agency
6801 Telegraph Road
Alexandria, VA 22310

Ms Michelle Van Cleave
Asst Dir/National Security Affairs
Office/Science & Technology Policy
New Executive Office Building
Washington, DC 20506

Mr. Richard Vitali
Director of Corporate Laboratory
US Army Laboratory Command
2800 Powder Mill Road
Adelphi MD 20783-1145

Dr. Edward C. Whitman
Dep Assist. Sec. of the Navy
C3I Electronic Warfare & Space
Department of the Navy
Washington, DC 20350-5000

Mr. Donald J. Yockey
U/Secretary of Defense for
The Pentagon, Room 3E933
Washington, DC 20301-3000

Dr. Linda Zall
Central Intelligence Agency
Washington, DC 20505

Mr. Charles A. Zraket
Trustee
The MITRE Corporation, A130
202 Burlington Road
Bedford, MA 01730